WADD TECHNICAL REPORT 60-768

COMPARISON OF RELATIVE COSTS OF THERMAL ANALYSIS METHODS FOR HYPERSONIC VEHICLE COMPARTMENTS

JOHN R. MALCOLM
ROBERT L. SLACK

THE BOEING COMPANY

JULY 1961

AERONAUTICAL ACCESSORIES LABORATORY
CONTRACT No. AF 33(616)-6339

PROJECT No. 9(15-6146)
TASK No. 60753

AERONAUTICAL SYSTEMS DIVISION
AIR FORCE SYSTEMS COMMAND
UNITED STATES AIR FORCE
WRIGHT-PATTERSON AIR FORCE BASE, OHIO

McGregor & Werner, Inc., Dayton, O.
300 - November 1961 - 9-293

FOREWORD

This report was prepared by the Environmental Control Development Group, Engineering Design Department, Aero-Space Division of the Boeing Airplane Company. The program was conducted under Contract Number AF33(616)-6339, "Research of Thermal Analysis Methods Specifically Applicable to Compartments of Hypersonic Vehicles and Satellite Re-entry Vehicles," Project Number 9(15-6146), Task Number 60753. The contract was administered under the direction of Mr. E. G. Koepnick and Mr. R. J. Gillen, Project Engineers of the Environmental Branch (WWRMFE) of the Flight Accessories Laboratory, Wright Air Development Division, Wright-Patterson Air Force Base, Ohio.

The authors wish to acknowledge the advice and helpful suggestions of Mr. A. L. Inglefinger (WWRMFE-2), the Task Engineer for this study.

ABSTRACT

In order to design the cooling systems of re-entry vehicles, judgment must be exercised in selecting the appropriate method for determining the transient heat transfer through complex structure into manned and equipment compartments. The accuracy must be consistent with the available calendar time, manpower and dollar cost in making this judgment. The heat flow can be determined analytically by several computing methods and experimentally by several laboratory testing methods.

This report presents the results of a study to examine the relationships between accuracy and cost in manhours, calendar time and dollars, in determining this transient heat flow for two hypothetical re-entry vehicles.

Accuracy and cost information were obtained for analytical methods: hand calculations, digital computers, differential analyzers, and passive element analogues; and for experimental methods: various size panels, half and full size vehicles, and vehicle compartments. Results are presented as curves of accuracy as a function of cost.

For the problems of this study, a general heat transfer digital computer program provides the most accuracy for the least cost. The other computing techniques rank in the following order: differential analyzer, passive element analogue, and hand calculations. The differential analyzer is the best method for parameter studies where a large number of runs is expected.

Experimental methods cannot compete with analytical methods in dollar cost, calendar time, or manhours. However, by obtaining material thermal properties experimentally, confidence can be increased in analytical solutions.

PUBLICATIONS REVIEW

This report has been reviewed and is approved.

FOR THE COMMANDER:

William C Savage

WILLIAM C. SAVAGE
Chief, Environmental Branch
Flight Acessories Laboratory

TABLE OF CONTENTS

Section		Page
	List of Illustrations	vi
	List of Tables	ix
	Nomenclature	xi
I.	Introduction	1
II.	Vehicle Design	3
	A. General	3
	B. Trajectories	3
	C. Thermal Environment	5
	D. Structural Design	6
	E. Optimum Insulation Thickness	8
III.	Equations and Calculation Methods	9
	A. General	9
	B. Glide Vehicle Equations	9
	C. Drag Vehicle Equations	14
	D. Calculation Methods	23
IV.	Analytical Methods Cost Comparison	29
	A. General	29
	B. True Answer	29
	C. Ground Rules for Cost and Accuracy Comparisons	31
	D. Cost Comparisons	35

TABLE OF CONTENTS (Continued)

		Page
V.	Experimental Methods Cost Comparison	43
	A. General	43
	B. Ground Rules for the Cost and Accuracy Comparison	44
	C. Testing Cost for Glide and Drag Vehicles	45
	D. Testing Inaccuracies for Glide and Drag Vehicles	47
	E. Cost and Accuracy Comparison	48
	F. Summary	50
VI.	Material Thermal Property Testing	53
	A. General	53
	B. Cost Ground Rules and Accuracy Discussion	53
	C. Material Property Cost and Influence on Heat Transfer Accuracy	55
	D. Summary	56
VII.	Conclusions	59
	References	61
	Appendix I - Spherical Stagnation Heat Transfer Coefficients	65
	Appendix II - Optimum Insulation Trade Study	67
	Appendix III - Theory of Finite Differences	73
	Appendix IV - Calculation Procedures	83
	Appendix V - Experimental Facilities	97
	Appendix VI - Testing Inaccuracies for Radiant Heat Testing	109
	Appendix VII - Similitude in Heat Transfer Tests	119

LIST OF ILLUSTRATIONS

Figure		Page
1.	Glide Vehicle Trajectory	139
2.	Drag Vehicle Trajectory	139
3.	Surface Temperatures Versus Time - Glide Vehicle $\alpha = 0^{o}$	140
4.	Surface Temperatures Versus Time - Glide Vehicle $\alpha = 12^{o}$	140
5.	Lines of Uniform Temperatures Glide Vehicle	141
6.	Drag Vehicle Equilibrium Skin Temperatures Versus Time	142
7.	Skirt and Heat Shield Temperatures - Drag Vehicle	143
8.	Weight Required for Thermal Protection Versus Heat Flux	143
9.	Glide Vehicle	144
10.	Structural Details - Glide Vehicle	145
11.	Drag Vehicle	146
12.	Structural Details - Drag Vehicle	147
13.	Weight Chargeable to the Cooling System Versus Insulation Thickness - Drag Vehicle	148
14.	Outer Insulation Thermal Conductivity Versus Mean Temperature	149
15.	Water Boiling Temperature - Glide Vehicle	150
16.	Thermal Conductivity Simulation	151
17.	Heat Flow Versus Number of Physical Subdivisions - Glide Vehicle	152
18.	Forward Side Heat Flow Versus Number of Physical Subdivisions - Drag Vehicle	152
19.	Total Heat Flow Versus Number of Physical Subdivisions - Drag Vehicle	153
20.	Solution % Error Versus Manhours - Glide Vehicle	153

LIST OF ILLUSTRATIONS (Continued)

Figure		Page
21.	Solution % Error Versus Total Dollar Cost - Glide Vehicle	154
22.	Solution % Error Versus Calendar Time - Glide Vehicle	155
23.	Total Dollar Cost Versus Number of Repeat Solutions - Glide Vehicle	156
24.	Manhour Cost Versus Number of Repeat Solutions - Glide Vehicle	157
25.	Solution % Error Versus Manhours - Drag Vehicle	158
26.	Solution % Error Versus Calendar Time - Drag Vehicle	159
27.	Solution % Error Versus Dollar Cost - Drag Vehicle	160
28.	Solution % Error Versus Calendar Time - Forward Side Drag Vehicle	161
29.	Total Dollar Cost Versus Number Repeat Solutions - Drag Vehicle	162
30.	Manhour Cost Versus Number Repeat Solutions - Drag Vehicle	163
31.	Radiant Heat Test Facilities Cost	164
32.	Radiant Heat Test Facilities Calendar Lead Time	165
33.	Experimental Manhours Versus Accuracy - Glide Vehicle	166
34.	Experimental Dollar Cost Versus Accuracy - Glide Vehicle	167
35.	Experimental Calendar Time Versus Accuracy - Glide Vehicle	168
36.	Experimental Manhours Versus Accuracy - Drag Vehicle	169
37.	Experimental Dollar Cost Versus Accuracy - Drag Vehicle	170
38.	Experimental Calendar Time Versus Accuracy - Drag Vehicle	171
39.	Material Property Test Apparatus Cost and Calendar Lead Time	172
40.	Effect on Heat Transfer of Errors in the Outer Insulation Diffusivity - Glide Vehicle	173

LIST OF ILLUSTRATIONS (Continued)

Figure		Page
41.	Effect on Heat Transfer of Errors in the Acoustical Insulation Diffusivity - Glide Vehicle	173
42.	Effect on Heat Transfer of Errors in the Honeycomb Diffusivity - Glide Vehicle	173
43.	Effect on Heat Transfer of Errors in the "Load Carrying" Insulation Diffusivity - Drag Vehicle	174
44.	Effect on Heat Transfer of Errors in the Radiation Factor - Drag Vehicle	174
45.	Spherical Nose Heat Transfer Coefficient for One-Foot Diameter Nose - Velocity up to 14,000 ft/sec	175
46.	Spherical Nose Heat Transfer Coefficient for One-Foot Diameter Nose - Velocity up to 28,000 ft/sec	176
47.	Stagnation Region Factor - Laminar Flow	177
48.	Geometric Definition of Angles Used to Find Angle between Flow and Surface Normal	178
49.	Typical Re-entry Vehicle Wall Temperature	179
50.	Maximum Cabin Wall Temperature Versus Insulation Thickness Forward Side - Drag Vehicle	180
51.	Water Boiling Temperature - Drag Vehicle	180
52.	Block Diagram of Differential Analyzer Setup	181
53.	Hand Calculation Data Sheet	182
54.	Radiant Heating Equipment	183
55.	Air Force Heat Test Facility Located at Inglewood, California (Photo Courtesy of Thompson Ramo-Woolridge, Inc.)	183
56.	Error in Heat Transfer from Vehicle Skin to Water Wall Resulting from Errors in Surface Temperature Simulation for Sea Level Testing - Glide Vehicle	184
57.	Error in Heat Transfer from Vehicle Skin to Water Wall Resulting from Errors in Surface Temperature Simulation with Altitude Error Curve "A" of Figure 59 - Glide Vehicle	184

LIST OF ILLUSTRATIONS (Continued)

Figure		Page
58.	Error in Heat Transfer from Vehicle Skin to Water Wall Resulting from Errors in Surface Temperature Simulation with Altitude Error Curve "B" of Figure 59 - Glide Vehicle	185
59.	Vehicle Trajectory Error Curves Used for Figures 57 and 58 - Glide Vehicle	185
60.	Error in the Heat Transfer to the Vehicle Resulting from Errors in Surface Temperature Simulation for Sea Level Testing - Drag Vehicle.	186
61.	Error in the Heat Transfer to the Vehicle Resulting from Errors in Surface Temperature Simulation with Altitude Error Curve "A" of Figure 63 - Drag Vehicle	186
62.	Total Error in the Heat Transfer to the Vehicle Resulting from Errors in Surface Temperature Simulation for Altitude Simulation Errors of Figure 63 - Drag Vehicle	187
63.	Vehicle Trajectory Error Curves Used for Figures 61 and 62 - Drag Vehicle	187

LIST OF TABLES

Table		Page
I.	Cost Summary Glide Vehicle	125
II.	Cost Summary Drag Vehicle	126
III.	Specimen Fabrication Estimates	127
IV.	Sea Level - Manhour Estimates - Radiant Heat Testing	128
V.	Vehicle Altitudes Simulated - Manhour Estimates - Radiant Heat Testing	129
VI.	Sea Level - Cost Estimate - Radiant Heat Testing	130
VII.	Vehicle Altitudes Simulated - Cost Estimate - Radiant Heat Testing	131
VIII.	Sea Level - Calendar Time Estimates - Radiant Heat Testing	132
IX.	Vehicle Altitudes Simulated - Calendar Time Estimates - Radiant Heat Testing	133
X.	Total Experimental Cost and Time Estimates - Radiant Heat Testing	134
XI.	Glide Vehicle - Cost and Time Estimates - Material Thermal Properties	135
XII.	Drag Vehicle - Cost and Time Estimates - Material Thermal Properties	136
XIII.	Total Experimental Cost and Time Estimates - Material Thermal Properties - Glide and Drag Vehicles	137
XIV.	Glide Vehicle - Heat Flow Errors from Errors in Material Thermal Properties	138

NOMENCLATURE

A	-	Area	ft^2
C	-	Thermal conductance	$BTU/hr\text{-}ft^2\text{-}^oF$
C	-	Electrical capacitance	farads
C_D	-	Drag coefficient	dimensionless
C_L	-	Lift coefficient	dimensionless
C_p	-	Specific heat	$BTU/lb\text{-}^oF$
D	-	Drag	lbs
D	-	Leading edge diameter	ft
E	-	Error	^oF
F_a	-	Radiation shape factor	dimensionless
F_e	-	Radiation emissivity factor	dimensionless
g	-	Local gravitational acceleration	ft/sec^2
g_o	-	Earth gravitational acceleration, standard	ft/sec^2 32.17
h	-	Convection coefficient	$BTU/hr\text{-}ft^2\text{-}^oF$
h_D	-	Average heat transfer coefficient for a sphere of diameter D	$BTU/hr\text{-}ft^2\text{-}^oF$
h_1	-	Average heat transfer coefficient for a one-foot diameter sphere	$BTU/hr\text{-}ft^2\text{-}^oF$
K	-	Thermal conductivity	$BTU/hr\text{-}ft^2\text{-}^oF/ft$
L	-	Lift	lbs
L	-	Insulation thickness	ft
L_H	-	Latent heat expendable coolant	BTU/lb
M	-	Free stream Mach number	dimensionless
Q/L	-	Total aerodynamic heat entering compartment	BTU
q	-	Heat transfer rate	BTU/hr

R	-	Earth radius	ft
R	-	Range	ft
S	-	Wing area	ft^2
T	-	Temperature	^oR
t	-	Thickness	ft
U	-	Velocity in the x direction	ft/sec
V	-	Velocity	ft/sec
V	-	Potential difference	volts
W	-	Weight	lbs
w	-	Weight flow rate	lbs/hr
x	-	Space coordinate	ft
y	-	Space coordinate	ft
z	-	Space coordinate	ft
α	-	Thermal diffusivity	ft^2/hr
α	-	Angle of attack	degrees
β	-	Total heat from internal source	BTU
γ	-	Altitude plus earth radius	ft
Δ	-	Increment	dimensionless
ϵ	-	Emissivity	dimensionless
η	-	Lbs. of power source (including expendable fuel) per unit blower energy	lbs/BTU
θ	-	Percentage of expendable coolant weight to account for tanks, plumbing, brackets, etc.	dimensionless
λ	-	Lbs. of blower and drive weight per unit blower energy	lbs/BTU/hr
Λ	-	Angle of sweepback	degrees
μf	-	Capacitance	microfarads

ρ	-	Density	lbs/ft^3
σ	-	Stefan - Boltzmann's constant	$BTU/hr\text{-}^{o}R^{4}\text{-}ft^{2}$
σ	-	Ratio of local atmosphere density to earth atmosphere density	dimensionless
Σ	-	Summation	dimensionless
τ	-	Time	hours
ψ	-	Heat exchanger weight per unit heat removal rate	#/BTU/hr

SUBSCRIPTS

a - Air

aw - Adiabatic wall

bl - Blower

c - Cabin

e - Electrical

f - Final

h - Honeycomb

i - Insulation

i - i^{th} location

o - initial

s - Spring

S - Skin

T - Thermal

w - Water wall

1, 2, 3, etc. - location in space

SUPERSCRIPTS

n - Evaluated at the n^{th} time interval

$\cdot$ - Time derivative

$'$ - Evaluated after the $\Delta\tau$ time has elapsed

I. INTRODUCTION

Large changes in the heat transfer rate occur at the surfaces of vehicles re-entering the earth's atmosphere. The task of determining the resultant transient heat flow through complex structure into the manned and equipment compartments is a complex problem and one that must be solved to design the vehicle cooling system.

There are two ways, analytically and experimentally, a designer may determine the size of the vehicle heat load. There are several computing methods he may choose to implement his analytical approach and several different ways in which he may conduct laboratory tests. The choice of method should be compatible with the desired solution accuracy and the calendar time, manpower and facilities available. The purpose of this study is to examine the relationships between accuracy and cost in manhours, calendar time and dollars.

Parameters were chosen that are typical of vehicles that will experience the maximum and minimum rates of change of conditions. Trajectories and a thermal environment were established for two vehicles, one a drag-retarded vehicle consisting of a sphere and a stability skirt, the other a lift sustained vehicle. Basic structural details were established. Approximate optimum insulation thicknesses were chosen for each vehicle.

The study was divided into two parts at this point. One was to compute the heat flow into the vehicles utilizing various computing techniques and to determine the cost in manhours, calendar time and dollars versus accuracy. The heat transfer into the manned compartments of these two vehicles was computed using the following four calculation methods:

1. Desk Calculations
2. Digital Computer
3. Differential Analyzer Computer
4. Passive Element Analogue Computer

The other part was to analytically examine experimental methods of obtaining the heat flow, determine the cost of fabricating and testing various size and type specimens, determine what accuracy might be expected, determine the cost and accuracy of obtaining various material properties, and assess the role that accuracy of material properties plays in the calculation of the overall heat flow.

Manuscript released for publication as a WADD Technical Report on 31 May 1961.

II. VEHICLE DESIGN

A. General

The type of vehicle being studied will have an effect upon the assumptions that can be validly made. These assumptions in turn will affect the relative merits of the various methods used to obtain the heat flow. Two vehicles were chosen that typify vehicles that will experience the maximum and minimum rate of change of conditions affecting the heat transfer. The two vehicles chosen for study are: (a) a drag retarded manned re-entry vehicle consisting of a 6.5 foot diameter sphere with a 15 degree tangent cone, and (b) a lift sustained manned re-entry vehicle of 30 feet overall length.

Trajectories were established for each of these vehicles. Vehicle velocity and altitude in turn determine the heat transfer coefficients and the adiabatic wall temperatures for each point in the vehicle trajectory. This temperature environment, along with air loads, accelerations, etc., was used to design the basic structure typical for vehicles of this class. The temperature environment was also used to determine approximate optimum insulation thickness for both vehicles.

The configurations thus established are not "finished" products in that the structures, trajectories, aerodynamic shapes, etc., are not optimized or designed in detail. However, both configurations are very close to what detail designs would produce and contain all of the elements essential to a typical heat transfer problem for vehicles of their type.

B. Trajectories

1. Glide Vehicle

The glide vehicle is a lift sustained manned re-entry vehicle with a wing loading of 30 lbs. per square foot, a lift coefficient of 0.07, and a lift drag ratio of 3.0. The initial speed and altitude are consistent with a 25,000 mile range, rotation of the earth neglected.

The initial speed of the glide vehicle for a range of 25,000 miles was determined by solving for the initial speed in the range equation.

$$R = \frac{L}{D} \frac{\gamma}{2} \operatorname{Log}_e \left[\frac{1 - \frac{V_o^2}{\gamma g}}{1 - \frac{V_f^2}{\gamma g}} \right]$$

For R = 25,000 nautical miles and L/D = 3, the initial velocity is 24,960 ft/sec. The glide trajectory was computed for a straight equilibrium glide at a constant lift coefficient. The lift coefficient and the wing loading give a glide parameter of W/SC_L = 428 lbs. per ft^2. With this constant value, the altitude was determined as a function of time from the expression

$$\sigma = \frac{W}{SC_L} \left(1 - \frac{V^2}{\gamma g}\right) \Big/ \frac{1}{2} \rho_a V^2$$

The ARDC 1956 Model Atmosphere was used for the properties of the atmosphere. These equations and assumptions will give trajectories within ± 10% of a more detailed and sophisticated approach.

The glide vehicle trajectory used in this study is shown on Figure 1.

The sample glide trajectory presented here used a constant lift coefficient for the entire flight path. More refined trajectories require modulation of the lift coefficient in order to achieve the best performance within the heating and acceleration limits of a manned vehicle. In an actual glide re-entry, the vehicle must operate within a re-entry corridor. The upper boundary of this corridor is formed by the altitude-speed combinations that permit recovery pullouts to be made without excessive g-loads and above altitudes at which heating becomes excessive. The lower boundary is formed by the temperature limit for various speed-altitude combinations. These boundaries are also functions of the shape, material, and lift coefficient. To fully exploit the vehicle performance capabilities for broadening the re-entry corridor, a re-entry would be initiated at the maximum available lift coefficient. When the temperature limit for this high lift coefficient is reached during the descent, the vehicle angle of attack and lift coefficient are reduced with altitude and the descent is continued along the temperature limit.

The constant lift coefficient glide re-entry would result in less deceleration initially with subsequent higher heating rates during the glide. The rates of change of conditions in the constant lift coefficient trajectory are sufficiently close to those of the variable lift coefficient trajectory, however, to represent a typical slow-change re-entry trajectory.

2. Drag Vehicle

The drag-retarded manned re-entry vehicle consists of a 6.5 foot diameter basic sphere with a 15 degree tangent cone with a base diameter of 10.3 feet. This results in a drag mass parameter $\frac{C_D A}{W}$ = 0.0192, and a gross weight of 2500 lbs. An altitude of 290,000 feet, speed of 25,900 ft/sec and a flight path angle of 5° below the horizontal were chosen for initial conditions.

The equations of motion were solved by a 704 IBM computer. The following two dimensional equations of motion, simplified by the omission of lift and thrust terms were used:

$$\frac{d\dot{\gamma}}{dt} = \gamma\dot{\beta}^2 - g_o \frac{R^2}{\gamma^2} - \frac{C_D \rho g A V \dot{\gamma}}{2W}$$

$$\frac{d\dot{\beta}}{dt} = \frac{2\dot{\gamma}\dot{\beta}}{\gamma} - \frac{C_D \rho g_o A V(\gamma\dot{\beta} + W)}{2\gamma W}$$

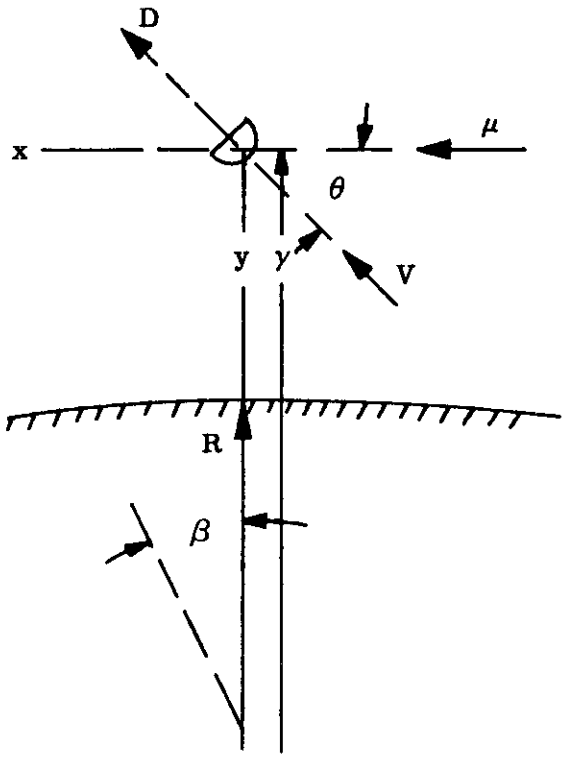

$$y = \gamma - R$$

$$x = \gamma \tan \beta$$

$$\dot{\gamma} = V \sin \theta$$

$$\gamma\dot{\beta} = V \cos \theta$$

The ARDC 1956 Model Atmosphere was used for the properties of the atmosphere. The resulting trajectory for the drag vehicle is shown on Figure 2. This trajectory is judged to be a fair representation of an actual trajectory for the given parameters and initial conditions.

C. Thermal Environment

Before the structural details of the vehicle can be established, some appreciation of the thermal environment must be obtained. The altitude, velocity, vehicle attitude and geometry determine the heat transfer coefficients, stagnation temperatures and adiabatic wall temperatures. These values, along with the emissivity of the vehicle surface, were used to obtain the vehicle equilibrium skin temperatures from the basic equation

$$h \left[T_{aw} - T_S \right] = \epsilon \sigma T_S^4$$

In computing the heat transfer coefficients and the adiabatic wall temperature, turbulent flow was assumed for all parts of the vehicle except for the nose and stagnation line of the wing. Laminar flow was assumed for these points.

Curves of the equilibrium skin temperatures versus time are shown on Figures 3 to 6. In computing the skin temperature for the stability skirt, radiant heat flow was considered out of both surfaces. The curve for the drag vehicle equilibrium temperature shows temperatures beyond the thermal limits for known structural materials. Clearly thus, either an ablative or heat shield structure is required. A beryllium heat shield of sufficient thickness that the thermal lag holds the temperature to safe values was chosen. (This decision is discussed in more detail below.) The resulting temperature for the inner and outer surfaces of the heat shield is shown on Figure 7. The heat shield thickness varies from 0.8 inches thick at the stagnation point to 0.25 inches thick at the sides. The thickness is varied so that the maximum temperature attained is the same at each point. Using the heat sink material at close to the maximum allowable temperature results in the lowest weight heat shield and a uniform surface temperature.

The heat transfer coefficients used in establishing the skin temperature of the spherical stagnation regions were obtained by the methods outlined in Appendix I. The remainder of the heat transfer coefficients were obtained from Reference 1.

D. Structural Design

1. General

When faced with the problem of designing the structure for re-entry vehicles, the designer can choose between one of four general types of structures: (a) insulated and cooled structure, (b) heat sink materials, (c) ablation materials, and (d) hot structure. The choice of structural configuration is influenced by several factors among which are weight, expansion problems, reliability, cost, ease of fabrication, heat flux, maximum temperature, time exposed to high heat flux, etc. Figure 8 is a plot of weight required for thermal protection versus the heat flux and shows the general regions of applicability of the various types of structure. The heat fluxes associated with the drag re-entry vehicle are noted on the curve and show that the structure should be of the heat sink or ablative type.

2. Glide Vehicle

The structural design of the glider allows thermal deformations to take place with as little restraint as possible. The skin panels are not rigidly attached to the internal structure and transmit air loads to the primary load carrying members by simple beam action. The internal structure is essentially statically determinate trusswork.

The skin, which experiences the higher temperatures and temperature

differences, is not rigidly attached to the primary structure. It is required only to carry the air load to the primary structural members. The flexible edge supports which hold the skin in its place do not have sufficient rigidity to allow the skin to develop net end loads of any significant magnitude.

The truss members, with exception of a few of the highly loaded elements, have sufficiently reduced moments of inertia at the joints to allow them to act as pin ended members. The thermal gradients across the structure do not impose major thermal stresses because of the determinate nature of the truss.

The skin panels and space truss are constructed of J-1500 (vacuum melted M-252). The nose cone and leading edges which are subjected to much higher temperatures are constructed of graphite and refractory materials. The structure is sketched on Figures 9 and 10.

3. Drag Vehicle

The structural design of the drag vehicle allows thermal deformation of the heat shield to take place with as little restraint as possible. The heat shield is connected to the structural shell with flexible attachments which are intended primarily for tension. Compression between the heat shield and structural shell would be carried by the insulation due to the deflection of the flexible attachments.

The structural shell is constructed as two hemispheres of .06 in. 2024-T3 spun aluminum joined at a circular ring which also supports the flared skirt.

Preliminary calculations show that the two types of thermal protection, heat shield and ablative, have comparable weights with a slight edge in favor of the ablative material. Nevertheless, a beryllium heat shield will be used for this study because this is a manned vehicle. The state of the art of ablating structure does not offer the margin of safety necessary for a manned vehicle. One reason for this is the heat transfer mechanism to ablating structure is not as well defined as is heat transfer to more conventional structure. If the quality control is not good, an ablative structure can spall off rather than ablate. If this happens, the results are disastrous to the vehicle.

The heat shield is beryllium shell which varies from .80 in. thick at the stagnation point to .25 in. thick at the sides. The thickness is varied so that the maximum temperature attained is the same at each point. This is done to keep the shield weight to a minimum and results in a uniform temperature over the heat shield surface. The flared skirt is composed of J-1500 (vacuum melted M-252) corrugated sheet over circular stiffeners. The structure is sketched on Figures 11 and 12.

E. Optimum Insulation Thickness

The next step toward setting up typical problems to solve is to obtain reasonable values of the insulation thickness. The basic theory and approach for our optimum insulation studies are outlined in Appendix II. The results of the brief studies showed that a water wall configuration (see Figure 13) resulted in approximately the same weight system as an insulated cabin with no water wall for the glide vehicle and a weight advantage in favor of insulated structure for the drag vehicle. There are many arguments that may be presented in favor of either a water wall or insulated structure. A discussion of the pros and cons of the various types of configurations is beyond the scope of this study. One potent factor in favor of a water wall is the thermal protection afforded a compartment in the event of failure of the cabin pressurization system. In this event, no air is available to act as a transport fluid to remove heat from the walls and to transport heat to the heat absorbing equipment. With this in mind, the decision was made to use a water wall for the glide vehicle with its long re-entry time and an insulated structure for the drag vehicle. A secondary reason for these choices is to cover both classes of structure so that problems unique to each type are covered.

III. EQUATIONS AND CALCULATION METHODS

A. General

This section outlines the derivation of the equations describing the heat transfer into the occupied compartments of both study vehicles. In addition, the four calculation methods that are to be compared, digital computer, differential analyzer, direct analogue, and hand calculations, are briefly described. The equations that are derived and solved are finite difference approximations to the basic equation.

$$\frac{\partial\left(K(T,\tau)\frac{\partial T}{\partial X}\right)}{\partial X} + \frac{\partial\left(K(T,\tau)\frac{\partial T}{\partial Y}\right)}{\partial Y} + \frac{\partial\left(K(T,\tau)\frac{\partial T}{\partial Z}\right)}{\partial Z} = \rho(X,T)\, C_p(X,T)\, \frac{\partial T}{\partial \tau}$$

Appendix III outlines the theory of finite differences, discusses the inherent errors and describes the direct analogue method of solving the above equation. References are given that will provide a more detailed treatment.

B. Glide Vehicle Equations

One of the major considerations in mathematically describing a heat transfer situation is to determine if a two and three dimensional description of temperature distribution must be written or if a one dimensional description will suffice. The sketch below represents a section through the structure of the glide vehicle.

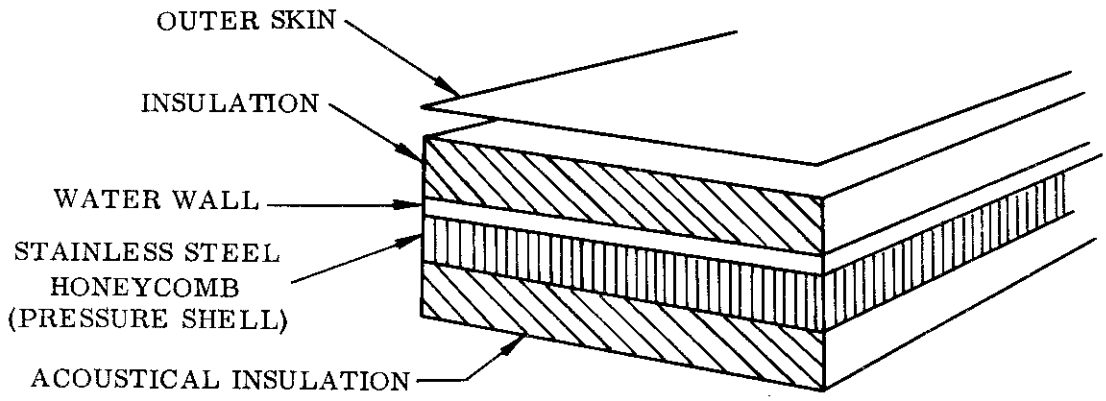

The heat entering the vehicle is transferred from the outer skin to the insulation almost solely by radiation. Most of the vehicle trajectory is sufficiently outside of the earth's atmosphere so that convection may be neglected except for the brief period at the end of the flight.

Figures 3 and 4 show that the temperature of the skin varies with length along the vehicle and around the vehicle. The first step will be to determine if this variation of temperature necessitates a two or three dimensional approach. This will be done by comparing the relative magnitude of the resistance to heat transfer along the vehicle and around the vehicle to the resistance toward the water wall.

The sketch below shows a section of skin, insulation, and water wall removed from a length along the vehicle lower surface.

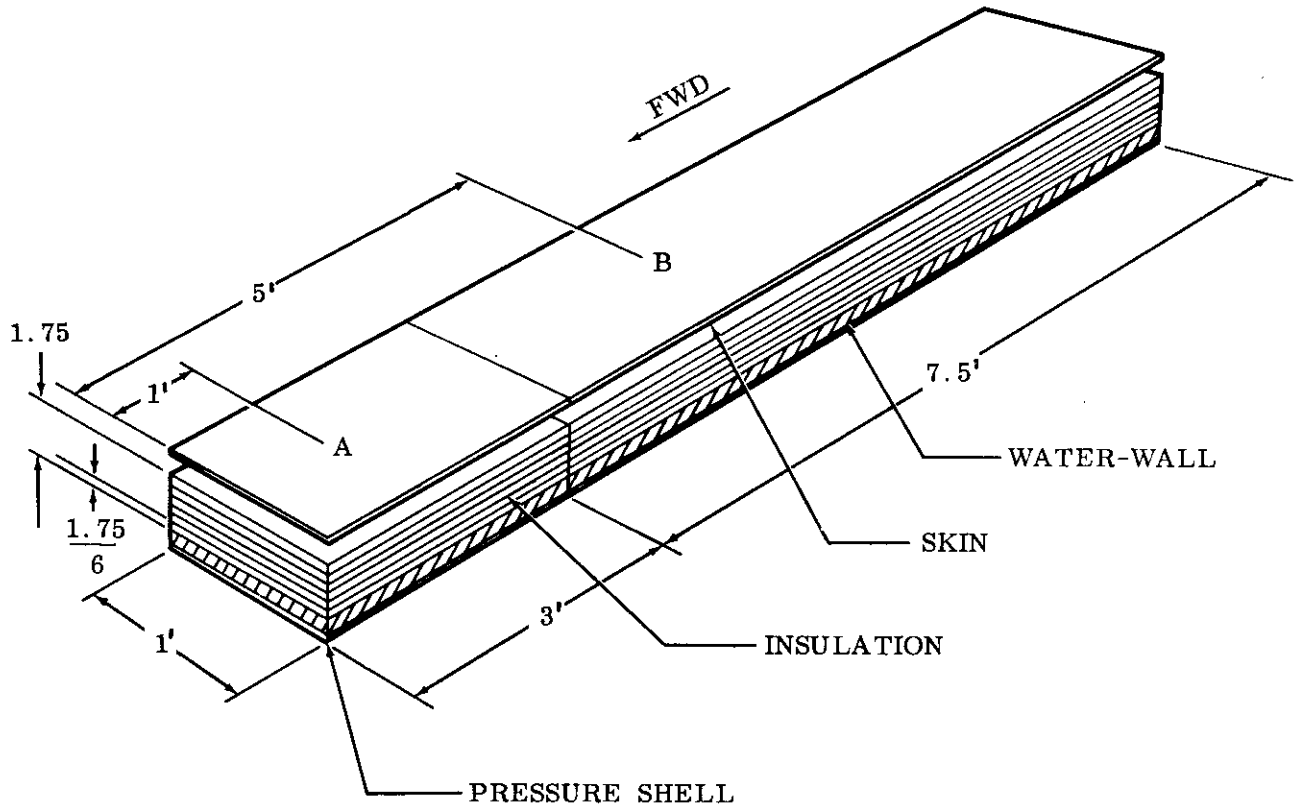

The temperatures are at the points A and B, one and five feet back from the leading edge along the vehicle. These two points are chosen because they have the maximum temperature gradient. The insulation has been sub-divided into six equal slabs by planes parallel to the skin and divided into two sections by a plane midway between the points A and B and a plane 7.5 ft. back. The thermal resistance values between any two nodes is given by $\frac{\Delta x}{KA}$. Resistance values through the insulation are identified with subscript 1 and along the vehicle with subscript 2.

Resistance toward the water wall per layer of insulation $= \left[\frac{1.75}{(6)(12)}\right]\left[\frac{1}{(3)(1)K_1}\right] = \frac{0.0081}{K_1}$

Resistance along the vehicle $= (4)\left[\frac{1}{\frac{(K_2)(1.75)}{(12)(6)}}\right] = \frac{164}{K_2}$

$$\frac{\text{Resistance along the vehicle}}{\text{Resistance toward water wall}} = \frac{\frac{164}{K_2}}{\frac{0.0081}{K_1}} = 20{,}300\ \frac{K_1}{K_2}$$

The thermal conductivity of the insulation is a function of the mean temperature; the mean temperature through the vehicle (direction 1) is lower than along it (direction 2), making K_1 slightly lower than K_2. Nevertheless, the ratio of the resistance values shows the resistance to heat flow along and around the vehicle is very much greater than the resistance through the insulation. The remaining factor to be examined is the influence of the potential for heat flow. The maximum temperature gradient along the body exists at $\alpha = 12^\circ$ and between one and five feet back from the leading edge where the potential is approximately 420° F. For estimating purposes, the thermal conductivity can be assumed constant giving a potential of $\frac{2670 - 40}{6} = 438^\circ$F in steady state. From this, it can be concluded that the potential through the vehicle (direction 1) is the same order of magnitude as the potential along the vehicle (direction 2). Therefore, the heat transfer along the vehicle may be ignored by comparison with the heat transfer through the vehicle. A similar analysis was made to show that the heat transfer around the vehicle may be ignored by comparison with the heat transfer through the vehicle.

Having established that a one-dimensional description is sufficiently accurate, the sketch below illustrates how the physical problem was subdivided in one particular case.

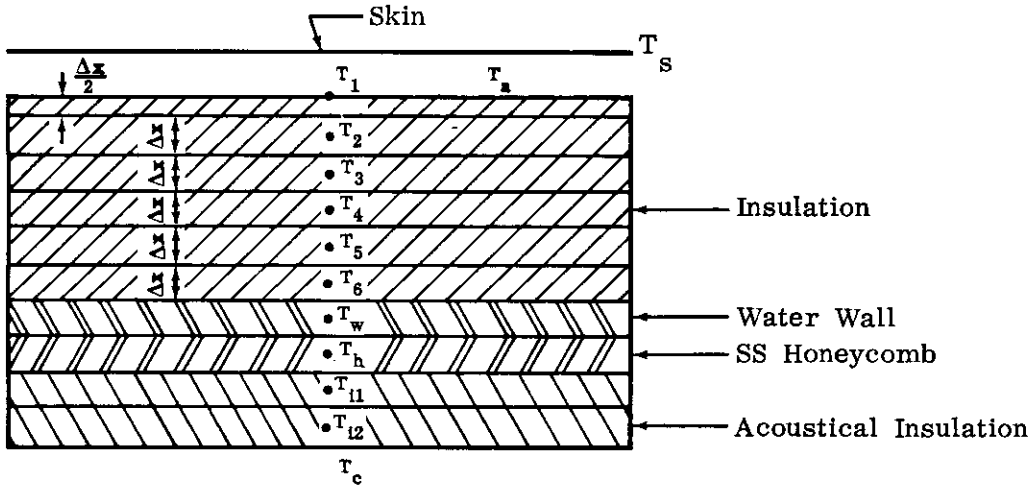

The following set of equations were written for this particular case.

Heat flow from skin to insulation:

$$\sigma Fe Fa A\left[(T_S)^4 - (T_1)^4\right] + h_{(\tau)} A\left[Ta_{(\tau)} - T_1\right] = \frac{K_1 A}{\Delta X}\left[T_1 - T_2\right] - \frac{\rho A \Delta x C_p}{2\Delta\tau}\left[T_1' - T_1\right]$$

Subsequent investigation showed the influence of the convection term $h_{(\tau)} A\left[Ta(\tau) - T_1\right]$ to be negligible.

Heat flow through the insulation:

$$\frac{K_1 A}{\Delta X}\left[T_1 - T_2\right] = \frac{K_2 A}{\Delta X}\left[T_2 - T_3\right] + \frac{\rho A \Delta X C_p}{\Delta\tau}\left[T_2' - T_2\right]$$

$$\frac{K_2 A}{\Delta X}\left[T_2 - T_3\right] = \frac{K_3 A}{\Delta X}\left[T_3 - T_4\right] + \frac{\rho A \Delta X C_p}{\Delta\tau}\left[T_3' - T_3\right]$$

$$\frac{K_3 A}{\Delta X}\left[T_3 - T_4\right] = \frac{K_4 A}{\Delta X}\left[T_4 - T_5\right] + \frac{\rho A \Delta X C_p}{\Delta\tau}\left[T_4' - T_4\right]$$

$$\frac{K_4 A}{\Delta X}\left[T_4 - T_5\right] = \frac{K_5 A}{\Delta X}\left[T_5 - T_6\right] + \frac{\rho A \Delta X C_p}{\Delta\tau}\left[T_5' - T_5\right]$$

$$\frac{K_5 A}{\Delta X}\left[T_5 - T_6\right] = \frac{2K_6 A}{\Delta X}\left[T_6 - T_w\right] + \frac{\rho A \Delta X C_p}{\Delta\tau}\left[T_6' - T_6\right]$$

$$\frac{2K_6 A}{\Delta X}\left[T_6 - T_w\right] + \frac{CA}{2}\left[T_h - T_w\right] = w\left(L_H(\tau)\right) + \frac{W_w C_p}{\Delta\tau}\left[T_w' - T_w\right]$$

$w(L_H(\tau))$ is the product of the flow rate of the water evaporated and the latent heat of the water as a function of time.

$W_{wo} - \Sigma w \Delta\tau = W_w$ Mass Balance

Heat balance on honeycomb

$$\left[\frac{1}{\frac{\Delta Xi}{2K_i A} + \frac{2}{CA}}\right]\left[T_{i_1} - T_h\right] = \frac{CA}{2}\left[T_h - T_w\right] + \frac{W_h C_{ph}}{\Delta\tau}\left[T_h' - T_h\right]$$

The term CA is the conductance value of the honeycomb. The finite difference theory assumes that the temperature of the honeycomb is represented by a single temperature at the midpoint. Therefore, the thermal resistance between the midpoint and the edge of the honeycomb is $\frac{2}{CA}$. The thermal resistance from the edge of the honeycomb temperature T_{i_1} is $\frac{\Delta X_i}{2K_iA}$. The total thermal resistance of resistances in series is their sum; thence the coefficient of the $\left[T_{i_1} - T_h\right]$ term is $\left[\frac{1}{\frac{\Delta X_i}{2K_iA} + \frac{2}{CA}}\right]$

Heat balance on acoustical insulation

$$\frac{K_iA}{\Delta X_i}\left[T_{i_2} - T_{i_1}\right] = \left[\frac{1}{\frac{\Delta X_i}{2K_iA} + \frac{2}{CA}}\right]\left[T_{i_1} - T_h\right] + \frac{\rho_iA\Delta X_iC_{pi}}{\Delta\tau}\left[T'_{i_1} - T_{i_1}\right]$$

$$\left[\frac{1}{\frac{1}{hA} + \frac{\Delta X_i}{2K_iA}}\right]\left[T_C - T_{i_2}\right] = \frac{K_iA}{\Delta X_i}\left[T_{i_2} - T_{i_1}\right] + \frac{\rho_iA\Delta X_iC_{pi}}{\Delta\tau}\left[T'_{i_2} - T_{i_2}\right]$$

In writing this set of equations, certain assumptions were made. The most important of these are:

1. The skin temperature is the equilibrium skin temperature. This assumption is justified by comparing the magnitude of the heat transferred into the skin from the boundary layer, the radiation from the skin, the heat flow into the cabin, and the amount of heat the skin is capable of absorbing.

2. The shape factor between the skin and the insulation is that for radiation between parallel plates.

3. The thermal conductivity of the insulation is given by Figure 14 as a function of mean temperature and altitude. The specific heat was assumed constant.

4. The pressure in the water wall was assumed to be held at the pressure corresponding to 40°F while the vehicle was at altitudes where this was possible. Figure 15 shows the saturation temperature vs time. Preliminary calculations show that the heat rejection from the cabin is sufficient to hold the water at 40°F during the early portions of the trajectory. This assumption requires the calculation technique to be capable of allowing the heat flow into the water wall to do two things: (a) evaporate water during the major portion of the re-entry, and

(b) increase the sensible heat of the water and associated structure to keep pace with the change in saturation pressure and allow the remaining heat flow, if any, to evaporate water.

5. The honeycomb is represented by a single conductance value. Fortunately, the temperature of the honeycomb does not undergo large temperature changes, making this assumption adequate.

6. The thermal conductivity of the acoustical insulation does not change with time because (a) the change in insulation means temperature is small, and (b) being inside the pressure shell, the cabin pressure prevents change due to pressure.

7. Heat is transferred to and from the acoustical insulation by a constant heat transfer coefficient. This assumption is justified on the basis of: constant cabin pressure, small temperature change of the insulation, and constant air velocity in the cabin.

8. The cabin temperature is assumed constant. This assumption rests on another assumption: the cabin conditioning system responds essentially instantly to changes in the vehicle heat load regardless of source, internal or aerodynamic.

9. The resistance to heat transfer through the mechanical joint between materials is assumed zero. Ordinary values of contact conductance are at least two orders of magnitude larger than the conductance values of interest in this problem.

Different assumptions could have been made. However, the ones made are reasonable estimates of the actual situation and should typify vehicles of this class. The only assumption that has a major effect on the economics of the solution is the one concerning the variation of thermal conductivity with temperature and pressure. In a later section, the influence of this assumption on the various computing techniques will be shown.

The above equations were derived for the insulation divided into six slabs. Equations were also written for the insulation divided into 2, 4, 8, and 10 slabs. The constants for these equations were computed and the equations supplied to specialists for machine solutions and engineering aides for solution by hand calculation methods.

C. Drag Vehicle Equations

The sketch below represents a section through the heat shield of the drag vehicle.

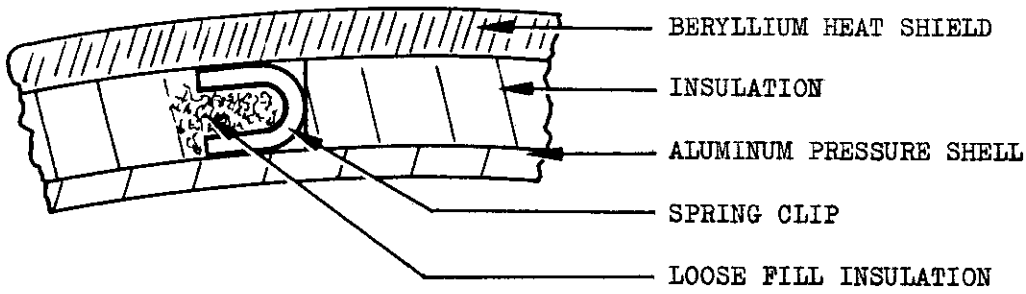

The first step will be to evaluate the effect of the spring on the total heat flow. The springs are located on 6" centers in all directions as shown on the sketch below. Dashed lines on the sketch represent lines across which there is no heat transferred since each point on these lines is equidistant from springs or points of equal potential.

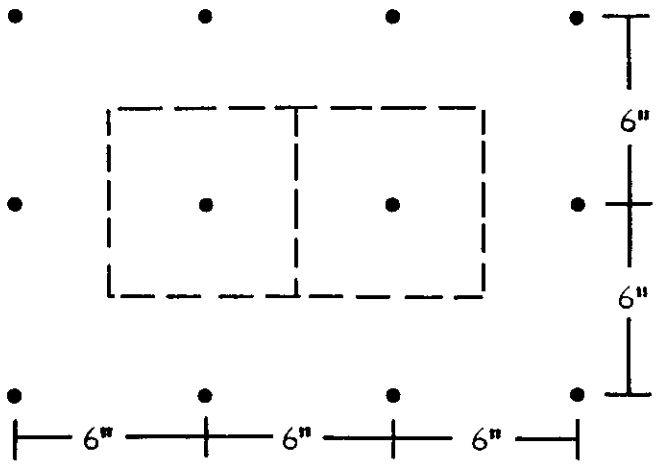

The sketch below is a spring surrounded by an adiabatic boundary described above. The spring is labelled Point 1 and the nodes representing the insulation 2, 3, 4, and 5. The purpose is to evaluate the thermal conductance along the paths 1-2, 1-3, 1-4, 1-5, 2-3, 3-4, 4-5, and 5-2.

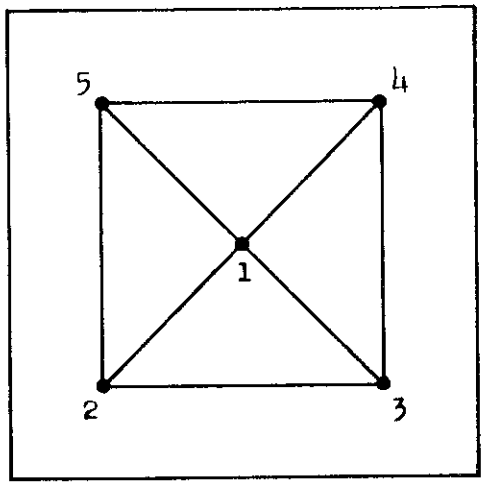

Reference 2 outlines a manner in which the problem may be attacked. To illustrate the technique, the following example will be used. The points on the sketch below represent nodes for a general case. The area and length of the heat transfer paths, a-b, a-c, b-c, between the nodes is desired. The dotted lines are the perpendicular bisectors of the various flow paths.

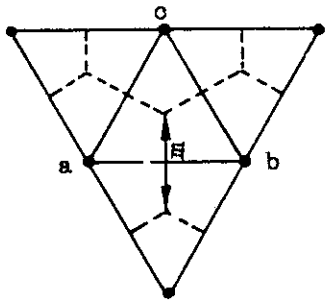

Reference 2 shows that the area associated with the heat flow from a to b is the thickness of the material multiplied by the length m in the sketch where m is the length of the line connecting the intersections of the perpendicular bisectors of the flow path. The length associated with the conductance value is a-b.

Erecting the perpendicular bisectors for the case of interest here as shown below, it can be seen that the intersection of the perpendicular bisectors fall on the paths 2-3, 3-4, 4-5, and 5-2. Therefore, the distance for the heat flow area is zero which means that no heat is transferred along paths

2-3, 3-4, 4-5, and 5-2. This same conclusion could be obtained by reasoning that since points 2, 3, 4, and 5 are equidistant from each other and equidistant from Point 1, they will be at the same potential. The sketch also shows that the area for heat flow along 1-2 is the thickness of the material times the length 2' - 5' and the length associated with the conductance is the length 1-2.

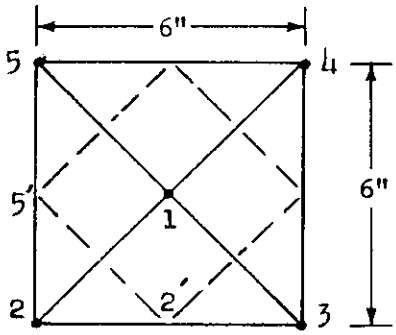

The above discussion shows that an adiabatic boundary can be drawn as illustrated in the sketch below.

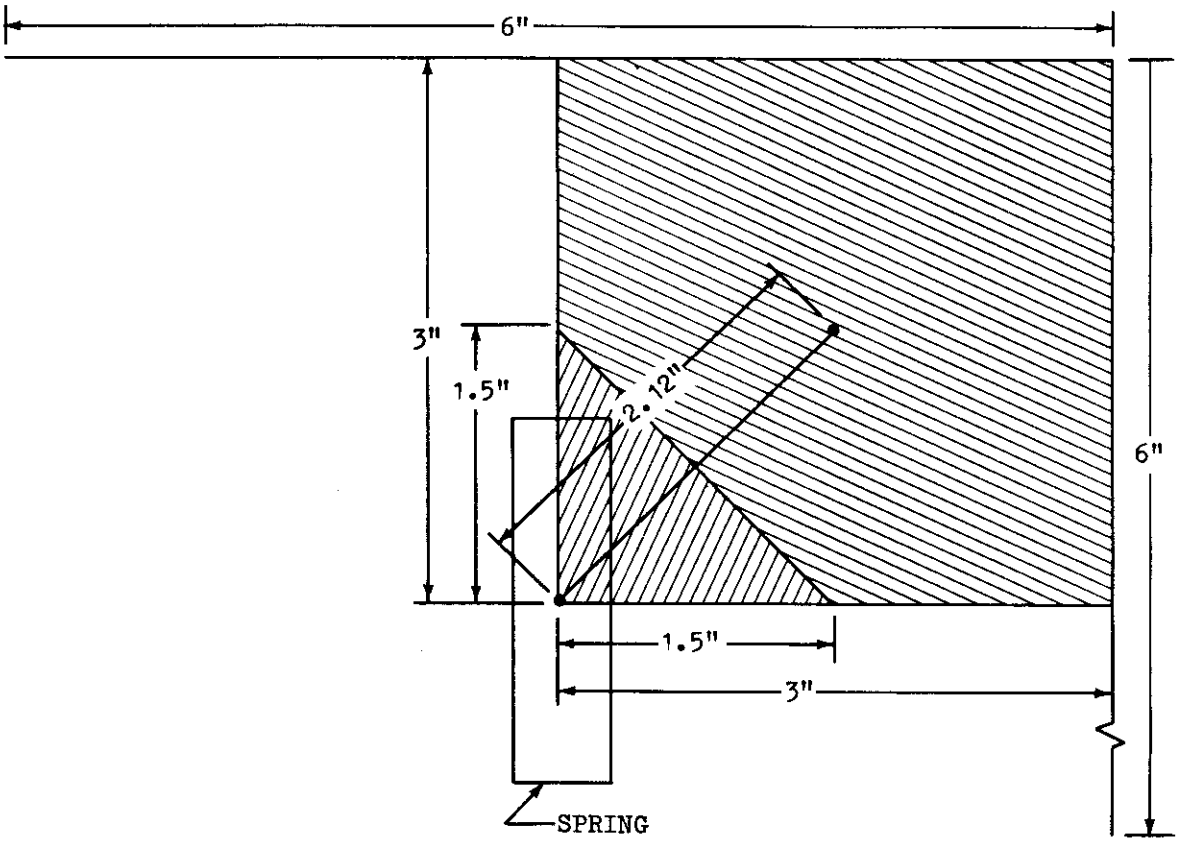

The sketch below is a cross section through the vehicle. The insulation and springs have been divided into six slabs by planes parallel to the skin and divided into two stacks of slabs by the plane a-b which is the perpendicular bisector of the line 1-4.

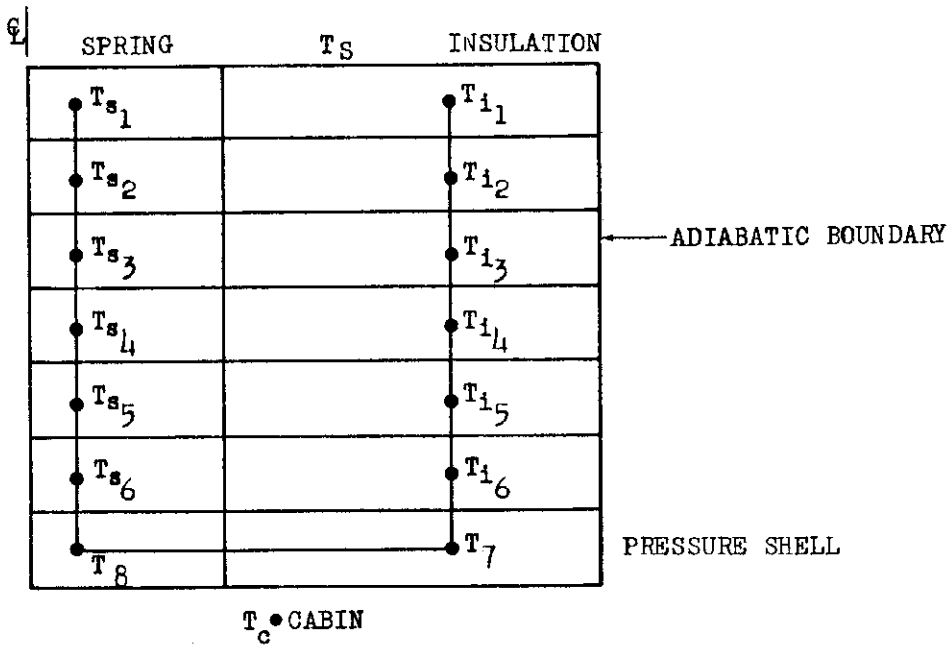

SECTION THROUGH FORWARD SIDE

The relative magnitude of the thermal resistances through the spring toward the cabin, through the insulation toward the cabin, and between the insulation and the spring are compared in the discussion below. The thermal resistance is given by $\frac{\Delta x}{KA}$. Values through the spring are identified with the subscript s, through the insulation with the subscript i, and between the spring and insulation with the subscript si. Detail dimensions of the spring and insulation are shown on Figure 12.

Resistance through the insulation

$$\frac{\Delta X_i}{K_i A_i} = \frac{\frac{(0.375)}{(6)}\left(\frac{1}{12}\right)}{\frac{(K_i)\left(3^2 - \frac{(1.5)^2}{2}\right)}{144}} = \frac{.09509}{K_i}$$

Resistance through the spring

$$\frac{\Delta X_s}{K_s A_s} = \frac{\left(\frac{1.339}{6}\right)\left(\frac{1}{12}\right)}{(K_s)\ \frac{(0.066)(2)}{(4)(144)}} = \frac{81.2}{K_s}$$

Using $K_s = 9.05\ \frac{\text{Btu - ft}}{\text{ft}^2\text{ - hr - }^\circ\text{F}}$

$$\frac{\Delta X_s}{K_s A_s} = \frac{81.2}{9.05} = 8.97$$

Resistance between spring and insulation

$$\frac{\Delta X_{si}}{K_{si} A_{si}} = \frac{\frac{2.12}{12}}{K_{si}\ \frac{(2.12)\ \frac{(0.375)}{6}}{144}} = \frac{191.9}{K_{si}}$$

Ratios of resistance values:

$$\frac{\text{Resistance through insulation}}{\text{Resistance between spring and insulation}} = \frac{0.09509\ K_{si}}{192\ K_i} = 0.000495$$

(Assuming K_{si} and K_i are evaluated at the same mean temperature)

$$\frac{\text{Resistance through spring}}{\text{Resistance between spring and insulation}} = \frac{8.97\ K_{si}}{192}$$

Using the conservative approach of evaluating K_{si} at sea level conditions and at a maximum mean temperature results in a value of 0.00933 for the above ratio.

On the basis of resistance values, the problem can be regarded as one-dimensional flow in parallel until the pressure shell is reached where the problem becomes two-dimensional. The question of potential has not been answered. The situation here is not as clear cut as in the case of the glide vehicle due to differences in capacitance values. Therefore, a study was initiated that used very fine physical subdivisions. The results of this study verified the conclusions reached on the basis of resistance values alone.

The following set of equations illustrate how the finite difference equations were written for the particular set of physical subdivisions illustrated on the sketch, page 18. Values associated with the insulation are identified with the subscript i, those associated with the spring use the subscript s, and the subscript ps with pressure shell.

Heat through the insulation:

$$\frac{2K_{i_1}A_i}{\Delta X_i}\left[T_S - T_{i_1}\right] = \frac{K_{i_2}A_i}{\Delta X_i}\left[T_{i_1} - T_{i_2}\right] + \frac{\rho A_i C_{pi} \Delta X_i}{\Delta T}\left[T'_{i_1} - T_{i_1}\right]$$

$$\frac{K_{i_2}A_i}{\Delta X_i}\left[T_{i_1} - T_{i_2}\right] = \frac{K_{i_3}A_i}{\Delta X_i}\left[T_{i_2} - T_{i_3}\right] + \frac{\rho A_i C_{pi} \Delta X_i}{\Delta T}\left[T'_{i_2} - T_{i_2}\right]$$

$$\frac{K_{i_3}A_i}{\Delta X_i}\left[T_{i_2} - T_{i_3}\right] = \frac{K_{i_4}A_i}{\Delta X_i}\left[T_{i_3} - T_{i_4}\right] + \frac{\rho A_i C_{pi} \Delta X_i}{\Delta T}\left[T'_{i_3} - T_{i_3}\right]$$

$$\frac{K_{i_4}A_i}{\Delta X_i}\left[T_{i_3} - T_{i_4}\right] = \frac{K_{i_5}A_i}{\Delta X_i}\left[T_{i_4} - T_{i_5}\right] + \frac{\rho A_i C_{pi} \Delta X_i}{\Delta T}\left[T'_{i_4} - T_{i_4}\right]$$

$$\frac{K_{i_5}A_i}{\Delta X_i}\left[T_{i_4} - T_{i_5}\right] = \frac{K_{i_6}A_i}{\Delta X_i}\left[T_{i_5} - T_{i_6}\right] + \frac{\rho A_i C_{pi} \Delta X_i}{\Delta T}\left[T'_{i_5} - T_{i_5}\right]$$

$$\frac{K_{i_6}A_i}{\Delta X_i}\left[T_{i_5} - T_{i_6}\right] = \frac{1}{\frac{\Delta X_i}{2K_{i_7}A_i} + \frac{\Delta X_{ps}}{2K_{ps}A_i}}\left[T_{i_6} - T_7\right] + \frac{\rho A_i C_{pi} \Delta X_i}{\Delta T}\left[T'_{i_6} - T_{i_6}\right]$$

Heat through the spring:

$$\frac{2K_{s_1}A_s}{\Delta X_s}\left[T_S - T_{s_1}\right] = \frac{K_{s_2}A_s}{\Delta X_s}\left[T_{s_1} - T_{s_2}\right] + \frac{\rho_s A_s C_{ps1} \Delta X_s}{\Delta T}\left[T'_{s_1} - T_{s_1}\right]$$

$$\frac{K_{s_2}A_s}{\Delta X_s}\left[T_{s_1} - T_{s_2}\right] = \frac{K_{s_3}A_s}{\Delta X_s}\left[T_{s_2} - T_{s_3}\right] + \frac{\rho_s A_s C_{ps2} \Delta X_s}{\Delta T}\left[T'_{s_2} - T_{s_2}\right]$$

$$\frac{K_{s_3}A_s}{\Delta X_s}\left[T_{s_2} - T_{s_3}\right] = \frac{K_{s_4}A_s}{\Delta X_s}\left[T_{s_3} - T_{s_4}\right] + \frac{\rho_s A_s C_{ps3} \Delta X_s}{\Delta T}\left[T'_{s_3} - T_{s_3}\right]$$

$$\frac{K_{s_4}A_s}{\Delta X_s}\left[T_{s_3} - T_{s_4}\right] = \frac{K_{s_5}A_s}{\Delta X_s}\left[T_{s_4} - T_{s_5}\right] + \frac{\rho_s A_s C_{ps4} \Delta X_s}{\Delta T}\left[T'_{s_4} - T_{s_4}\right]$$

$$\frac{K_{s_5}A_s}{\Delta X_s}\left[T_{s_4} - T_{s_5}\right] = \frac{K_{s_6}A_s}{\Delta X_s}\left[T_{s_5} - T_{s_6}\right] + \frac{\rho_s A_s C_{ps5} \Delta X_s}{\Delta T}\left[T'_{s_5} - T_{s_5}\right]$$

$$\frac{K_{s_6}A_s}{\Delta X_s}\left[T_{s_5} - T_{s_6}\right] = \frac{1}{\frac{\Delta X_s}{2K_{s_7}A_s} + \frac{\Delta X_{ps}}{2K_{ps}A_s}}\left[T_{s_6} - T_8\right] + \frac{\rho_s A_s C_{ps6} \Delta X_s}{\Delta T}\left[T'_{s_6} - T_{s_6}\right]$$

Heat balance on pressure shell:

$$\left[\frac{1}{\frac{\Delta X_{ps}}{2K_{ps}A_i}+\frac{\Delta X_i}{2K_{i7}A_i}}\right]\left[T_{i6}-T_7\right]=\left[\frac{1}{\frac{\Delta X_{ps}}{K_{ps}A_i}+\frac{1}{hA_i}}\right]\left[T_7-T_c\right]+\frac{K_{ps}A_{7-8}}{\Delta X_{7-8}}\left[T_7-T_8\right]$$

$$+\frac{\rho A_i \Delta X_{ps} C_{pps7}}{\Delta \tau}\left[T_7'-T_7\right]$$

$$\left[\frac{1}{\frac{\Delta X_s}{2K_{s7}A_s}+\frac{\Delta X_{ps}}{2K_pA_s}}\right]\left[T_{s6}-T_8\right]=\left[\frac{1}{\frac{\Delta X_{ps}}{2K_{ps}A_s}+\frac{1}{hA_s}}\right]\left[T_8-T_c\right]-\frac{K_{ps}A_{7-8}}{\Delta X_{7-8}}\left[T_7-T_8\right]$$

$$+\frac{\rho A_s \Delta X_{ps} C_{pps7}}{\Delta \tau}\left[T_8'-T_8\right]$$

Aft Side of Drag Vehicle

The following sketch shows a section through the aft portion of the drag vehicle. Preliminary calculations for optimum insulation thickness revealed that the heat transfer is by radiation and the minimum vehicle penalty occurs with no insulation. Symmetry indicates that one-half or any other fraction of the vehicle may be analyzed. Radiation between the skirt and the sphere will depend upon the shape factor which will vary from point to point on the sphere. The following equations for one-half the sphere divided into four nodes will illustrate the method.

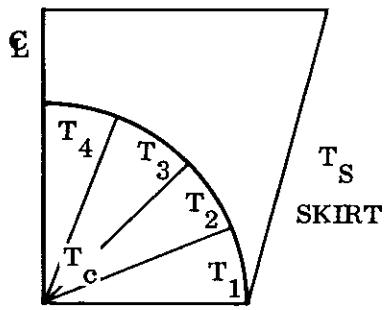

SECTION THROUGH AFT SIDE

$$A_1 \sigma \, FeFa \left[T_S^4 - T_1^4\right] = \frac{K_{ps1} A_{ps1-2}}{\Delta X_{1-2}} \left[T_1 - T_2\right] + hA_1 \left[T_1 - T_c\right] + \frac{\rho_{ps} A_1 tC_{pps1}}{\Delta \tau} \left[T_1' - T_1\right]$$

$$A_2 \sigma \, FeFa \left[T_S^4 - T_2^4\right] + \frac{K_{ps1} A_{ps1-2}}{\Delta X_{1-2}} \left[T_1 - T_2\right] = \frac{K_{ps2} A_{ps2-3}}{\Delta X_{2-3}} \left[T_2 - T_3\right] + hA_2 \left[T_2 - T_c\right] + \frac{\rho_{ps} A_2 tC_{pps2}}{\Delta \tau} \left[T_2' - T_2\right]$$

$$A_3 \sigma \, FeFa \left[T_S^4 - T_3^4\right] + \frac{K_{ps} A_{ps2-3}}{\Delta X_{2-3}} \left[T_2 - T_3\right] = \frac{K_{ps3} A_{ps3-4}}{\Delta X_{3-4}} \left[T_3 - T_4\right] + hA_3 \left[T_3 - T_c\right] + \frac{\rho_{ps} A_3 tC_{pps3}}{\Delta \tau} \left[T_3' - T_3\right]$$

$$A_4 \sigma \, FeFa \left[T_S^4 - T_4^4\right] + \frac{K_{ps} A_{ps3-4}}{\Delta X_{3-4}} \left[T_3 - T_4\right] = hA_4 \left[T_4 - T_c\right] + \frac{\rho_{ps} A_4 tC_{pps4}}{\Delta \tau} \left[T_4' - T_4\right]$$

In writing the equations for the drag vehicle, certain assumptions were made. The most important of these are:

1. The radius of the vehicle is sufficiently large so that curvature effects may be ignored.

2. The thermal conductivity of the insulation is given by Figure 14 as a function of insulation mean temperature and altitude.

3. The heat transfer path into and out of the spring is the end area where the spring is attached to the heat shield and the pressure shell. The flat faces of the spring will not come in contact with either the pressure shell or the heat shield because the heat shield expands and the spring is extended.

4. Heat is transferred into the cabin by a constant heat transfer coefficient as was the case for the glide vehicle and for the same reasons advanced in that case.

5. The cabin temperature is assumed constant for the same reasons advanced for the glide vehicle.

6. The variation in metal thermal conductivity and specific heat with temperature were assumed to be linear. The specific heat of the insulation was assumed constant.

7. The emissivity of the skirt and sphere were assumed constant.

8. The assumptions regarding contact resistances for this vehicle are the same as for the glide vehicle for the same reason as in the preceding section.

9. The temperature variation along the skirt is small and was neglected. The skirt temperature used in the calculation was taken from Figure 7.

10. The assumptions listed above are not the only ones possible, but were chosen as reasonable for vehicles of this class. As mentioned in the discussion for the drag vehicle, the variation of thermal conductivity with both mean temperature and altitude is the assumption that has the major effect on the economics of obtaining a solution. This will be discussed later.

Equations were written for the heat transfer paths divided into 2, 4, 6, and 10 nodes. The constants for the equations were computed and the equations supplied to specialists for programming for machine solution and to engineering aides for solution by hand calculation methods.

D. Calculation Methods

1. General

After deriving equations, obtaining material properties and computing constants, the engineer is faced with deciding what calculation procedure to employ. There are in general four choices open to him: a) high speed digital computers, b) direct analogue methods, c) differential analyzers, and d) hand calculation techniques. The equations derived for both vehicles were given to specialists in each of these fields for solution and the costs of obtaining answers recorded. The following discussion briefly outlines the machine capability as applicable to this type of problem and explains how the problems were programmed and scaled.

2. Digital Computers

The digital computer available for solving the equations derived for the two vehicles was an IBM 704. In general, there are two types of programs that may be used to formulate problems for a digital computer: 1) a program written specifically for the task at hand, 2) a program written in sufficiently general terms so that it is capable of solving a wide variety of problems by the inclusion or omission of terms. The latter course was chosen for this study. The program used was the Lockheed Thermal Analyzer Program which is available to the industry through Share. The Lockheed Program used is not entirely in its original form, some modifications having been made; however, the program is a typical general heat transfer program.

The program input is based on the analogy between heat transfer and the flow of current in a resistance-capacitance network. The program is written in electrical terms but, unlike direct analogues, no scaling is

necessary. This requires the physical heat transfer problem to be expressed as an equivalent resistance capacitance network.

Any elements in the network that vary with either time or temperature are identified. Examples are variation of thermal conductivity with altitude and mean temperature, radiation, and variation of specific heat with temperature. Every element in the network is given an identifying number and the input data compiled.

The input data is divided into 7 separate blocks:

1. The first block contains the identifying number and the initial value of the temperature for each node in the network.

2. The second block contains the value of each resistor in the network and identification of what nodes are connected by the resistor.

3. The third block contains the capacitor numbers and values.

4. The fourth block is the variables block. This block, along with the curves in block five, gives the programmer the ability to make the voltage, the resistor, or capacitor of any node any desired function of time or of the voltage at any other node or combinations of two nodes. Nodes with radiant heat transfer are included in this block of data.

5. Block five contains tables of the relationships between dependent and independent variables.

6. Block six lists printing instructions.

7. Block seven specifies at what time interval the variables listed in block six will be printed out.

The alternate method of writing a specific program for the two vehicles has some advantages and at least one disadvantage. The main advantage is, in general, tailor-made programs consume less machine time than do general programs. However, this advantage is usually lost in the time required to write the program. The time required to write a program specifically for the two vehicles was estimated and shown on the curves. This estimate is probably valid as an average time required for a competent programmer to write a program but any given program may require more time than the average. If a general program is available, it does not pay to write a specific program to gain the advantage of less machine time, unless a large number of conditions are to be evaluated.

3. Differential Analyzer

The differential analyzer available was a PACE (Precision Analogue Computing Equipment) manufactured by Electronic Associates, Inc. The PACE

is a modern, general-purpose differential analyzer with central console control and metering and removable patch boards. The facility used consists of four consoles, each of which contains 48 operational amplifiers which may be used for summing, and twenty of which may be used as integrators, four servo resolver units, five dual channel electronic multiplier units, six diode function generators, and eighty ten-turn helical potentiometers. The four consoles are interconnected by control and signal trunk lines so that they may be used individually or in any combination required by the particular problem. When more than one console is used, the problem is centered at one console and the others slaved to it.

The engineer preparing his problem for solution on a differential analyzer thinks a little differently than when preparing the problem for solution by digital or hand methods. The finite difference equation derived for digital and hand calculation methods will resemble the following equation:

$$\frac{T_i' - T_i}{\Delta \tau} = \frac{K}{\rho C_p \Delta X^2} \left[T_{i-1} - T_i \right] - \frac{K_1}{\rho C_p \Delta X^2} \left[T_i - T_{i+1} \right]$$

where the term $\frac{T_i' - T_i}{\Delta \tau}$ approximates $\frac{\partial T}{\partial \tau}$ or, in view of the assumption made in deriving the equations that all the heat absorbing capability is concentrated at the midpoint of the length, $\frac{T_i' - T_i}{\Delta \tau}$ more properly approximates $\frac{d T}{d \tau}$. The approximation is, of course, necessary when using digital or hand methods, neither of which is capable of integration. Since the differential analyzer can integrate, the above equation when written for solution by a differential analyzer becomes:

$$T_i = \int \left[\frac{K}{\rho C_p \Delta X^2} \left[T_{i-1} - T_i \right] - \frac{K}{\rho C_p \Delta X^2} \left[T_i - T_{i+1} \right] \right] d\tau$$

The conductivity of the insulation for both vehicles is a function of both altitude and insulation mean temperature. The conductivity function was indirectly simulated by assuming that the conductivity at a given altitude could be expressed by the sum of a product of a function of time and a function of temperature plus a function of temperature plus a constant. By manipulating the family of conductivity curves given on Figure 14 and the variation of altitude with time as given by Figures 1 and 2, a form was obtained expressing the conductivity for a given altitude as:

$$K = f(\tau)\, g(T) + y(T) + \text{Constant}$$

This relationship was obtained for the conductivity at 250,000 feet and above. In order to obtain the conductivity at any other altitude, it was assumed that a percentage of the 250,000 feet and above curve could be added to above relationship regardless of temperature. The validity of this assumption can be checked by reference to Figure 16 which plots both the thermal conductivity given and the conductivity calculated using the relationship and assumptions listed above.

Heat is transferred by radiation into the manned compartment on both the glide vehicle and the aft side of the drag vehicle. Temperatures raised to the fourth power were obtained using servo-multipliers. When solving the larger number of node cases, it was found that the temperature of the outer surface of the insulation differed from the skin temperature by less than ten degrees. In those cases, the skin temperature was applied directly on the outer surface of the insulation.

4. Direct Analogue

A facility designed for solution of problems by the direct analogue method is manufactured by Computer Engineers Associates. Unfortunately, the facility lacks the ability to simulate the variation of thermal conductivity with mean temperature and altitude. Therefore, the passive elements (decaded capacitors) of the passive element analogue were used with the active elements of the differential analyzer. Radiation and the variation of thermal conductivity with temperature and time were simulated in the same manner as described above.

The joining of the passive element analogue and the differential analyzer did not cause any difficulty when solving the glide vehicle problems but the partners were found to be somewhat incompatible when solving the drag vehicle problems. The problem arose in the following manner. In Appendix III it is shown that in scaling a problem for solution by analogue technique, one has some freedom in choosing the scale factors between the analogous quantities to match the equipment at hand. Servo potentiometers were used as part of the equipment simulating the thermal conductivity. The maximum electrical resistance available was 30,000 ohms. As Appendix III points out, the scale factors for resistance, capacitance and time are inter-related and the size of capacitors required is reduced either by increasing the resistance or reducing the time. In this case, the resistance cannot be increased because it is an integral part of the servo potentiometer and the time can be reduced only to the point where the readout instruments will follow without serious error. This gave capacitors in the order of 100-900 μf . In order to obtain capacitors of this size, it was necessary to use electrolytic type which have accuracies rated at $\pm$ 20%. The effect of this will be shown in a later section.

Heat transferred into the aft side of the drag vehicle was not obtained with the passive element analogue because the problem is largely one of radiant heat transfer. The majority of the equipment used are non-linear

elements and the set up essentially duplicates the corresponding setup for the differential analyzer.

5. Hand Calculations

The facilities used for the hand calculations have little bearing on the time required for solution, at least by comparison to the human element. A discussion of what various individuals accomplished follows in a later section.

6. Calculation Procedure

Appendix IV contains a brief summary of how the equations were translated into machine setups.

IV. ANALYTICAL METHODS COST COMPARISON

A. General

This chapter presents the cost versus accuracy comparison for the various methods of computing the heat flow into the compartments of both study vehicles. Before making the comparison, some index of accuracy is necessary. A discussion is included that defines a "true" answer and how it was obtained. Also included is a discussion of the ground rules and assumptions that were made in gathering and presenting the cost data.

B. True Answer

The exact determination of the heat flow into the two study vehicles is impossible. Appendix III discusses why mathematical answers of this study will always contain an element of the unknown, due solely to the errors associated with the computation technique. In addition, there will be errors from other sources such as the accuracy to which the physical properties are known, the degree to which they can be simulated, failure of the analytical technique to account for all of the heat flow paths, and other factors that are either completely unknown or inadvertently overlooked. Examples of the latter might be the change in emissivity of a surface due to corrosion or handling between the time it is assembled and the actual flight of the vehicle.

The following are types of "true" answers that might be defined:

1. The actual heat flow into the vehicle that will result when the vehicle follows its design trajectory. This number can never be completely known, although it can be very closely approximated with adequate flight test data.

2. The answer that would be obtained if it were possible to express precisely the physical situation in mathematical terms and to solve exactly the resulting partial differential equations with associated initial and boundary conditions.

3. The third type of "true" answer is that answer that is the best reasonably obtainable, making the assumption that the input data is absolutely correct. That is, skin temperatures, material properties, dimensions, etc., are all known with absolute precision. This is the "true" answer that will be used in this study to compare solution cost versus accuracy.

The "true" answers were obtained by plotting the resulting heat flow versus the number of physical subdivisions as in Figures 17 to 19. Figure 17 shows the total heat into the glide vehicle plotted against the number of physical subdivisions. The figure shows that as the number of nodes approaches 6, the heat load changes only very slightly with increasing the number of nodes. Appendix III states that the error in a finite difference approximation for a one-dimensional case with constant physical properties is given by:

$$E = \left.\frac{\partial^2 T}{\partial \tau^2}\right]_i^{n+\theta_3} \frac{\Delta \tau}{2!} - \propto \left(\left.\frac{\partial^4 T}{\partial X^4}\right]_{1+\theta_1}^{n} + \left.\frac{\partial^4 T}{\partial X^4}\right]_{1-\theta_2}^{n} \right) \frac{\Delta X^4}{4!}$$

For the following discussion, the assumption will be made that the above equation derived for one-dimensional heat flow with constant physical properties is at least approximately correct for the problems under consideration. The temperature gradients on the skin of the glide vehicle are small enough so that the flow can be considered one-dimensional. The heat flow of the forward side of the drag vehicle is in parallel, the insulation and the spring serving as essentially two parallel paths with no flow between them. The resistance to heat flow between the spring and the insulation is substantially greater than the path through the insulation directly into the vehicle. On the other hand, the physical properties are not constant and this effect on the error equation is not known. However, conclusions based on this equation should be at least quantitative.

Δx is equal to the insulation thickness in feet divided by the number of nodes. For example on the glide vehicle, the insulation thickness is 1.75 inches; $\Delta x = \frac{1.75}{(12)(n)}$ where n is the number of nodes. It can be seen from the foregoing that as n increases, $(\Delta x)^4$ decreases rapidly; hence this portion of the error decreases rapidly with increasing number of nodes.

The equation for E also states that the remainder of the truncation error is proportional to $\Delta \tau$. Once establishing that the heat flow changes only very slightly with increasing number of nodes above 6, it remains to show that the error due to $\Delta \tau$ is small. As is shown in Appendix III, $\Delta \tau$ and Δx cannot be chosen independently; rather, the maximum allowable $\Delta \tau$ is inversely proportional to n^2. Hence, as the number of nodes increases, $\Delta \tau$ must decrease as the square of n. To demonstrate that the influence of $\Delta \tau$ is negligible, the 10-node case was repeated with $\Delta \tau$ that were 1/2 and 1/4 of the maximum allowable. The differences in the heat flows, as calculated with various $\Delta \tau$, were essentially zero.

Before accepting the 10-node case as calculated by the digital machine as being the best practical answer, the discrepancy between the answers as obtained by the different calculation methods must be explained. These discrepancies arise in the following way: Both the passive element analogue and the differential analyzer use non-linear elements to obtain the insulation thermal conductivity as a function of mean temperature and altitude, and the simulation is not perfect. For example, Figure 16 shows the assumed variation of thermal conductivity with mean temperature and altitude. The variation used by the differential analyzer is also shown. The simulation is good, but not perfect. In general, the thermal conductivity simulated is lower than the actual. This will result in a slightly lower heat flow as shown on Figure 17. The case for the passive element analogue is similar.

The digital machine time consumed in obtaining these answers may be found in Table I. The time for the 10-node case is 3.2 hours. The machine time for a 12-node case is estimated to be 4.9 hours. It is difficult to state what the practical maximum machine time is for a given problem; it depends upon the value of the answer but, from the rate of change of the heat flow per square foot with number of nodes, very little change could be expected for the additional 1.7 hours of machine time.

The foregoing removes the last objection to using the 10-node case as the best practical answer. This answer will be used as the "true" answer and errors will be computed on this basis. To compare cost versus accuracy for one calculation method, the actual value of the "true" answer is not important since it forms the basis for comparison. However, to compare methods, the "true" answer should be as exact as possible since the accuracies are to be compared as well as the costs.

C. Ground Rules for Cost and Accuracy Comparisons

Before discussing the cost versus accuracy results, the ground rules under which the data were gathered will be discussed.

1. Analytical Methods Data Presentation

During the course of this study, it became apparent that basic ground rules must be established for gathering and presenting cost data as a function of solution accuracy. The cost data that are gathered as the result of our experience may not be exactly representative of what someone else may expect or even what we might expect if the problem were to be repeated. The time to solve any given problem is dependent upon many factors, a number of which are extraneous to the merits of the particular solution method. Examples of these extraneous factors are: the priority for men and machine time, the errors that people make, and the ability of the people assigned to the problem. The following discussion will point out why the raw data has been adjusted and how this will make the results more meaningful.

The first basic assumption is that the problems were solved by high caliber, experienced people who made no major errors and experienced no machine failures. The costs have been adjusted where necessary to reflect this point of view.

a. Problem Priority

The assumption of a high priority problem was made because the problem flow time between the engineer and the various other people involved in the solution is a function of a given company's internal organization and varies considerably. This flow time varies not only from company to company, but within a given company depending upon the work load.

Since there is no assurance that the actual flow time required for these problems is representative of either our own organization flow time or some other organization's flow time, the actual time was adjusted to represent how long it would take if all equipment and personnel were available when needed.

An example will illustrate why this adjustment is necessary. Figure 28 is a plot of solution % error versus calendar time required for the various calculation methods for the forward side of the drag vehicle. The hand calculations were performed by experienced aides assigned to this problem. As soon as the engineer wrote the finite difference equations, there was an engineering aide available to start working on the hand calculations. However, this was not the situation in the case of the digital solution. A programmer was not immediately available. When the programmer finished programming the equations, there was a time lag while cards were punched and an additional waiting period for machine time. During this period of time, another group had a high priority task which preempted the card punching and computing facilities. If the actual time were reported without adjustment, the difference between hand and digital methods would be smaller than that shown and would not be representative.

b. Human Error

Unfortunately, people do not make mistakes in a predictable manner. The errors made by any given individual are randomly distributed and in general may be divided into two classes, major and minor. For the purpose of this discussion, a major error will be defined as any error causing the waste of one day or more and a minor error as any error causing the waste of less than a day. A competent and experienced person is by definition one who knows and understands his subject thoroughly and makes few major errors. The people working on all phases of these problems made mistakes both major and minor. On some phases of this program, people made no mistakes; other phases contained several errors. Since it is impossible to state with any assurance that the number of mistakes made on any particular phase is representative, the time wasted due to major mistakes will not be shown.

The following example will illustrate how these errors may occur and why adjustment is necessary. One phase of this problem was under the direction of an experienced electrical engineer with substantially more than average ability. During the course of his investigation, the engineer read degrees Fahrenheit for degrees Rankine on a curve of thermal conductivity versus mean temperature and set up his analogue computer accordingly. The setup and solution time took approximately three days, which of course was wasted. The engineer redid the problem correctly in about the same length of time that it took to do it incorrectly. If the total time to do the problem is reported as the sum of the time it took to do it

correctly, plus the time it took to do it incorrectly, a fallacious impression is created. It is improbable that another engineer with the same experience and ability would make a similar mistake causing the same time waste. That particular mistake should be averaged over a large number of problems and the number of problems this engineer did on this study does not give a statistically valid sample.

c. Machine Failures

Exactly the same reasoning applied to human errors can be applied to machine failures. Machine failure will follow a random distribution and the number of problems that were done in connection with this study is not large enough to be statistically valid. For example, during this investigation a change was made in the digital readout instructions. During the following three days, the digital machine failed to correctly print out the results of this study's problems. This has been the only incident of this type with the digital machine. It is obviously wrong to charge the digital method for that particular problem with the time lost due to that machine failure. The adjustments in the raw data discussed above are necessary to prevent misleading conclusions, but the adjusted results can lead to misunderstandings unless the reader keeps in mind that the curves represent a situation that is approximately normal. Any given similar problem may take much more time due to major human error, machine failure, or machines and personnel not being available when required.

d. Experience Level

Considerable difference exists between the time required for experienced and inexperienced engineering aides to perform the hand calculations. Most of this is in setting up the data sheets. The hand calculations, except for the simplest case, require very large amounts of time because the step by step nature of a hand calculation procedure precludes more than one individual working on a given problem at one time.

The finite difference equations were given to two engineering aides with varying experience and ability. The experienced aide was an engineering aide with more than average ability. The other data sheet was prepared by an engineering aide whose experience has not included heat transfer calculations of this type, hence can be considered inexperienced. The difference in solution time was almost entirely in the time to set up the data sheets. Another difference arises from the manner in which the sheets are set up. Many short cuts are learned through experience. For this reason, an inexperienced person will never quite equal the output of an experienced person at the peak level.

In the initial stages of the problem, a wide gap exists between the two outputs. However, these calculations are routine and repetitious and boredom soon reduces the experienced aide's output. At the same time, after two or three days of this type of calculation, there are no inexperienced operators. Were it not for the initial setup, they would equal out - both succumbing to boredom with resulting loss of production. The curve below was obtained by actual test cases.

A previously set up data sheet was given to two people to calculate, an experienced engineering aide and a typist who has had little, if any experience using desk calculators. The curve shows that the number of operations the experienced aide performed per unit time decreased with time while the typist first improved, then her performance deteriorated as she became bored with the routine operations.

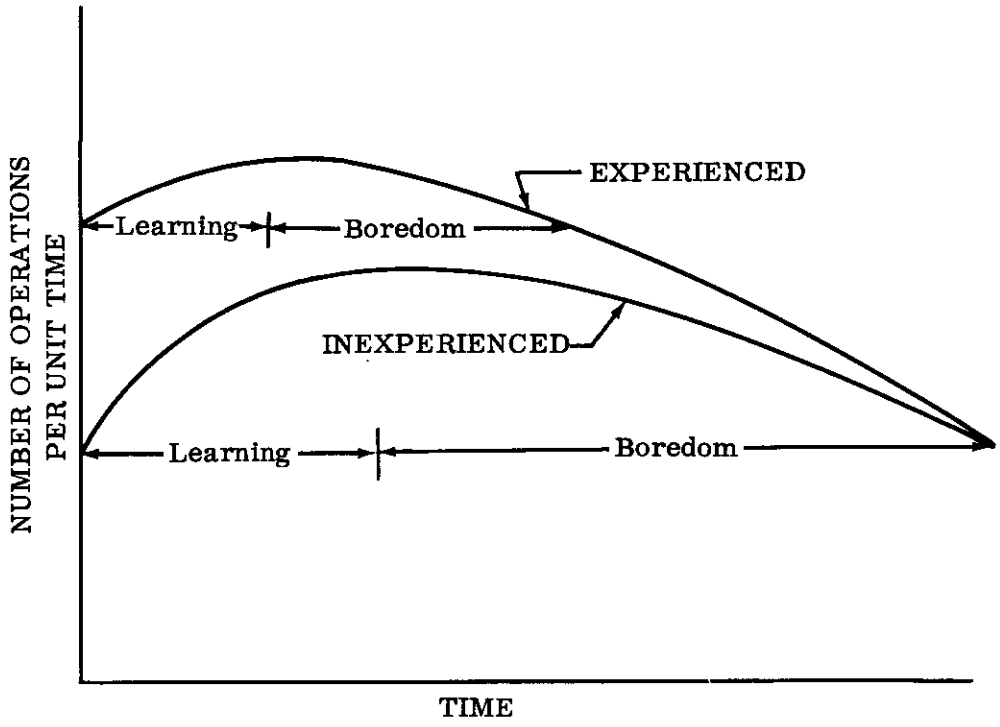

e. Number of Sections Analyzed

The number of sections analyzed for each vehicle to obtain the total heat transferred into the vehicle requires discussion. This item has no bearing on comparisons of manhours, dollar cost or calendar time when comparing one calculation method to another since the same number of sections were used for each. However, to compare the costs of analytical methods to experimental methods

the number of sections analyzed has a direct bearing on the costs; the costs in general, being linearly proportional to the number of sections analyzed.

Seven different areas were analyzed to obtain the total heat into the cabin of the glide vehicle. These areas were, upper surface, two lower surfaces, forward bulkhead, aft bulkhead upper side and lower side. Only one temperature was taken at each of these areas, except on the bottom. The gradient in the fore and aft direction is shallow in the cabin area.

The thickness of the heat shield on the drag vehicle was varied from 0.80 inch thick at the stagnation point to 0.25 inch thick at the sides. The thickness was varied so that the maximum temperature attained was the same at each point. Therefore, it was necessary to analyze only one section of the forward side of this vehicle to have a heat transfer situation that was representative of the whole. The entire aft section of this vehicle was analyzed. Since the aft position of this vehicle was not insulated, the section was broken up into nodes to account for the shape factor variation around the vehicle and the metal induction around the vehicle.

D. Cost Comparisons

This section presents the results of tabulating the costs of various methods of calculation versus the accuracy of the method. Figure 20 to 24 are curves for the glide vehicle and Figures 25 to 30 are for the drag vehicle.

For this study, percent error in the total heat transferred into the compartment was defined as one-hundred times the difference between the heat flow as calculated and the "true" answer, divided by the "true" answer.

A side point of interest is the sign of the error. The sign of the error is negative for both glide and drag vehicle which means that there is more heat transferred in the "true" answer than in the less accurate cases. This is contrary to what one might think. Consider the case of a plane wall of a homogeneous material, constant physical properties, and exposed to a step change in temperature on one face. The sketch below shows how, as the number of nodes increases, the temperature of a point as calculated by the finite difference approximation approaches the exact answer.

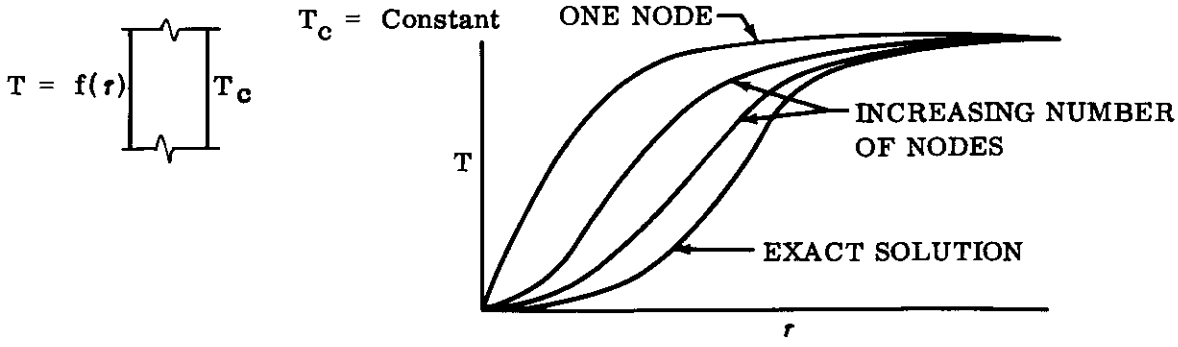

The area under this curve is proportional to the heat transferred and is highest for the one node approximation and becomes progressively smaller as the number of nodes increases and approaches the exact answer as a limit.

The cases studied behave differently, that is, as the number of nodes increases the heat transferred increases. The explanation for this behavior lies in the variation of the thermal conductivity with mean temperature. Considering a small number of nodes case, there is a large temperature difference between nodes and as the number of nodes increases the temperature difference between adjacent nodes decreases. The thermal conductivity for the conductance value between any two adjacent nodes is determined by the mean temperature. In the small number of nodes case the mean temperature is low giving a low thermal conductivity. As the number of nodes increases, the mean temperature between adjacent nodes increases giving higher thermal conductivities. Incidentally, using higher thermal conductivities between adjacent nodes increases their temperature and in turn increases the thermal conductivity between them and "snowballs" the effect.

1. Comparison of Solution Accuracy for Glide Vehicle

Figure 20 plots the solution error versus the manhour cost of obtaining the solution for the glide vehicle.

The desired solution accuracy does not greatly influence the manhours required for the digital computer, the passive element analogue, or the differential analyzer whereas the time required for a solution by hand methods is very dependent upon desired solution accuracy. The manhours to obtain a digital solution is only slightly influenced by accuracy because the more accurate cases differ from the less accurate cases only in the time required to compute the input, keypunch the cards, and write the machine instructions. These times are small by comparison to the other times required, such as learning. The same reasoning is applicable to the differential analyzer and passive element analogue. The difference between the more accurate and less accurate cases is the time required to compute input and wire the circuits. There is, however, an element missing in these data and that is the influence of the number of opportunities for error. The possibility of an error increases with the number of physical subdivisions. In the case of the digital computer, this means listing more input on the key-puncher's instruction sheet, computing more constants, and punching more cards. In the case of the analogue and differential analyzer, more nodes mean more wiring problems and more constants to compute. For the hand calculations, smaller physical subdivisions again mean more constants to compute, larger data sheets to be set up to accommodate the large number of equations and more times the equations must be solved, giving more opportunity for human error.

The simple cases involving the smallest number of nodes were solved first and the same individuals repeated the problems for the larger number of node cases. This procedure gave them a certain advantage in solving the problems in that the simple cases made the people familiar with the

problems. As a consequence, it is highly probable the people made fewer mistakes in the larger number of node cases by this procedure than they would have had the larger number of nodes case been the only one they solved.

However, the hand calculations present a different picture. The accuracy obtained is dependent upon the number of physical subdivisions and, as was discussed in the preceding work on errors, the maximum allowable time step is inversely proportional to the square of the number of physical subdivisions. This means that the total time to solve a problem by hand, using finite differences, is proportional to the cube of the number of physical subdivisions. Therefore, the time required for hand solutions increases sharply with increasing accuracy, soon becoming prohibitive for this particular problem at least. The times shown in Table I are estimated, using experienced gained from the simpler cases.

The accuracy obtainable by the various machine methods is roughly comparable and the best accuracy is obtainable with the IBM. As was noted in the preceding discussion, the accuracy of the analogues depends, in part, upon the simulation of the thermal conductivity with mean temperature and time. In this particular case, the simulation was fairly good. In general, the IBM is more flexible in the types of variation than can be simulated.

Digital computers show the least manhours for a given accuracy. The machine program used was the Lockheed Thermal Analyzer and the man assigned was familiar with the use of this program. If it had been necessary to write a specific program, or the engineer assigned had to familiarize himself with the Lockheed Program, more time would have been required. Again note that the time required is only slightly influenced by accuracy. The above statement is only partially true in that the curve shown was estimated for the case where the programmer made a few errors. As was pointed out earlier, the more accurate the solution, the more opportunities for error; thus, on the average, the more accurate solutions will require more time.

The dollar cost for the solutions is shown on Figure 21. The cost figures that were used as a basis for obtaining dollar cost are representative of an aircraft industry average. $3.90 per hour is representative of the average direct labor charge for the lesser experienced people and $4.50 per hour for the more experienced people. The overhead charge is $4.50 per hour. $350 and $150 per hour was used as the cost of the IBM facility, $42.50 per console hour for the analogue computer. Two curves of a digital computer are shown, $350 representing the approximate cost of "outside" machine time and $150 as a lower limit of "in house" machine time. The IBM machine has the least dollar cost when using the Share Program. Note the dollar cost for the IBM calculation increases rather sharply as the accuracy improves. This is due to the increase in machine time required when calculating for the large number of node cases, because, as discussed earlier, the number of repeat calculations increases as the cube of the number of physical subdivisions. This is not the case

however for either the differential analyzer or the passive element analogue since they both integrate the time and the actual problem solution time is a relatively small percent of the total time spent on the machine. The majority of the machine time is consumed in setting up the problem and checking out the circuits. As might be expected from the manhour curve, there is little difference in cost between a differential analyzer and a passive element analogue.

Figure 22 shows the calendar time required versus solution accuracy. Note that manhours cannot be directly translated into calendar time because there are delays of various types. Some examples would include: keypunching for IBM machines, manpower scheduling problems, machine scheduling, etc. Again, the IBM solution utilizing the Share Program requires the least time, with the differential analyzer and the analogue following in that order. The hand calculations, except for the simplest case, require very large amounts of time.

Figure 23 shows how the cost in dollars increases with the number of times a problem is repeated. The curve for hand calculations shows that two solutions cost essentially twice as much as one solution. There is no reason for the cost for hand calculation to diminish except for the experience level of the people doing the work and it has been stated that experience gained as the problem progresses means nothing for practical purposes. Another point to be noted is the small slope of the curves for the passive element analogue and the differential analyzer. This comes about because the cost of obtaining an additional solution is a very small amount of time to change potentiometer's setting and the time required to run the problem again. On the other hand, the slope of the cost curves for the digital solution is steeper than the curve for either the passive element analogue or the differential analyzer because of the difference in cost for digital machine time. The curves show that if a number of parameter runs are desired it is cheaper in dollar cost to use the differential analyzer or a passive analogue solution.

It should be noted that the errors in these solutions are not equal. The curves were plotted for the same physical subdivisions. The error for the digital solution is close to zero, the error in the differential analyzer is approximately 2% and the error in the passive element solution is approximately 9%.

Figure 24 plots the manhour cost versus the number of parameter runs made. The manhours for a hand solution, like the dollar cost, increase directly as the number of parameter runs made while the manhours for passive element analogue, differential analyzer and digital solutions increase slowly with number of parameter runs. For a digital solution, the increased time is the time to compute inputs, punch cards and reduce the data. For passive element analogue and differential analyzer, the additional manhours represent the time to compute inputs, make changes on the machine, run the machine and reduce the data. These times are relatively small by comparison to the total. These curves state that if

manhours is the criterion, the digital solution is the most attractive. Assuming that machine time is available, the curve for calendar time required for additional parameter runs is identical in appearance to Figure 24, meaning that if calendar time is the criterion, the digital computer is again the most desirable.

2. Comparison of Solution Accuracy for Drag Vehicle

Figures 25 to 30 are curves showing the relationships between cost and solution error for calculating the heat flow into the drag vehicle. Many of the comments and conclusions applicable to the curves for this vehicle are identical to those made on the curves for the glide vehicle. This section will discuss the points where the curves differ and why they differ.

The first major point of difference is that it was impractical to obtain accurate heat flows into the vehicle by using a passive element analogue due to problems with capacitor size and problems simulating the radiation on the aft side. It was stated in the section on calculation methods that due to the size of the capacitors involved, it was necessary to use electrolic capacitors on the analogue of the forward side. Electrolic capacitors have a stated accuracy of $\pm$ 20%. Figure 28 compares the results obtained for the forward side with results for the other methods and shows the large errors that resulted.

Figure 25 plots solution error versus manhours required. The curves are similar to the corresponding curves for the glide vehicle with the exception of the curve for a hand solution. The curve shows that if one is willing to accept larger errors, a hand solution requires less manhours. This situation comes about because of two factors. First, in the lesser accuracy cases, the stability criteria allow the use of reasonably large $\Delta\tau$ and second, the total flight time of this vehicle is in the order of 200 seconds. Hand calculation manhours are directly proportional to vehicle flight time. If the flight time had been half again as large, the manhours would exceed that for solution by digital means.

Figure 26 plots solution error versus calendar time. Again, the curves are similar to the corresponding curves for the glide vehicle with the exception of the curve for hand calculation. The same remarks made for manhours apply here; calendar time is less due to the favorable stability criteria and the chart flight time.

The total dollar cost as a function of solution error may be found on Figure 27. Here again the cost of hand calculation is less than for the other methods for the reasons previously stated. There is an additional point of difference between this figure and the corresponding curve for the glide vehicle and that is the cost for the digital solution. (On this vehicle, the dollar cost is only slightly influenced by error and the curve for the two different costs of machine time are superimposed.) Total machine time used for these calculations is small by comparison to machine time used for the glide vehicle due to the short flight time.

The dollar cost for repeating the problem a number of times may be found on Figure 29. This curve, like the corresponding curve for the glide vehicle, is based on the 8 node solution. For the glide vehicle, if the problem were to be repeated more than four times and digital machine time cost $350.00 per hour (or seven times if digital machine time costs $150 per hour), it is cheaper to solve the problem on a differential analyzer. The corresponding number of solutions for the drag vehicle are 23 and 47. Again, this is due to the vehicle's short flight time, making the machine costs a smaller percentage of the total.

Manhour costs versus the number of repeat solutions may be found on Figure 30. As was the case for the glide vehicle, the slopes of the curves are small, illustrating that the majority of the time is spent in preparing for one solution rather than in the actual solution.

3. Summary

There are advantages and disadvantages to all of the calculation methods used. No one method is a panacea for heat transfer calculations.

It has been shown that the study problems can be considered one-dimensional and the conclusions reached are based on a one-dimensional study. If it had been necessary to use a two or three-dimensional approach, in general, the problem size would preclude the use of differential analyzers, passive element analogues or hand calculations.

One advantage of using either a differential analyzer or passive element analogue that is difficult to numerically evaluate, is the "feel" for his problem that an engineer gets while using these machines. For example, if a parameter study is being conducted on either a differential analyzer or passive element analogue, changes to the problem are made by changing potentiometer settings, changing capacitors, removing or adding additional circuits, etc. Each change has some physical significance and the person conducting the problem mentally equates what he is doing electrically to what he is doing to the heat transfer problem. Most people will develop more understanding of their problems by this method than they will by making changes in instructions to keypunch operators for a digital machine.

Analogues and differential analyzers have another advantage in that the results of parameter variations are immediately available on the recording instrument. This can enable the engineer running the problem to monitor the critical element in his setup, temperature, heat transfer, etc. He therefore can eliminate some runs or add additional runs without delay.

Solutions were obtained for both vehicles using a passive element analogue that did not employ non-linear elements to simulate the variation in the thermal properties with time and temperature. This reduces the machine setup time a great deal. If an insulation mean thermal conductivity is obtained by the following successive approximation technique,

answers within about 20% of the true answer can be cheaply obtained. For example, a solution to the forward side of the drag vehicle costs less than $300.

Mean values for the conductivity were obtained from Figure 14. A mean altitude was assumed, and a guess of the mean temperature of each node was made. Using these values, the problem was solved. Using the time-temperature history obtained and the vehicle trajectory, a new mean thermal conductivity was obtained. This process was repeated until there was no change in the time-temperature history. This technique proved to be valuable in that not only did it give the engineer the "feel" for his problem as discussed above, but provided answers that are at least approximate, thus serving as a valuable check on the other problems during their initial phases. For example, when the first answers were obtained for the drag vehicle forward side using the passive element analogue, they were found to differ widely from the answers obtained by the simple solution. A little investigation uncovered a large scaling error. Without the simple solution available as a check, the problem runs might have been completed before the error was discovered.

Digital computers have an advantage over other computation methods in the types of variation of thermal properties with either temperature or time that they are capable of simulating. The non-linear elements of a differential analyzer can be used for these simulations; however, the range of simulation is limited not only by the function but by the amount of equipment available for the task. This ability, along with other factors, makes the digital machine the most accurate of all methods studied.

Digital computers also have an advantage in the size of problem they are capable of simulating. For example, the two dimensional problem on the forward side of the drag vehicle used essentially all of the elements of two consoles of differential analyzer equipment. This is one half of the total differential analyzer equipment available, whereas this problem required very little of the total digital capacity available.

There is no one best calculation method for making parameter runs. The possible combinations of manhours, calendar time, vehicle flight time, solution error, number of runs, etc., are endless. However, some general conclusions can be drawn. Hand calculations are not suited to parameter studies. Digital machines have a limited place in parameter studies. They are more adaptable to short flight problems like the drag vehicle of this study, to situations where the best possible accuracy is required and where calendar time is the most important criterion or only a few runs are desired. Using a digital machine for parameter runs on long flight time vehicles will very likely monopolize the available digital machine capacity.

Passive element analogues and differential analyzers are best suited to situations calling for large numbers of parameter runs and where manhours and calendar time are not the primary consideration. Network analyzers can provide the engineer with a feel for the problem at very nominal cost.

V. EXPERIMENTAL METHODS COST COMPARISON

A. General

The previous chapters have described several analytical methods which can be used to calculate the quantity of heat entering a re-entry vehicle. The next two chapters will examine experimental methods to determine if a test method or methods can compete in accuracy, dollar cost, manhours, or calendar time with the mathematical calculation of heat transfer.

Ordinarily, testing is done after the vehicle and environmental control systems have been designed and built. These tests are actually "proof tests" to show if the system has satisfied the design requirements. The type of testing considered here, however, is to obtain information needed to design the system, and therefore is conducted in the design stage of the program. Since the test objectives and timing are different for "design testing" than for "proof testing", this distinction must be kept in mind when considering the experimental approach. The conclusions of this study are not necessarily valid for "proof testing".

Two basic testing concepts are considered:

1. Experimental determination of the heat transfer by simulating the vehicle skin temperature versus time on a specimen.

2. Experimental determination of the thermal properties of the materials of the vehicles.

Occasionally material properties are not available in the literature and must be experimentally determined before the analytical methods can be used to calculate the heat flow.

The first testing concept is presented in this chapter, and material thermal property testing is discussed in Chapter VI.

The tungsten filament-quartz tube radiant heater has been selected as the best available method for simulation of the required surface temperatures. Because of the importance of the transient heat flow for the design, the testing method must be capable of simulating not only the maximum required temperature but also the variation of surface temperature with time. Appendix V shows which facilities could be used to test the vehicles of this report. From this survey, the radiant heater was selected as the test method to use for the methods study. Cost and accuracy will be presented for testing of panels, reduced and full size specimens, both with and without simulation of the altitude profile.

B. Ground Rules for the Cost and Accuracy Comparisons

1. Testing Cost

a. Test Facilities Cost

The cost of the facility required to test these various specimens will not be included as a cost (similarly the cost of the calculating machine is not included in the analytical solutions). However, the cost of the required facilities has been estimated to provide an indication of the capital value of the required test equipment, and are shown on Figure 31. These costs include the equipment and installation cost, assuming that the installation site and utilities are provided. The cost shown does not include the building to house the facilities. The cost estimate is for a "minimum" facility with only the capability to test the specimen identified. An actual facility very likely would include additional capabilities (such as provisions for structural, human engineering, or equipment testing) which would increase the total cost. Approximate lead time which would be required to design, procure, and install the facility is shown on Figure 32.

Existing radiant heat facilities can be leased from several organizations. Reference 3 includes organizations who have indicated an interest in performing subcontract heat testing. An Air Force facility located in Inglewood, California, with operational responsibility assigned to the West Coast Laboratory of Thompson Ramo Wooldridge Incorporated, is available for testing on a contract basis. Details of this facility are shown in Appendix V.

b. Testing Cost for Radiant Heat Testing

The cost of testing, as estimated for the comparisons of this report, include the following items:

(1) Specimen fabrication - This includes engineering time to prepare drawings of the specimen and the actual fabrication cost of labor and materials. The specimen drawings have been assumed to be simplified drawings for experimental manufacturing.

(2) Testing cost - This includes the engineering cost to design the heater array, and shop labor to construct the test set-up and to install the thermocouples on the specimen. The cost of the heaters and reflectors is considered as a facility cost. Data reduction is based on manual reduction of test data and subsequent calculation of the experimental heat transfer. A cost is included for post test disassembly.

The manhour cost of $8.35 per hour for shop labor, $9.35 per hour for engineering time, and $8.75 per hour for drafting and engineering aides was used for the dollar cost estimate. These rates include overhead in each case.

The calendar time estimates are based on two eight-hour shifts, five days a week.

2. Testing Inaccuracies

Error, as used in this report, has been previously defined as the deviation from the true value. For the experimental section, it is more specifically the difference between the measured value and the true value. The true value may be either a condition to be simulated for the test or the true value corresponding to a measured value. If the true value corresponds to a measured value, and is unknown, the error cannot be expressed. For example, if a surface temperature of 2000°F is to be simulated and the temperature determined from the test is 1900°F, the error is 100°F. However, if from the same test, the heat transfer was measured as 900 BTU, the error cannot be defined since the true value for the heat transfer is unknown.

Inaccuracy is different from error and will be used to denote the difference which can occur in a measured value. Using the above example, if the measured value of 1900°F surface temperature was estimated to be within 1950°F to 1850°F, then the inaccuracy would be +50°F to -50°F. Similarly, if the heat transfer was estimated to be between 1000 BTU to 800 BTU, the inaccuracy would be +100 BTU to -100 BTU.

Because the study did not include any actual radiant heat testing, experimental inaccuracies were estimated for each test condition. These individual inaccuracies were analytically combined on the differential analyzer to determine the total effect on the heat transfer. Since the actual amount of heat transfer is unknown, these differences are inaccuracies, not errors. To interpret the differences as errors would be assuming the heat transfer calculated by the differential analyzer is the true heat transfer. The analytical methods defined a "true" mathematical answer and compared errors for the various methods on this basis. Since neither the analytical errors nor experimental inaccuracies are based on the actual heat transfer, they cannot be directly compared.

The range of inaccuracy which is shown for each experimental method is, therefore, the total inaccuracy in the heat transfer resulting from various individual testing inaccuracies.

C. Testing Cost for Glide and Drag Vehicles

The detailed manhour, dollar cost, and calendar time estimates are shown on Tables III through X.

1. Specimen Fabrication Costs

The estimates of manhours, dollar cost, and calendar time for fabricating each of the specimens are shown on Table III. The cost and time for these specimens are very dependent on the structure of each vehicle, the priority of the project, and the capabilities of the manufacturer. Since the specimens are fabricated during the design phase of the vehicle, and some of the structure advances the state-of-the-art, useful by-products (structural and manufacturing research) will be obtained. Therefore, some of the cost shown in this table possibly could be charged to manufacturing and structural research.

Table III also includes estimates for building a second specimen. The cost of the second item is much less because the tooling cost has been absorbed by the first specimen. If another test program required a specimen similar to the heat test specimen, the average cost of both specimens would be less. For example (from Table III), the cost of the second full size specimen of the glide vehicle is less than that of the first half size. Several other methods should be considered to reduce specimen cost. In some cases a specimen built for other test programs may be modified and used if timing permits. These factors may all be important considerations in selecting the test method to be used.

The estimates for the full and reduced size glide vehicle do not include the nose cone or leading edges. These items were not included because of their high cost. The calculated temperatures on the attaching structure would be simulated to obtain the heat flow path of these components. The drag vehicle specimens likewise do not include the beryllium heat shield. A thin skin would replace the beryllium for the test. This thin skin is used both because of the high cost of the beryllium and the health hazard of fabricating and heating beryllium. Special control procedures would be required during the testing to prevent exposure of personnel to beryllium vapor. The calculated temperature on the inner face of the shield is then simulated on the thin skin for the test.

The weight which was used in estimating the fabrication cost of each specimen is also shown on Table III.

2. Cost for Testing in the Radiant Heat Facility

The itemized testing cost for the actual testing in the radiant heat facility is shown on Tables IV through IX for both sea level and altitude simulated testing. The cost for retesting is also shown for each specimen. The retest estimates include a cost for removing and reinstalling a different thickness insulation on the specimen prior to the next test.

The number of thermocouples and heat zones assumed for each specimen are also shown on these tables.

a. Manhour Cost

Table IV shows the manhour cost for sea level testing and Table V is for the altitude simulated test. These charts show the detailed engineering, shop, drafting, and engineering aide manhours for each specific operation related to performing the test. The retest does not require any "test plan" charges, and the "test setup" is less since the heater array is the same as was used for the first test. "Data reduction" hours are the same for both tests.

b. Dollar Cost

Table VI shows the dollar cost for sea level testing and Table VII is for the altitude simulated test. These charts are similar to the manhour charts except "material cost" is included for the "test setup." Thermocouples, anticipated lamp replacement, and the materials for the lamp array are included in this cost.

c. Calendar Time

The calendar time is shown on Table VIII for sea level testing and on Table IX for altitude testing. Calendar time is shown for the "test plan"; however, this would easily be absorbed by the specimen fabrication calendar time shown on Table III. The calendar time to change the insulation thickness is included in the "test setup" time for the second test.

3. Total Cost for Experimental Test Methods

Table X shows the total testing cost which includes both specimen fabrication and the testing cost for the radiant heat facility. The totals shown on this table assume three tests will be made on each specimen to allow selection of the optimum insulation thickness. These totals represent the summary of the itemized costs shown on Tables III through IX.

As shown on this table, the testing cost varies from $18,000 for testing a small panel at sea level, to nearly $3,000,000 for testing a full size glide vehicle specimen with altitude simulation.

Comparing this cost with the analytical cost shown on Figures 20 through 22 for the glide vehicle and Figures 25 through 27 for the drag vehicle, shows that even the least expensive test method is several times as expensive as the analytical methods (except hand calculations). The experimental methods also require more manhours and calendar time than the analytical solutions.

D. Testing Inaccuracies for Glide and Drag Vehicles

The inaccuracies and other experimental assumptions are discussed for each of the specimens in Appendix VI.

E. Cost and Accuracy Comparison

1. Glide Vehicle

The comparison of accuracy and cost is shown on Figures 33, 34 and 35 for each test method considered. The positive range of inaccuracy indicates more heat transfer into the vehicle than without the inaccuracies, and the negative range indicates less.

a. Manhour Cost

The total manhour cost versus range of inaccuracy is shown on Figure 33. From this figure it can be seen that testing of panels is the least expensive test, followed by crew compartment test, half size vehicle test, and full size vehicle test.

Comparing the range of inaccuracy for sea level testing and altitude testing shows that for a moderate increase in manhours, an altitude simulated test gives greatly increased accuracies. Comparing different specimens shows, for instance, that the accuracy for an altitude test on a panel is greater than the much more expensive sea level test on a half or full size vehicle. Since a large percentage of the total cost is for building the specimen, the difference in manhours of the sea level and altitude test is not as great as one might think.

The inaccuracy range shown for testing a single panel assumes the test heat transfer occurs on the entire surface area of the vehicle. Since the temperature profile selected for the single test would necessarily be hotter than that of some areas of the vehicle, the resulting total heat transfer is relatively inaccurate. If two temperature profiles are tested, the resulting accuracy is much greater. The cost of testing the second panel is still more expensive than the analytical solution and for panel testing the analytical and experimental methods should supplement each other. Thus, the parameter runs for each of the temperature profiles could be done analytically.

The crew compartment testing deserves special consideration. The accuracy range for this test specimen is very similar to the half and full size complete vehicles; however, the testing cost is much less. This specimen would also be invaluable for such items as developing the water wall, cabin leakage, and internal film coefficients in addition to the heat test. Some of the specimen fabrication costs could undoubtedly be charged to these items. The main increases in accuracy of half or full size vehicle result from simulation of the radiation shape factors between the vehicle skin and the crew compartment, and the simulation of the forward and aft bulkhead temperatures.

b. Dollar Cost

The dollar cost is shown on Figure 34. The difference between the manhour cost and the dollar cost is in the cost of the materials used. This cost does not change the results for accuracy versus dollar cost from what has been discussed for the manhour cost versus accuracy.

c. Calendar Time

The calendar time for each test is shown on Figure 35. Since this is a design test, the information from the test is required to size the environmental control system. This timing will, in some cases, preclude the use of some test methods.

One significant item concerning calendar time is that for many of the specimens the lead time to obtain the testing facility is less than the calendar time to fabricate the specimen. Thus, for many testing methods, even if a test facility is not available, the calendar time to obtain the test facility is not an important consideration.

2. Drag Vehicle

The comparison of accuracy and cost is shown on Figures 36, 37, and 38 for each test method. The positive range of inaccuracy indicates more heat transfer into the vehicle than without the inaccuracies, and the negative range indicates less. Because of the different structure and temperature of the forward and aft sections of the drag vehicle, the estimates for panel testing have assumed that two panels would be required, one for the forward and one for the aft section.

a. Manhour Cost

Manhour cost versus range of inaccuracy is shown on Figure 36. Comparing the accuracies of panel testing for sea level and altitude would lead one to believe that altitude testing is not required for the drag vehicle. Actually, the sea level test seems accurate compared to the altitude test because of the inside convection coefficient influence. This coefficient, as calculated for the sea level test conditions, compensated for the higher sea level conductivity of the insulation. The resulting heat flow coincided by chance.

If the inside convection coefficient had been more closely simulated, the resulting inaccuracies would have been greater than shown for the sea level test of the half size vehicle. The problem of simulating the heat transfer off the interior wall is discussed in more detail in Appendix VI.

Because of the size of the drag vehicle, the larger (six-foot by ten-foot) panels actually cost more to test than the half size vehicle. These larger panels are not recommended because the half size vehicle provides better simulation and undoubtedly could be used for other testing after the heat test had been accomplished. A possible exception is discussed under "Calendar Time" below. As was previously discussed for the glide vehicle, the additional cost of the altitude simulated test is moderate compared to the increased accuracy.

b. Dollar Cost

The dollar cost is shown on Figure 37. The results of the dollar cost versus accuracy are the same as for the manhours.

c. Calendar Time

The calendar time estimates are shown on Figure 38. Testing of larger panels, although more costly than the half size vehicle, does have the advantage of less required calendar time. The comments concerning calendar time for the glide vehicle apply for the drag vehicle.

F. Summary

1. Cost and accuracy of experimental and analytical methods cannot be compared for two reasons:

   a. Comparison of the two methods requires that the actual amount of heat entering the vehicle be known; the "true" analytical solution is not the actual amount of heat entering and to use this mathematical "true" answer would greatly handicap the experimental methods.

   b. Analytical and experimental approaches are supplemental methods rather than different solutions.

Testing provides insight into the factors which, at present, cannot be analytically resolved. However, experimental methods cannot be efficiently or accurately applied unless supplemented by a mathematical program. For example:

a. Parameter studies should be done by an analytical program.

b. Development of the optimum wall configuration, rather than only a wall which will work, is aided by a parallel analytical program.

c. Evaluation of test inaccuracies and development of the test procedures require an analytical program.

d. The art of calculating heat transfer may be improved when a test program is conducted in parallel with an analytical program. Often refinements to analytical approaches result from findings of a test.

2. Testing inaccuracies can nullify any possible increase in accuray gained by testing. If testing is to provide the answers which cannot be analytically derived, the testing techniques and apparatus must be developed to increase test accuracy. For example, panel testing, which is the most attractive from cost considerations, should be developed to the point where the measurement of transient heat transfer through a panel approaches the accuracy with which thermal conductivity is measured. The basic heater is available for providing the temperature requirements, but the test apparatus and procedures must be developed to reduce temperature measurement inaccuracy, pressure simulation inaccuracy, edge effects, buckling of the panels, and inaccuracy in measuring the heat transfer through the panel.

3. Each vehicle and wall configuration must be individually examined to determine what specimen should be tested. Vehicle walls containing pressure dependent thermal properties must be tested with the vehicle altitude trajectory simulated unless the inaccuracy of a sea level test can be tolerated.

Panel tests will provide the basic heat flow into the typical wall and will allow such factors as contact resistance and heat shorts to be resolved. Reduced and full size tests provide simulation of radiation shape factors, bulkhead temperatures, and possibly inside film coefficients. For some vehicles, such as the glide vehicle of this study, the testing of the crew compartment rather than the complete vehicle should be considered because of the much reduced cost.

The cost of a specimen could also be greatly influenced by calculating the temperature conditions to some component within the wall, thus eliminating the cost of the super alloys or other high cost items on the outer section of the wall. For some wall configurations, the outer section of the wall does not significantly affect the heat transfer but accounts for a large part of the specimen fabrication cost.

4. Tests conducted with temperature and altitude versus time simulation are still unable to exactly reproduce the thermal environment of the actual vehicle re-entering the atmosphere. Some of the items not simulated are:

a. Deflections of the structure during the re-entry and the effect on heat flow paths, insulation, and other geometry changes.

b. The actual pressure in the insulation (different from the vehicle altitude pressure because of air currents, leakage, and other factors).

c. The temperature on the vehicle (calculated temperatures may be in error).

d. The convection effects such as between the skirt and aft section of the drag vehicle.

VI. MATERIAL THERMAL PROPERTY TESTING

A. General

Chapter V presented the cost and accuracy of experimentally determining the heat transfer into a re-entry vehicle by simulating the vehicle skin temperature on a test specimen. This chapter examines the second experimental method, material thermal property testing.

The analytical solutions for the heat transfer into the vehicle assume that the material thermal properties are known and are exactly correct. The cost and accuracy of thermal properties and the influence the accuracy of the properties has on the overall heat transfer is considered in this chapter.

Radiation shape factors, although not material properties, are required for the calculation of the heat transfer and have been included in this discussion.

B. Cost Ground Rules and Accuracy Discussion

1. Cost Ground Rules

a. Test Apparatus Cost

Consistent with the analytical approaches and the surface temperature simulation test methods, the test apparatus cost is shown independent of the testing costs. The cost and lead time estimates for each apparatus are shown on Figure 39. These estimates are based on building equipment from present designs and do not include any development cost. The value shown for the low conductivity tester is for a guarded hot plate which has a maximum hot plate temperature of 1200°F. The apparatus for a hot plate temperature of 2500°F required for the study vehicles is now being developed and the equipment costs are unknown.

b. Testing Cost

The cost of determining material thermal properties depends on the number of specimens tested, the temperature range, and, for some properties, the order of magnitude of the property and the number of test pressures.

Estimates have been made for the required thermal properties of each material for both vehicles, although many of the thermal properties are well documented in the literature and would not require testing.

The cost shown is based on testing several insulation thicknesses because the thickness effect on the radiant heat transfer through fibrous insulation subject to large temperature differences is not predictable.

The estimates for the insulation testing are based on apparatus similar to the guarded hot plate. Since this apparatus does not have the capabilities for the required temperatures, these estimates might change, depending on the apparatus developed for the higher temperatures.

The manhour cost consists of the same hourly rates as previously presented in Chapter V.

The calendar time estimates are based on two eight-hour shifts, five days per week. Calendar time for data reduction is not shown since this could be done concurrently with the testing. Each thermal property is evaluated on a separate apparatus so the total calendar time is determined by the property requiring the most time.

2. Property Accuracy Discussion

Appendix V outlines the test apparatus used for material thermal properties and shows the accuracy for each property which is representative of literature values. Additional differences are very likely to exist between the construction material of the actual vehicle and the specimen tested for material properties. Differences also exist between the environment of the actual vehicle and the environment in which the properties were tested. The following examples will illustrate:

a. Thermal Conductivity

(1) The method generally used for presenting test data (as a function of mean temperature) can introduce errors. The more accurate method would show the test data as a function of cold plate temperatures for each test hot plate temperature.

(2) The moisture content of some types of insulation will produce errors because the installed insulation may have a moisture content different from the test conditions.

(3) Changes in thickness and density of compressible materials will change the thermal conductance from the values used for the heat transfer calculations.

b. Emissivity

Many factors can change the emissivity of a sample from the value determined experimentally. Changes in surface conditions caused by handling, corrosion, heating, dirt and roughness are some examples. Since the emissivity is usually determined in an atmosphere free of carbon dioxide and water vapor (because of the absorption of certain wave lengths of radiation), the presence of

these substances can change the total normal emissivity. Often the literature values are not given for the temperature and surface conditions desired, and approximate values must be used.

c. Radiation Shape Factors

If geometry simplifications were required to determine the shape factors, the actual vehicle shape factors might be different from the values which were derived.

C. Material Property Cost and Influence on Heat Transfer Accuracy

1. Glide Vehicle

a. Test Cost

The detailed testing cost for the materials of the glide vehicle are shown in Table XI. The cost of determining the thermal conductivity of the outer insulation is the major cost of the thermal property testing of the glide vehicle. Most other properties can be determined relatively inexpensively. Table XIII summarizes the cost of testing all the thermal properties of the glide vehicle.

b. Effect of Material Properties on Analytical Solution Accuracy

Figures 40, 41 and 42 show the effect of errors in the outer insulation, acoustical insulation and honeycomb diffusivity on the heat entering the water wall. These factors are shown on these figures for the $\alpha = 0^{\circ}$, $\ell = 5$ feet, and $\alpha = 12^{\circ}$, $\ell = 5$ feet temperature profiles. The errors in the outer insulation diffusivity cause large errors in the total heat entering the water wall. The acoustical insulation errors result in only minor errors for the $\alpha = 12^{\circ}$ condition, but somewhat larger for the $\alpha = 0^{\circ}$ condition. This situation arises because of the $\alpha = 0^{\circ}$ case, the heat entering the water wall through the acoustical insulation is a significant portion of the total heat. The resulting error based on the overall vehicle would be between the $\alpha = 0^{\circ}$ and $\alpha = 12^{\circ}$ conditions. From Figure 42, it can be seen that relatively large errors in the diffusivity of the honeycomb result in only minor heat transfer errors. Since the acoustical insulation and honeycomb are in a series heat flow path, the total error was solved on the differential analyzer for several combinations of errors. The results are shown in Table XIV. This table also shows the outer insulation to be the most important of the three factors in determining the heat transfer.

2. Drag Vehicle

a. Test Cost

The detailed testing cost for the materials of the drag vehicle are shown in Table XII. For this vehicle, the cost of testing the load carrying insulation and the loose insulation represents a very large percentage of the total cost. The remaining properties can be tested at small cost. Table XIII summarizes the cost if all the thermal properties of the drag vehicle were tested.

b. Effect of Material Properties on Analytical Solution Accuracy

Figures 43 and 44 show the effect on the total heat entering the vehicle if errors occur in the thermal diffusivity of the load carrying insulation on the forward section of the sphere or in the radiation factor for the aft section.

These figures show that both of these errors significantly change the overall heat transfer into the vehicle.

Combinations of the heat transfer error can be obtained by adding the resulting heat transfer error for each material property error. For example, a $\pm$ 10% error in the insulation diffusivity results in a $\pm$ 5% error in the heat transfer (Figure 43) and a $\pm$ 10% error in the radiation factor results in a $\pm$ 7% error in the heat transfer (Figure 44). The total heat transfer error will then be in the range of + 12% to -12%.

D. Summary

1. The total cost of an analytical solution must include both the solution cost and the necessary material property testing cost. If considerable testing is required, the material property testing dollar and manhour cost can be as important as the solution cost. Calendar time for material property testing could result in extension of the analytical calendar time; however, the analytical part could be concurrent with the thermal property testing.

   Preliminary results of the analytical programs can usually reduce the testing required. For example, preliminary analytical results for the glide vehicle would show that the testing emphasis should be on the outer insulation and with thicknesses over one inch. This would materially reduce the total testing time.

2. Usually, a vehicle wall will contain a key thermal property which directly influences the precision of the analytical approach. This property for the glide vehicle is the outer insulation diffusivity. The drag vehicle has a key property for each section: the load carrying

insulation for the forward section and the radiation factor for the aft section.

a. Glide Vehicle

A ± 10% error in the outer insulation of the glide vehicle will result in a + 10% to -9% range of error for the heat transfer to the water wall.

b. Drag Vehicle

A ± 10% error in the load carrying insulation of the forward section and a ± 10% error in the radiation factor for the aft section result in a total error of + 12% to -12% for the drag vehicle analytical solution.

VII. CONCLUSIONS

The following conclusions have been reached as a result of this study.

1. Hand calculations have a limited place in heat transfer calculations for re-entry vehicles: for low accuracy problems on short flight time vehicles and in those limited number of problems where only one solution is desired.

2. Assigning experienced engineering aides to a hand calculation problem is advantageous only in setting up the problem. After the problem has been set up, the calculations are so boring and routine that an experienced operator's output is not essentially different from the output of a less experienced person.

3. Experience level has a large impact on the manhours, calendar time, and dollar cost for all other solution methods.

4. Solving heat transfer problems with a general program for a digital computer requires the least manhours, calendar time, and dollar cost for problems similar to those of the glide vehicle. Writing a special digital program makes the digital solution more expensive in dollars, calendar time and manhours than the other machine calculation methods.

5. The cost of solutions obtained by differential analyzers and passive element analogues are larger than the cost of digital methods; the differential analyzer is a little cheaper than the passive element analogue in all respects. The passive element analogue is best suited to linear problems rather than the non-linear problems studied.

6. Passive element analogues that do not use non-linear elements can be used in an iterative manner to cheaply obtain approximate answers to problems similar to those of this study. The approximate answers thus obtained can be valuable in large problems by establishing boundaries on the possible answers before more sophisticated methods are used.

7. Passive element analogues and the differential analyzers give an engineer a "feel" for his problem because he mentally equates what he is doing electrically to the thermal equivalent.

8. Appreciable reductions in the total dollar cost can be realized in a digital solution by accepting about 2 or 3% less than the best obtainable accuracy for problems similar to those of the glide vehicle.

9. A general digital heat transfer program has the least cost in dollars, manhours and calendar time for problems similar to those of the drag vehicle. The next best method is the differential analyzer, followed by a specific digital program.

10. In general, digital computers are not as limited in problem size or scope as are either differential analyzers or passive element analogues. Digital

computers are normally used to solve two or three dimensional problems that involve temperature or time dependent thermal properties.

11. If several parameter runs are desired, the selection of calculation method depends upon the accuracy desired, the number of runs, and which criterion (dollar cost, calendar time or manhours) is the most important. In general, the differential analyzer is the best suited to parameter studies.

12. Experimental and analytical methods should be regarded as supplemental approaches. Testing can provide simulation of the physical problem that cannot be obtained analytically.

13. Testing cost can be reduced and accuracy improved if the test program is supplemented by a parallel analytical study.

14. Experimental methods are very much more costly than analytical programs.

15. The cost of experimental methods, particularly in calendar time, precludes the use of reduced and full size vehicle experimental methods for design testing.

16. Experimental approaches are not suited to parameter studies.

17. Accurate test results are obtained from testing the wall configurations studied only if the altitude as well as the temperature history is simulated.

18. The best accuracy is obtained by testing a full size specimen for vehicles similar to the drag vehicle; however, significant reductions in cost can be realized for small reduction in accuracy by testing a half-size specimen.

19. Where the type of vehicle permits testing of a crew or equipment compartment only, large cost reductions can be obtained with little sacrifice of accuracy.

20. Ground testing, even with the temperature and altitude history simulated, still does not account for all of the factors influencing the heat transfer. Examples of factors not simulated include air leakage from the cabin and structural distortion from temperature effects.

21. In some problems, a key material property, such as thermal diffusivity, is the most important single factor in determining the heat transfer through a composite structure. If the value of the key property is known with high confidence from test data, high confidence can be generated in an analytical solution.

REFERENCES

1. Nagel, A. L., Handbook for Heat Transfer Computations, January 14, 1958, Boeing Airplane Company document number D2-2481, Secret.

2. MacNeal, R. H., An Asymmetrical Finite Difference Network, Journal of Applied Mathematics, 1952.

3. A.I.A. Survey 58-98, Survey of Transient Elevated Temperature Facilities, Aircraft Industries Association, December, 1958.

4. Fay, J. A., and Riddell, R. R., Theory of Stagnation Point Heat Transfer In Disassociated Air, Journal of Aeronautical Sciences, 1958.

5. Pournell, J. E., and Stuhring, D. H., Preliminary Evaluation of ILC SPD-117 and MC-2 Full Pressure Ventilation Suit Under Anticipated Thermal Profiles Encountered During Manned Re-Entry from Orbit, May 22, 1959, Boeing Airplane Company document number D2-4395.

6. Carslaw, H. S., Mathematical Theory of the Conduction of Heat in Solids, Dover Publications, New York, 1945.

7. Courant, R., Friedricks, K. O., and Lewy, H., Über die partiellen Differenzen-gleichungen der Mathematischen Physik, Math. Ann., Vol. 100, p. 32, 1928.

8. Dufort, E. C., and Frankel, S. P., Stability Conditions in the Numerical Treatment of Parabolic Differential Equations, Math. Tables and Aids to Computation, p. 135, July, 1953.

9. Grabbe, E. M., Ramo, S., and Wooldridge, D. E., Handbook of Automation, Computation, and Control, Vol. 1, John Wiley and Sons, New York, 1958.

10. Milne, W. E., Numerical Solution of Differential Equations, John Wiley and Sons, New York, 1953.

11. O'Brien, G. G., Hyman, M. A., and Kaplan, S., A Study of the Numerical Solution of Partial Differential Equations, J. Math. Physics, Vol. 29, p. 223, 1951.

12. Richtmyer, R. D., Difference Methods for Initial Value Problems, Interscience Publishers, New York, 1957.

13. Schneider, P. J., Conduction Heat Transfer, Addison-Wesley, Reading, Mass., 1955.

14. Infrared Lamps and Their Application, General Electric Large Lamp Department Brochure.

15. Elevated Temperature Test Equipment, Research Incorporated Brochure.

16. Kitchar, A. F., The Development of High Density Radiant Heating Equipment and Materials to Simulate Aerodynamic Heating, W.A.D.C. TR 57-159, March, 1957.

17. Rothenberg, A. J., Facility and Capability Description, West Coast Laboratory of Thompson Ramo Wooldridge, Inc.

18. Hoff, N. J., Induction Heating and Theory in the Solution of Transient Problems of Aircraft Structures, W.A.D.C. TR 56-145, August, 1956.

19. Arnold Engineering Development Center Test Facilities Handbook, January, 1959.

20. Hogness, T. R., Arc Heated Plasma for Laboratory Hypersonics, Astronautics, March, 1959.

21. Brogan, The Electric Arc Wind Tunnel - A Tool for Atmospheric Re-entry Research, American Rocket Society Journal, September, 1959.

22. Ferri, A., and Libby, A. A., The Hypersonic Facility of Polytechnic Institute of Brooklyn and its Application to Problems of Hypersonic Flight, W.A.D.C. TR 57-369, August, 1957.

23. Potter, J. Leith, Aerodynamic Heating Facilities, AEDC TR 58-7, July, 1958.

24. Bailey, J. F., Analysis of an Electrical-Resistance Type Gas Heater, AEDC TN 58-3.

25. Gross, Robert A., A High Temperature, Steady-Flow, Supersonic Tunnel, Journal of the Aero Space Sciences, October, 1959.

26. Allen, J. M., and others, Determination of Preferred Method of Producing Air Temperatures Encountered in Flight by Hypersonic Aircraft and Missiles, AEDC TR 57-11, July, 1957.

27. Lucus, William R., and Huston, Myron E., Planning a Re-entry and Recovery Test Program, Astronautics, March, 1959.

28. Stollenwerk, E. J., and Perry, R. W., Preliminary Planning for a Hyper-velocity Aeroballistic Range at Arnold Engineering Development Center, AEDC TN 58-25, June, 1958.

29. Goldsmith, A., and Waterman, Thermophysical Properties of Solid Materials, W.A.D.C. 58-476, January, 1959.

30. Woodside, William, Deviations from One-dimensional Heat Flow in Guarded Hot Plate Measurements, Review of Scientific Instruments, Vol. 28, No. 12, pp 1033.

31. Somers, E. V., and Cyphers, J. A., Analysis of Errors in Measuring Thermal Conductivity of Insulating Materials, Review of Scientific Instruments, Vol. 22, pp 583, 1951.

32. Dusinberre, G. M., Errors in Measuring Thermal Conductivity, Review of Scientific Instruments, Vol. 23, pp 649, 1952.

33. Fieldhouse, I. B., Hedge, J. C., and Lang, J. I., Measurement of Thermal Properties, W.A.D.C. TR 58-274, November, 1958, pp. 1-5.

34. Seibel, Richard D., and Mason, George L., Thermal Properties of High Temperature Materials, W.A.D.C. TR 58-468, June, 1958, pp. 44-56.

35. Fieldhouse, I. B., and others, Thermal Properties of High Temperature Materials, W.A.D.C. TR 57-487, February, 1958, pp. 3, 4, 5, 31.

36. Lucks, C. F., and others, The Experimental Measurement of Thermal Conductivities, Specific Heats, and Densities of Metallic, Transparent, and Protective Materials, AF Tech. Report 6145, pp. 7-12, 59.

37. Rasor, M. S., and McClelland, Thermal Properties of Materials, W.A.D.C. Report 56-400, Part I, March, 1957, pp. 14-18, 23-28.

38. Seibel, Richard D., Survey and Bibliography on the Determination of Thermal Conductivity of Metals at Elevated Temperatures, Office of Technical Services, United States Dept. of Commerce, Report PB 111756, August, 1954.

39. Hsu, S. T., Theory of a New Apparatus for Determining the Thermal Conductivities of Metals, Review of Scientific Instruments, Vol. 28, Number 5, May, 1957, pp. 333-336.

40. Betz, H. T., and others, Determination of Emissivity and Reflectivity Data on Aircraft Structural Materials, W.A.D.C. TR 56-222, October, 1958, Sec. II, pp 1-3.

41. Hamilton, D. C., and Morgan, W. R., Radiant-Interchange Configuration Factors, NACA TN 2836, December, 1952.

42. Jakob, Max, Heat Transfer, Vol. II, John Wiley, pp. 54-85.

43. Tea, P. L., Jr. and Baker, H. D., A Model Method for Determining Geometric Factors in Solid to Solid Radiation Heat Transfer, ASME Transactions, Vol. 80 #2, pp. 367-372.

44. Moen, W. K., Surface Temperature Measurement, Instruments and Control Systems, January, 1960, pp. 70-73.

45. Bussell, B., Analog Study of a Thermocouple Instrumentation Error, University of California, Dept. of Engineering Report C 57-65, August, 1957.

46. Lever, R. C., Development of High Temperature Thermocouple Materials, Society of Automotive Engineers Reprint 105V.

47. Shaw, V. G., High Temperature Measurement, Instruments and Control Systems, January, 1960, pp. 58-61.

48. Temperature - Its Measurement and Control in Science and Industry, Vol. II, American Institute of Physics.

APPENDIX I

SPHERICAL STAGNATION HEAT TRANSFER COEFFICIENTS

Heat transfer coefficients for spherical stagnation regions were calculated using the methods of Fay and Riddle, Reference 4. The coefficients are given in Figures 45 and 46 which show the average heat transfer coefficient for a one-foot diameter sphere as a parameter on a plot of altitude and velocity. The coefficient for any other diameter is obtained by dividing by the square root of the diameter in feet. The coefficient at the stagnation point can be obtained from the relatsbnship:

$$\frac{h \text{ stagnation point}}{h \text{ average nose}} = 2.1$$

The coefficient at the stagnation line is obtained from:

$$\frac{h \text{ stagnation line, } \Lambda = 0}{h \text{ stagnation point}} = \frac{1}{\sqrt{2}}$$

Correction factors to find the heat transfer coefficient as a function of distance back from the leading edge are obtained from Figure 47. This correction can also be used for sweep angle corrections by using the following relationships:

$$\cos \Theta = (\cos \theta_1)(\cos \phi_1) + (\cos \theta_2)(\cos \phi_2) + (\cos \theta_3)(\cos \phi_3)$$

The geometric interpretation of these angles is given on Figure 48.

Drag Vehicle Sample Problem

To illustrate the use of these curves and correction factors, two sample problems will be solved. The first sample problem will be to find a stagnation heat transfer coefficient at some point in the drag vehicle trajectory. At one point, the velocity is 24,960 ft/sec and the altitude is 290,000 ft. With this altitude and velocity, Figure 46 gives an average h over the stagnation region for a one-foot diameter sphere of 2.0 Btu/hr-ft^2-°F. To obtain the average h over the stagnation region of the sample vehicle, divide by the square root of the vehicle diameter, in this case 6.5 feet.

$$\frac{2}{\sqrt{6.5}} = 0.784 \text{ Btu/hr-ft}^2\text{-°F}$$

To obtain h stagnation point

$$h \text{ stagnation point} = (2.1)(0.784) = 1.65 \text{ Btu/hr-ft}^2\text{-°F}$$

GLIDE VEHICLE SAMPLE PROBLEM

The next problem will be to find the heat transfer coefficient at a point in the glide vehicle trajectory for a point 30° from the leading edge of a wing with a sweep angle of 70° and an angle of attack of 12° and a leading edge radius of 1.5 inches. At one point in the trajectory the altitude is 320,000 feet and the velocity is 24,960 ft./sec.

The first step will be to find the heat transfer coefficient for the stagnation line and then correct for the sweep angle and position around the leading edge.

From Figure 46, the average h over the nose for a one-foot diameter sphere at the problem altitude and velocity is 0.85 BTU/hr-ft^2-°F.

The correction for the leading edge diameter is made by dividing by the square root of the diameter in feet.

$$\frac{0.85}{\sqrt{\frac{(1.5)(2)}{12}}} = 1.700 \text{ BTU/hr-ft}^2\text{-°F}$$

To obtain h stagnation point:

$$\text{h stagnation point} = (2.1)\ (1.70) = 3.57 \text{ BTU/hr-ft}^2\text{-°F}$$

To obtain h stagnation line:

$$\frac{3.57}{\sqrt{2}} = 2.53 \text{ BTU/hr-ft}^2\text{-°F} = \text{h stagnation line } \Lambda = 0$$

The next step is to calculate the angle Θ so Figure 47 may be used to correct for sweep angle and distance from the leading edge.

With a sweep angle Λ of 70°, an angle of attack α of 12° and the location of the point in question 30° from the stagnation line θ_1 = 20°27' and θ_2 = 23°12'.

With the above information, cos Θ can readily be calculated from

$$\cos\Theta = (\cos\ \theta_1)\ (\cos\ \phi_1) + (\cos\ \theta_2)\ (\cos\ \phi_2) + (\cos\ \theta_3)\ (\cos\ \phi_3)$$

$$\Theta = 79°18'$$

$$\frac{h}{h_{\Theta = 0}} = 0.16 \quad \text{From Figure 47}$$

$$h = (0.16)\ (2.53) = 0.405 \text{ BTU/hr-ft}^2\text{-°F.}$$

APPENDIX II

This appendix outlines a study that was conducted to obtain insulation thicknesses that represented the minimum total penalty to the study vehicles. The sketch below represents a manned or a pressurized equipment compartment of a re-entry vehicle. The compartment is experiencing aerodynamic heating and has internal heat sources such as electronic equipment. Both the aerodynamic heat and the heat from internal sources are removed by an air transport fluid and absorbed in a heat exchanger by an expendable coolant.

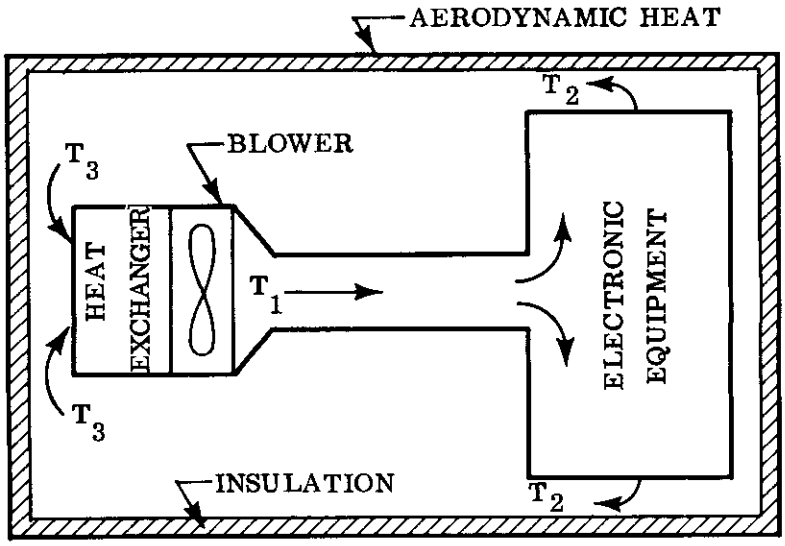

T_1 - Temperature of heat transport medium leaving the blower

T_2 - Temperature of heat transport medium leaving the electronic equipment.

T_3 - Maximum allowable temperature of heat transport medium entering the heat exchanger.

The weight of the cooling system and other items that can be charged to the cooling system can be described as follows:

$$W = \rho AL + \left[\frac{Q}{LL_H} + \frac{\beta}{L_H}\right]\left[1+\theta\right] + \left[\frac{\dot{Q}}{L} + \dot{\beta}\right]\psi$$

$$+ \left[\frac{\dot{Q}}{L\Delta T_{1-3}} - \frac{\dot{\beta}\,\Delta T_{2-3}}{\Delta T_{1-3}\,\Delta T_{1-2}} + \frac{\dot{\beta}}{\Delta T_{1-2}}\right]\Delta T_{bw}\left[\lambda + \eta_T + \frac{\tau}{L_H}\right]$$

where the terms have the following significance:

ρAL is the insulation weight.

$\frac{Q}{LL_H} + \frac{\beta}{L_H}$ is the weight of expendable coolant required to absorb the aerodynamic and internally generated heat.

θ is a factor to account for the expendable coolant heat sink tankage.

$\frac{\dot{Q}}{L} + \dot{\beta}$ is the maximum heat transfer rate that must be absorbed by the heat exchanger.

ψ is the heat exchanger weight as of function of the maximum heat transfer rate.

The term $\left[\frac{\dot{Q}}{L\Delta T_{1-3}} - \frac{\dot{\beta}\Delta T_{2-3}}{\Delta T_{1-3}\,\Delta T_{1-2}} + \frac{\dot{\beta}}{\Delta T_{1-2}}\right]\Delta T_{bw}\left[\lambda + \eta r + \frac{r}{LH}\right]$ is the penalty due to the blower and drive, fuel, fuel tankage, and the expendable coolant required to cool the blower power.

$\left[\frac{\dot{Q}}{L\Delta T_{1-2}} - \frac{\dot{\beta}\Delta T_{2-3}}{\Delta T_{1-3}\Delta T_{1-2}} + \frac{\dot{\beta}}{\Delta T_{1-2}}\right]$ is equal to the product of the transport medium flow rate and specific heat necessary to pick up the heat transferred into and generated in the compartment.

$\frac{\Delta T_{1-2}}{\Delta T_{1-3}}$ is a factor that related the amount of heat absorbing capacity left in the transport medium after absorbing the heat generated by the electrical equipment to the maximum possible heat absorbing capability of the transport medium.

When $\left[\frac{\dot{Q}}{L\Delta T_{1-3}} - \frac{\dot{\beta}\Delta T_{2-3}}{\Delta T_{1-3}\,\Delta T_{1-2}}\right] < 0$, these terms are omitted because the aerodynamic heat can be absorbed by the flow the electrical equipment requires without exceeding T_3.

When $\left[\frac{\dot{Q}}{L\Delta T_{1-3}} - \frac{\dot{\beta}\Delta T_{2-3}}{\Delta T_{1-3}\,\Delta T_{1-2}}\right] > 0$, a weight flow rate of transport fluid over and above that required for absorbing the internal heat generated must be provided to take care of the aerodynamic heat.

ΔT_{bw} is the temperature rise across the blower. The product

$\left[\frac{\dot{Q}}{L\Delta T_{1-3}} - \frac{\dot{\beta}\Delta T_{2-3}}{\Delta T_{1-3}\,\Delta T_{1-2}} - \frac{\dot{\beta}}{\Delta T_{1-2}}\right]\Delta T_{bw}$ is the power in BTU/hr

required to drive the blower.

λ is the weight of the blower power including fuel and fuel tankage as a function of the total energy required to drive the blower.

η is the blower and drive weight as a function of blower power.

$\frac{r}{L_H}$ is the weight of expendable coolant required to absorb the blower energy

The minimum system weight occurs when $\frac{dW}{dL} = 0$. In simple systems or systems with long flight times where transients are a small percentage of the overall time, $\frac{dW}{dL}$ may be obtained analytically. The systems employed in this study are too complex for simple analytical description of the aerodynamic heat entering the compartment. Therefore, the minimum system weight was determined by graphing systems weight versus insulation thickness.

The following discussion illustrates the use of the above equations as applied to the drag vehicle. The study for the glide vehicle is analogous.

Drag Vehicle Optimum Insulation Study

A study was made to determine the total cooling system weight as a function of the insulation thickness on the forward and aft sections of the occupied compartments. The results of this study for the forward wall are shown on Figure 13, where the weight chargeable to the cooling system is plotted against insulation thickness for the water wall and the insulated wall cases. The graph shows that the minimum system penalty is obtained by using an insulated wall. Since the cabin temperature was held constant, both the heat flow and the cabin wall temperature are variables. Figure 50 is a plot of maximum cabin wall temperature versus insulation thickness. The design wall temperature selected was 300°F. This selection was based on the work described in Reference 5 which demonstrates that test subjects can endure ambients of the type shown on Figure 49. It was felt that at the end of the trajectory shown, some excape mechanism would be employed to remove the occupant from the compartment. If the man were to be returned to earth inside this vehicle, additional insulation would be required to keep the cabin walls below 300°F.

The aft portion of the vehicle presents a different picture. Here the heat flow is by radiation from the stability skirt to the aft portion of the sphere and the minimum weight system occurs with no insulation. The maximum temperature is below the design criteria of 300°F. Therefore, the design was based on no insulation.

As was discussed in the body of this report, subsequent investigations showed that the choice for both the fore and aft sections of the vehicle were rather poor from a design standpoint, in that the total heat flow is very dependent upon the value of emissivity and the inside heat transfer coefficient, parameters whose value are not subject to exact predictions. This point was recognized at the time the configurations were set, but the decisions were made because the configurations afford excellent examples of a different class of problems from those of the glide vehicle. Also, because payload weight is so costly, the design may well be as shown and the predicted heat transfer coefficients substantiated by test.

The following sample calculation will illustrate how the preceding equations were

applied to this specific vehicle.

Six different insulation thicknesses, 0.25, 0.30, 0.35, 0.40, 0.45, and 0.50 inches, were examined. For the insulated wall case the cabin air temperature was assumed constant at 80°F and the heat exchanger, blower, blower power penalty and expandable coolant weight necessary to obtain that goal were calculated. In the water wall case, the cabin wall temperature is a function of the water boiling temperature which, in turn, is a function of altitude (Figure 51).

The total system weight for the insulated wall configuration is made up of the weights of water heat sink, water tank, heat exchanger, insulation, and the weight of the power supply plus fuel and blower that is chargeable to the aerodynamic heat. The following table illustrates the use of the optimizing equations.

Insulation Thickness	Weight Insulation	Heat	Weight Water	Weight Heat Exchanger + Tank	Weight Power Supply + Fuel + Blower	Total
In.	Lbs.	Q/L BTU	$\frac{Q}{LL_H}$ Lbs.	Lbs.	Lbs.	Lbs.
0.25	25.95	957.6	0.958	1.10	15.32	43.5
0.30	31.14	633.3	0.6333	0.896	10.14	42.9
0.35	36.33	406.0	0.406	0.753	6.49	44.0
0.40	41.5	251.0	0.251	0.657	4.02	46.5
0.45	46.7	151.0	0.151	0.595	2.42	49.9
0.50	51.9	83.7	.0837	0.552	1.34	53.9

Figure 13 plots total system weight and Figure 50 plots maximum wall temperature versus insulation thickness. The minimum system penalty occurs with an insulation thickness of 0.30 inches and a wall temperature of 440°F. To bring the wall temperature down to the maximum of 300°F that was set as the maximum allowable, it was necessary to increase the wall insulation thickness to 0.375".

An identical calculation was performed for a water wall system. In this case, the weights of the heat exchanger, blower and power supply system are omitted and a water distribution system added. The water distribution system consists of a fibrous insulation material used for wick and a thin aluminum shell. Admittedly, this assumption ignores some very real design problems such as filling, venting,

etc., that are beyond the scope of this study. Cabin wall temperature will very closely follow the boiling temperature of the water which is a function of the altitude. This curve is also plotted on Figure 51. The curve for the water wall shows that this system weighs more than an insulated wall designed for a maximum of 300°F. Therefore, an insulated wall case was chosen for study.

APPENDIX III

THEORY OF FINITE DIFFERENCES

Many problems on heat transfer to the occupied compartments of high speed aircraft do not lead themselves to exact mathematical solution. Usually the heat flow paths are not composed of a single material, and are arranged in combinations of series and parallel flow. Some of the material properties may be temperature dependent, the boundary conditions may be temperature and time dependent and the initial value of the temperature distribution may be complex. All in all, the prospects of obtaining an exact solution to a given heat transfer problem are dim, but solutions that are at least approximately true must be obtained for design purposes. There are two techniques widely used, finite differences and analogies.

The usual engineering approach to this problem is to employ finite differences. This section will outline briefly the theory of forward finite differences and discuss the inherent errors. References 6 to 13 contain more detailed treatment of the theory and applications. There are two types of finite differences, forward and backward. The sketch below and following discussion will illustrate the types.

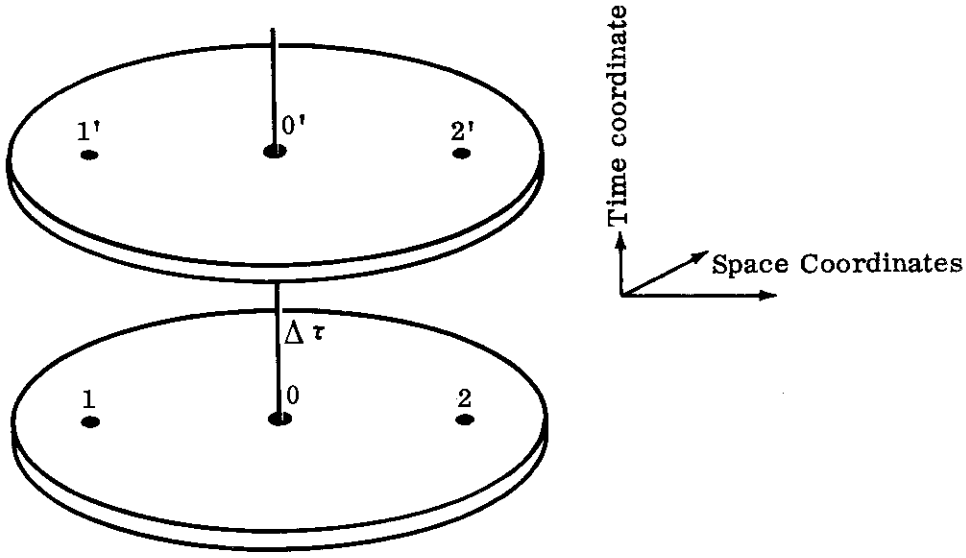

The temperature at points, 0, 1, 2 are at the present time and are known. The unknown temperatures at the points 0', 1', 2' are at a future time: $\Delta\tau$ later than the present. The forward difference method uses the known present temperatures of the points 0, 1 and 2 to calculate the temperature of the point 0' after $\Delta\tau$ time has elapsed. The backward difference method uses the unknown temperatures 1' and 2' along with the known temperature 0 to calculate the temperature at 0'. Since the expression for the temperature at the point 0' contains the unknown temperatures 1' and 2', the expression must be solved simultaneously with similar expressions for 1' and 2'. The forward difference method is the most commonly used technique and is the one used for this report.

Two different roads may be followed to arrive at the finite difference equations and to determine the limitations upon them. The first road is mathematical in nature and involves expansion in a Taylor's Series about a point and will be

employed in a later discussion on errors.

The other path involves physical reasoning and is the method outlined here. The simple, one-dimensional case sketched below will be used to illustrate the method. Assume that the left side of the slab undergoes an arbitrary change of temperature with time, the initial temperatures are some arbitrary function of length, and the right side is perfectly insulated. The first step is to divide the length into increments Δx long.

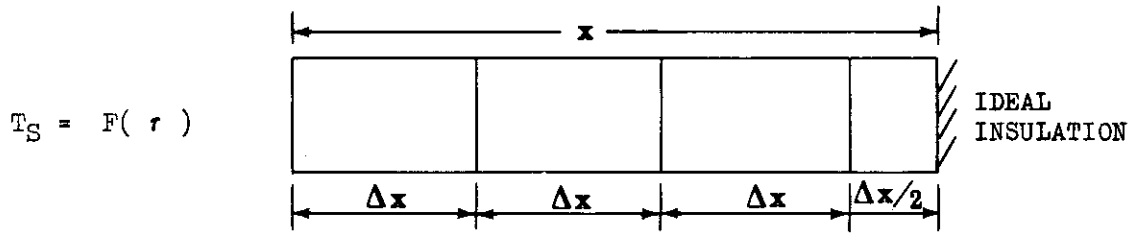

The following assumptions are made:

1. The total mass within the volume associated with Δx is concentrated at its midpoint.

2. Heat is conducted between nodes by fictitious massless conducting rods between midpoints.

Writing a heat balance on the ith slab:

q in from i-1 slab during the time $\Delta\tau$

$$\frac{K A}{\Delta X}\left[T_{i-1} - T_i\right]\Delta\tau$$

q out to i+1 slab during the time $\Delta\tau$

$$\frac{K A}{\Delta X}\left[T_i - T_{i+1}\right]\Delta\tau$$

q change in the internal energy during the time $\Delta\tau$

$$\rho A\, C_p\, \Delta X \left[T_i' - T_i\right]$$

q in = q out + q change in the internal energy

$$\frac{KA}{\Delta X}\left[T_{i-1} - T_i\right] = \frac{KA}{\Delta X}\left[T_i - T_{i+1}\right] + \frac{\rho A C_p \Delta X}{\Delta T}\left[T_i' - T_i\right]$$

$$T_i' = T_i\left(1 - \frac{2K\Delta T}{\rho C_p \Delta X^2}\right) + \frac{K\Delta T}{\rho C_p \Delta X^2}\left[\left(T_{i-1}\right) + \left(T_{i+1}\right)\right]$$

An equation such as the above is written for each slab. The time-temperature history

is determined by solving each equation again and again until the summation of $\Delta\tau$ covers the desired time span. Unfortunately $\Delta\tau$ cannot be chosen large arbitrarily to reduce the number of times each equation must be solved. Aside from considerations of approximating $\frac{\partial T}{\partial \tau}$, there are limitations on the choice of $\Delta\tau$.

The above equation states that the temperature of the i th slab after time has progressed $\Delta\tau$ units depends upon the present temperature of the i th node, the present temperature of its surroundings, the thermal properties of the material, and the physical dimensions. This equation also implies some limitations. If, in the equation for the i th node, the coefficient of the present temperature is negative, the equation would state: the hotter an object is at the moment, the colder it will be in the future. Such a statement is not only physical nonsense; it violates the Second Law of Thermodynamics. From this, it must be concluded that the coefficient of the present temperature has to be positive. An identical conclusion can be reached by mathematical reasoning. If the coefficient of the present temperature must be positive, then for this equation the stability criterion is $\Delta\tau \leq \frac{\Delta x^2}{2\alpha}$

It will be shown in a later section that the error in a finite difference approximation is proportional in part to Δx. This point is also apparent from the physical point of view in that the assumption was made that the heat absorbing capacity is assumed to be concentrated at the midpoint of the finite length Δx. The smaller the Δx, the more closely this assumption approximates a continuum. Therefore, from the standpoint of accuracy, Δx should be as small as possible. The other side of the coin is that $\Delta\tau$ will decrease as the square of Δx and the number of temperatures to be calculated increases inversely as Δx. Therefore, to cover the same time span, the total number of calculations increases inversely as the cube of Δx.

An equation similar to the above is written for each node. For example, the equations for a 4-node problem would be:

$$T_1' = T_1\left[1 - \frac{2K\Delta\tau}{\rho C_p \Delta X^2}\right] + \frac{K\Delta\tau}{\rho C_p \Delta X^2}\left[T_S + T_2\right]$$

$$T_2' = T_2\left[1 - \frac{2K\Delta\tau}{\rho C_p \Delta X^2}\right] + \frac{K\Delta\tau}{\rho C_p \Delta X^2}\left[T_1 + T_3\right]$$

$$T_3' = T_3\left[1 - \frac{2K\Delta\tau}{\rho C_p \Delta X^2}\right] + \frac{K\Delta\tau}{\rho C_p \Delta X^2}\left[T_2 + T_4\right]$$

$$T_4' = T_4\left[1 - \frac{2K\Delta\tau}{\rho C_p \Delta X^2}\right]$$

If any of the physical properties are temperature or time dependent, they are evaluated at the present temperature T and at the present time τ. If the geometry is not as simple as that used for illustration purposes, overall conductance values are used.

The solution procedure for the set of equations is as follows: The stability criterion discussed above is employed to find the minimum $\Delta\tau$ in the system. The coefficient of each term in the equations is then calculated. Using the initial temperatures of the nodes, the temperature at the end of the time interval $\Delta\tau$ is calculated for each node. These temperatures now become the initial values with which to calculate the temperature at the end of the next time interval. This process is repeated again and again until the summation of $\Delta\tau$ covers the desired time period.

ERRORS IN THE FINITE DIFFERENCE APPROXIMATION TO THE HEAT FLOW EQUATION

A truly exact solution to any physical heat flow problem is impossible. The cause of inaccurate solutions may come under several classifications.

1. Inadequate Mathematical Representation of Physical Conditions

The mathematical model (a set of differential equations with initial and boundary conditions) will not represent the physical conditions exactly. This discussion is not concerned with difficulties of this kind. Rather, the differential equations, initial and boundary conditions, and all physical properties will be assumed to represent the physical situation accurately. In some simple cases, exact analytical solutions can be obtained. This discussion, however, is concerned with the errors in the approximation techniques that are necessary in the more complex cases.

2. Truncation Error

Differential equations with initial and boundary conditions which are difficult to solve are often replaced by difference equations. If the boundary conditions involve derivatives, they are replaced by the corresponding conditions involving differences. The truncation error is a measure of the difference between the differential equation and the difference equation which replaces it.

For example, if $T(x, \tau)$ is the solution of the simplest heat equation:

$$\alpha \frac{\partial^2 T}{\partial X^2} - \frac{\partial T}{\partial \tau} = 0 \qquad (1)$$

where α is the thermal diffusivity

and if $T_i^n = T(i\,\Delta X, n\,\Delta\tau)$, where i and n are integers, i is the i th mesh point and n is the n th time increment. Equation (1) may be replaced with the difference equation.

$$\frac{\alpha}{\Delta X^2}\left[T_{i+1}^n - 2T_i^n + T_{i-1}^n\right] - \frac{T_i^{n+1} - T_i^n}{\Delta\tau} = 0 \qquad (2)$$

The truncation error at mesh point (i, n) is defined to be the difference

$$E_i^n = \alpha \left.\frac{\partial^2 T}{\partial X^2}\right]_i^n - \left.\frac{\partial T}{\partial \tau}\right]_i^n - \frac{\alpha}{\Delta X^2}\left[T_{i+1}^n - 2T_i^n + T_{i-1}^n\right] + \frac{T_i^{n+1} - T_i^n}{\Delta \tau} \qquad (3)$$

If it is assumed that $T(x, \tau)$ possesses continuous fourth partial derivatives with respect to x and second partial derivatives with respect to τ, the following Taylor expansions with remainder apply:

$$T_{i+1}^n = T_i^n + \left.\frac{\partial T}{\partial X}\right]_i^n \Delta X + \left.\frac{\partial^2 T}{\partial X^2}\right]_i^n \frac{\Delta X^2}{2!} + \left.\frac{\partial^3 T}{\partial X^3}\right]_i^n \frac{\Delta X^3}{3!} + \left.\frac{\partial^4 T}{\partial X^4}\right]_{i+\theta_1}^n \frac{\Delta X^4}{4!}$$

$$T_{i-1}^n = T_i^n + \left.\frac{\partial T}{\partial X}\right]_i^n \Delta X + \left.\frac{\partial^2 T}{\partial X^2}\right]_i^n \frac{\Delta X^2}{2!} + \left.\frac{\partial^3 T}{\partial X^3}\right]_i^n \frac{\Delta X^3}{3!} + \left.\frac{\partial^4 T}{\partial X^4}\right]_{i+\theta_2} \frac{\Delta X^4}{4!}$$

$$T_i^{n+1} = T_i^n + \left.\frac{\partial T}{\partial \tau}\right]_i^n \Delta \tau + \left.\frac{\partial^2 T}{\partial \tau^2}\right]_i^{n+\theta_3} \frac{\Delta \tau}{2!}$$

Here θ_1, θ_2, and θ_3 are numbers between 0 and 1. In a Taylor expansion with a remainder, the last term is evaluated at a different point in space and time than the preceeding terms. Just where the last terms are evaluated cannot be defined but they must lie between i and i +1 and i and i -1 in space and n and n +1 in time. Substituting these expressions in equation (3), the expression for the truncation error is:

$$E_i^n = \left.\frac{\partial^2 T}{\partial \tau^2}\right]_i^{n+\theta_3} \frac{\Delta \tau}{2!} - \alpha\left\{\left.\frac{\partial^4 T}{\partial X^4}\right]_{i+\theta_1}^n + \left.\frac{\partial^4 T}{\partial X^4}\right]_{i-\theta_2}^n\right\} \frac{\Delta X^4}{4!} \qquad (4)$$

This truncation error expression expresses roughly how rapidly the error decreases when working with mesh point (i, n) and adjacent points, as the mesh size is decreased because Δx is inversely proportional to the mesh size and $\Delta \tau$ is related to Δx through the stability criterion.

3. Round-Off Error

If numerical methods are used to solve the difference equation, there will be round-off errors in many of the steps. Individual round-off errors are usually relatively small. For example, an IBM 704 Digital Computer has a word length of about 8 decimal places. Given a set of equations of the form:

$$T_i^{n+1} = T_i^n\left(1 - \frac{2\alpha\Delta\tau}{\Delta X^2}\right) + \frac{\alpha\Delta\tau}{\Delta X^2}\left(T_{i+1}^n + T_{i-1}^n\right)$$

and if for some reason it is necessary to use a small mesh size, it is possible that more than 8 significant figures will be required for T_i^{n+1} to be different from T_i^n.

4. Instability of Difference Equations

The last item to be investigated is the possibility of error due to the instability of the difference equations. The difference system is said to be unstable if in the step-by-step solution of the difference equation any errors made at a particular step such as round-off errors, truncation errors or mistakes grow with time.

In the solution of complicated heat problems on a digital computer, care must be taken that none of the last three types of errors affect the answer greatly. The finite difference equation gives information about the temperature at certain mesh points, depending on one or more space variables and a time variable. If the solution of the difference equation converges to that of the differential equation, the truncation error may be made smaller by cutting down the increment sizes. However, this causes the amount of calculation needed to increase and, as discussed previously, the total round-off error may be prohibitive. The stability criterion determines how small the time increment has to be in relation to the increments in the space variables. In practice, round-off and truncation errors may be grouped as one worry and stability as another worry.

In complicated problems the truncation and round-off worries may be handled by doing the problem twice, once with the mesh size twice as large as at the other time but still using stable formulas. If the answers are practically the same at all common mesh points, it is a good indication that truncation and round-off are not causing trouble. The sketch below illustrates the interrelationship between truncation and round-off errors.

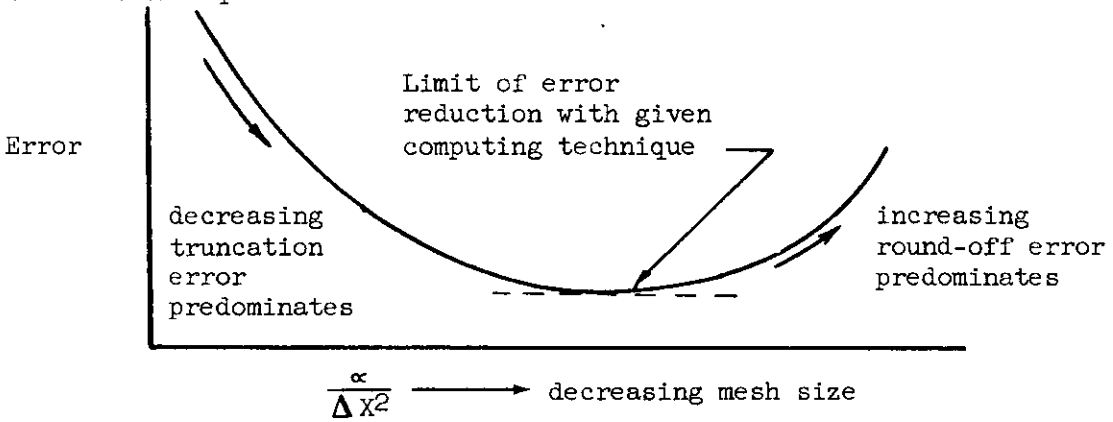

Books on heat transfer, References 6 and 13, and books discussing parabolic partial differential equations, References 9 and 10, derive intuitively or rigorously the stability requirement for equation (2). It is

$$\frac{\alpha\left(\Delta\tau\right)}{\Delta X^2} \leq \frac{1}{2} \qquad (5)$$

This criterion tells how small $\Delta\tau$ must be in comparison with Δx. Richtmyer, in Reference 12 derives many similar relationships. In non-linear problems, it is usually not possible to find a simple criterion such as this. In a rigorous criterion, the bound on the ratio would be a function of the unknown temperature. It is best to obtain an "effective" diffusion constant α so that this may be substituted into inequality (5) or into a similar formula for a linear difference equation different from equation (2). When the problem contains radiation terms as well as conduction terms, the usual practice is to consider a conduction term which would have somewhat the same effect on the solution for the particular temperatures involved. For example, an equation of the following form arises in the glide vehicle case:

$$\frac{T_i^{n+1} - T_i^n}{\Delta\tau} = \frac{2\sigma Fe Fa}{\rho C_p \Delta X}\left[\left(T_{i-1}^{\,n}\right)^4 - \left(T_i^{\,n}\right)^4\right] - \frac{\alpha}{\Delta X^2}\left[T_i^n - T_{i+1}^{\,n}\right]$$

See sketch below:

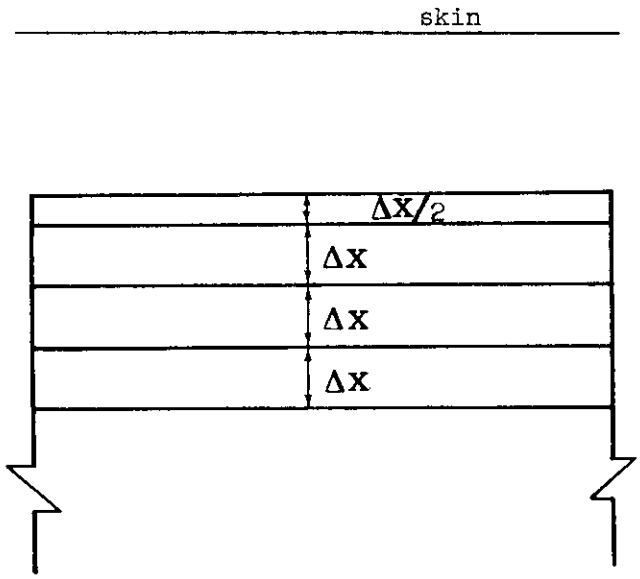

This equation can be written in the form

$$\frac{T_i^{n+1} - T_i^{-n}}{\Delta\tau} = \frac{2\,hr}{\rho C_p \Delta X}\left[T_{i-1}^{\,n} - T_i^{\,n}\right] - \frac{\alpha}{\Delta X^2}\left[T_i^n - T_{i+1}^{\,n}\right]$$

$$\text{Where } hr \equiv \frac{\left[\left(T_{i-1}^{\,n}\right)^4 - \left(T_i^n\right)^4\right]\sigma Fe Fa}{T_{i-1}^{\,n} - T_i^{\,n}}$$

Solve for either $\Delta\tau$ max each time step and use current values of T_{i-1}^{n} & T_i^{n} or use the maximum possible value of T_{i-1} and T_i with the assurance that hr will never exceed the value thus obtained. The stability criterion for this problem can be written as:

$$\Delta\tau \leq \frac{\rho C_p \Delta X}{2\ hr} + \frac{\Delta X^2}{\alpha}$$

A mathematical discussion of stability for various difference equations associated with certain parabolic partial differential equations is given by many authors, References 8, 9, 10, 11, 12, 13. The digital methods used in these investigations were all explicit methods. That is, the difference equation used gives each value of the temperature at time $(n + 1)\ \Delta\tau$ explicitly if the values at previous times are given.

ELECTRICAL ANALOGY

Another technique used to solve complex heat transfer problems is an extension of finite differences. It involves the use of the analogy that exists between heat transfer and the flow of current in a resistance capacitance network. The differential equation governing the voltage distribution in a body with uniformly distributed resistance and capacitance is:

$$\frac{1}{R}\ \frac{\partial^2 V}{\partial x^2} = C\ \frac{\partial V}{\partial \tau_e}$$

The differential equation governing the temperature distribution in a body with uniformly distributed conductance and thermal capacitance is:

$$K\ \frac{\partial^2 T}{\partial x^2} = \rho C_p\ \frac{\partial T}{\partial \tau_T}$$

Comparing the two equations term by term, the following table of analogous quantities can be prepared:

Current is analogous to rate of heat transfer
Voltage is analogous to temperature
Resistance is analogous to thermal resistance
Capacitance is analogous to thermal capacitance
Electrical time is analogous to thermal time

A table of the constants of proportionality can be prepared as follows:

$$a = \frac{\text{Electrical time}}{\text{Thermal time}}$$

$b = \frac{\text{Electrical capacity}}{\text{Thermal capacity}}$

$d = \frac{\text{Voltage}}{\text{Temperature}}$

$e = \frac{\text{Electrical resistance}}{\text{Thermal resistance}}$

$f = \frac{\text{Electrical current}}{\text{Rate of heat transfer}}$

The following algebraic relationships between the proportionality constants can be derived:

$$a = be = \frac{bd}{f}$$

$$b = a/e = \frac{af}{d}$$

$$d = ef = \frac{af}{b}$$

$$e = a/b = d/f$$

$$f = \frac{d}{e} = \frac{bd}{a}$$

Three of the above proportionality constants may be arbitrary. A simple procedure often used is to determine the maximum voltage, resistance and capacitance available from the facility and then using the maximum expected values of temperature thermal resistance and thermal capacitance, choose b, d and e such that as much as possible of the total facilities capability is used, then calculate a and f to insure that the time is within the measuring instrument's ability. Ordinarily the time will be well within the capability of strip chart recorders, in fact, it is usually possible to speed up the solutions by using smaller values of capacitance.

APPENDIX IV

This appendix presents a brief discussion of how the finite difference equations were translated into machine setups. A detailed discussion is beyond the scope of this report but the general method will be outlined in block diagram form. The method will be illustrated by indicating how a sample problem might be setup for each of the four calculation methods under consideration.

Two common problems are encountered with all of the calculation methods studied: (1) the thermal conductivity must be expressed as a function of insulation mean temperature and altitude, and (2) the proper equations must be selected to properly represent the glide vehicle water wall conditions. The sample problem chosen will contain the first of these problem areas. The water wall case will be discussed separately.

Sample Problem:

The sketch below represents the heat transfer situation to be simulated:

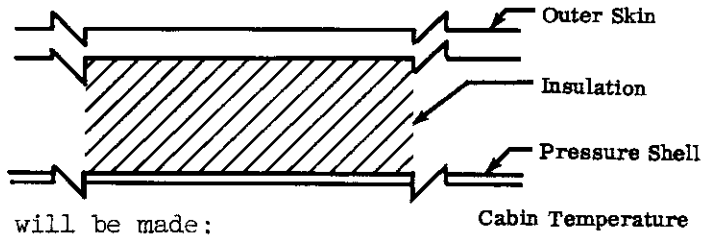

The following assumptions will be made:

1. The skin temperature is a variable with time and transfers heat to the insulation by radiation only.
2. The insulation thermal conductivity varies with altitude and temperature.
3. Heat is transferred to a constant cabin temperature by a constant heat transfer coefficient.
4. The specific heat is constant.
5. The thermal resistance of the pressure shell is negligible by comparison to the resistance of the insulation.

The sketch below shows how the insulation was divided into nodes in the manner illustrated in Appendix III.

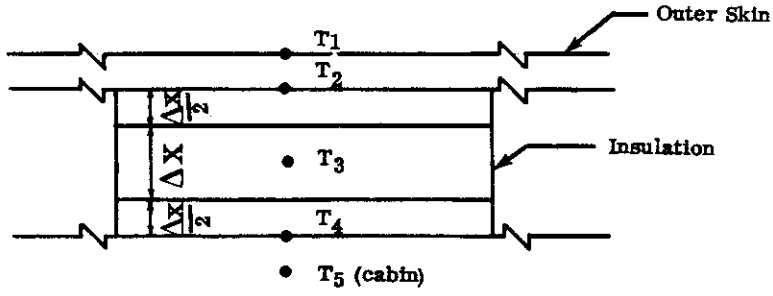

Heat Balance:

Rate of heat transfer into a node = rate of heat transfer out of a node plus the rate of change of the nodes internal energy.

The finite difference equations are:

$$\sigma A \, FeFa \, (T_1^4 - T_2^4) = \frac{K_1 A}{\Delta X} (T_2 - T_3) + \frac{\rho c_p A \, \Delta X}{2 \, \Delta \tau} (T_2' - T_2)$$

$$\frac{K_1 A}{\Delta X} (T_2 - T_3) = \frac{K_2 A}{\Delta X} (T_3 - T_4) + \frac{\rho c_p A \Delta X}{\Delta \tau} (T_3' - T_3)$$

$$\frac{K_2 A}{\Delta X} (T_3 - T_4) = h A (T_4 - T_5) + \frac{\rho c_p A \, \Delta X}{2 \, \Delta \tau} (T_4' - T_4)$$

Digital Computers

The digital computer available for solving the equations derived for the two study vehicles was the IBM 704. The machine program used for this study was the Lockheed Thermal Analyzer Program which is available to the industry through Share. The program is a general purpose heat transfer program and is based on the analogy between heat transfer and current flow in a resistance capacitance network. The way the digital computer was used in this study will be illustrated by solving the sample problem shown above. The first step in solving equations with this program is to draw an analogous electrical network. The equivalent electrical circuit for the sample thermal problem is shown below.

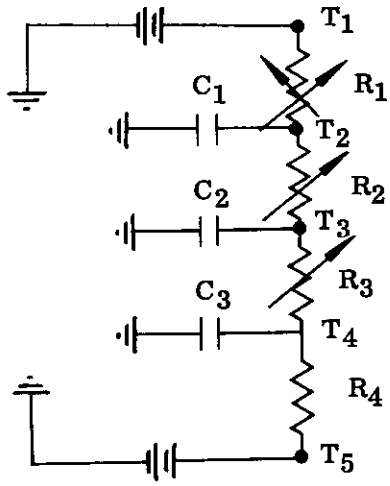

Where the following symbols are used:

Radiation resistor 

A variable resistor 

A fixed resistor 

A capacitor 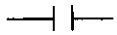

A voltage source 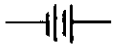

In the analogy between heat transfer and current flow the electrical resistance is proportional to the thermal resistance. No electrical analogy for heat transfer by radiation exists; therefore, the value of the radiation resistor is calculated from $R_1 = \frac{1}{h_r A}$ where

$$h_r = \frac{\sigma \, FeFa \left[T_1^{\,4} - T_2^{\,4} \right]}{T_1 - T_2}$$

The voltage sources supply voltages proportional to T_1 and T_5. The capacitance values are the heat absorbing capability of each node. $C_1 = C_3 = C_2/2 = \frac{\rho Ac_p \Delta X}{2}$.

R_4 is equal to $\frac{1}{h\,A}$. R_2 and R_3 are equal to $\frac{\Delta X}{K_1 A}$ and $\frac{\Delta X}{K_2 A}$ respectively. Since the thermal conductivity of the exterior insulation is a function of both mean temperature and altitude, the resistance must vary with these two parameters. Therefore, some provisions must be made in the equivalent thermal circuit to obtain the mean temperature.

The mean temperatures are obtained by using cathode followers as illustrated below.

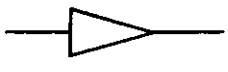

Cathode Follower

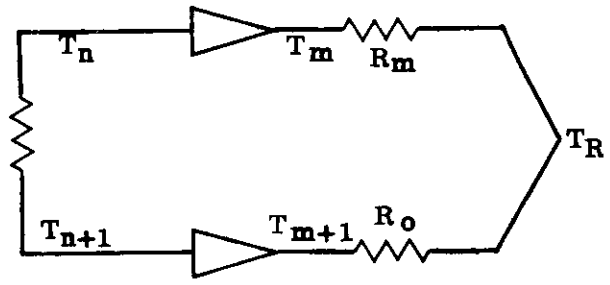

The voltage input to a cathode follower is impressed on the output with no current drain from the input side. In heat transfer terms, the temperature T_n equals T_m and no heat is transferred from T_n to T_m. Applying Kirchoff's law to the point R, current in = current out.

$$\frac{T_m - T_R}{R_m} = \frac{T_R - T_{m+1}}{R_o}$$

$$\frac{T_m}{R_m} + \frac{T_{m+1}}{R_o} = \left[\frac{1}{R_m} + \frac{1}{R_o}\right] T_R$$

If R_m is made equal to R_o

$T_R = \frac{T_m + T_{m+1}}{2}$ or the average temperature of T_n and T_{n+1}

The diagram becomes:

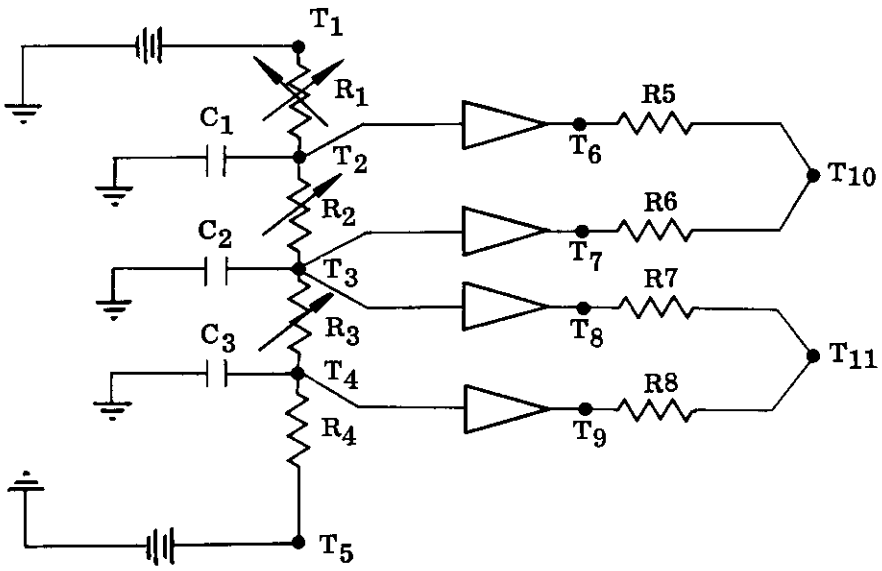

T_{10} and T_{11} are $\frac{T_2 + T_3}{2}$ and $\frac{T_3 + T_4}{2}$ respectively.

Using the altitude as a function of time from a trajectory curve such as Figure 1, and the plot of insulation thermal conductivity versus mean temperature and altitude such as Figure 14, a table of thermal conductivity as a function of time and mean temperature can be constructed. An example of such a table is shown below:

TIME-	MEAN TEMPERATURE ~ °F															
hr	100	200	300	400	500	600	700	800	900	1000	1100	1200	1300	1400	1500	1600
0																
0.01																
0.02						THERMAL CONDUCTIVITY										
0.03																
0.04																

The mean temperatures T_{10} and T_{11} and the problem time are used to obtain the correct thermal conductivity for the appropriate resistor at that particular time in the trajectory. The program has the ability to interpolate in the table.

A variable voltage supply is connected to T_1 and a constant voltage supply to T_5. Since voltage is analogous to temperature, the voltage supplied to the outer skin represents the variation in the skin temperature with time. The voltage supplied to T_5 represents the cabin temperature.

The next step is to calculate and assemble the various pieces of input data such as:

σ FeFa A, A/ Δ X, $\rho c_p A \Delta X$, $\frac{\rho c_p A \Delta X}{2}$, hA, and the variation of T_1 with time,

the initial temperatures, etc.

Each circuit element is given an identifying number. The problem is now ready for machine coding (writing keypunching instructions).

Keypunching instructions, in essence, build the resistance capacitance network and associated equipment by instructing the machine which resistors are connected together, which capacitor goes with which resistor, what elements are variable, how they vary, etc.

The first block of data contains the initial value of the temperature for each node.

The second block contains the value of each resistor and identifies which resistors are connected together. In the sample problem, this block of information would contain the constant portions of the variable resistors R_1, R_2, and R_3, the constant values of R_4, R_5, R_6, R_7, and R_8. It would also contain the information that T_1 is connected to T_2 via R_1, T_2 is connected to T_6 via a cathode follower, T_2 is also connected to T_3 via R_2, etc.,until the entire circuit is described.

The third block of data contains the capacitor values that are attached to each node. For example, C_1 has the value of $\frac{\rho c_p A \Delta X}{2}$ and goes with T_2.

Block four states which circuit elements are variable, how they vary and which resistors are radiation resistors. In the example, R_1, R_2, R_3, and T_1 are identified as variables, R_1 as a radiation resistor, R_2 and R_3 as variable resistors varying with time and T_{10} and T_{11} respectively (their mean temperatures), and T_1 is a variable with time.

Block five contains the specific information of how each of the variables in the preceeding block of information vary. For example, the variation of T_1 with time is given and the table of thermal conductivity as a function of mean temperature and time are contained in this block.

Block six lists which items are to be printed out. Not all of the information available is desired. In the example the temperatures T_{10} and T_{11} are of little interest. The most likely item of interest is T_4 so that the heat rate into the cabin may be calculated by the relationship $\frac{T_4 - T_5}{R_4}$ = heat transfer rate. The total heat may be obtained by graphical integration. (It is possible to combine circuit elements to obtain both the rate of heat transfer and the total heat transferred.)

Block seven specifies at what time interval the variables listed in block six are printed out. As stated earlier the time interval for calculation is not arbitrary and in general is small. Therefore, all of the possible information describing how the temperatures vary is not normally desired. The printouts are specified at some convenient time interval consistant with the problem requirements.

DIFFERENTIAL ANALYZER

The equations on pages 12, 20 and 21 are written as finite difference equations in time. Since the differential analyzer is capable of integration, there is no need of approximating the derivative with respect to time. A typical equation written for solution by the differential analyzer would be written as:

$$T_n = \int_0^\tau \frac{(q_{in} - q_{out})\, d\tau}{\rho A c_p \Delta X} = \int_0^\tau \frac{\left\{ \frac{K_n A}{\Delta X} \left[T_{n-1} - T_n \right] - \frac{K_{n+1} A}{\Delta X} \left[T_n - T_{n+1} \right] \right\} d\tau}{\rho A c_p \Delta X}$$

The major problem areas are the same for the differential analyzer as for the digital solution methods, viz., simulation of the variation of thermal conductivity with mean temperature and time, and selection and execution of the water wall calculation procedures. Discussion of the water wall calculation procedure will be deferred. As stated in the body of the report the thermal conductivity was obtained from the relationship $K = f(\tau)g(T)+y(T)+\text{Constant}$. To illustrate the application of the differential analyzer to a thermal problem of this type, the sample problem used to illustrate the digital application will be repeated and use the same assumption regarding thermal conductivity. The finite difference equations are:

$$\sigma \, FeFa(T_1^4 - T_2^4) = \frac{KA}{\Delta X} (T_2 - T_3) + \frac{\rho c_p A \Delta X}{2 \Delta \tau} (T_2' - T_2)$$

$$\frac{K_1 A}{\Delta X} (T_2 - T_3) = \frac{K_2 A}{\Delta X} (T_3 - T_4) + \frac{\rho c_p A \Delta X}{\Delta \tau} (T_3' - T_3)$$

$$\frac{K_2 A}{\Delta X} (T_3 - T_4) = hA (T_4 - T_5) + \frac{\rho c_p A \Delta X}{2 \Delta \tau} (T_4' - T_4)$$

The corresponding integral equations are:

$$\frac{\rho c_p A \Delta X T_2}{2} = \int_0^\tau \left[\sigma Fe \; Fa \; A(T_1^4 - T_2^4) - \frac{K_1 A}{\Delta X} (T_2 - T_3) \right] d\tau$$

$$\rho c_p A \Delta X T_3 = \int_0^\tau \left[\frac{K_1 A}{\Delta X} (T_2 - T_3) - \frac{K_2 A}{\Delta X} (T_3 - T_4) \right] d\tau$$

$$\frac{\rho c_p A \Delta X T_4}{2} = \int_0^\tau \left[\frac{K_2 A}{\Delta X} (T_3 - T_4) - hA (T_4 - T_5) \right] d\tau$$

The first step in the solution process is to scale the problem; that is to find the constants of proportionality between electrical quantities and the analogous thermal properties. This subject was discussed on pages 80 and 81 . The next problem is to determine how the various variable elements can be generated. A discussion of the various function generating equipment is beyond the scope of this study. Each thermal problem will have certain requirements for variable elements. Sufficient

equipment may or may not be availble to simulate all the variables in the problem. In general, compromises must be made. In fact, one must examine the effects of the variables, the cost of accurately simulating the variables and the desired solution accuracy. There is no substitute for experience in this area. In the sample problem, it will be assumed that sufficient equipment is available to simulate the radiation terms and the variation of thermal conductivity with time and mean temperature can be simulated by the expression:

$K = f(\tau)\, g(T) + y(T) + y(T) + \text{Constant}$. A block diagram for the sample problem would be as shown on Figure 52. Each block is numbered and the functions performed by the block are listed below:

Block 1 - generates τ by integrating $d\tau$

Block 2 - function generator - generates T_1 as a function of time

Block 3 - function generator - received T_1 from Block 2 and generates $\sigma FeFaAT_1^4$

Block 4 - generates T_2 by integrating the expression

$$T_2 = \int_0^{\tau} \frac{\left[\sigma FeFaA\,(T_1^4 - T_2^4) - \frac{K_1 A}{\Delta X}\,(T_2 - T_3)\right]}{\rho C_p \Delta XA}\, d\tau$$

Block 5 - receives T_2 from Block 4 and generates $\sigma FeFaAT_2^4$

Block 6 - receives T_2 from Block 4 and T_3 from Block 10 and generates

$$g\left(\frac{T_2 + T_3}{2}\right) \text{ necessary for } K_1$$

Block 7 - receives T_2 from Block 4 and T_3 from Block 10 and generates

$$y\left(\frac{T_2 + T_3}{2}\right) \text{ necessary for } K_1$$

Block 8 - receives $y\left(\frac{T_2 + T_3}{2}\right)$, $g\left(\frac{T_2 + T_3}{2}\right)$, and $f(\tau)$ from Blocks 9, 7 and 6 respectively and generates K_1

Block 9 - receives τ from Block 1 and generates $f(\tau)$ necessary for K_1

Block 10 - generates T_3 by integrating the expression:

$$T_3 = \int_0^{\tau} \frac{\left[\frac{K_1 A}{\Delta X}\,(T_2 - T_3) - \frac{K_2 A}{\Delta X}\,(T_3 - T_4)\right]}{\rho c_p \Delta XA}\, d\tau$$

Block 11 - receives T_3 from Block 10, T_4 from Block 14 and generates

$$g\left(\frac{T_3 + T_4}{2}\right) \text{ necessary for } K_2$$

Block 12 - receives T_3 from Block 10, T_4 from Block 14 and generates

$$y\left(\frac{T_3 + T_4}{2}\right) \text{necessary for } K_2$$

Block 13 - receives $g\left(\frac{T_3 + T_4}{2}\right)$ from Block 1, $y\left(\frac{T_3 + T_4}{2}\right)$ from Block 12 and $f(\tau)$ from Block 9 and generates K_2

Block 14 - generates T_4 by integrating the expression

$$T_4 = \int_0^{\tau}\left[\frac{\frac{K_2 A}{\Delta X}\left(T_3 - T_4\right) - hA\left(T_3 - T_5\right)}{\rho c_p A \frac{\Delta X}{2}}\right] d\tau$$

Block 15 - generates T_5

DIRECT ANALOGUE

The direct analogue utilizes the same basic analogy between electrical and heat transfer quantites as the digital and differential analyzer. The usual steps in solving problems with the direct analogue method is to draw an equivalent electrical circuit, compute the values of the resistors and capacitors, scale the problem as discussed in Appendix III and wire the resistance capacitance network. However, the direct analogue machine available did not have the capability of simulating the variation of thermal conductivity with temperature and time. Therefore, it was necessary to use the active elements of the differential analyzer to obtain variable thermal conductivity. In the body of the report it was stated that passive element analogues that do not employ non-linear elements may be used in an iterative manner to obtain approximate answers economically. The approximate answers obtained in this manner are valuable in two ways: first, they establish boundaries on the possible answer when more sophisticated techniques are used and secondly, the analogue technique gives the engineer solving the problem an excellent understanding of the important elements of the problem. The reasons for this increased understanding are discussed on page 40.

Since the block diagram for the direct analogue with non-linear elements is similar to the block diagram for the differential analyzer, the sample problem will be repeated here to illustrate how the problem would be approached using linear elements.

The first step is to draw an equivalent electrical network as shown below:

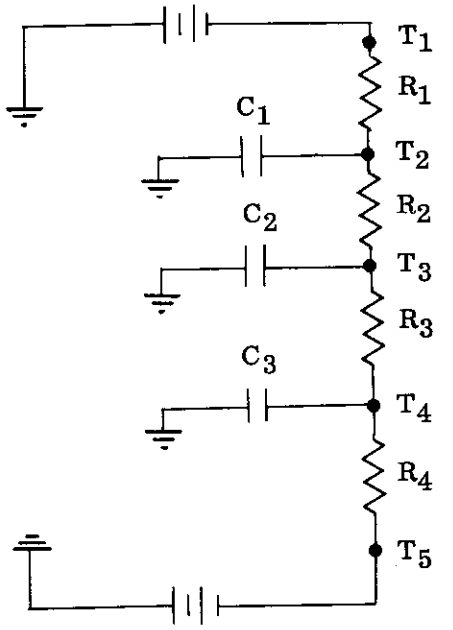

$$R_1 = \frac{1}{hr\ A} \qquad R_2 = \frac{\Delta X}{K_1\ A} \qquad R_3 = \frac{\Delta X}{K_2\ A} \qquad R_4 = \frac{1}{h\ A}$$

$$C_1 = C_3 = \frac{C_2}{2} = \frac{\rho A c_p\ \Delta X}{2}$$

Since hr, K_1 and K_2 are functions of temperature and time, a mean value must be estimated to start the problem. The next step is to scale the problem using the procedure outline in Appendix III. After scaling a resistance capacitance network is assembled and temperature versus time obtained. Using the trajectory and the temperatures thus obtained, a plot of thermal conductance versus time can be prepared and an average found by graphical integration. The problem is repeated using the new values of R_1, R_2, and R_3. The temperature obtained in the second trial is compared with the temperatures obtained in the preceding case. This procedure is repeated until the assumed temperatures equals the calculated temperatures. Occasionally the problem time scaling will be sufficiently slow so that the resistances may be varied with time by hand during the problem by setting potentiometers. The problems of this study were solved by passive elements employing non-linear elements as well as using the iterative procedure outlined above. The advantages and disadvantages are discussed on page 40 .

HAND CALCULATIONS

The hand calculation procedure is basically performing by hand the same calculations as the digital machine performs. To facilitate the step by step procedure a data sheet is usually employed. The sample problem finite difference equations are:

$$\sigma A\ FeFa \left[T_1^4 - T_2^4\right] = \frac{K_1 A}{\Delta X}\left(T_2 - T_3\right) + \frac{\rho c_p A\ \Delta\ X}{2\ \Delta\tau}\left(T_2' - T_2\right)$$

$$\frac{K_1 A}{\Delta X}\left(T_2 - T_3\right) = \frac{K_2 A}{\Delta X}\left(T_3 - T_4\right) + \frac{\rho c_p \; A \; \Delta X}{\Delta \tau}\left(T_3' - T_3\right)$$

$$\frac{K_2 A}{\Delta X}\left(T_4 - T_5\right) = h\, A\left(T_4 - T_5\right) + \frac{\rho c_p A \; \Delta X}{2\, \Delta \tau}\left(T_4' - T_4\right)$$

Solving each equation for T_2', T_3', and T_4' and substituting equivalent electrical quantities for thermal quantities:

$$T_2' = T_2\left[1 - \left[\frac{C_1}{R_1} + \frac{C_2}{R_2}\right]\Delta\tau\right] + C_1 \frac{\Delta\tau}{R_1} T_1 + \frac{C_1}{R_2}\Delta\tau\, T_3$$

$$T_3' = T_3\left[1 - \left[\frac{C_2}{R_2} + \frac{C_2}{R_3}\right]\Delta\tau\right] + C_2 \frac{\Delta\tau}{R_2} T_2 + \frac{C_2}{R_3}\Delta\tau\, T_4$$

$$T_4' = T_4\left[1 - \left[\frac{C_3}{R_3} + \frac{C_3}{R_4}\right]\Delta\tau\right] + \frac{C_3}{R_3}\Delta\tau\, T_3 + \frac{C_3}{R_4}\Delta\tau\, T_5$$

It has been shown on page 75 that $\Delta\tau$ cannot have any value desired, rather the coefficients of T_2, T_3, and T_4 must be positive. Therefore, part of the calculation procedure must be to solve for $\Delta\tau$ allowable. Since R_1, R_2, and R_3 vary with time, $\Delta\tau$ allowable will vary with time. Therefore, one may either solve for the allowable $\Delta\tau$ each time step or he may calculate the minimum value $\Delta\tau$ could ever be and use that value throughout the calculation procedure. The latter course is the method assumed for the sample problem. A sample data sheet prepared for this problem appears in Figure 53.

To start the calculation procedure, the initial values of all the tmperatures are placed in the appropriate columns. To find the temperatures T_2, T_3 and T_4 $\Delta\tau$ time units later, the initial values of T_2, T_3 and T_4 are used in the equation with the values of T_1 and T_5 at the time τ. The values of T_2, T_3 and T_4 thus calculated become the past values for the next calculation. The computation procedes in this step by step manner until the summation of $\Delta\tau$ covers the time period of interest.

WATER WALL

At altitudes below 106,000 ft., the water will boil at a temperature above 40°F and the boiling temperature will vary with altitude. Therefore, the equations used to represent the heat transfer in the flight regime below 106,000 ft. must account for the change in the sensible heat of the water and the change in the heat stored in the water wall materials, as the boiling point changes as well as calculating the

heat absorbed by evaporating water and the amount of water remaining.

Two possible conditions exist:

(1) The heat input to the water wall is insufficient to heat both water and water wall materials to the boiling temperature. In this case, no water is evaporated.

(2) The heat input to the water wall is more than sufficient to heat both water and materials to the boiling temperature. In this case, some water is evaporated and the amount of heat carried overboard by the steam and the water remaining must be calculated.

Means must be provided in the calculation procedure to determine when each of the above conditions exist and to select the proper equations. The technique accomplishing this is indicated schematically below:

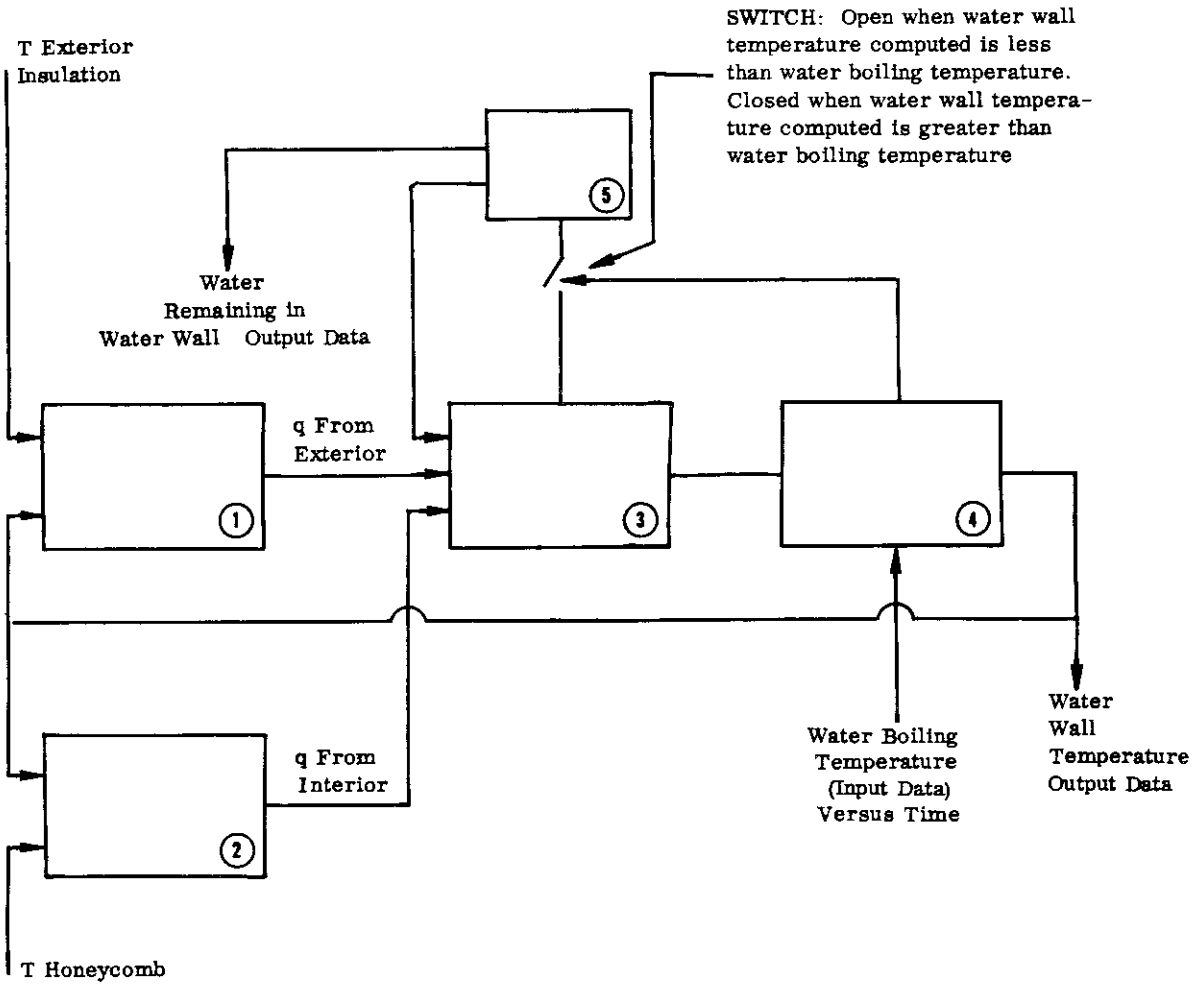

Block 1 receives the temperature of the exterior insulation adjacent to the water wall and the water wall temperature, and calculates the heat transfer rate from the exterior to the water wall.

Block 2 receives the temperature of the honeycomb and the water wall temperature and calculates the heat transfer to or from the vehicle interior.

Block 3 receives the heat transfer rates from Blocks 1 and 2 and the amount of water remaining in the water wall and the heat absorbing capacity of the equipment associated with the water wall to calculate the water wall temperature. The excess heat transferred over and above that necessary to increase the sensible heat of the water wall is used to evaporate water.

Block 4 compares the calculated water wall temperature with the water boiling temperature as a function of time. If the calculated value exceeds the input temperature by a small amount a switch is closed to allow the heat balance in Block 3 to include the water evaporation term. If the calculated temperature is below the input temperature, the water evaporation term is not included in Block 3.

Block 5 calculates amount of heat absorbed by water evaporating when the switch is closed. The water evaporation rate is also integrated in this block to determine the amount of water remaining in the water wall.

APPENDIX V

EXPERIMENTAL FACILITIES

The test facilities discussed in this appendix are (I) heating sources which can be used to simulate a desired surface temperature on a specimen, and (II) test apparatus required to experimentally determine material thermal properties.

I. HEAT FACILITIES

Many heating methods have been developed which could be used to heat a test specimen; however, only a few are capable of providing the temperatures and heat fluxes for the test time of the two vehicles in this study. This section is a general survey of the various heating methods to determine which faciilties have the capabilities to provide the necessary skin temperature and test time simulation. Of the numerous heat sources which are discussed in this chapter, the tungsten filament quartz tube radiant heater is the most capable of providing the heat required to test specimens of the vehicles of this study. The importance of the temperature-time simulation eliminates many heat sources which are unable to provide the heat for the operating times required. Some of the heating methods are not capable of producing the maximum temperatures required. The heat sources remaining which can adequately supply the required temperature and time simulation are either more costly or require further development. Some of the heating methods of the last group are likely to become more important in the future if the maximum temperature required exceeds the capability of the quartz-tube heater.

The heaters have been arranged into the following groups: (a) heating methods which directly heat the specimen, (b) heating methods which use heated gas to heat the specimen (convection heating), and (c) miscellaneous other heating methods.

A. Heating Methods Which Directly Heat the Specimen

Conduction, induction, and radiant heating facilities fall into this category. The development of these heating systems has been largely the result of the need for structural data from vehicles subjected to transient heating. The requirements for a heating system for structural testing and heat transfer testing are very similar; however, several differences do exist. Since structural test specimens are externally loaded during the test, the heaters must be located to allow the loading apparatus to be installed on the specimen. A second difference is that the required heat fluxes will generally be less for the heat transfer test than for the structural test for a given vehicle.

1. Conduction Heating

Strip heaters, blanket heaters, and conductive film heaters have been successfully used in the 1000°F range. Since the temperatures are lower than required for the study vehicles, conduction heating is not satisfactory. This method does have several advantages in

the lower temperature range which will be briefly discussed.

This heater provides a uniform heating source provided good contact is maintained between the specimen and heater (for metallic specimens an electrical insulator is required between the heater and specimen). This heater is especially attractive for testing in an altitude chamber because of the reduced oxidization effects on the heater and the reduction of corona problems with the low voltage which can be used. One of the disadvantages of conduction heating for structural testing is the attachment of the loading mechanisms which are located in the same physical location as the heaters. Since these loading devices are not required for heat transfer testing, conduction heaters do not pose this problem. Buckling of the test specimen during test and providing good thermal contact on curved specimens are two problems which must be resolved when considering resistance heating for heat transfer testing. Additional development of conduction heating methods is being done by the University of Colorado.

2. Radiant Heating

Radiant heat is the best method of heating the specimens of the study vehicles.

Various types of heating elements have been tested as radiant heaters, including nickel-chromium, carbon rod and tungsten. Both the carbon rod and the nickel-chromium elements have the serious disadvantage of relatively high thermal inertia, requiring 15 to 30 seconds to reach operating temperature. This thermal lag, for some temperature-time profiles, would not cause serious errors but for other profiles, such as the drag vehicle of this study, an appreciable error in skin temperature would result. A removable shield between the heater and specimen has been used for high inertia heaters. After the heater attains the desired temperature, the shield is removed, allowing the specimen to be heated. The use of a shield for even small panels complicates the test facility and becomes impractical for a large test involving a reduced or full size vehicle. The high thermal inertia heater also makes the simulation of the desired temperature-time profile more difficult during the decreasing temperature portion of the test.

The radiant heater in extensive use for structural testing is the quartz tube-tungsten filament heater. It has very low thermal inertia, requiring less than one second to reach operating temperature. The quartz tubes enclosing the tungsten filament are 0.375 inches in diameter and can be purchased in varying lengths (5 inches to 50 inches lighted length). Probably the most common length is the 10-inch heater which is rated at 1 kilowatt at 220 volts. The heaters are often operated at higher voltage (440 volts may be used) to increase the heat output. The increased voltage results in reduced life but is usually satisfactory for testing

purposes. The maximum operating temperature is limited by the quartz tube which softens at approximately 3400°F. Reference 14 describes a commercially available quartz tube heater.

Heater support assemblies, reflectors, power control equipment and programming equipment are commercially available for the tungsten filament heater (see Reference 15). Reference 16 outlines the development of this associated equipment. The power controllers can be programmed to supply power to automatically impose either a skin temperature or heat flux on a specimen. Thermocouples attached to the specimen provide the sensor for the desired skin temperature or heat flux. Manual control can also be used with visual readout equipment for the thermocouples. The power control equipment generally uses ignitron tubes although saturable reactors have been used. Reflectors are usually used to increase the efficiency of the heaters. The reflectors have been fabricated from aluminum, stainless steel, and stainless steel base metal covered with ceramic and coated with gold on the reflecting surface, depending on the maximum temperature and time encountered.

The overall heating configuration is made by mounting the lamps in an array around the specimen, the density of the lamps depending on required temperatures and estimated heat flux for the specimen.

Maximum specimen surface temperatures attainable with the quartz tube heater are near 3000°F (depending somewhat on the specimen) with power inputs near 100 kilowatts per square foot with a commercially available unit operated at 440 volts.

If during the time versus temperature profile the desired specimen temperature requires faster cooling than is attained with the heaters off, cold air or carbon dioxide can be blown over the surface. An excess cooling would be used and the heaters would supply heat to control the surface to the desired temperature.

Since the heat transfer through a vehicle may be a function of the ambient pressure, the simulation of the altitude-time variation of the vehicle may be required to obtain the accuracy desired. This altitude simulation could be accomplished either by enclosing the specimen and heaters in an altitude chamber or possibly (at least for a panel test) by fabricating the specimen so that the specimen could be evacuated to the desired pressure. If the heaters are operated in an altitude chamber, certain problems occur which are not experienced at sea level pressure. One problem results from the corona effect. This requires that the lamps either be operated at reduced voltage or be used with specially designed assemblies. These assemblies have isolation coatings applied to the surfaces, edges, or points where corona could occur. A second problem is the overheating of the lamp ends and reflectors because of the reduced convective cooling in the altitude chamber. Numerous approaches are now being considered to solve these problems,

such as developing higher allowable temperatures on the reflectors and water or forced air cooling of the components. Another problem in testing in an altitude chamber is providing cooling on the specimen if the desired temperature decreases faster than the specimen will cool with the heaters off. A special radiant heat sink would be required to increase the specimen cooling rate.

The extensive use of the quartz tube tungsten filament heater was demonstrated by a survey of heating methods conducted in 1958 by The Aircraft Industries Association (Reference 3). The results of this survey showed that some thirty organizations had facilities and used this heater for transient temperature testing.

Figure 54 shows radiant heaters and power equipment being used to heat a specimen.

The costs of the radiant heat facilities for testing the specimens of this study are shown on Figure 31; however, Reference 3 includes a list of organizations who have indicated an interest in performing heat testing on a subcontract basis.

The Air Force facility located in Inglewood, California, with operational responsibility assigned to the West Coast Laboratory of Thompson Ramo Wooldridge Incorporated, is also available for testing on a contract basis. This facility has an electrical substation rating of 15,000 KVA continuous service. Approximately 10,000 kilowatts of this power are available for heating equipment. A steam ejector evacuation system is available on the site for altitude simulation testing. Reference 17 describes the capabilities of this facility. Figure 55 is an aerial photograph of the facility.

3. Induction Heating

Induction heating can provide the required simulation but the costs are higher than the radiant heating costs.

Induction heating is caused by eddy currents in an electrically conducting material. The eddy currents result from a changing magnetic field. Since the heat is generated within the material rather than on the surface, good simulation is not attained unless the heating occurs in the outer layer of the skin. The depth of penetration for a given material and temperature depends on the frequency of the electrical energy. Polytechnic Institute of Brooklyn and the University of Florida have done development work on induction heating. Reference 18 includes some testing experience with a 20 kilowatt heater. It has been demonstrated that induction heating equipment can simulate the required temperatures and heat flux required for the vehicles of this study; however; this form of heating at the present is several times as expensive

as the radiant heating facility previously discussed. Numerous problems such as the design of the heating coils and development of power control systems must still be solved before induction heating can be extensively used.

Continued development of induction heaters is being done at the University of Florida for Wright Air Development Division Structural Test Laboratory. The largest induction heating facility planned at present is the 10,000 kilowatt facility (40 units of 250 kilowatts each) at Wright Air Development Division. Heat fluxes in the order of 250 kilowatts per square foot are considered practical for induction heating although higher rates have been obtained. The specimen can be heated to the melting temperature of the material with induction heating. Because of the higher costs, compared to the radiant heaters, induction heaters are likely to be used only for higher temperatures or heat fluxes than are attainable with the radiant heaters.

B. Heating Methods Which Use Heated Air to Heat the Specimen

Various facilities which transfer heat to the specimen by convection are briefly evaluated in this section. Included in this group are the "wind tunnel facilities." Wind tunnels are primarily designed to simulate airstream conditions for investigations of heat transfer coefficients, flow regime, structural and control problems. Since the comparisons of this study originate from the vehicle outer surface temperature, the various facilities will only be evaluated as a method of producing a required skin temperature on a specimen.

The numerous facilities included in this section can be separated into either continuous or intermittent operating heat sources.

1. Intermittent Heat Sources

These heat sources do not have the capability to simulate the test time of the vehicles. A brief description is included to identify the facilities in this group.

a. Shock Tubes and Hypersonic Shock Tubes

Operating time of these tunnels is in the order of 40 milliseconds. The heating is done by electrical arc discharge. The facility consists of a driver section, driven section, test section and the vacuum source. The driver gas is at a high pressure and is separated from the driven gas by a diaphragm. The diaphragm between the driven and driver gas is broken, the resulting mixture ruptures a second diaphragm and enters the test section. By using a supersonic nozzle, the Mach number can be increased to approximately 20 with stagnation temperatures of 20,000°F. Tunnels included in this area are the "Hotshots" of Arnold Engineering Department

Center. Reference 19 further describes these tunnels.

b. Gatling Gun Hypersonic Shock Tunnels

To extend the operating time of the hypersonic shock tubes, numerous shock tubes can be operated similar to a Gatling Gun. Cornell Aeronautical Laboratory has developed this principle with the "Little Rollo" tunnel. Although these tunnels have longer operating time, the time is still too short for the vehicles of this study.

c. High Intensity Electric Arc Jets (Plasma Jets)

Heating is accomplished by using a high current arc enclosed in a chamber. The arc is surrounded by injecting water or gas to thermally confine the arc current. Temperatures in the range of 10,000°F to 20,000°F are possible. Test periods of several minutes have been attained (Reference 20). This high temperature energy source is extensively used for high temperature material studies. Reference 21 also includes a description of a plasma jet.

2. Continuous Heat Sources

Convection heating, using one of the heater sources discussed in this section, has only been used on very limited scale as for the study of ablation with very small specimens. Since the theoretical temperatures are higher than the present radiant heat capabilities, it is believed that the future of these heat sources will depend primarily on a future requirement for high temperatures. Convection heating has several basic limitations and major development problems. One limitation in testing a full or reduced size specimen is that the temperature can be controlled on one zone only, the remainder of the vehicle would not be controlled unless the actual flight conditions of the vehicle are reproduced. The control system, even to accomplish control on one zone, would present some difficult development problems. Altitude simulation would require fabrication of the test specimen to allow evacuation of the pressure dependent components. The design of the facility to control and transport the air at temperatures of 3000°F would be difficult because of the high heating rates the facility would experience.

a. Continuous Operating Tunnels

Present continuous operating tunnels cannot simulate the airstream conditions for the vehicle re-entry trajectory. Some of the facilities have heaters which are capable of supplying air at temperatures sufficiently high to heat a model to the desired surface temperature. Various air heating methods are

used including electric resistance heaters, mechanical compressors, and chemically fueled heaters. To reduce the heater size, some designs incorporate large heat reservoirs in the form of sheet metal lattices, steel balls, or heated refractory materials. The heat stored in the reservoir supplies the required heat to the tunnel gas during the test. This type of heater has supplied gas heated to over 3000°F. Reference 22 describes an existing facility.

Electric resistance heaters used to directly heat the tunnel gas have the advantage of the rapid response required for simulation of time dependent temperature profiles. Reference 23 indicates the upper temperature limit for electric resistance heaters as approximately 2500°F for air and possibly 4000°F for nitrogen. Recent work on this heater for transient simulation of temperature is Reference 24.

Reference 25 describes a continuous operating tunnel with a unique heat source. The inlet air is preheated to 1200°F followed by burning hydrogen upstream of the throat to obtain temperatures of approximately 3500°F.

Reference 26 discusses the many considerations involved in designing a heating source.

b. Combustion or Chemical Jets

Chemical jets such as jet and rocket engine exhaust gases are a source of high energy gases. These combustion jets have been used by the Army Ballistic Missile Agency for the development of ablation materials for nose cones. Reference 27 is an unclassified description of this heat source.

C. Miscellaneous Other Heating Methods

Several other test facilities are capable of providing some degree of simulation but are not easily classified in the previous sections. A description and evaluation of the capabilities of each is included below. At the present, none of these methods are competitive with the radiant heaters discussed previously.

1. Aeroballistic Ranges and Magnetic Accelerators

Desired skin temperatures with these facilities are attained by "firing" or accelerating the model to a high velocity. These facilities have very short flight times, small model sizes, and high accelerations on the model. Reference 28 describes planning done by Arnold Engineering Development Center for an aeroballistic range. This facility, because of the above limitations, is not satisfactory for the simulation required for the vehicles of this study.

2. Arc-Image, Solar Furnaces

The arc-image furnace focuses the high temperature carbon arc with a parabolic mirror to obtain temperatures in the 10,000°F range. The test area is limited to less than one square inch. The solar furnace which focuses the sun's rays also is limited to very small test areas and is not satisfactory for testing considered in this study.

3. Rocket-Propelled Model

The rocket propelled model is a very important test method for determining heat transfer coefficients and flow regime. Since the vehicle structure would require simulation to determine heat transfer, a relatively large model would be required. Instrumentation of the model, recovery of the model, and reproducing the re-entry trajectory are other problems of the rocket propelled model. Further development of this test method may result in increased importance in the future.

4. Flame Heating

The use of flames (such as acetylene) has been considered as a means of heating a specimen. Even temperature distribution on the surface would require developing controllable nozzles which could be spaced at very small intervals. This method may have possibilities but would require considerable development. Specimen contamination could occur for some materials using flame heating.

II. MATERIAL THERMAL PROPERTY TESTING

This section describes test methods used to determine the material thermal properties required for the analytical calculation of heat flow. Many of the thermal properties could be determined by any one of several methods which have been developed. The various methods can be compared by considering accuracy, speed of operation, dependence of results on independent properties, reliability of results, range of temperature, geometry of the samples, and the cost of the test apparatus. The error in the thermal property will be discussed in detail for only one method. The method selected for the error discussion is not necessarily the most accurate, but is one of the more common methods which have been used and therefore is representative of the error which exists in literature values of thermal properties.

Material thermal properties to be considered are: thermal conductivity, specific heat, density, diffusivity and emissivity. Radiation shape factors, although not material thermal properties, are included in this section since they are required for calculation of radiant heat transfer.

Reference 29 contains literature values for the thermal properties of many materials.

A. Thermal Conductivity

The type of apparatus used for thermal conductivity testing of solids depends on the relative (high or low) conductivity and the temperature range of the testing.

1. Low Conductivity Materials

The conductivity test accepted as a standard for testing materials with conductivities less than 5.0 BTU/hr-ft^2-$^\circ$F/in. is the American Society of Testing Materials Procedure C177-45 (guarded hot plate). This procedure assumes one dimensional heat flow from the specimen to the cold plates. Temperature differences between the specimen and the guard heaters will cause deviations in this unidirectional heat flow. These conditions have been evaluated in References 30, 31 and 32.

Assuming the apparatus can hold the temperature difference between the guard plate and test specimen to less than 1°F, the resulting error is less than 3% for specimens not exceeding the specified thicknesses of the American Society of Testing Materials Procedure. Other test differences for the guarded hot plate procedure include inaccuracies in temperature measurement, heat flow measurement (watt meter) and errors from misalignment of heaters. These account for an estimated additional 3% inaccuracy for an overall error in the neighborhood of 5%.

This type of apparatus is usually limited to temperatures on the hot plate of 1000 to 1200°F, allowing a maximum mean temperature of 700-900°F depending on the apparatus. Since knowledge of material properties at higher temperatures is becoming more important, apparatus is currently being developed for hot side temperatures of 2500°F.

The thermal conductivity of some materials (such as the fibrous insulations) is both temperature and pressure dependent. Since the vehicles operate at high altitude for a portion of the flight profile, the conductivity of these materials is required for various ambient pressures. Conductivity testing at reduced pressure introduces additional problems in maintaining and measuring the pressure in the specimen. This additional error introduced for reduced pressure depends on the pressure range of the testing and the sensitivity of the conductivity to pressure. Since the conductivity (for a given mean temperature) may be only one half or one third as great at 300,000 feet altitude as at sea level, a total error of 10% is estimated.

2. High Conductivity Materials

Several techniques have been developed for determining the thermal conductivity of metals. References 33, 34, 35, 36 and 37 describe

the various techniques which have been used.

One method which is used by Armour Research Foundation is described in Reference 33. This procedure determines the conductivity by measuring the temperature at two radial locations on a disk shaped specimen heated from the center. Radial heat flow is assured by using disks made of the same material as the specimen on each side of the specimen. These disks are also heated until the axial temperature gradient is negligible. The accuracy of this apparatus depends on alignment of the heaters, resistance of the heater coils, location of the thermocouples, and thermocouple inaccuracy. The estimated error of the conductivity is 5% (Reference 33). This apparatus has been used for maximum temperatures of 3000°F.

Reference 37 also shows a thermal conductivity tester for metals. This reference estimates the error to be within 5% to 8%, depending somewhat on the heater used for a given sample. This tester can be used for temperatures as high as 6000°F.

B. Specific Heat

A literature survey (Reference 38) found three basic methods of determining the specific heat of material at high temperature: (1) liquid calorimeters, (2) ice calorimeters, and (3) heat flow apparatus.

The liquid calorimeter has been used by Armour Research Foundation for the temperature range of 1000°F to 3000°F (Reference 35). The sample is heated to the desired temperature and immersed in a liquid calorimeter. The resulting change in enthalpy of the specimen is used to compute the specific heat.

The specimen in this procedure is dropped into a dry receiver to prevent splashing of liquid which occurs if the sample is dropped directly into the fluid. At high temperature the heat loss of the sample during the drop from the furnace to the calorimeter temperature can cause significant error. This is minimized by incasing the specimen in a graphite capsule. The test is then performed both with the specimen in the capsule and with the empty capsule. The difference between the two tests is used to determine the specific heat of the specimen.

Reference 35 includes an analysis of the accuracy of the liquid calorimeter. The analysis shows that the largest inaccuracy is measuring the sample temperature in the furnace. A test was conducted comparing temperature in the sample with the temperature measured in special tubes placed in the furnace. The thermocouples in the samples agreed with the arithmetic average of the protected thermocouples to within 4°F. The unsteady behavior of the furnace from line voltage fluctuations resulted in a 15°F deviation at temperatures above 2400°F. These conditions were estimated to introduce an error of 1%. A 1% error was also estimated because of inaccuracies in measuring the heat content of the sample in

the calorimeter. The total error of the specific heat measurements was estimated to be about 3% for the temperature range of the materials tested.

Heat flow apparatus have also been developed for specific heat measurements. Reference 37 describes an apparatus which has been used for temperatures as high as 6000°F. The error estimated for this apparatus was 5%.

C. Density

Various methods for determining the density of solid materials can be used. Reference 38 includes a bibliography of methods used for determining density. Density of materials at temperatures other than that used in the test can be calculated using the thermal expansion properties of the specimen to determine the volume at specified temperature. An accuracy analysis done by Battelle Memorial Institute on density determination estimated the error as 0.1% at the temperatures where the density was directly measured, and 0.2% for other values involving the uses of a dilatometer to determine linear coefficients of expansion (Reference 36). Test specimens included various metals at temperatures to 1800°F.

D. Thermal Diffusivity

The thermal diffusivity α, can be calculated from the thermal conductivity, K; specific heat, C_p; and density, ρ as follows:

$$\alpha = \frac{K}{\rho C_p}$$

Apparatus have been developed however, which allow the thermal diffusivity to be experimentally determined. Reference 38 includes a bibliography of various methods which can be used. One technique imposes a sinusoidal heat pulse on one end of the specimen. Time-temperature measurements are made at a given location in the specimen. The heat pulse is then changed and the measurements are repeated. The diffusivity can then be calculated. A slight modification of this procedure uses time-temperature measurements at two locations in the specimen and requires only one heat pulse to calculate the diffusivity. Reference 39 discusses another method which uses a second material with known thermal properties adjacent to the specimen. From the time-temperature measurements and the thermal properties of the known substance, the diffusivity of the specimen is determined. The reported error of the diffusivity using this equipment is 3% (Reference 39).

E. Emissivity

Total normal emissivity is experimentally determined by comparing the amount of radiation received from the sample with that received by a black body for exactly the same conditions. The samples are heated to

the specified temperature and the resulting radiation is then measured. Since carbon dioxide and water vapor absorb certain wave lengths of radiation, the tests are usually done at reduced pressure. One of the largest inaccuracies is the measurement of the temperature of the specimen. To determine the inaccuracy in temperature measurement, Armour Research Foundation (Reference 40) used an optical pyrometer to compare the temperature of a platinum sample measured with a thermocouple at 1000°F. A difference of 20°F was found. This was estimated to produce an error of 8% in the emissivity value.

The accuracy of the emissivity also depends on changes in sensitivity of the detector system. Periodic checks with the black body response curve by Armour Research Foundation showed that over a testing period of two years, the detector experienced a 20% decrease in sensitivity. This difference was assigned a 5% indeterminate value.

A 2% inaccuracy was estimated for electronic measurement of the detector signal. The total error estimated by Armour Research Foundation was 10%.

F. Radiation Shape Factors

Radiation shape factors may be analytically derived for simple combinations of surfaces. Reference 41 includes factors for many special cases. Several experimental methods have been devised using mechanical or optical integrating devices, electrical analogues or models. Reference 42 includes a discussion of various analytical and experimental methods used to find shape factors.

A recently developed apparatus is discussed in Reference 43. This apparatus provides a plane source of diffused light for experimentally determining shape factors between surfaces. The apparatus uses a special detector to minimize the cosine error. Sources of error include the lack of perfectly diffuse emission on the plane and the inaccuracy in simulating the model configuration and reading the detector. Comparison of the experimental results of certain simple configurations which were analytically determined showed very close agreement.

Since the accuracy is greatly dependent on the complexity of the configuration and the skill of the operator, the overall error is difficult to assess. Assuming a high skill level of the operator, the experimental techniques should provide shape factors within 10% for most configurations.

APPENDIX VI

TESTING INACCURACIES FOR RADIANT HEAT TESTING

This appendix discusses in detail various testing inaccuracies. Panel, reduced and full size vehicle specimens are considered both for sea level and altitude simulated testing. The first two sections discuss inaccuracies in general, followed by the last section which discusses inaccuracies for the specific specimens of this study.

I. EXPERIMENTAL INACCURACIES FOR PANEL, REDUCED OR FULL SIZE SPECIMENS

A. Inaccuracies Common to Panel, Reduced or Full Size Specimens

One error which is common to radiant heat testing of panels, reduced or full size specimens, is the inability to exactly reproduce the desired surface temperatures on the test specimen. This error may have numerous sources, including inaccuracy in measuring the surface temperature, inaccuracy in reproducing exactly the time-temperature profile, and errors caused by non-uniform temperature distribution on the specimen.

The measurement of transient surface temperatures of a specimen heated in the range of 1000°F to 2500°F is subject to significant inaccuracies with presently used instrumentation. If thermocouples are used, inaccuracies occur because of thermocouple attachment methods, radiation to (or from) the thermocouple bead (because of differences in the emissivity of the thermocouple and the surface), inadequate response rates of the thermocouples and measuring devices, induced currents in the thermocouple from stray electric sources, and conduction of heat from the thermocouple leads. Reference 44 discusses the magnitudes of some of these inaccuracies. Reference 45 shows the effect of attaching the thermocouple to the back surface of the skin to reduce the radiation error. These factors generally will cause the indicated temperature to be less than the actual surface temperature. Reference 46 is a comprehensive list of thermocouples and corresponding operating temperatures.

Other high temperature measurement instruments include (1) total radiation devices, (2) brightness or optical pyrometers, and (3) two color pyrometers. Reference 47 outlines the advantages and disadvantages of each method. These temperature indicating devices are less reliable than properly attached and shielded thermocouples, especially for measuring transient temperatures. Reference 48 is a current publication on methods and application of temperature measurement.

With the automatic temperature-time programmers commercially available, the error caused from not following exactly the time-temperature profile during heating is very small unless the required temperature or heat fluxes are near the maximum capability of the heaters. When the required surface temperature is decreasing, cooling might be required on the specimen. If the test is conducted at sea level, air or carbon dioxide can be used for cooling, but for tests conducted in an altitude chamber, cooling is more difficult. This problem is discussed in more detail in the next section.

The error from non-uniform temperature distribution on the surface of the specimen will depend on the required heat transfer and the resulting complexity of the array of lamps. For low heat rates, close lamp spacing is required to obtain even distribution. For high heat rates, the lamps are spaced as closely as possible, and for some tests, double rows of lamps are required to obtain the desired heat rates.

Another source of error is in the determination of the amount of heat which is transferred through the specimen. Heat gages or heat sinks would be used, depending on the specimen and testing conditions. The inaccuracy associated with measuring the heat transfer will be discussed in more detail later for the specific specimens.

B. Inaccuracies of Panel Testing

Edge effects allow heat to flow parallel to the panel which introduces one of the major error sources for testing panels. These effects can be minimized by insulating the edges, testing larger panels, or possibly by providing guard heaters on the edges. A second error source results from the buckling which often accompanies the heating of panels. The buckling causes extreme changes in geometry of the components. Erroneous temperature measurements on the unheated side of the panel will result from convection and radiation unless the panel is properly shielded.

C. Scale Vehicles

Scaled vehicles, as considered in this report, are actually reduced surface area specimens since the specimen is fabricated from the full thickness materials. If the material thickness is not full size, the problems of similitude must be considered. Appendix VII discusses these problems.

Testing reduced size specimens of the complete vehicle will eliminate the edge effects which occur from testing panels. If a temperature gradient exists on the vehicle, the testing with each zone simulated will be more accurate than using the test results from one or two panels for the vehicle as would be done with panel testing. The actual size of the reduced size specimen to be tested will depend on the cost of specimen fabrication and testing; however, the specimen must be of sufficient size to allow full size thickness to be used and to allow satisfactory temperature distribution on the specimen.

D. Full Size Vehicles

The full size specimen will have errors very similar to the reduced size test. Depending on the size of the vehicle, using the full size specimen should increase the uniformity of the temperature distribution on the vehicle. The full size specimen obviously requires more heating equipment than a reduced size test, but individual heater failures are likely to be less important in maintaining the desired temperature distribution.

E. Crew Compartment Testing

The crew (and equipment) compartments for some vehicles could be tested without testing the complete vehicle. The surface temperature on the outer surface of the compartment would be calculated and this temperature would be imposed on the specimen for the test. This crew compartment specimen could be either full or reduced size. The errors for this type of testing are similar to the reduced and full size vehicles except for the additional error caused by calculating the temperature on the outer surface of the crew compartment. The importance of this additional error will depend on the specific vehicle considered.

II. INACCURACIES FOR SEA LEVEL AND ALTITUDE SIMULATED TESTING

A. General

To determine the test to be accomplished, it is necessary to consider not only the test specimen, but also if the test should be conducted at sea level or with altitude simulation. Since some of the thermal properties of the vehicle wall change with pressure, errors will exist unless the pressure variation of the vehicles during the flight profile is pressure-time simulated. Altitude testing at any constant altitude (other than sea level) is not recommended because the additional cost would be very nominal to simulate the time-altitude profile.

B. Sea Level Testing

If the test is conducted at sea level pressure, the test results must either be accepted with the test inaccuracy or some method must be applied to account for the varying altitude (pressure) of the actual vehicle. Assuming first that an attempt will be made to correct the sea level test results, two approaches are possible. The first approach would be to use similitude during the test. This entails changing a test parameter (such as time or temperature) during the test to account for the changes in altitude which have not been simulated. Appendix VII shows that for even a simple wall containing only one material with pressure dependent thermal conductivity, this similitude is not practical.

The second approach would be to analytically correct the sea level test results to reflect the changes in altitude which were not simulated. The manner to be used would be:

1. Analytically predict the results for test conditions (sea level pressure).
2. Compare these analytical predictions with the test results.
3. Adjust the analytical procedure to obtain correlation with the test at sea level.

4. Analytically determine the heat transfer for the altitude-time trajectory using the adjusted analytical procedures.

Careful analysis of this procedure, which at first seems entirely satisfactory, shows that adjustment of test data by this method is likely to introduce rather than correct errors.

There are two possible situations that can arise when comparing analytical and experimental data. The first possibility is that there is a comparable uncertainty in the test data and the analytical results. If this is the case, it could not be determined what direction the analytical results should be corrected.

The second possibility is that there is high confidence that the test data is accurate. For this situation the direction of correction of the analytical results is known and it remains to determine how to perform the adjustments.

The experimentally determined heat transfer through the specimen would not give sufficient information to adjust the analytical program, since it would not be known what factor in the analytical method should be corrected to correlate the experimental data. The correlation procedure required would be to compare both the heat transfer and temperature-time profiles for each component of the wall. Knowing the experimental results are correct, the analytical study could then be adjusted to correspond to the experimental heat transfer and temperature profiles. This correlation would be very complex and, because of thermocouple inaccuracy, large errors very likely would be introduced into the analytical study. In addition to inaccuracy in the thermocouple and heat flow measurements, any location errors of the thermocouples would result in incorrect adjustments. Another problem would be to resolve the experimental heat transfer for each flow path, if the wall section contained parallel paths. The heat transfer measured would be the total for all paths. Even assuming the analytical and experimental methods could be correlated at sea level, the analytically determined heat transfer for the altitude condition does not include any experimental altitude effects.

Because of the difficulty in using an analytical adjustment procedure for sea level testing, this report assumes the test data will be accepted without attempting to decrease the error by subsequently using a mathematical method. The error in accepting this data will, of course, depend on how important the pressure dependent components are to the heat transfer. By examining the pressure variable components of the wall, it can often be determined if the experimental sea level heat transfer is greater or less than the actual altitude-time heat transfer. For example, if the only pressure variable component is an insulation which has decreased conductivity with increased altitude (for a given mean temperature) the sea level test would show higher heat transfer than the actual heat transfer. This data could be then accepted as being "conservative" compared to the altitude heat transfer.

C. Altitude Simulated Testing

Altitude testing could be accomplished either by (1) testing the whole specimen in an altitude chamber or (2) fabricating the specimen so that the pressure sensitive components could be evacuated individually. The second method probably could be used for panel tests but it is very doubtful if it could be applied to reduced or full size specimens. The cost comparison assumes the testing is accomplished within an altitude chamber and the facility cost shown on Figure 31 includes suitable chamber and evacuation equipment. Fabrication of a specimen to allow evacuation of a component would be more expensive, although the facility cost would be somewhat less. Note, however, on Figure 31 that the evacuation chamber for many of the test specimens considered, is not a large part of the total facility cost.

When the heat transfer testing is conducted with altitude simulation, some errors can occur which require evaluation. The most obvious error results from pressure differences between the actual trajectory and the simulated chamber pressure. This error includes inaccuracies in measuring the chamber pressure and the inaccuracies in admitting air to simulate the decreasing altitude of the re-entry.

Another error is caused by failure to simulate the convective coefficient on the unheated side of the specimen. In the vehicle the unheated side is maintained at cabin pressure. The coefficient which exists for altitude testing is probably very unlike the design conditions unless special simulation is provided. This error is discussed in more detail for the drag vehicle testing where the coefficient is very important.

A problem may also occur in providing cooling to the specimen during the decreasing temperature part of the simulation. If the specimen does not cool sufficiently fast with the heaters off, special radiant panels may be required.

III. EXPERIMENTAL ACCURACY FOR GLIDE AND DRAG VEHICLES

A. Glide Vehicle

1. General

The accuracy comparison for the glide vehicle is based on the amount of heat entering the water wall from the outer skin. To show the resulting heat transfer errors caused from errors in simulating the specimen surface temperature, Figures 56, 57, and 58 are included. These figures are for the $\alpha = 12°$, $\ell = 5$ feet and $\alpha = 0°$, $\ell = 5$ feet conditions of the glide vehicle. (The temperature error shown on Figures 56, 57, and 58 (shown in °F) is the error which occurs at the maximum temperature of the temperature-time profile. The percentage error which corresponds to this temperature error was then used to determine the temperature error at all other times.

This same procedure was used for the panel, reduced size, full size, and crew compartment speciments discussed later.) The curves on Figure 56 are for a sea level test and reflect, in addition to the temperature error, the sea level conductivity of the insulation, the sea level water boiling temperatures, and the convective effects between the outer skin and outer insulation at sea level. The curves on Figures 57 and 58 are for altitude simulated testing. These curves include an error from not exactly simulating the altitude-time trajectory. Figure 59 shows the altitude errors used for Figures 57 and 58. Figure 57 shows the resulting heat transfer which would be obtained if the altitude chamber were evacuated to a maximum of 250,000 feet (Curve A, Figure 59). The heat transfer for the test with a maximum evacuation altitude of 150,000 feet (Curve B, Figure 56) is shown on Figure 58. The importance of accurate altitude simulation for the glide vehicle can be seen by comparing the errors of Figures 57 and 58.

The upper surface temperatures of the glide vehicle (Figure 3) are below room temperature for the first hour of re-entry. It has been assumed that temperatures below room temperature would not be simulated, and this error is included for each test.

Figures 56, 57 and 58 do not include the inaccuracy of measuring the test heat transfer through the specimen.

2. Panel Testing

Two sizes of panels were considered for the glide vehicle, a two-foot by four-foot panel and a six-foot by ten-foot panel. For each of these panels, two testing possibilities were assumed.

The first possibility assumes that only one temperature-time test will be done and the results of this test will be applied to the total surface area of the vehicle to obtain the total heat transfer. For this condition, it was assumed that the temperature profile of $\alpha = 12°$, $\ell = 5$ feet would be used.

The second condition assumes that two time-temperature tests would be done and the results of both tests would be applied to the vehicle. The $\alpha = 0°$, $\ell = 5$ feet profile would be used in addition to the $\alpha = 12°$, $\ell = 5$ feet for the two temperature conditions.

Using estimated-film coefficients and air temperatures which occur on the unheated side of the panel during the test resulted in significant errors in the heat entering the water wall. Since heat flowing from the cabin to the water wall can be accurately calculated (knowing the thermal conductance of the honeycomb and the acoustical insulation), the accuracy of the test would be increased by experimentally determining only the heat transfer from the skin. This would require heavily insulating the cabin side of the water wall during the test.

The temperature simulation inaccuracies for each of the panel tests used were:

a. Two-Foot by Four-Foot Panel

A surface temperature error range from +200°F to -150°F was assumed for the $\alpha = 12°$, $\ell = 5$ feet and +100°F to -75°F for $\alpha = 0°$, $\ell = 5$ feet. The smaller errors for the $\alpha = 0°$, $\ell = 5$ feet were assumed because of the lower temperatures of this profile.

b. Six-Foot by Ten-Foot Panel

The error range for the temperature simulation on the six-by-ten panel was assumed to be +150°F to -100°F for $\alpha = 12°$, $\ell = 5$ feet, and +75°F to -50°F for $\alpha = 0°$, $\ell = 5$ feet. The six-by-ten panel was assumed to have three temperature zones. Simulation of the three zones allows the heat transfer to be determined more accurately from the center zone.

The altitude simulated testing assumed the error curve A of Figure 59.

The amount of heat which is transferred through the wall would be determined from the increase in the heat content of the water wall. It was assumed that this heat increase could be measured with an inaccuracy not exceeding 10%.

3. Reduced and Full Size Vehicle Testing

The half and full size specimens are complete structural models of the vehicles with the exception of the nose cone and leading edges. These items have been removed since these areas represent only a small area compared to the total vehicle area. The calculated temperature on the attaching structure of the nose cone and leading edges would be simulated to reproduce the heat transfer which results from these paths. Six heat zones are imposed on the specimen (additional zones could be used with essentially no increase in cost), corresponding to the calculated temperatures and areas. The areas of the vehicle with temperature profiles approximating the $\alpha = 12°$, $\ell = 5$ feet condition have been assumed to have a temperature simulation error range of +125°F to -75°F for the half size vehicle and +100°F to -50°F for the full size vehicle. The lower temperature areas approximating the $\alpha = 0°$, $\ell = 5$ feet condition have been assumed to have a temperature simulation error range of +50°F to -25°F for both the half and full size vehicles.

The amount of heat entering the vehicle would be obtained from measuring the increase in heat in the water wall. It was assumed that this heat increase could be measured with an inaccuracy not exceeding 10%.

The altitude simulated test assumed the error Curve A of Figure 59.

4. Crew Compartment Testing

The crew compartment of some vehicles (such as the glide vehicle of this study) could be tested without testing the complete vehicle. For this test the temperatures on the outer surface of the crew compartment would be calculated. Five heat zones were assumed for this specimen (additional zones could be used with essentially no increase in cost). Half size and full size specimens were both considered. The areas of the compartment with temperature profiles approximating the $\alpha = 12°$, $\ell = 5$ feet conditions have been assumed to have a temperature simulation error range of +150°F to -100°F for the half size specimen and +125°F to -75°F for the full-size specimen. The lower temperature areas approximating the $\alpha = 0°$, $\ell = 5$ feet condition have been assumed to have a temperature simulation error range of +50°F to -25°F for both specimens.

The amount of heat entering the specimen would, as for the previous glide vehicle specimens, be determined from the increase in the heat content of the water wall. The inaccuracy of measuring the heat transfer was assumed to be 10%.

The altitude simulated test assumed the error curve A of Figure 59.

B. Drag Vehicle

1. General

The accuracy comparison for the drag vehicle is based on comparing the total heat entering the vehicle which includes the forward and aft sections of the sphere. To show the resulting error in heat transfer caused by errors in simulation of the specimen surface temperature, Figures 60, 61, 62, and 63 have been included. (The temperature error shown on Figures 60, 61, and 62 (shown in °F) is the error which occurs at the maximum temperature of the temperature-time profile. The percentage error which corresponds to this temperature error was then used to determine the temperature error at all other times. This same procedure was used for the panel, reduced and full size specimens discussed later.) The curves on Figure 60 are for a sea level test and therefore reflect the sea level conductivity in addition to the surface temperature error. The curves on Figure 61 are for the altitude simulated test. These curves include an error caused by not exactly simulating the altitude-time trajectory. The error trajectory of Curve A, Figure 63 was used for these curves.

Figures 60 and 61 show the errors in heat transfer for both the forward and aft sections of the sphere, and the total vehicle.

Figure 62 compares the resulting total heat transfer which would result from various errors in the altitude-time trajectory of the vehicle. The curves on Figure 63 show the error profiles which were assumed.

Comparison of the total heat transfer errors occurring for these altitude errors shows that the heat transfer for the drag vehicle, unlike the glide vehicle, is less sensitive to altitude simulation errors. Accurate simulation of the re-entry profile would be more difficult, however, because of the short flight time of the drag vehicle.

Figures 60, 61, and 62 assume that the inside film coefficient (h_c) and the vehicle compartment temperature (T_c) have been perfectly simulated to the design conditions. The convective heat transfer from the vehicle drag skirt to the aft section of the vehicle which would occur during the test was also included for the sea level and altitude test conditions. The inaccuracy of measuring the heat transfer through the specimen has not been included on these figures.

The inside film coefficient and temperature on the unheated side of the specimen were estimated for the test conditions. The simulation of the inside film coefficient for the altitude test would require the use of radiant panels since the convective film is very small for these conditions. The radiant panels would be located parallel to the unheated side of the specimen. The selection of F_e and the radiant sink temperature to simulate the desired film coefficient requires that the temperature on the unheated side of the speciman be known. Since this temperature is not known until after the test, one of two methods could be used to find the required F_e and radiant panel temperature. The first, and the one assumed for this study, is to analytically determine the temperature. The second method would require testing at various combinations of F_e and radiant panel temperature to obtain a range of inside film coefficients. This approach would involve the expense of testing the panel numerous times. The heat transfer into the aft section of this vehicle is extremely sensitive to this film coefficient and large errors will result unless this parameter is accurately simulated.

2. Panel Testing

Two sizes of panels were considered for the drag vehicle, a two-foot by four-foot panel and a six-foot by ten-foot panel. Because the structure of the forward section of the drag vehicle is different from the structure of the aft secion, two different panels must be fabricated and tested for each size panel considered.

For the two-by-four panel, a surface temperature error range of +200°F to -150°F was assumed. The temperature error range for the six-by-ten specimen was assumed to be +150°F to -100°F.

The panel corresponding to the aft section of the vehicle would be fabricated to include a portion of the drag skirt. The surface temperature would be imposed on the skirt and the heat would be transferred to the part of the panel representing the aft sphere by radiation and convection. Shielding would be required to simulate the radiation from the aft section of the sphere to space.

Heat transfer through the panel for the altitude testing would probably be measured by the temperature rise in the radiant panel. If this method were used, the radiant panel would be insulated to receive only the heat from the test panel. A 10% inaccuracy is assumed for this measurement of heat transfer.

The sea level panel test would use some form of a heat meter: either a portion of the panel or an attached meter. One method would use a heat meter attached between the insulation and the aluminum pressure shell. By measuring the heat transferred through the meter and the transient storage heat of the adjacent aluminum, the heat transferred from the aluminum could be calculated. Another method would utilize the unheated side surface temperature on the panel and the film coefficient to calculate the heat transfer. This procedure would require calibration of the panel, both for various panel temperatures and ambient temperatures to provide values of film coefficients which occurred during the test. A 20% inaccuracy has been assumed for measuring the heat transfer for the sea level tests.

The altitude error curve A of Figure 63 was assumed for altitude simulated testing.

3. Reduced and Full Size Vehicle Testing

The half and full size specimens are complete structural models of the vehicle, except, as mentioned in Chapter IV, the beryllium heat shield has been replaced with a thin skin.

The temperature simulation error range for the half size specimen was assumed to be +125°F to -75°F, and +100°F to -50°F error range was assumed for the full size specimen.

The sea level test would probably use a convective heat sink to maintain the design temperature inside the specimen during the test. This heat sink would be used to measure the heat entering the vehicle. An inaccuracy of 5% was assumed for measuring the heat entering the vehicle.

The altitude tests could be conducted either with or without inside pressure simulation (8,000 feet compartment altitude). If the test was performed with the compartment pressure simulated, the heat entering the vehicles would be measured similar to the sea level testing. If the cabin altitude is not simulated, the radiant heat sink in the form of panels inside the vehicle would be required because of the extremely small inside film coefficients. The method selected in this study assumes the inside pressure is simulated and the inaccuracy of 5% was used for measuring the heat entering the vehicle.

The altitude error curve A of Figure 63 was also used for the altitude simulated tests for the reduced and full size vehicle tests.

APPENDIX VII

SIMILITUDE IN HEAT TRANSFER TESTS

Introduction

The situation under consideration is three-dimensional heat conduction in a body. The outer surface has a prescribed temperature that may vary with both time (τ) and distances (X, Y, and Z). The air temperature on the inner side is to be constant regardless of the heat flux. The heat transfer coefficients are prescribed. The body, in general, will consist of n distinct homogeneous layers of n different materials. The heat capacity of each material is temperature dependent and the conductivity is pressure and temperature dependent where the environmental pressure is a prescribed function of time. The initial temperature is uniform.

The problem is to determine if the solution for the temperature as a function of time and distance can be related to the temperature in a scale model. The scale model may be constructed geometrically similar to the full-size vehicle. The models initial temperature and the variation of the model outer surface temperature with time and distance may be prescribed. The air temperature, pressure and the heat transfer coefficients of the model on the inner side may be prescribed. Only a one-dimensional case will be considered in this investigation because it has been shown that the heat transfer in the study vehicles may be considered one-dimensional. In addition, the one-dimensional problem presents the minimum complexity.

One Dimensional Heat Conduction Equation With Temperature Dependent Properties

The first step in the investigation will be to consider the case where the material properties are functions of temperature only; the pressure history is constant. The one-dimensional conduction equation for the case of temperature-dependent thermal properties is:

$$\rho(x)C_p(x,T)\frac{\partial T}{\partial \tau} = \frac{\partial}{\partial x}\left[K(x,T)\frac{\partial T}{\partial x}\right] \qquad (1)$$

The equation applies at any point where the material properties are smooth functions of x, i.e., at points where the properties change discontinuously, Equation (1) does not apply. Therefore, it can be assumed that the body consists of n such regions and Equation (1) applies in any region of length L.

Making the changes of variables

$$\bar{u} = T/V \qquad (2)$$

$$\bar{x} = x/L \qquad (3)$$

where V is a fixed uniform temperature which can conveniently be taken as the initial

temperature. Equation (1) can be written

$$\rho(\bar{x})Cp(\bar{x},\bar{u})\frac{\partial \bar{u}}{\partial \tau} = \frac{1}{L^2}\frac{\partial}{\partial \bar{x}}\left[K(\bar{x},\bar{u}\frac{\partial \bar{u}}{\partial \bar{x}}\right] \quad (4)$$

Note that the functions ρ, C_p and K in Equation (1) and Equation (4) are not the same but are related through Equations (2) and (3). Equation (4) may be

$$\frac{Cp(\bar{x},\bar{u})}{Cp(\bar{x},1)}\left[\frac{\partial \bar{u}}{\partial \tau}\right] = \frac{K(\bar{x},1)}{\rho(\bar{x})Cp(\bar{x},1)L^2}\left[\frac{1}{K(\bar{x},1)}\frac{\partial}{\partial \bar{x}}(K(\bar{x},\bar{u}\frac{\partial \bar{u}}{\partial \bar{x}})\right] \quad (5)$$

where, for example, $C_p(\bar{x}, 1)$ is the initial heat capacity (at $\bar{u} = 1$ or $T = V$). If a characteristic time is defined as

$$\tau = \frac{K(\bar{x}, 1)\tau}{\rho(\bar{x})Cp(\bar{x}, 1)L^2} \quad (6)$$

(5) becomes

$$\frac{Cp(\bar{x},\bar{u})}{Cp(\bar{x}, 1)}\left[\frac{\partial \bar{u}}{\partial \bar{\tau}}\right] = \frac{1}{K(\bar{x}, 1)}\frac{\partial}{\partial \bar{x}}\left[K(\bar{x}, \bar{u})\frac{\partial \bar{u}}{\partial \bar{x}}\right] \quad (7)$$

In all cases of practical interest, the body consists of n distinct regions of uniform material properties. This simplifies the situation considerably. Equation (7) takes the form

$$\frac{Cp(\bar{u})}{Cp(1)}\frac{\partial \bar{u}}{\partial \bar{\tau}} = \frac{\partial}{\partial \bar{x}}\left[\frac{K(\bar{u})}{K(1)}\frac{\partial \bar{u}}{\partial \bar{x}}\right] \quad (8)$$

and (6) becomes

$$\bar{\tau} = \frac{K(1)\tau}{\rho Cp(1)L^2} \quad (9)$$

so that the characteristic time is now uniform within the region.

The special case of one region, one material, is of interest. It is required that the solutions be identical for the two Models A and B. Leaving aside for that moment the question of boundary conditions, Equation (8) would require that

$$\frac{Cp(\bar{u})}{Cp(1)} = \frac{c_p(\bar{u})}{c_p(1)} \qquad (10)$$

$$\frac{K(\bar{u})}{K(1)} = \frac{k(\bar{u})}{k(1)} \qquad (11)$$

where the upper case refers to the full-size Model A and the lower case refers to the small Model B.

Note the Equation (10) and Equation (11) do not require the two models to be of the same material, but only that corresponding thermal properties as a function of temperature ratio be of the same functional shape. For example, suppose that the heat capacity can be written.

$$C_p(\bar{u}) = A + Bg(\bar{u}), \quad c_p(\bar{u}) = a + b\,g(\bar{u}) \qquad (12)$$

where $g(1) = 0$ and $g(\bar{u})$ is the same function in both cases but where the initial temperature V and v need not be the same. Then (10) requires that $B/A = b/a$. A similar relationship would have to be satisfied by the conductivity at the same initial temperatures V and v as for the heat capacity.

It is extremely doubtful, however, if any practical situation exists where two different materials will yield the same solution. For example, considering the case where the thermal properties are linear functions of temperature as in the sketch below,

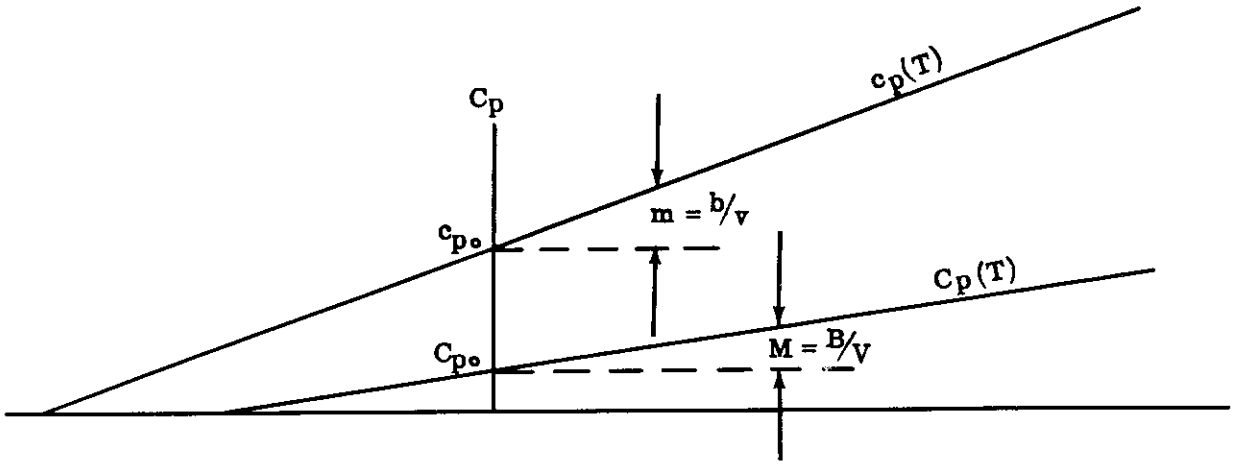

then,

$$C_p(T) = C_{po} + MT = C_{po} + \frac{B}{V}T = C_{po} + B\bar{u}$$
$$c_p(T) = c_{po} + mT = c_{po} + \frac{b}{v}T = c_{po} + b(\bar{u}) \qquad (13)$$

where M, m are the slopes of the respective lines and B,b are the coefficients in Equation (12). In order to put Equation (13) in the form of Equation (12) and have $g(1) = 0$ let

$$A = C_{po} + B, a = c_{po} + b \qquad (14)$$

then,

$$C_p(\bar{u}) = A + B\left[\frac{T}{V} - 1\right]$$
$$c_p(\bar{u}) = a + b\left[\frac{T}{v} - 1\right] \qquad (15)$$

The condition given by Equation (10), $B/A = b/a$, then gives $\frac{MV}{A} = \frac{mv}{a}$.

The quantities M, V, and A are fixed by the given conditions of Model A. The quantity m is fixed by the choice of the material for Model B. Then, from (14)

$$\frac{V}{a} = \frac{V}{c_{po} + mv} = \frac{MV}{mA} = C_1 \qquad (16)$$

where C_1 is a constant depending upon the choice of the material for Model B, Equation (16) can be solved uniquely for v giving

$$v = C_1 c_{po}/(1 - C_1 m) \qquad (17)$$

Equation (17) gives the initial temperature in Model B that must be required; this requirement results from the condition that must be satisfied by the temperature dependence of the heat capacity. However, Equation (11) will result in a similar equation, i.e.,

$$v = C_2 Ko/(1 - C_2 m') \qquad (18)$$

In general, Equations (17) and (18) will determine two different values of v. We conclude that as a practical matter both models must be constructed of the same material.

Having determine that Equations (10) and (11) require that the thermal properties of corresponding regions be identical, it remains to determine the remaining conditions that must be satisfied. Consider a multi-regional problem. The models must be geometrically similar, i.e., $L_1/l_1 = L_2/l_2 \ldots = Ln/ln$, same ratio of characteristic times. Note the initial conditions must be the same in both models.

The boundary conditions in Model B which correspond to those in Model A follow immediately from Equation (9). For if τ is real time when considering Model A, real time in Model B will be $(\tau l^2/L^2)$.

One Dimensional Heat Conduction Equation With Temperature & Pressure Dependent Properties

If the conductivity is pressure and temperature dependent and the heat capacity temperature dependent, the differential equation is

$$\rho Cp(T) \frac{\partial T}{\partial \tau} = \frac{\partial}{\partial x}\left[K(T,\tau) \frac{\partial T}{\partial \tau}\right] \qquad (19)$$

This cannot be put into the form of Equation (8) by a transformation of the type $\bar{x} = x/L$, $\bar{u} = T/V$, $\bar{\tau} = f(\tau)$. That is, a transformation of this type will not transform Equation (19) to the form of Equation (8); instead, the coefficient involving conductivity will always be time dependent. Hence, the pressure dependent and non-pressure dependent situations cannot be related by a transformation of this type.

It is possible that for special forms of $K(T,\tau)$ Equations (19) and (8) may be transformed to a common form by a non-linear transformation; for example, $\bar{x} = x/L$, $\bar{u} = T/V$, $\bar{\tau} = f(T,\tau)$. However, even if such a transformation could be found, it would probably be impractical; the most likely reason being that the boundary conditions could not be made identical in the two models. Linear equations can often be transformed, but, as has been previously demonstrated by the temperature dependent case, in a non-linear equation a change in the function form of a coefficient containing the dependent variable will generally result in an unrelated system. The opinion is, therefore, offered that the temperature-pressure dependent case represents an essentially different non-linear system from the temperature dependent case.

CONCLUSIONS

1. For the case of material properties dependent upon temperature only, it can be concluded that as a practical matter both models, full size and scale must be made of the same material and have the same initial temperature and temperature history. In addition, real time will be related by the ratio of the geometric scale factor squared.

2. For the case of material properties dependent upon both temperature and pressure, no simple relationship exists linking the heat flow in a model to that in a full size specimen if their pressure history are not identical.

3. For many insulations the variation in thermal conductivity with altitude is too large to be ignored in test planning. The foregoing investigation shows that the prototype's pressure history, temperature history and material should be duplicated in the test situation.

COST SUMMARY GLIDE VEHICLE

TABLE 1

NO. OF PHYSICAL SUBDIVISIONS	DIGITAL COMPUTER				DIFFERENTIAL ANALYZER				PASSIVE ELEMENT ANALOGUE				HAND CALCULATIONS			
	10	8	4	2	8	4	2	1	8	4	2	1	10	8	4	2
% ERROR	0	.46	3.75	10.65	1.74	7.50	25.5	37.6	9.14	16.8	29.3	43.6	0	.46	3.75	10.65
PRELIMINARY ENGINEERING HRS																
SET UP	198 ←															→198
MATERIALS PREPARATION	16 ←							→16	12	12	12	12	20	20	20	20
COORDINATION	9	9	9	9	24	24	24	24	27	27	27	27	1	1	1	1
SOLUTION																
ORIENTATION HRS	48	48	48	48	98.5	98.5	98.5	98.5	80	80	80	80	6	6	6	6
SETUP HRS	3	2.4	1.8	1.2	42	41.5	41	41	63	63	61	61	30	24	12	6
HR. DELAYS	16	16	16	16	40	40	40	40	40	40	40	40	-	-	-	-
CHECK OUT HRS	3	3	2	2	8	8	8	8	26	26	26	25	-	-	-	-
MACHINE RUN HRS	3.2	2.1	1.0	0.9	3.8	2.0	1.2	0.8	3.8	2.0	1.2	0.8	72.000	32.800	4600	576
DATA REDUCTION	1	1	.8	.6	.2	.2	.2	.2	.2	.2	.2	.2	1	1	.8	.6
TOTAL MAN HRS	58	56	54	53	153	150	149	148	173	171	168	167	72037	32831	4619	589
CONSOLE HRS.	3.2	2.1	1.0	0.9	51	50	50	50	65	65	65	65	-	-	-	-
CALENDAR DAYS	9	9	9	9	24	24	24	24	27	27	27	27	9005	4112	578	73
MAN HR $ COST	542	524	505	496	1431	1403	1393	1384	1618	1599	1571	1561	630000	288000	40000	5154
CONSOLE $ COST	1120	735	350	315	2142	2100	2100	2100	2730	2730	2730	2730	-	-	-	-
$ COST	1662	1259	855	811	3573	3503	3493	3484	4348	4329	4301	4291	630000	288000	40000	5154
SOLUTION + ENGINEERING																
TOTAL MAN HR	281	279	277	276	391	388	387	386	410	408	405	404	72256	33114	4846	795
TOTAL $ COST	3747	3344	2940	2896	5798	5728	5718	5709	6564	6545	6517	6507	632000	290000	42500	7202
TOTAL CALENDAR	36	36	36	36	51	51	51	51	56	56	56	56	9032	4139	606	99
REPEAT SOLUTION																
MAN HRS.	.5	.5	.5	.5	.1	.1	.1	.1	.1	.1	.1	.1	72000	328000	4600	576
$ COST	1120	735	350	315	162	85	51	34	162	85	51	34	630000	288000	40000	5154

COST SUMMARY DRAG VEHICLE

TABLE II

METHOD		DIGITAL COMPUTER					DIFFERENTIAL ANALYZER				PASSIVE ELEMENT ANALOGUE			HAND CALCULATIONS				
NO. OF PHYSICAL SUBDIVISIONS		10	8	6	4	2	8	6	4	2	8	4	2	10	8	6	4	2
FORWARD % ERROR (ALL ERRORS AFT % ERROR SHOWN ARE TOTAL % ERROR MINUS)		0 0 0	.23 0 .07	1.26 0 .38	3.46 0 1.05	21.16 0 6.40	9.75 0 2.95	12.3 0 3.72	18.2 0 5.50	37.6 0 11.4	42.3 0 12.8	40.2 0 12.2	28.9 0 8.75	0 0	.23 0	1.26 0	3.46 0	21.16 0
FORWARD SIDE PRELIMINARY ENGINEERING	SET UP & ORIENTATION HRS MATERIAL PREPARATION HRS COORDINATION HRS	99 6 7	99 5 7	99 5 7	99 5 7	99 4 7	99 5 7	99 5 7	99 5 7	99 4 7	99 5 7	99 5 7	99 4 7	99 6 7	99 5 7	99 5 7	99 5 7	99 4 7
FORWARD SIDE SOLUTION	ORIENTATION HRS SET UP HRS DELAYS HRS CHECKOUT MACHINE HRS ACTUAL MACHINE RUN HRS DATA REDUCTION HRS	80 10 24 3 .12 1	80 8 24 3 .08 1	80 6 24 2 .07 .8	80 4 24 2 .03 .6	80 2 24 1 .02 .5	68 3 40 7 .08 .2	68 2 40 6 .08 .2	68 2 40 6 .08 .2	68 1 40 5 .07 .2	72 24 40 12 .02 .2	72 24 40 9 .02 .2	72 24 40 8 .02 .2	2 14 1038 1	2 11 531 1	2 8 225 .8	2 6 67 .6	2 1.4 8 .5
	TOTAL MAN HRS TOTAL CONSOLE HRS TOTAL CALENDAR DAYS	94 .12 15	92 .08 15	89 .07 15	87 .03 15	84 .02 14	78 13 14	76 13 14	76 13 14	74 13 14	108 17 19	105 17 18	104 17 18	1054 133	547 68	236 29	76 9	12 2
	TOTAL MANHOUR $ COST TOTAL CONSOLE $COST TOTAL DOLLAR COST	878 41 919	860 29 889	832 23 855	813 12 825	785 6 791	729 536 1265	710 535 1245	710 535 1245	691 534 1225	1009 714 3461	981 714 3432	972 714 3422	9223 9223	4786 4786	2065 2065	665 665	105 105
FORWARD SIDE SOLUTION & ENGINEERING	TOTAL MANHOURS TOTAL CALENDAR DAYS TOTAL DOLLAR COST	206 29 1967	203 29 1927	200 28 1893	198 28 1863	194 27 1819	189 29 2303	187 28 2283	187 28 2283	184 28 2254	219 32 2711	216 32 2713	214 27 2715	1166 146 10270	658 82 5823	347 43 3102	187 23 1702	122 15 1133
AFT SIDE PRELIMINARY ENGINEERING	SET UP & ORIENTATION HRS MATERIAL PREPARATION HRS COORDINATION HRS	105 3 3	105 3 3	105 2 3	105 2 3	105 1 3	105 3 6	105 2 6	105 2 6	105 1 6				105 3 1	105 3 1	105 2 1	105 2 1	105 1 1
AFT SIDE SOLUTION	ORIENTATION HRS SET UP HRS DELAYS HRS CHECKOUT MACHINE HRS ACTUAL MACHINE RUN HRS DATA REDUCTION HRS	24 2.5 24 3 .03 .2	24 2.0 24 3 .03 .2	24 2.0 24 3 .03 .2	24 1.5 24 3 .03 .2	24 0.5 24 3 .02 .2	42 3 40 16 .09 .2	42 2 40 12 .08 .2	42 2 40 8 .06 .2	42 1 40 4 .05 .2				4.5 3.1 15 .2	4.5 2.8 12 .2	4.5 2.6 9 .2	4.5 2.4 6 .2	4.5 2.4 3 .2
	TOTAL MAN HOURS TOTAL CONSOLE HOURS TOTAL CALENDAR DAYS	30 .03 7	29 .03 7	29 .03 7	29 .03 7	28 .02 7	61 16 12	56 16 12	52 15 12	47 15 12				23 3	20 3	17 2	13 2	10 1
	TOTAL MANHOUR $ COST TOTAL CONSOLE $COST TOTAL $ COST	280 12 292	271 12 283	271 12 283	271 12 283	262 6 268	570 672 1242	524 672 1196	486 630 1116	439 630 1069				201 201	175 175	149 149	114 114	88 88
AFT SIDE SOLUTION & ENGINEERING	TOTAL MANHOURS TOTAL CALENDAR DAYS TOTAL $ COST	141 21 1330	140 21 1321	139 21 1312	139 21 1312	137 21 1287	175 28 2308	169 28 2853	165 28 2173	159 28 2116				132 17 1220	129 16 1194	125 16 1159	121 15 1124	117 14 1088
TOTAL DRAG VEHICLE	MANHOURS CALENDAR DAYS DOLLAR COST	347 50 3297	343 50 3248	339 49 3205	337 49 3175	331 48 3107	364 57 4611	356 57 4536	352 57 4456	343 57 4370				1298 163 11490	787 98 7018	472 59 4262	308 38 2827	239 29 2222
DOLLAR COST FOR REPEAT SOLUTION		41	29	23	12	6	6	6	6	6	6	6	6	11500	7000	4000	3000	2000

TABLE III

SPECIMEN FABRICATION ESTIMATES

RADIANT HEAT TEST SPECIMENS

SPECIMEN IDENTIFICATION		FIRST SPECIMEN								SECOND SPECIMEN		
SPECIMEN SIZE	SPECIMEN WEIGHT	FABRICATION TIME MANHOURS			SPECIMEN COST DOLLARS [1]			CALENDAR TIME WEEKS [2]		FABRICATION TIME MANHOURS	SPECIMEN COST DOLLARS [1]	CALENDAR TIME WEEKS [2]
		ENGINEERING		SHOP MANHOURS	LABOR		MATERIALS					
		DESIGN	FABRICATION		DESIGN	FABRICATION		DESIGN	FABRICATION			
GLIDE VEHICLE TEST PANEL (2 FT. X 4 FT.)	30	250	100	1400	2,300	12,500	1800	3	7	800	8000	1
GLIDE VEHICLE TEST PANEL (6 FT X 10 FT)	225	300	150	3400	2,800	29,700	4400	3	12	2000	20,000	3
HALF SIZE GLIDE VEHICLE	1520	1900	1100	222,000	17,800	1,866,000	182,000	8	55	84,700	805,000	8
HALF SIZE GLIDE VEHICLE CREW COMPT ONLY	100	750	600	21,000	5600	175,000	14,500	5	30	7,300	68,000	6
FULL SIZE GLIDE VEHICLE	3400	2500	1300	294,000	23,400	2,468,000	324,000	8	64	120,500	1,229,000	12
FULL SIZE GLIDE VEHICLE CREW COMPT. ONLY	320	1000	760	27,400	9,400	238,000	30,400	5	38	10,500	108,000	10
DRAG VEHICLE TEST PANEL (2 FT X 4 FT.)	24	200	100	660	1,900	6,500	2,200	3	6	300	4,500	1
DRAG VEHICLE TEST PANEL (6 FT. X 10 FT)	180	250	200	6,400	2,300	54,200	11,400	3	14	3,000	32,400	4
HALF SIZE DRAG VEHICLE	190	800	480	8,070	7,500	71,900	13,400	6	24	3,300	37,500	4
FULL SIZE DRAG VEHICLE	730	1000	640	26,600	9,400	228,000	47,500	6	32	12,100	140,000	8

[1] BASED ON THE FOLLOWING LABOR COSTS: ENGINEERING 9.35 DOLLARS / HR.
SHOP 8.35 DOLLARS / HR.

[2] BASED ON TWO 8-HOUR SHIFTS PER DAY.

TABLE IV

SEA LEVEL-MANHOUR ESTIMATES

RADIANT HEAT TESTING

TEST IDENTIFICATION			FIRST TEST MANHOURS							SECOND TEST MANHOURS [1]			
			TEST PLAN		TEST SETUP		TEST RUN		DATA REDUCTION	TEST SETUP		TEST RUN	
SPECIMEN DESCRIPTION	HEAT ZONES	THERMO-COUPLES	ENGR. HOURS	DRAFT. HOURS	ENGR. HOURS	SHOP HOURS	ENGR. HOURS	SHOP HOURS	AIDE HOURS	ENGR. HOURS	SHOP HOURS	ENGR. HOURS	SHOP HOURS
GLIDE VEHICLE TEST PANEL (2 FT. X 4 FT.)	1	30	85	25	26	48	12	10	114	22	35	10	2
GLIDE VEHICLE TEST PANEL (6FT. X 10 FT.)	3	75	120	40	71	120	44	22	233	54	78	40	6
HALF SIZE GLIDE VEHICLE	6	130	400	200	264	630	132	75	500	104	266	124	24
HALF SIZE GLIDE VEHICLE CREW COMPT. ONLY	5	130	290	90	200	545	70	50	500	70	170	70	10
FULL SIZE GLIDE VEHICLE	6	180	492	216	400	1060	160	104	700	230	580	120	24
FULL SIZE GLIDE VEHICLE CREW COMPT. ONLY	5	130	426	150	254	680	120	70	500	84	190	120	26
DRAG VEHICLE TEST PANEL (2 FT. X 4 FT.)	1	30	85	25	28	64	8	10	139	23	47	8	2
DRAG VEHICLE TEST PANEL (6 FT. X 10 FT.)	3	75	132	56	77	142	28	26	258	58	82	24	10
HALF SIZE DRAG VEHICLE	3	90	344	64	150	435	30	50	390	70	130	26	10
FULL SIZE DRAG VEHICLE	3	115	360	80	304	610	40	96	500	114	160	40	16

[1] DATA REDUCTION MANHOURS ARE SIMILAR FOR FIRST AND SECOND TESTS.

TABLE V

VEHICLE ALTITUDES SIMULATED - MANHOUR ESTIMATES

RADIANT HEAT TESTING

TEST IDENTIFICATION			FIRST TEST MANHOURS							SECOND TEST MANHOURS [1]			
			TEST PLAN		TEST SETUP		TEST RUN		DATA REDUCTION	TEST SETUP		TEST RUN	
SPECIMEN DESCRIPTION	HEAT ZONES	THERMO-COUPLES	ENGR. HOURS	DRAFT. HOURS	ENGR. HOURS	SHOP HOURS	ENGR. HOURS	SHOP HOURS	AIDE HOURS	ENGR. HOURS	SHOP HOURS	ENGR. HOURS	SHOP HOURS
GLIDE VEHICLE TEST PANEL (2 ft X 4 ft)	1	30	115	30	52	100	15	14	114	26	50	13	6
GLIDE VEHICLE TEST PANEL (6 ft X 10 ft)	3	75	160	50	142	240	52	30	233	62	108	48	10
HALF SIZE GLIDE VEHICLE	6	130	480	240	518	1250	150	95	500	120	465	144	44
HALF SIZE GLIDE VEHICLE CREW COMPT ONLY	5	130	370	130	400	1090	90	70	500	80	270	90	30
FULL SIZE GLIDE VEHICLE	6	180	572	256	675	2100	190	134	700	260	980	150	74
FULL SIZE GLIDE VEHICLE CREW COMPT. ONLY	5	130	506	190	450	1350	140	90	500	104	340	140	46
DRAG VEHICLE TEST PANEL (2 ft X 4 ft)	1	30	115	30	56	130	11	13	139	27	62	11	5
DRAG VEHICLE TEST PANEL (6 ft X 10 ft)	3	75	172	66	154	285	34	32	258	66	112	30	16
HALF SIZE DRAG VEHICLE	3	90	424	80	300	870	40	60	390	83	180	34	18
FULL SIZE DRAG VEHICLE	3	115	440	100	500	1200	50	105	500	134	240	50	26

[1] DATA REDUCTION MANHOURS ARE SIMILAR FOR FIRST AND SECOND TEST.

TABLE VI

SEA LEVEL-COST ESTIMATE

RADIANT HEAT TESTING

TEST IDENTIFICATION			FIRST TEST DOLLARS [1]					SECOND TEST DOLLAR-COST [1] [2]			
				TEST SETUP				TEST SETUP			
SPECIMEN DESCRIPTION	HEAT ZONES	THERMO-COUPLES	TEST PLAN	LABOR	MATER-IALS	TEST RUN	DATA REDUC-TION	LABOR	MATER-IALS	TEST RUN	DATA REDUC-TION
GLIDE VEHICLE TEST PANEL (2 ft X 4 ft)	1	30	1000	650	450	200	1000	500	100	100	1000
GLIDE VEHICLE TEST PANEL (6 ft X 10 ft)	3	75	1500	1,650	600	600	2050	1150	200	450	2050
HALF SIZE GLIDE VEHICLE	6	130	5500	7,750	1000	1850	4400	3200	265	1350	4400
HALF SIZE GLIDE VEHICLE CREW COMPT. ONLY	5	130	3500	6,400	800	1100	4400	2100	200	750	4400
FULL SIZE GLIDE VEHICLE	6	180	6500	12,600	1700	2350	6100	7000	400	1300	6100
FULL SIZE GLIDE VEHICLE CREW COMPT. ONLY	5	130	5300	8,050	1400	1700	4400	2400	350	1350	4400
DRAG VEHICLE TEST PANEL (2 ft X 4 ft)	1	30	1000	350	250	150	1200	600	100	100	1200
DRAG VEHICLE TEST PANEL (6 ft X 10 ft)	3	75	1750	1900	500	500	2250	1200	200	300	2250
HALF SIZE DRAG VEHICLE	3	90	3800	5000	600	700	3400	1750	265	325	3400
FULL SIZE DRAG VEHICLE	3	115	4000	8000	900	1200	4400	2400	450	500	4400

[1] BASED ON THE FOLLOWING LABOR COSTS: ENGINEERING 9.35 DOLLARS/HR, SHOP 8.35 DOLLARS/HR, DRAFTING & ENG. AIDE 8.75 DOLLARS/HR

[2] INCLUDES MANUAL REDUCTION OF DATA FROM TEMPERATURE-TIME STRIP RECORDERS AND CALCULATION OF HEAT FLOW. SPECIMEN FABRICATION COST NOT INCLUDED, SEE TABLE III

THESE COSTS ASSUME THE SECOND SPECIMEN IS TESTED CONSECUTIVELY WITH FIRST SPECIMEN.

TABLE VII

VEHICLE ALTITUDES SIMULATED - COST ESTIMATE

RADIANT HEAT TESTING

TEST IDENTIFICATION			FIRST TEST DOLLAR COST [1]					SECOND TEST DOLLAR COST [1] [2]			
DESCRIPTION	HEAT ZONES	THERMO-COUPLES	TEST PLAN	TEST SETUP		TEST RUN	DATA REDUC-TION	TEST SETUP		TEST RUN	DATA REDUC-TION
				LABOR	MATER-IALS			LABOR	MATER-IALS		
GLIDE VEHICLE TEST PANEL (2 ft X 4 ft)	1	30	1350	1300	550	250	1000	650	150	175	1000
GLIDE VEHICLE TEST PANEL (6 ft X 10 ft)	3	75	1950	3350	700	750	2050	1500	250	550	2050
HALF SIZE GLIDE VEHICLE	6	130	6600	15, 300	1200	2200	4400	5000	375	1700	4400
HALF SIZE GLIDE VEHICLE CREW COMPT. ONLY	5	130	4500	12,800	1000	1450	4400	3000	300	1100	4400
FULL SIZE GLIDE VEHICLE	6	180	7600	24, 000	2000	2900	6100	10, 600	600	2000	6100
FULL SIZE GLIDE VEHICLE CREW COMPT. ONLY	5	130	6400	15, 500	1650	2050	4400	3800	550	1700	4400
DRAG VEHICLE TEST PANEL (2 ft X 4 ft)	1	30	1350	1600	350	200	1200	775	150	150	1200
DRAG VEHICLE TEST PANEL (6 ft X 10 ft)	3	75	2150	3850	600	600	2250	1550	250	400	2250
HALF SIZE DRAG VEHICLE	3	90	4650	10, 000	700	900	3400	2300	375	475	3400
FULL SIZE DRAG VEHICLE	3	115	5000	14, 700	1100	1350	4400	3250	600	700	4400

[1] BASED ON THE FOLLOWING LABOR COSTS: ENGINEERING 9.35 DOLLARS/HR, SHOP 8.35 DOLLARS/HR, DRAFTING & ENGINEERING AIDE 8.75 DOLLARS/HR.
INCLUDES MANUAL REDUCTION OF DATA FROM TEMPERATURE-TIME STRIP RECORDERS AND CALCULATION OF HEAT FLOW. SPECIMEN FABRICATION COST NOT INCLUDED, SEE TABLE III

[2] THESE COSTS ASSUME THE SECOND SPECIMEN IS TESTED CONSECUTIVELY WITH FIRST SPECIMEN

TABLE VIII

SEA LEVEL - CALENDAR TIME ESTIMATES

RADIANT HEAT TESTING

TEST IDENTIFICATION			FIRST TEST CALENDAR WORK DAYS [1]				SECOND TEST CALENDAR WORK DAYS [1]		
SPECIMEN DESCRIPTION	HEAT ZONES	THERMO-COUPLES	TEST PLAN	TEST SETUP	TEST RUN	DATA REDUC-TION	TEST SETUP	TEST RUN	DATA REDUC-TION
GLIDE VEHICLE TEST PANEL (2 ft X 4 ft)	1	30	7	7	7	17	4	7	7
GLIDE VEHICLE TEST PANEL (6 ft X 10 ft)	3	75	7	14	7	21	8	7	14
HALF SIZE GLIDE VEHICLE	6	130	14	30	7	45	21	7	30
HALF SIZE GLIDE VEHICLE CREW COMPT. ONLY	5	130	14	30	7	45	19	7	30
FULL SIZE GLIDE VEHICLE	6	180	21	40	7	64	34	7	44
FULL SIZE GLIDE VEHICLE CREW COMP'T ONLY	5	130	14	30	7	45	21	7	30
DRAG VEHICLE TEST PANEL (2 ft X 4 ft)	1	30	7	7	7	17	4	7	7
DRAG VEHICLE TEST PANEL (6 ft X 10 ft)	3	75	7	14	7	21	8	7	14
HALF SIZE DRAG VEHICLE	3	90	14	30	7	34	17	7	24
FULL SIZE DRAG VEHICLE	3	115	14	30	7	45	18	7	30

[1] BASED ON TWO 8-HOUR SHIFTS PER DAY

TABLE IX

VEHICLE ALTITUDES SIMULATED-CALENDAR TIME ESTIMATES

RADIANT HEAT TESTING

TEST IDENTIFICATION			FIRST TEST CALENDAR WORK DAYS [1]				SECOND TEST CALENDAR WORK DAYS [1]		
SPECIMEN DESCRIPTION	HEAT ZONES	THERMO-COUPLES	TEST PLAN	TEST SETUP	TEST RUN	DATA REDUCTION	TEST SETUP	TEST RUN	DATA REDUCTION
GLIDE VEHICLE TEST PANEL (2 ft X 4 ft)	1	30	11	14	7	17	5	7	7
GLIDE VEHICLE TEST PANEL (6 ft X 10 ft)	3	75	11	28	7	21	10	7	14
HALF SIZE GLIDE VEHICLE	6	130	21	75	7	45	31	7	30
HALF SIZE GLIDE VEHICLE CREW COMPT. ONLY	5	130	21	60	7	45	24	7	30
FULL SIZE GLIDE VEHICLE	6	180	28	120	7	64	48	7	44
FULL SIZE GLIDE VEHICLE CREW COMP'T ONLY	5	130	21	90	7	45	28	7	30
DRAG VEHICLE TEST PANEL (2 ft X 4 ft)	1	30	11	14	7	17	5	7	7
DRAG VEHICLE TEST PANEL (6 ft X 10 ft)	3	75	11	28	7	21	9	7	14
HALF SIZE DRAG VEHICLE	3	90	28	55	7	34	21	7	24
FULL SIZE DRAG VEHICLE	3	115	28	75	7	45	24	7	30

[1] BASED ON TWO 8-HOUR SHIFTS PER DAY.

TABLE X

TOTAL EXPERIMENTAL COST AND TIME ESTIMATES

RADIANT HEAT TESTING

TEST SPECIMEN DESCRIPTION	SEA LEVEL TEST [3]			ALTITUDE SIMULATED TEST [3]		
	TOTAL MAN-HOURS-HOURS	TOTAL CALENDAR TIME-WEEKS [2]	TOTAL TEST COST-DOLLARS [1]	TOTAL MAN-HOURS - HOURS	TOTAL CALENDAR TIME-WEEKS [2]	TOTAL TEST COST-DOLLARS [1]
GLIDE VEHICLE TEST PANEL (2 FT. X 4 FT.)	2,440	19	23,300	2,610	20	25,000
GLIDE VEHICLE TEST PANEL (6 FT. X 10 FT.)	5,320	28	51,000	5,680	32	54,400
HALF SIZE GLIDE VEHICLE	229,300	88	2,105,000	230,800	101	2,118,000
HALF SIZE GLIDE VEHICLE CREW COMPT. ONLY	24,900	60	219,000	26,000	68	228,100
FULL SIZE GLIDE VEHICLE	304,200	107	2,875,000	306,800	128	2,897,000
FULL SIZE GLIDE VEHICLE CREW COMPT. ONLY	33,200	68	315,000	34,700	82	328,800
DRAG VEHICLE TEST PANEL (2 FT. X 4 FT.)	1,757	18	17,600	1,942	19	19,900
DRAG VEHICLE TEST PANEL (6 FT. X 10 FT.)	8,430	30	82,700	8,800	33	86,300
HALF SIZE DRAG VEHICLE	12,100	52	117,800	12,900	58	126,000
FULL SIZE DRAG VEHICLE	31,900	61	318,900	33,000	73	329,000

[1] BASED ON THE FOLLOWING LABOR COSTS: ENGINEERING 9.35 DOLLARS/HR, SHOP 8.35 DOLLARS/HR., DRAFTING & ENGINEERING AIDE 8.75 DOLLARS/ HOUR.

[2] CALENDAR TIME ESTIMATES ASSUME TWO 8-HOURS SHIFTS PER DAY.

[3] THESE ESTIMATES INCLUDE FABRICATION OF THE SPECIMEN AND THREE TESTS.

TABLE XI

GLIDE VEHICLE-COST AND TIME ESTIMATES

MATERIAL THERMAL PROPERTY

NO.	WALL COMPONENT TO BE TESTED	THERMAL PROPERTY TESTED	TEST ALTITUDES REQUIRED	NUMBER OF TESTS: MATERIAL THICKNESS REQUIRED	NUMBER OF TESTS: TEMP. AT EACH ALTITUDE	NUMBER OF TESTS: TOTAL TESTS	TEST COST DOLLARS [1]	TEST TIME CALENDAR WEEKS	TEST TIME MANHOURS: ENGINEERING	TEST TIME MANHOURS: SHOP
1.	OUTER INSULATION	K	6-(SEA LEVEL TO 250,000 FT)	4 (0.5 TO 2.0 IN)	10	240	14700	290	198	1540
		C_p	SEA LEVEL ONLY	1	10	10	80	2.0	4	5
		ρ	SEA LEVEL ONLY	1	1	1	40	0.1	4	-
		ϵ	SEA LEVEL ONLY	1	15	15	65	0.1	6	1
2.	ACOUSTICAL INSULATION	K	2-(SEA LEVEL AND 8,000 FT.)	1	6	12	370	1.0	4	40
		C_p	SEA LEVEL ONLY	1	6	6	70	1.2	4	4
		ρ	SEA LEVEL ONLY	1	1	1	40	0.1	4	-
3.	HONEYCOMB	K	3(SEA LEVEL TO 250,000 FT)	1	10	30	2110	5.1	36	212
		C_p	SEA LEVEL ONLY	1	10	10	70	2.1	4	4
		ρ	SEA LEVEL ONLY	1	1	1	40	0.1	4	
4.	M-252	K	SEA LEVEL ONLY	1	10	10	440	3.0	20	30
		C_p	SEA LEVEL ONLY	1	10	10	70	2.1	4	4
		ρ	SEA LEVEL ONLY	1	1	1	40	0.1	4	-
		ϵ	SEA LEVEL ONLY	1	15	15	65	0.1	6	1
5.	RADIATION SHAPE FACTORS BETWEEN OUTER SKIN & OUTER INSULATION	F_e	SEA LEVEL ONLY	-	--	4	185	0.8	16	4

[1] BASED ON ENGINEERING COST OF 9.35 DOLLARS/HR. & SHOP COST OF 8.35 DOLLARS/HR

TABLE XII

DRAG VEHICLE-COST AND TIME ESTIMATES

MATERIAL THERMAL PROPERTIES

NO.	WALL COMPONENT TO BE TESTED	THERMAL PROPERTY TESTED	TEST ALTITUDES REQUIRED	MATERIAL THICKNESS REQUIRED	TEMP. AT EACH ALTITUDE	TOTAL TESTS	TEST COST DOLLARS [1]	TEST TIME CALENDAR WEEKS	TEST TIME MANHOURS	
									ENGINEERING	SHOP
1.	LOAD CARRYING INSULATION	K	6 (SEA LEVEL TO 250,000 FT)	4 (0.5 TO 2.0 IN)	10	240	14700	30.0	198	1540
		C_p	SEA LEVEL ONLY	1	10	10	80	2.0	4	5
		ρ	SEA LEVEL ONLY	1	1	1	40	0.1	4	—
2.	LOOSE INSULATION	K	6 (SEA LEVEL TO 250,000 FT)	3(.3 TO 1.0 IN)	10	180	11100	20.0	144	1170
		C_p	SEA LEVEL ONLY	1	10	10	70	2.0	4	4
3.	ALUMINUM	K	SEA LEVEL ONLY	1	6	6	370	1.0	7	36
		C_p	SEA LEVEL ONLY	1	6	6	70	2.1	4	4
		ρ	SEA LEVEL ONLY	1	1	1	40	0.1	4	—
		ϵ	SEA LEVEL ONLY	1	15	15	65	0.1	6	1
4.	BERYLLIUM	K	SEA LEVEL ONLY	1	10	10	440	3.0	20	30
		C_p	SEA LEVEL ONLY	1	10	10	70	2.1	4	4
		ρ	SEA LEVEL ONLY	1	1	1	40	0.1	4	—
		ϵ	SEA LEVEL ONLY	1	15	15	65	0.1	6	1
5.	RADIATION SHAPE FACTOR BETWEEN SKIRT AND AFT SECTION	F_e	SEA LEVEL ONLY	—	—	8	365	1.6	32	8

[1] BASED ON ENGINEERING COST OF 9.35 DOLLARS/HR AND SHOP COST OF 8.35 DOLLARS/HR.

TABLE XIII

TOTAL EXPERIMENTAL COST AND TIME ESTIMATES-GLIDE & DRAG VEHICLES

MATERIAL THERMAL PROPERTY

TEST APPARATUS	GLIDE VEHICLE				DRAG VEHICLE			
	TOTAL MAN-HOURS ~ HOURS		TOTAL CALENDAR TIME ~ WEEKS	TOTAL TEST COST~DOLLARS	TOTAL MAN-HOURS ~ HOURS		TOTAL CALENDAR TIME ~ WEEKS	TOTAL TEST COST ~ DOLLARS
	ENGR.	SHOP	[2]	[1]	ENGR.	SHOP	[2]	[1]
1. LOW CONDUCTIVITY TESTER	202	1580	30	15,100	342	2710	50	25,800
2. HIGH CONDUCTIVITY TESTER	56	242	8	2,550	27	66	4	810
3. SPECIFIC HEAT TESTER	16	17	7	290	16	17	6	290
4. DENSITY TESTER	12	-	1	160	12	-	1	120
5. EMISSIVITY TESTER	12	2	1	130	12	2	1	130
6. RADIATION SHAPE FACTOR TESTER	16	4	1	185	32	8	2	365
TOTALS	314	1845	30	18 415	441	2803	50	27515

[1] BASED ON THE FOLLOWING LABOR COST: ENGINEERING 9.35 DOLLARS/HR AND SHOP 8.35 DOLLARS/HR

[2] CALENDAR TIME ESTIMATES ASSUME TWO 8-HOUR SHIFTS PER DAY. SINCE IT IS ASSUMED ALL THE TEST APPARATUS WILL BE USED CONCURRENTLY, THE TOTAL TIME REQUIRED IS DETERMINED FROM THE APPARATUS REQUIRING THE MAXIMUM CALENDAR TIME.

TABLE XIV

GLIDE VEHICLE-HEAT FLOW ERRORS

FROM ERRORS IN
MATERIAL THERMAL PROPERTIES

ASSUMED PERCENT ERRORS IN MATERIAL THERMAL PROPERTIES			CALCULATED PERCENT ERROR IN HEAT FLOW FOR GIVEN ERROR IN MATERIAL PROPERTIES	
OUTER INSULATION DIFFUSIVITY	HONEYCOMB DIFFUSIVITY	ACOUSTICAL INSULATION DIFFUSIVITY	$\alpha = 0^0$ $\lambda = 5$ FEET	$\alpha = 12^0$ $\lambda = 5$ FEET
50	100	50	51	47
-50	-75	-50	-58	-53
10	50	20	+ 18	+17
-10	-50	-20	-21	-23
5	25	10	+ 7	+7
-5	-25	-10	-13	-13

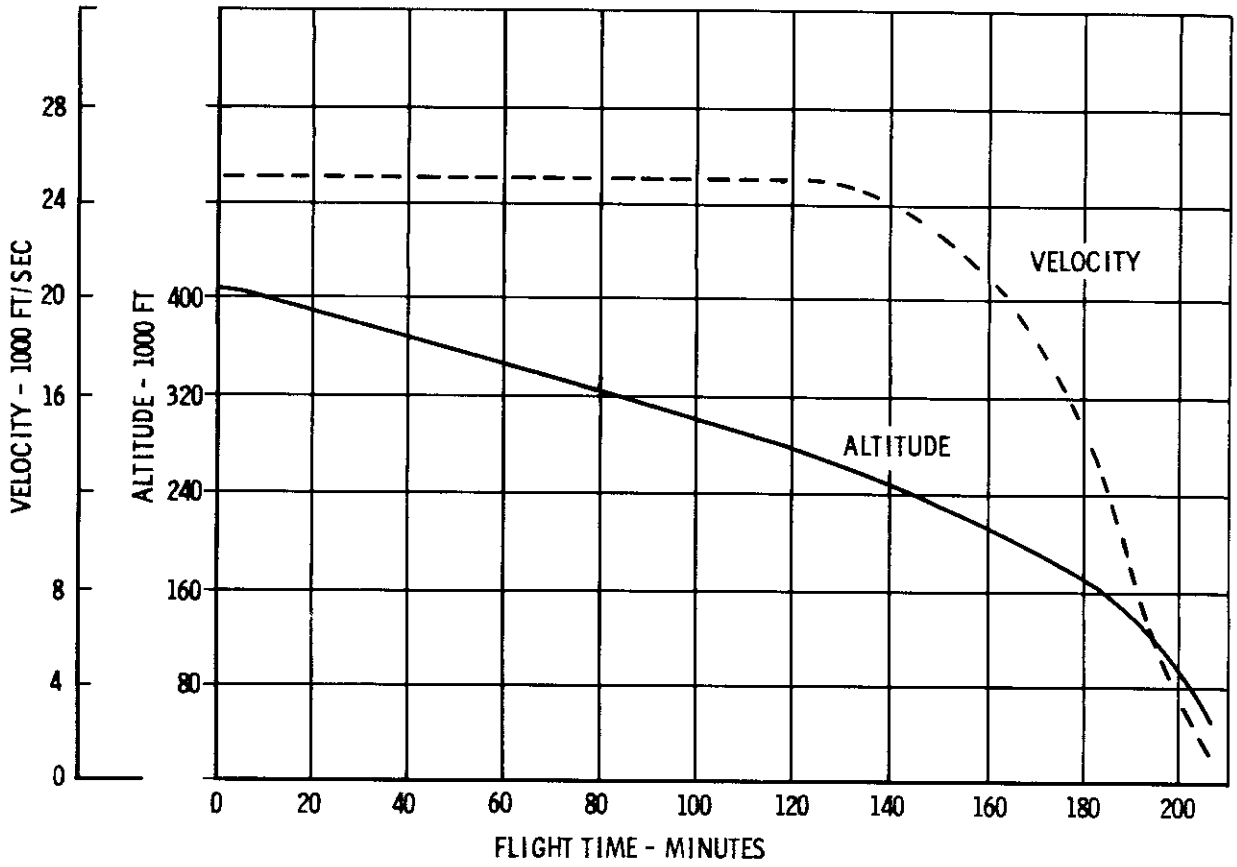

FIG. 1 GLIDE VEHICLE TRAJECTORY

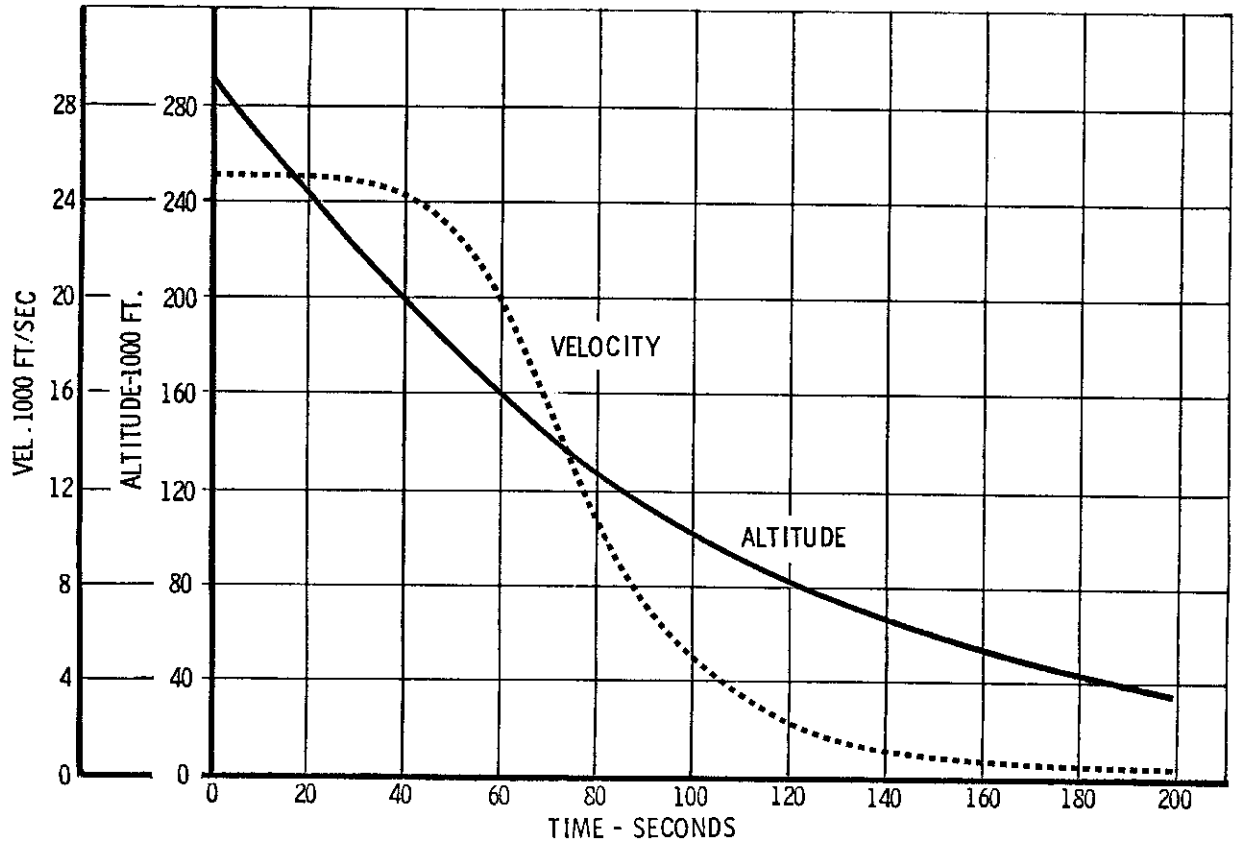

FIG. 2 DRAG VEHICLE TRAJECTORY

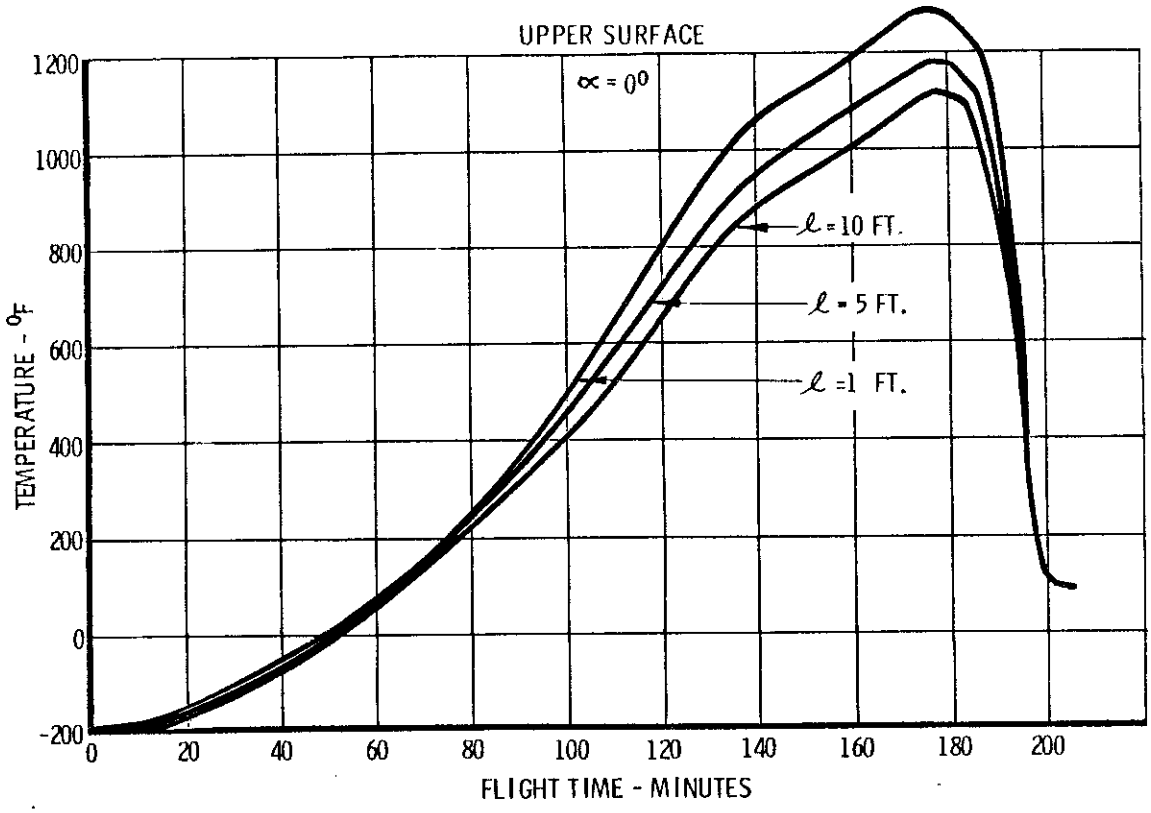

FIG.3 SURFACE TEMPERATURES VS TIME GLIDE VEHICLE

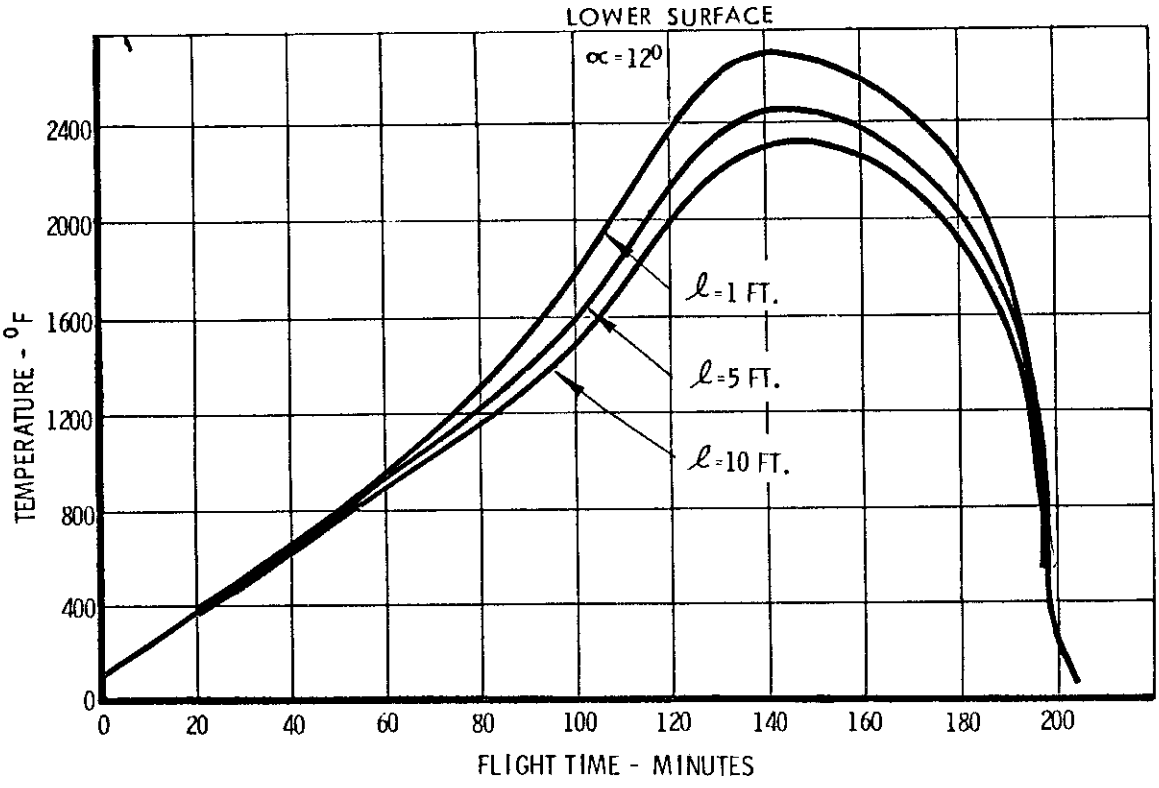

FIG.4 SURFACE TEMPERATURES VS. TIME GLIDE VEHICLE

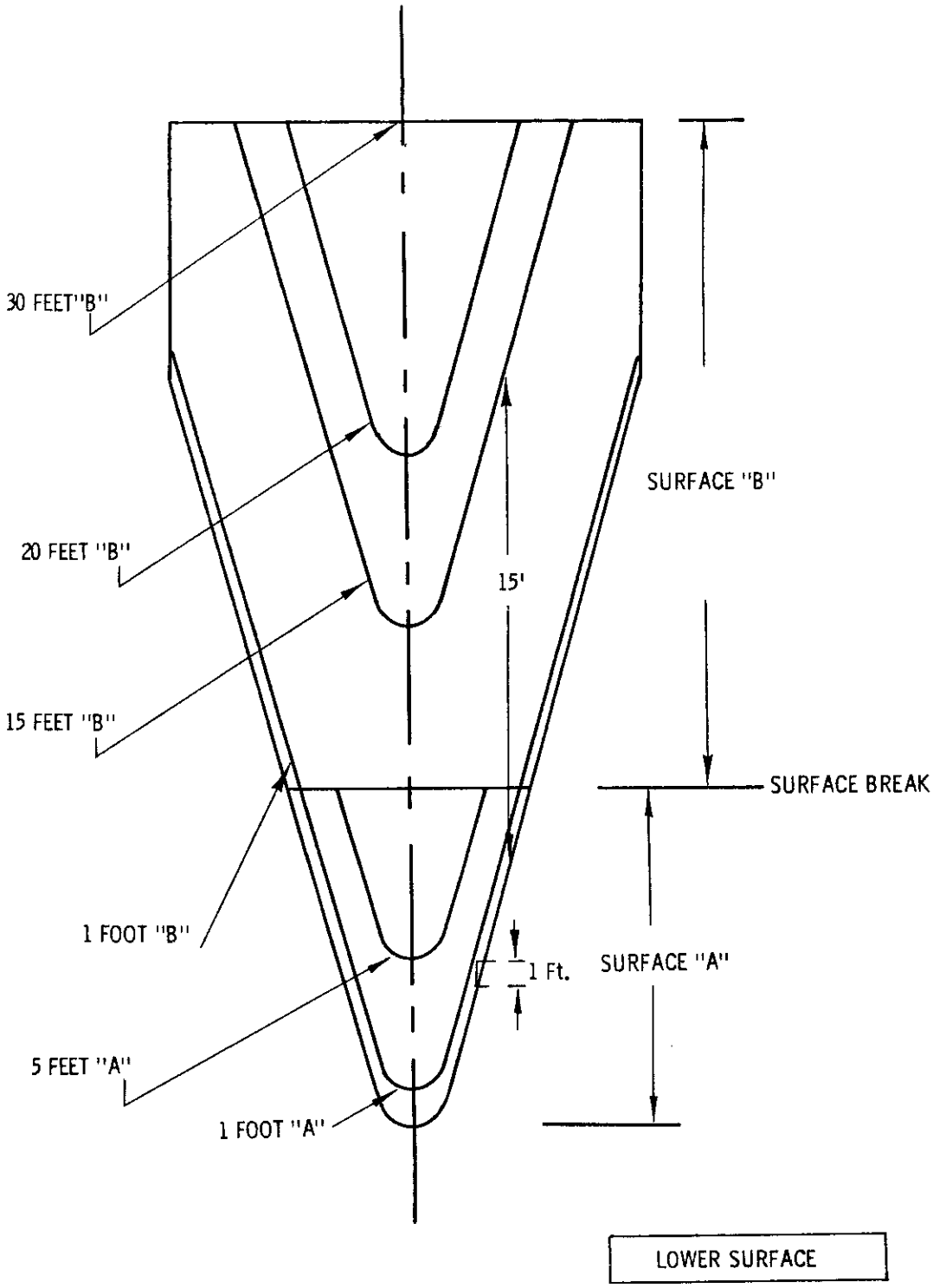

FIG.5 LINES OF UNIFORM TEMPERATURES
GLIDE VEHICLE

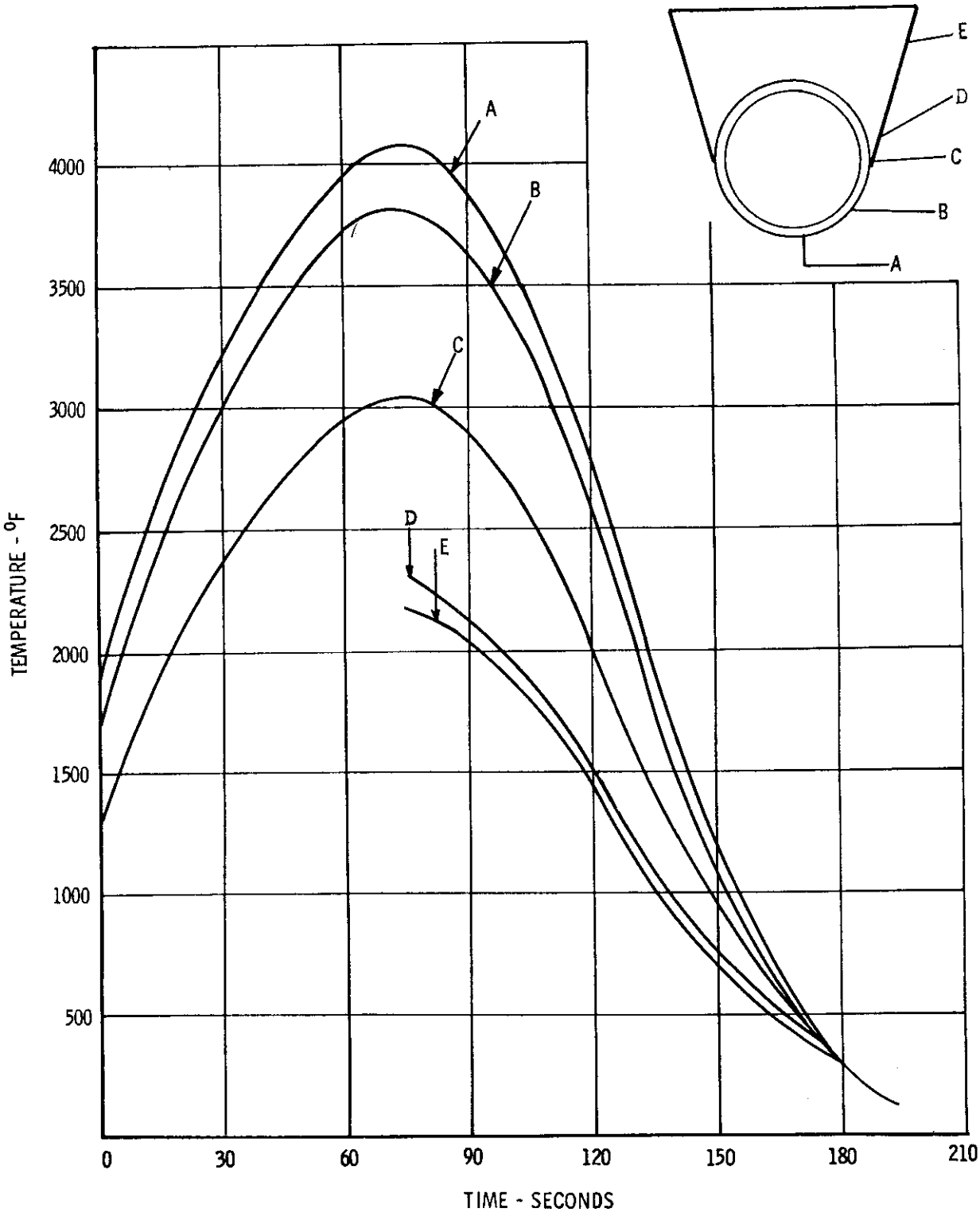

FIG.6 DRAG VEHICLE EQUILIBRIUM SKIN TEMPERATURES VERSUS TIME

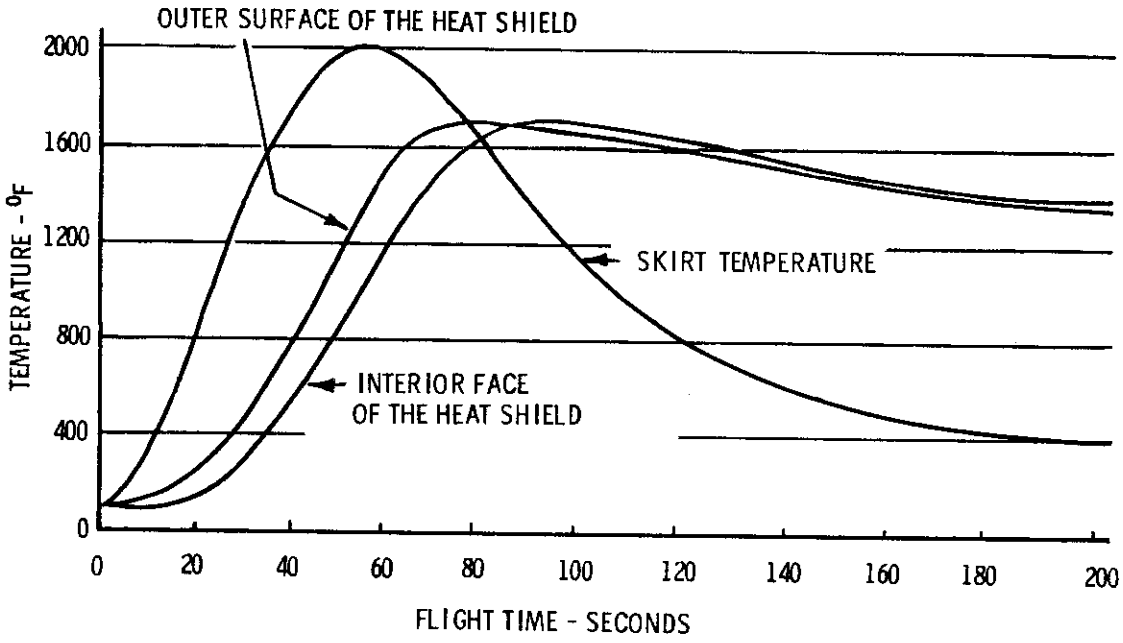

FIG.7 SKIRT HEAT SHIELD TEMPERATURES DRAG VEHICLE

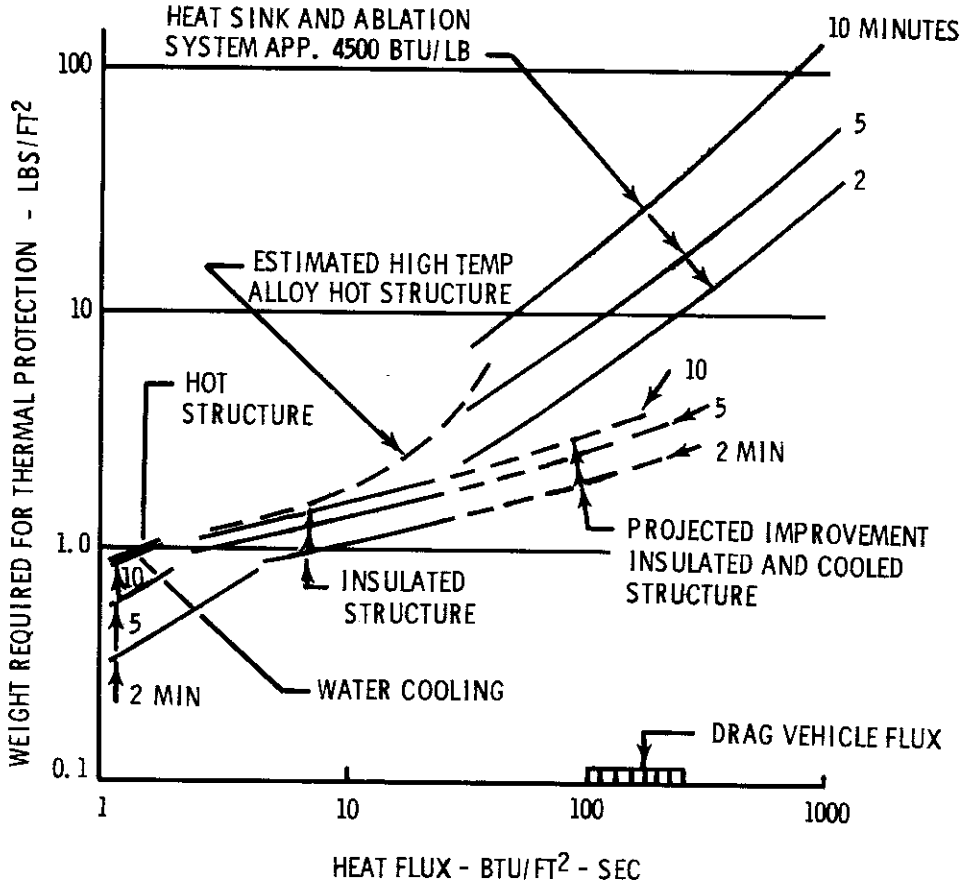

FIG. 8 WEIGHT REQUIRED FOR THERMAL PROTECTION VS. HEAT FLUX

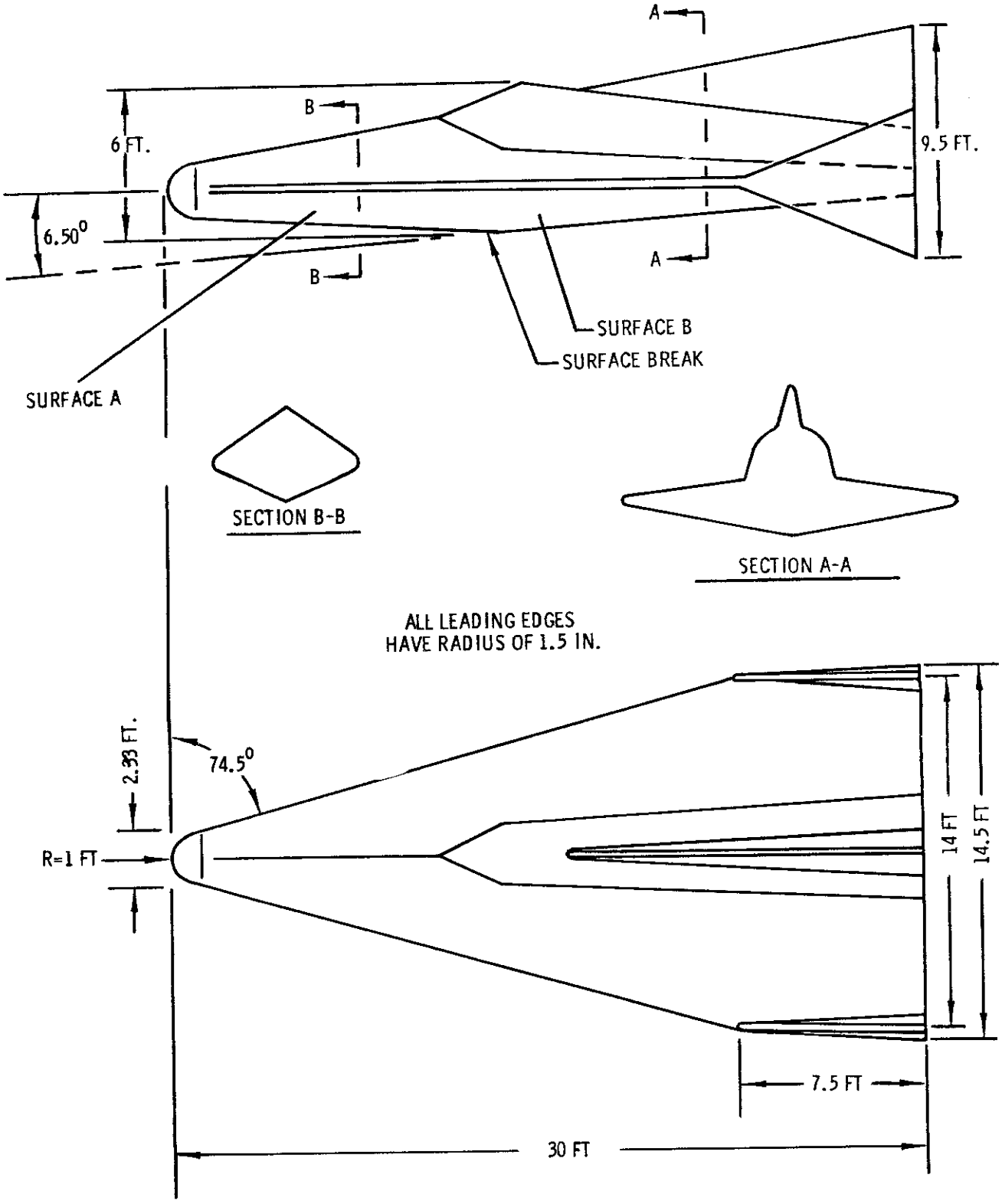

FIG. 9 GLIDE VEHICLE

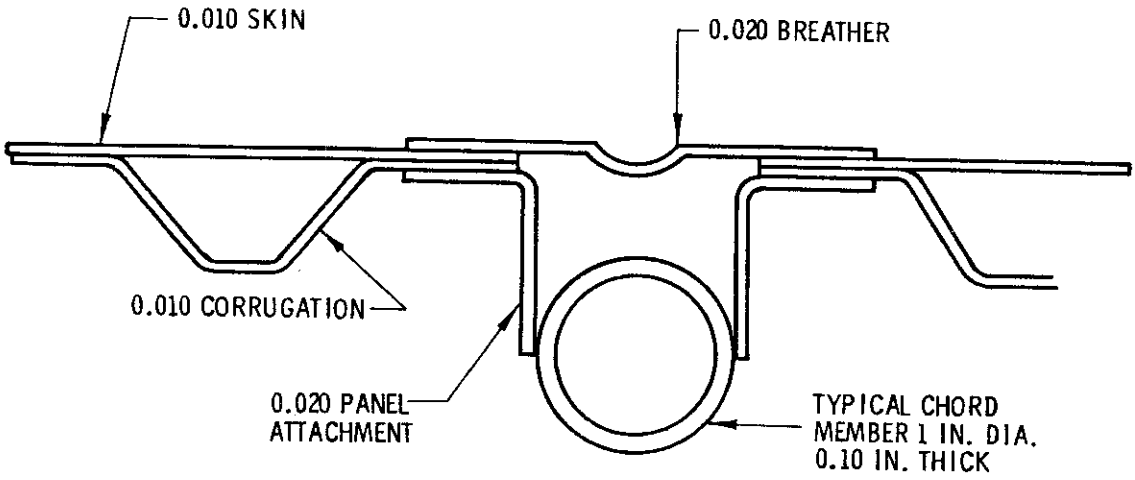

TYPICAL SKIN TO SPAR CHORD CONNECTION

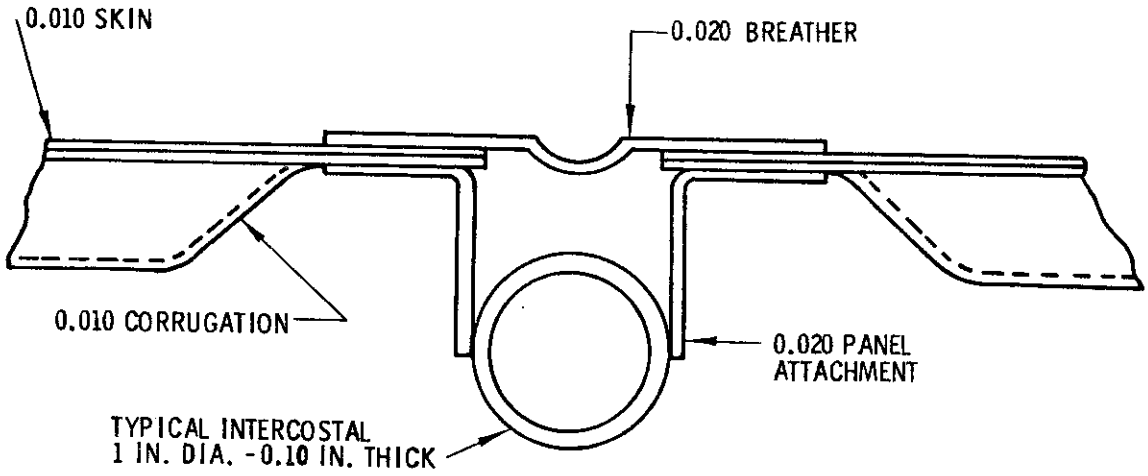

TYPICAL SKIN TO INTERCOSTAL CONNECTION

FIG. 10 STRUCTURAL DETAILS-GLIDE VEHICLE

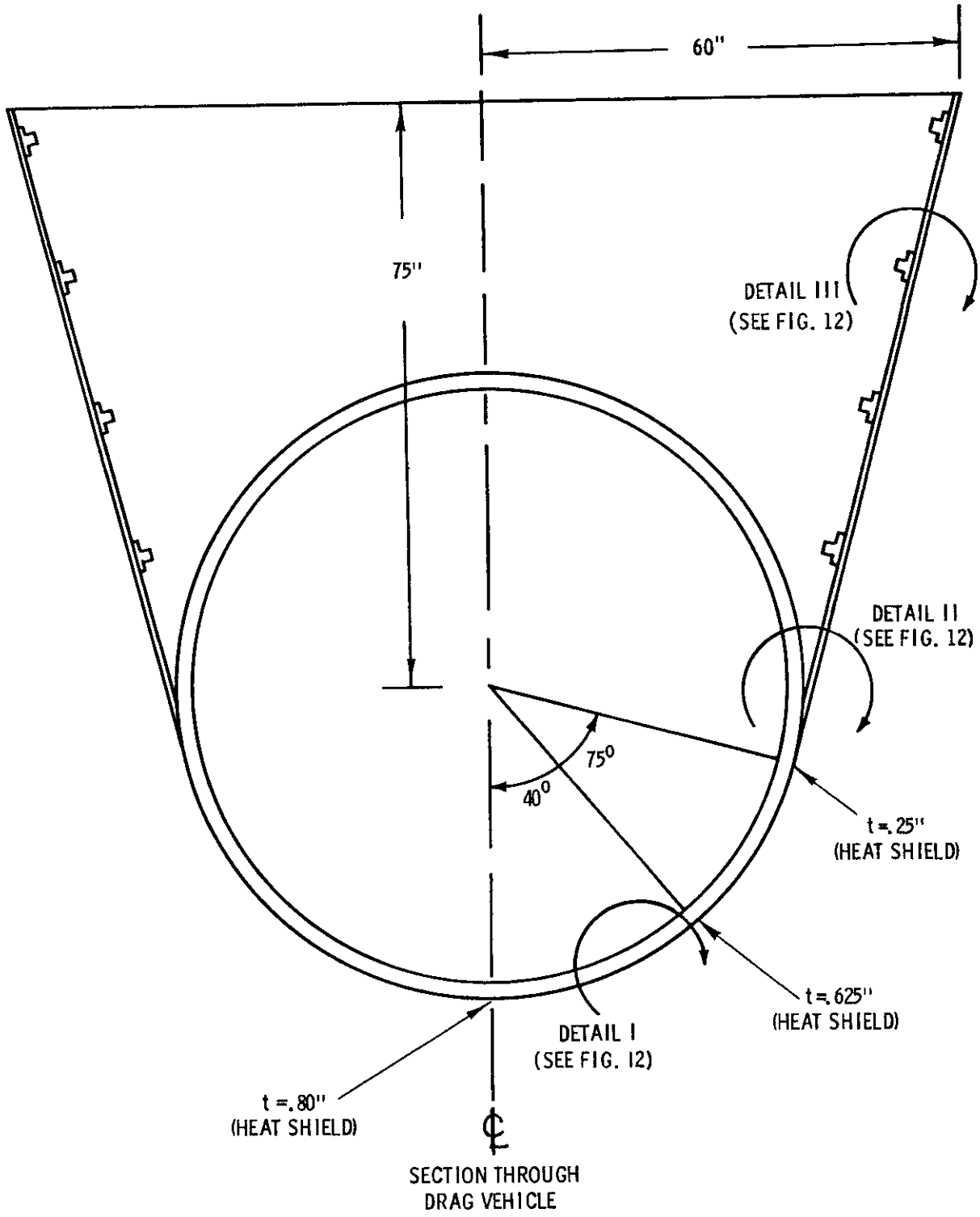

FIG. 11 DRAG VEHICLE

DETAIL I

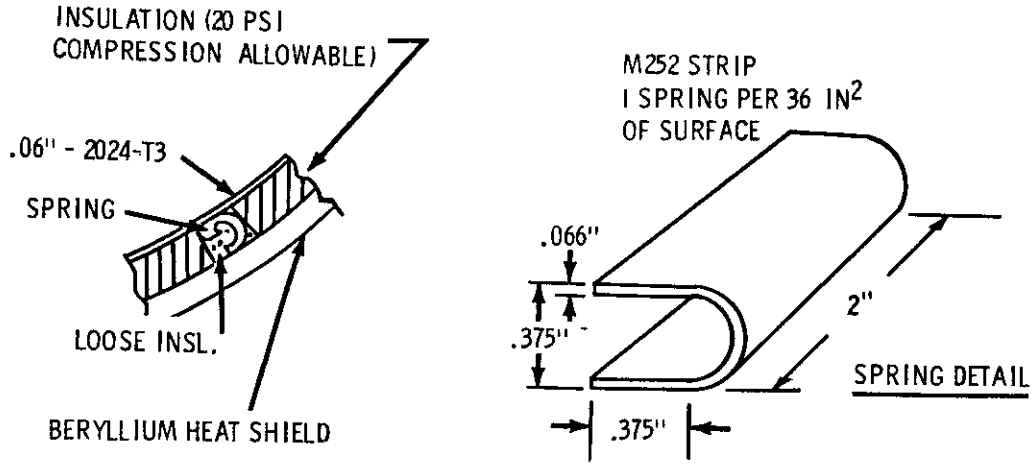

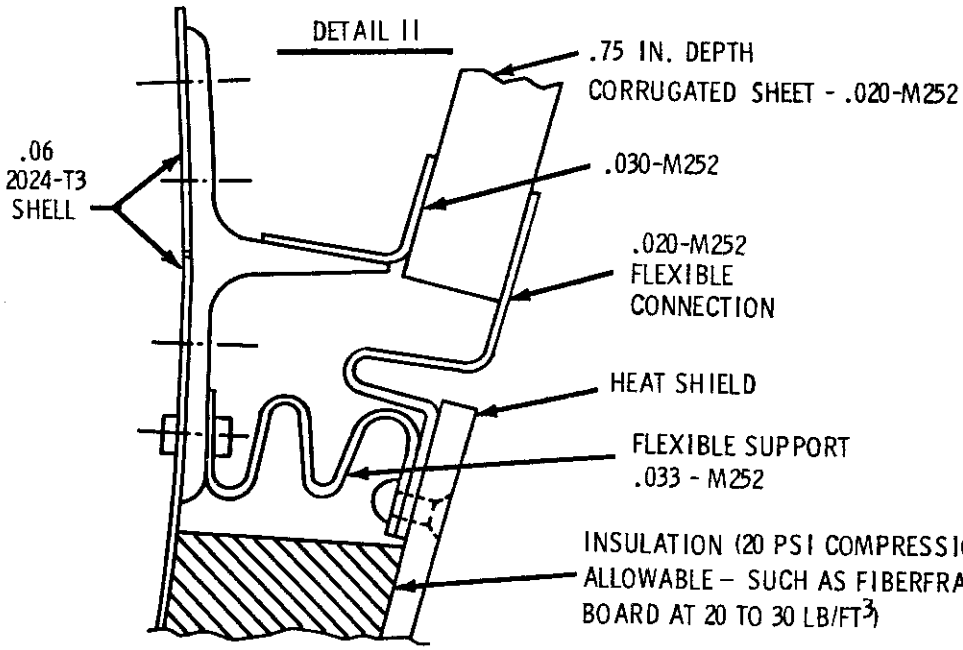

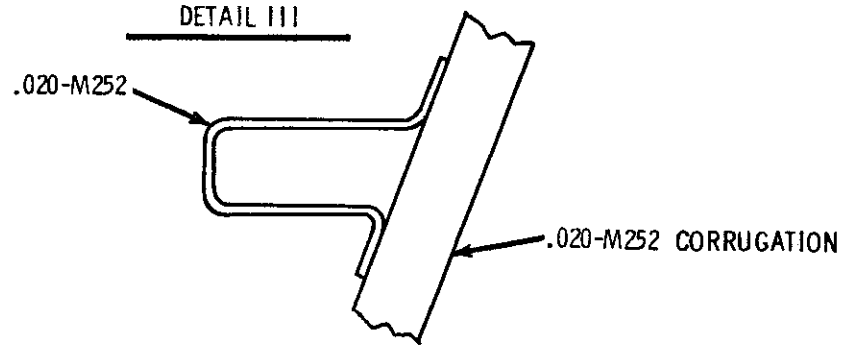

FIG. 12 STRUCTURAL DETAILS - DRAG VEHICLE

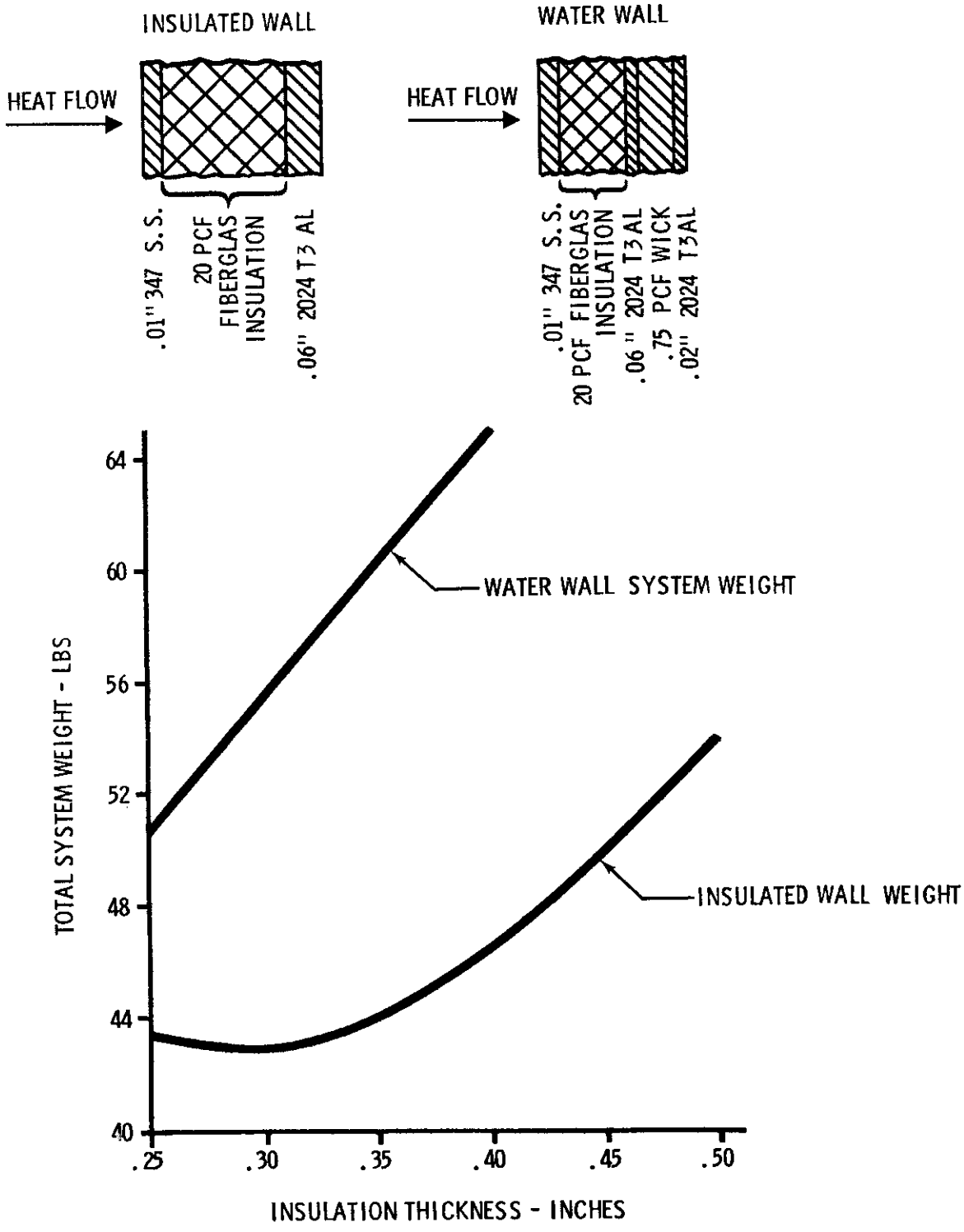

FIG. 13 WEIGHT CHARGEABLE TO THE COOLING SYSTEM VS INSULATION THICKNESS DRAG VEHICLE

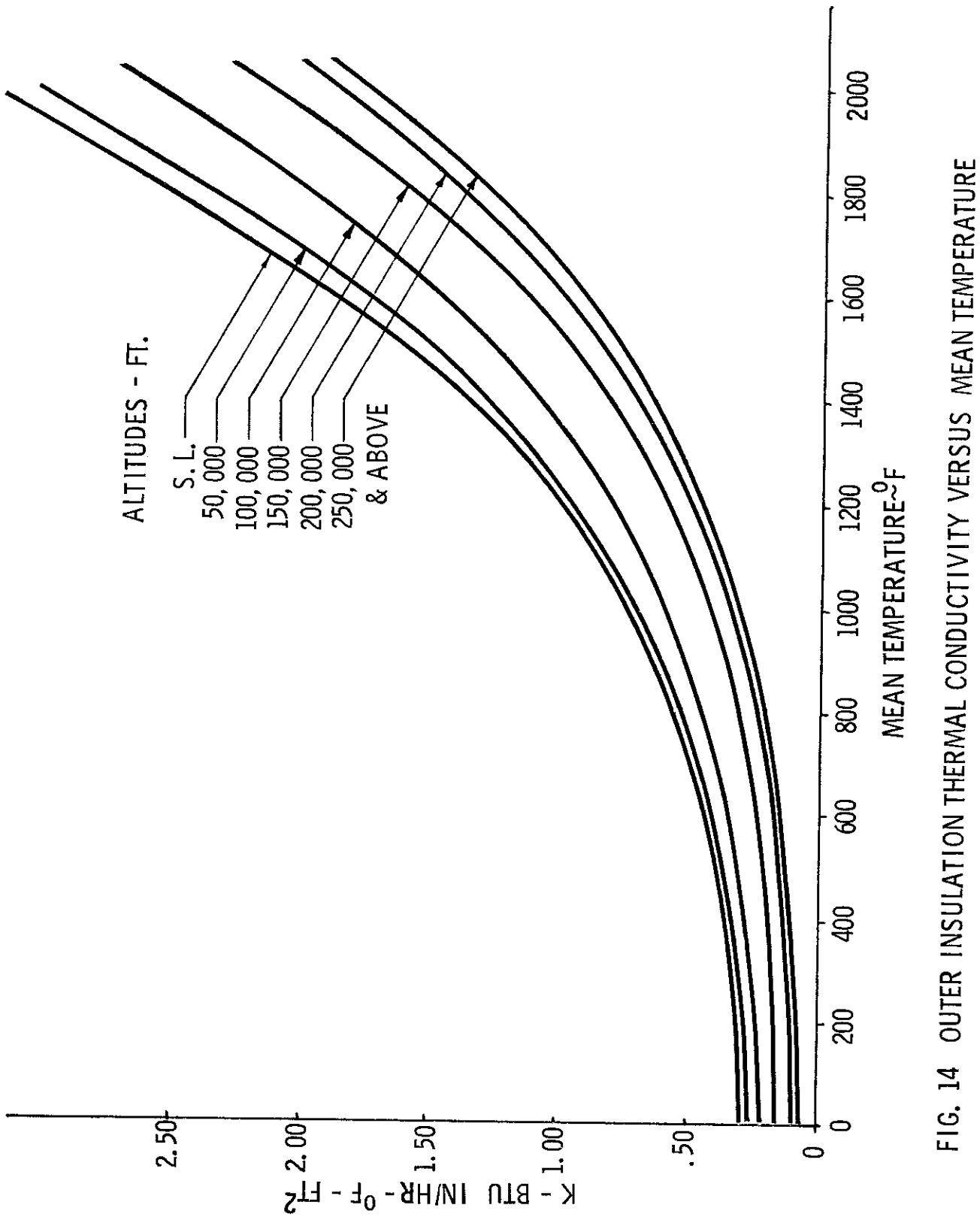

FIG. 14 OUTER INSULATION THERMAL CONDUCTIVITY VERSUS MEAN TEMPERATURE

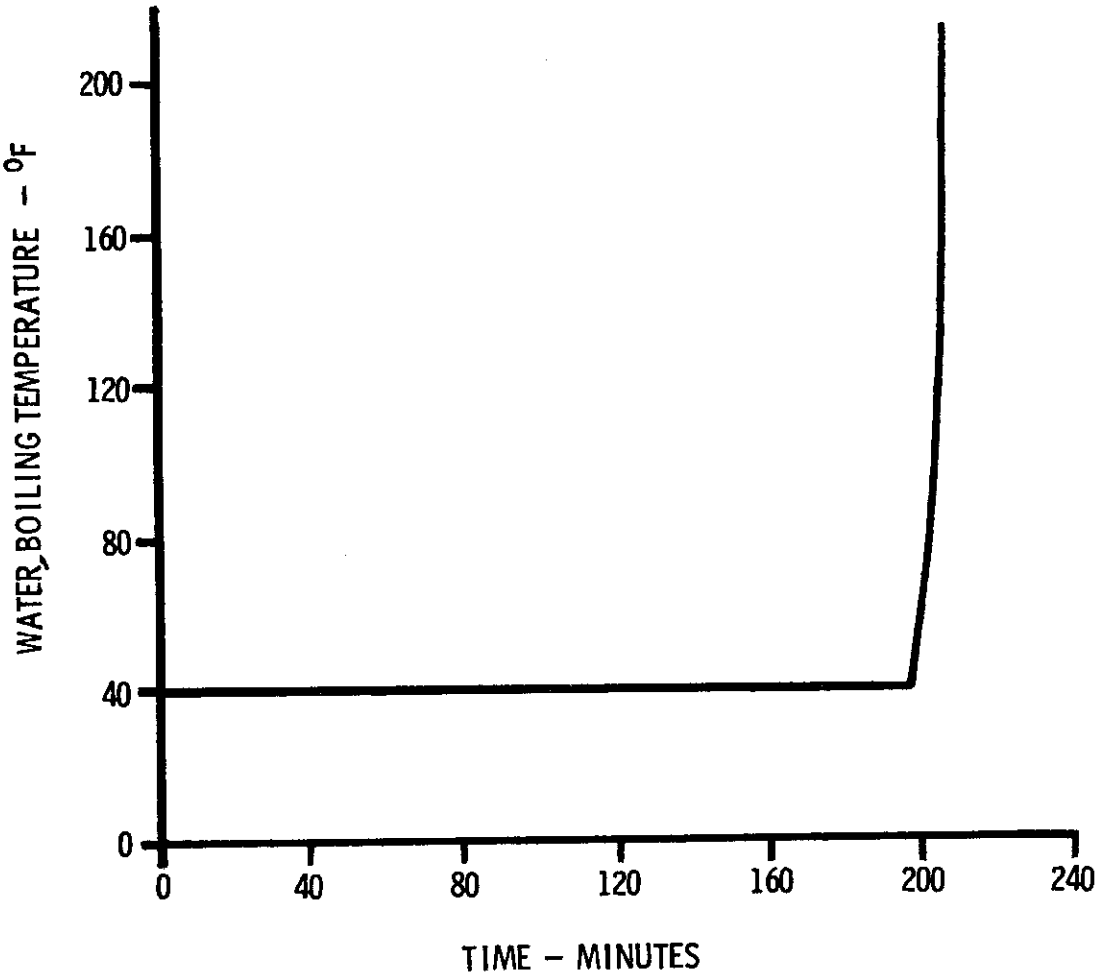

FIGURE 15 WATER BOILING TEMPERATURE - GLIDE VEHICLE

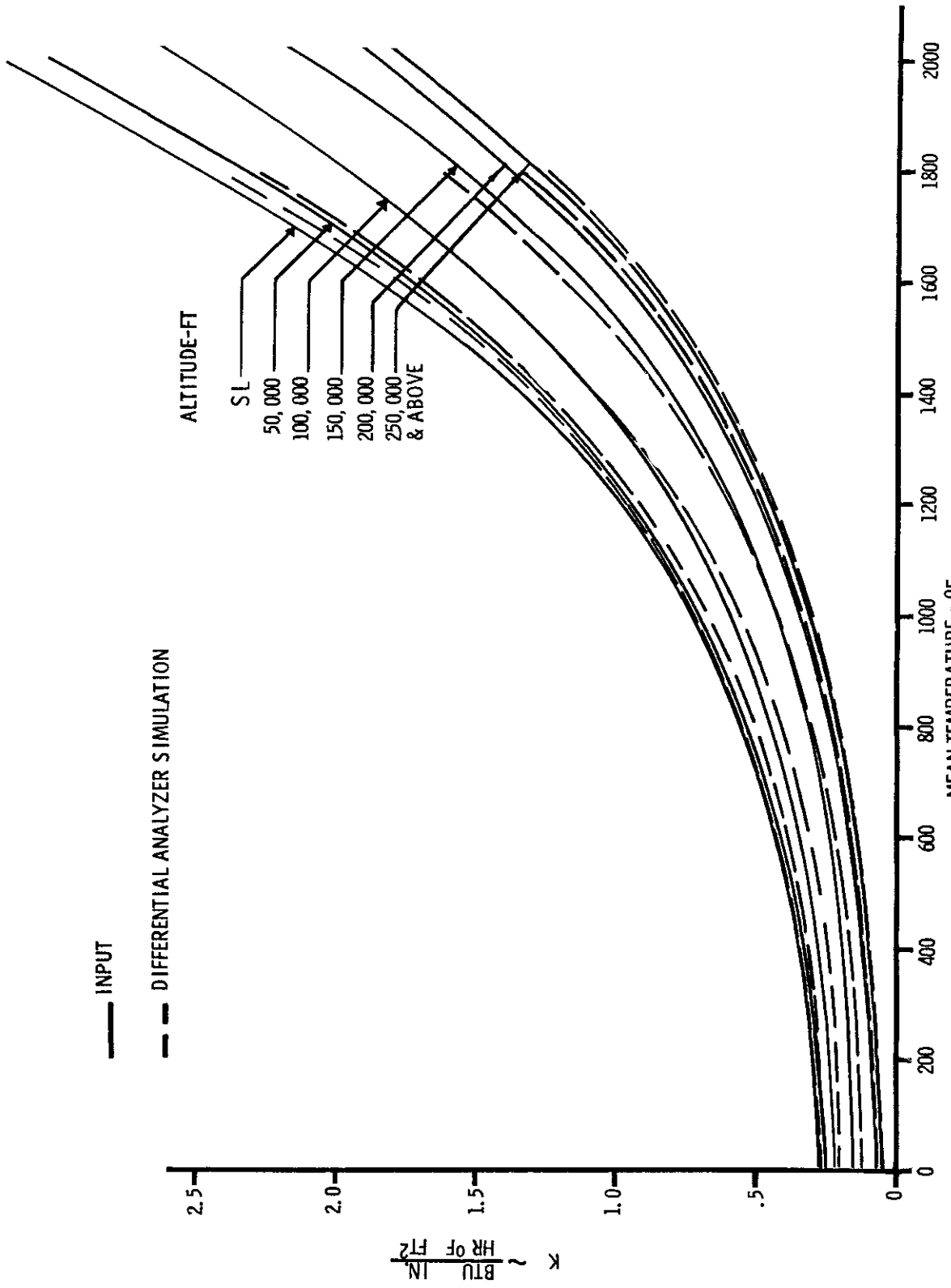

FIG. 16 THERMAL CONDUCTIVITY SIMULATION

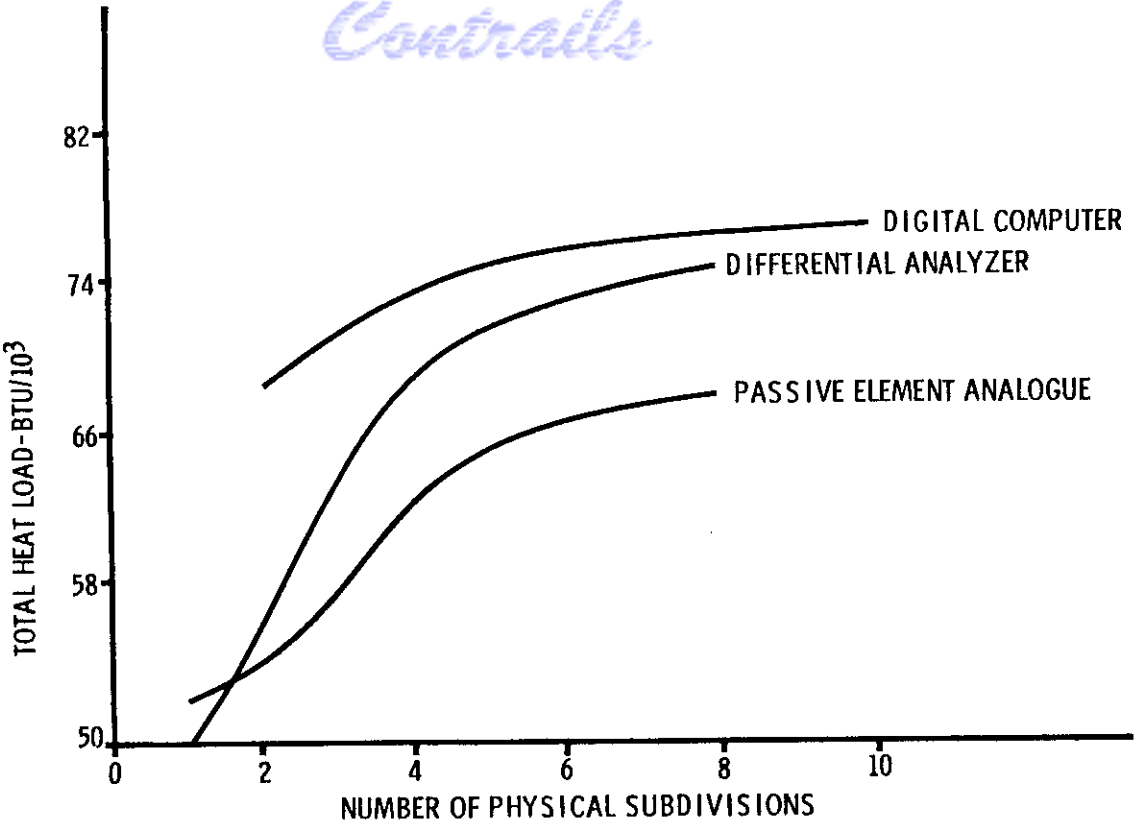

FIG. 17 HEAT FLOW VS NUMBER OF PHYSICAL SUBDIVISIONS-GLIDE VEHICLE

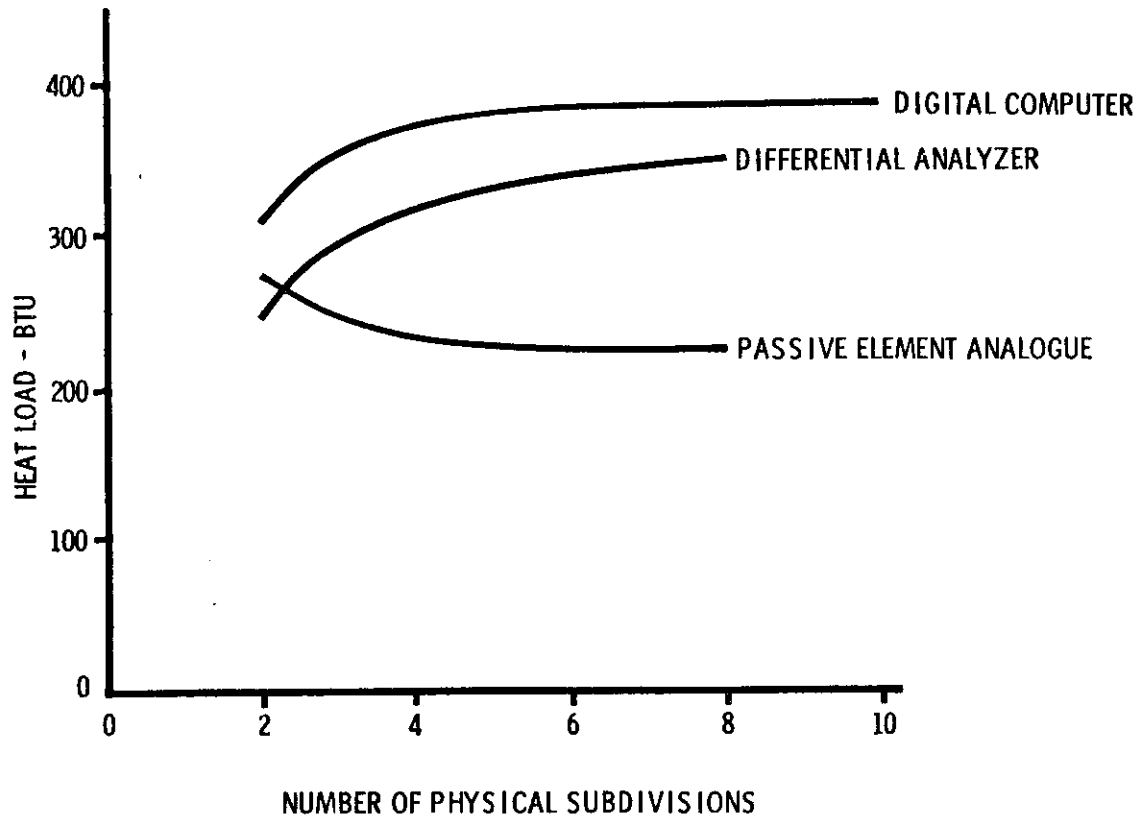

FIG. 18 FORWARD SIDE HEAT FLOW VS NO. OF PHYSICAL SUBDIVISIONS-DRAG VEHICLE

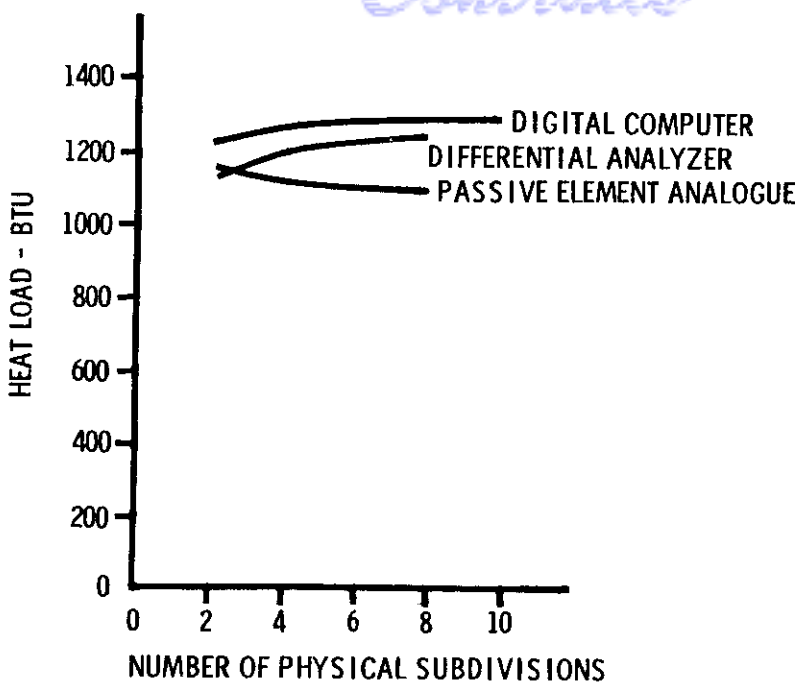

FIG. 19 TOTAL HEAT FLOW VS NUMBER OF PHYSICAL SUBDIVISIONS-DRAG VEHICLE

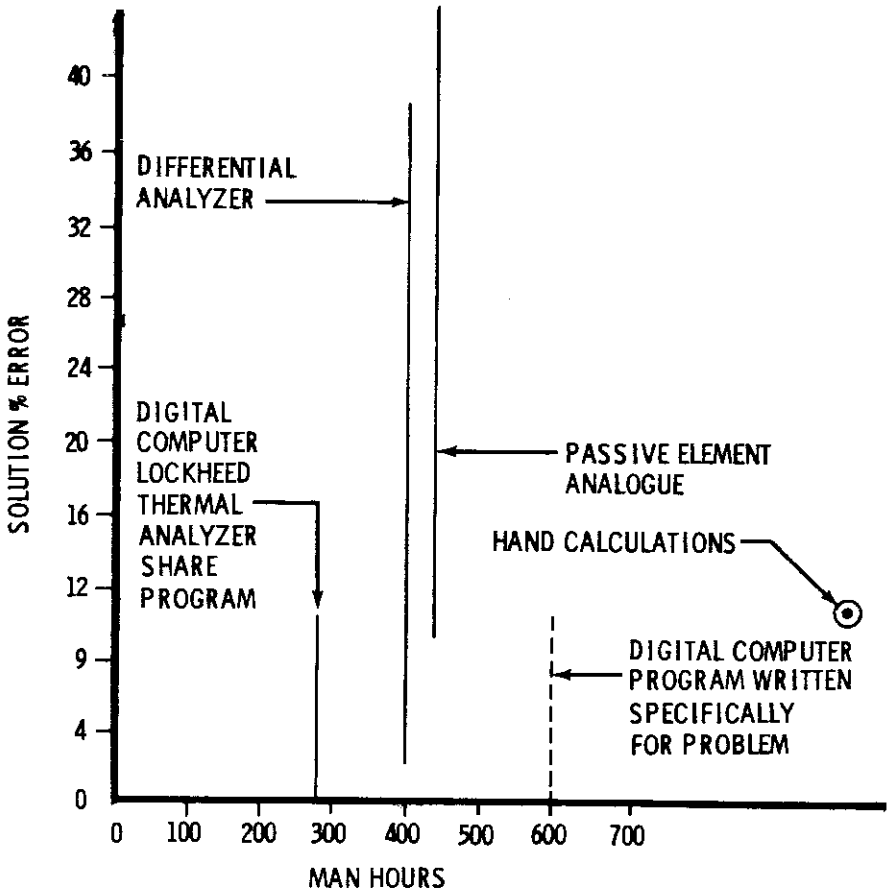

FIG. 20 SOLUTION % ERROR VS. MAN HOURS - GLIDE VEHICLE

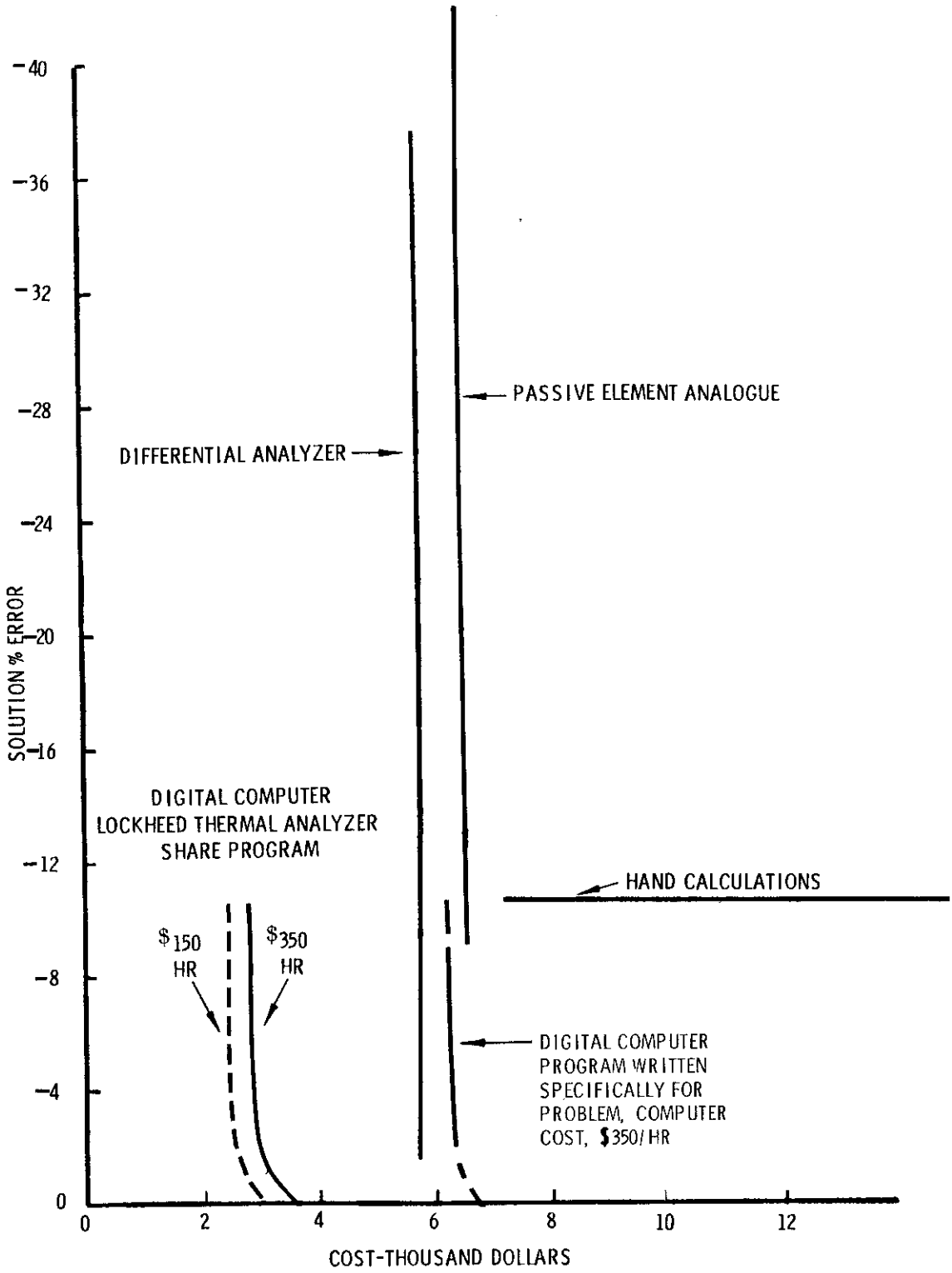

FIG. 21 SOLUTION % ERROR VS TOTAL DOLLAR COST-GLIDE VEHICLE

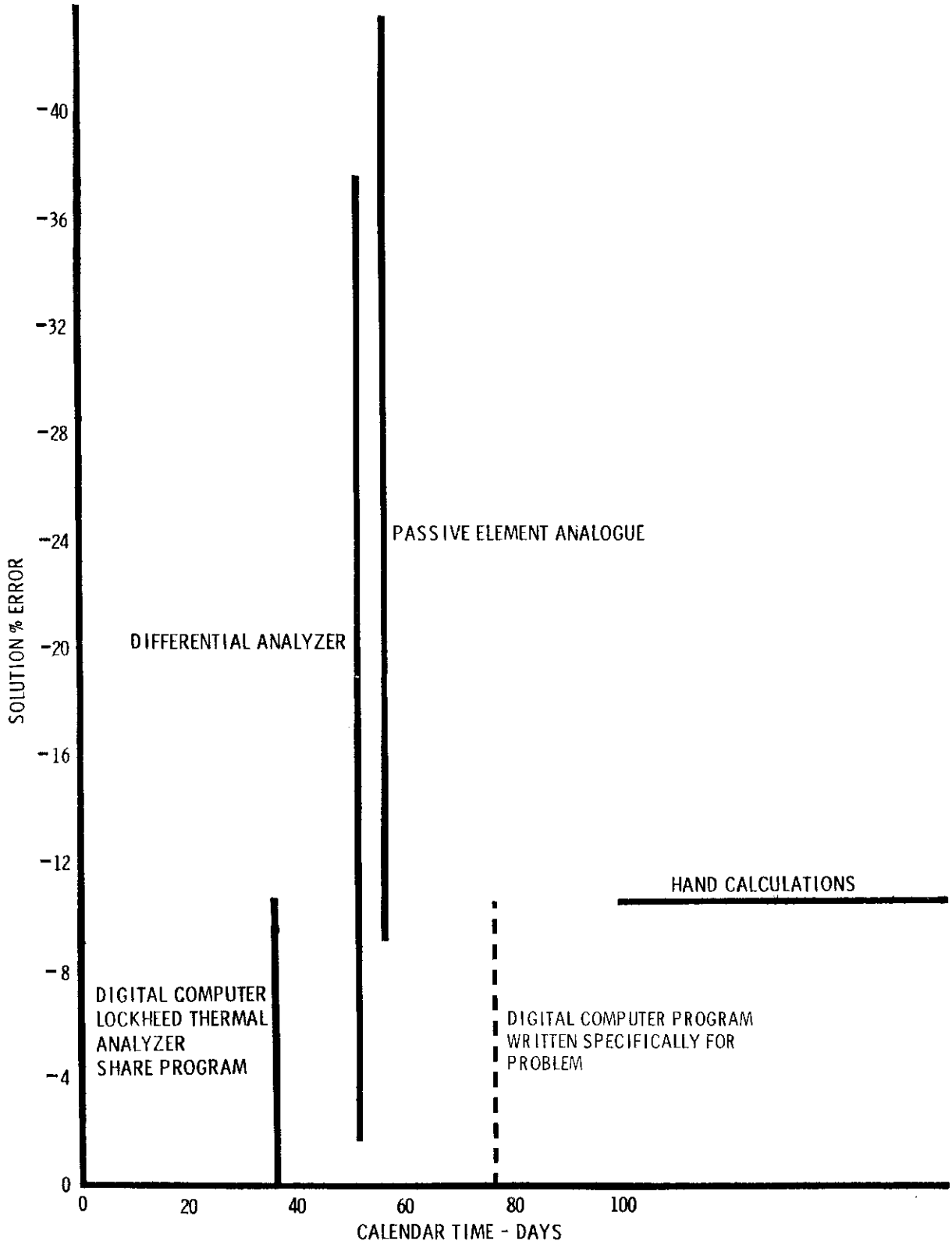

FIG. 22 SOLUTION % ERROR VS CALENDAR TIME-GLIDE VEHICLE

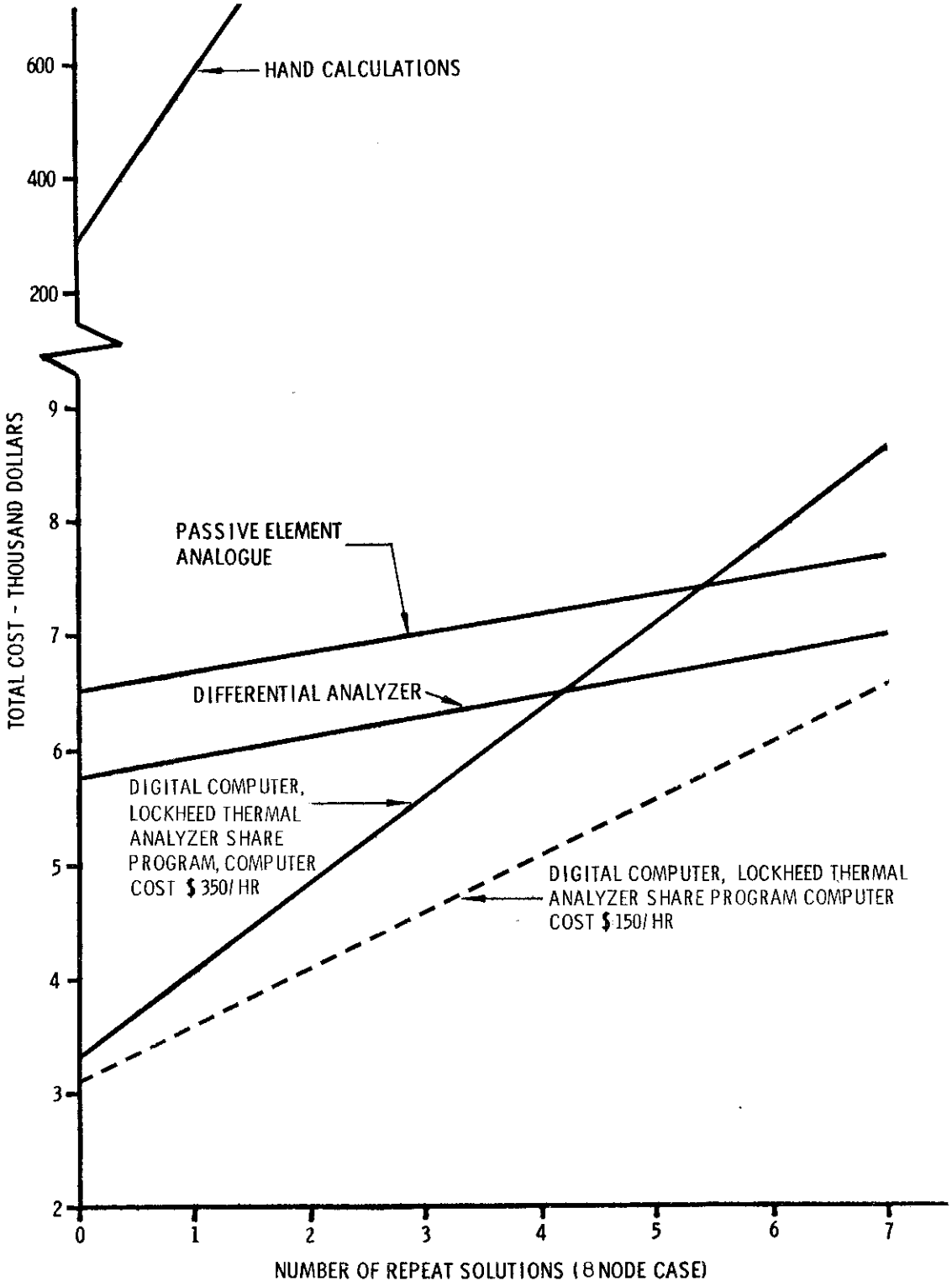

FIG. 23 TOTAL DOLLAR COST VS NO. REPEAT SOLUTIONS - GLIDE VEHICLE

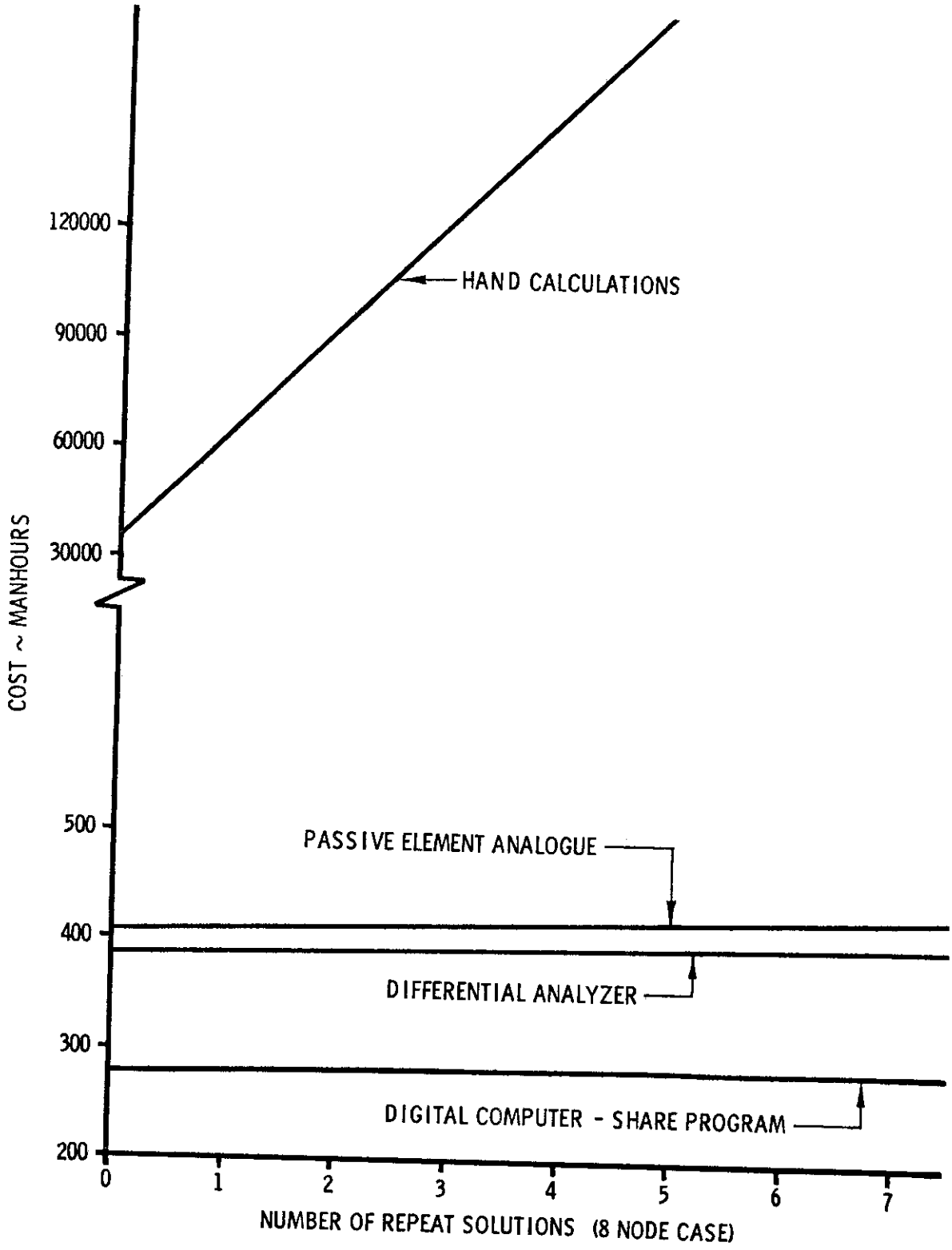

FIG. 24 MAN HOUR COST VS NO. REPEAT SOLUTIONS-GLIDE VEHICLE

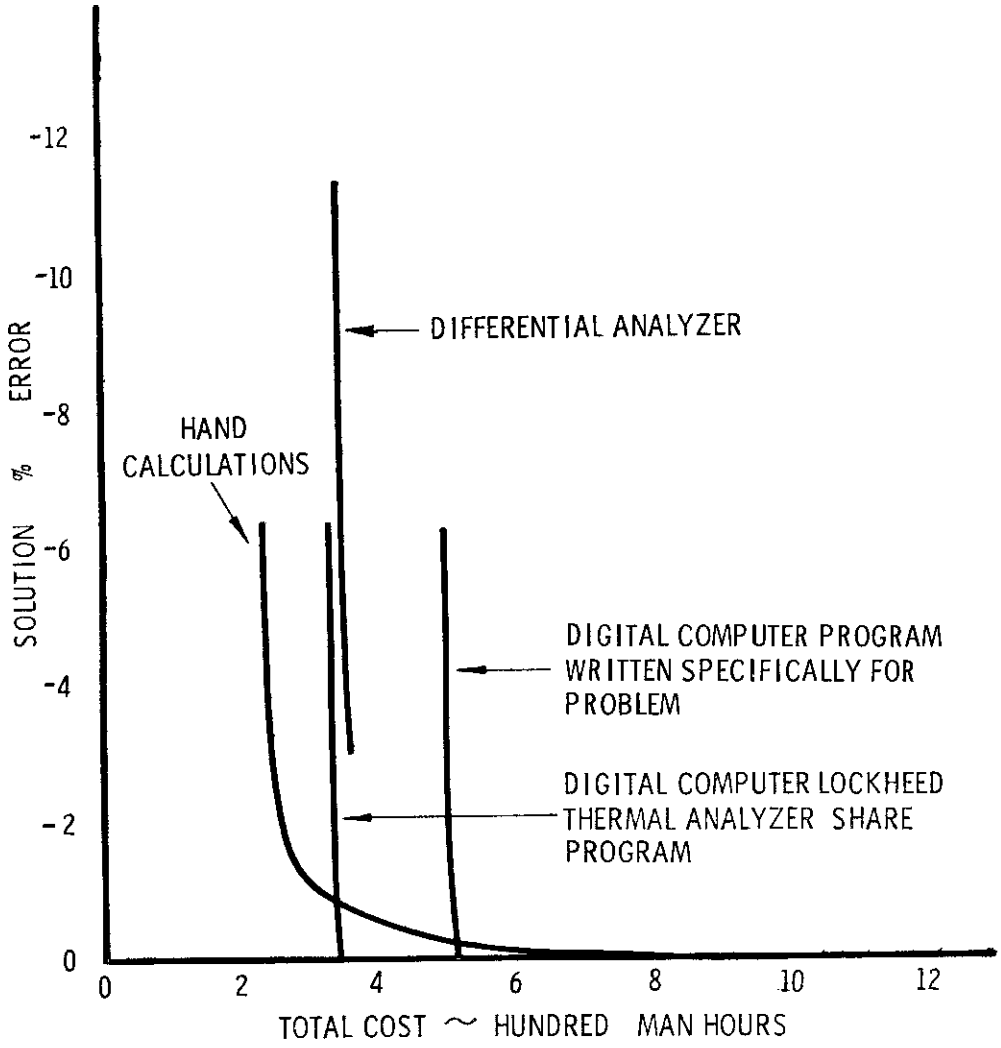

FIG. 25 SOLUTION % ERROR VS MAN HOURS - DRAG VEHICLE

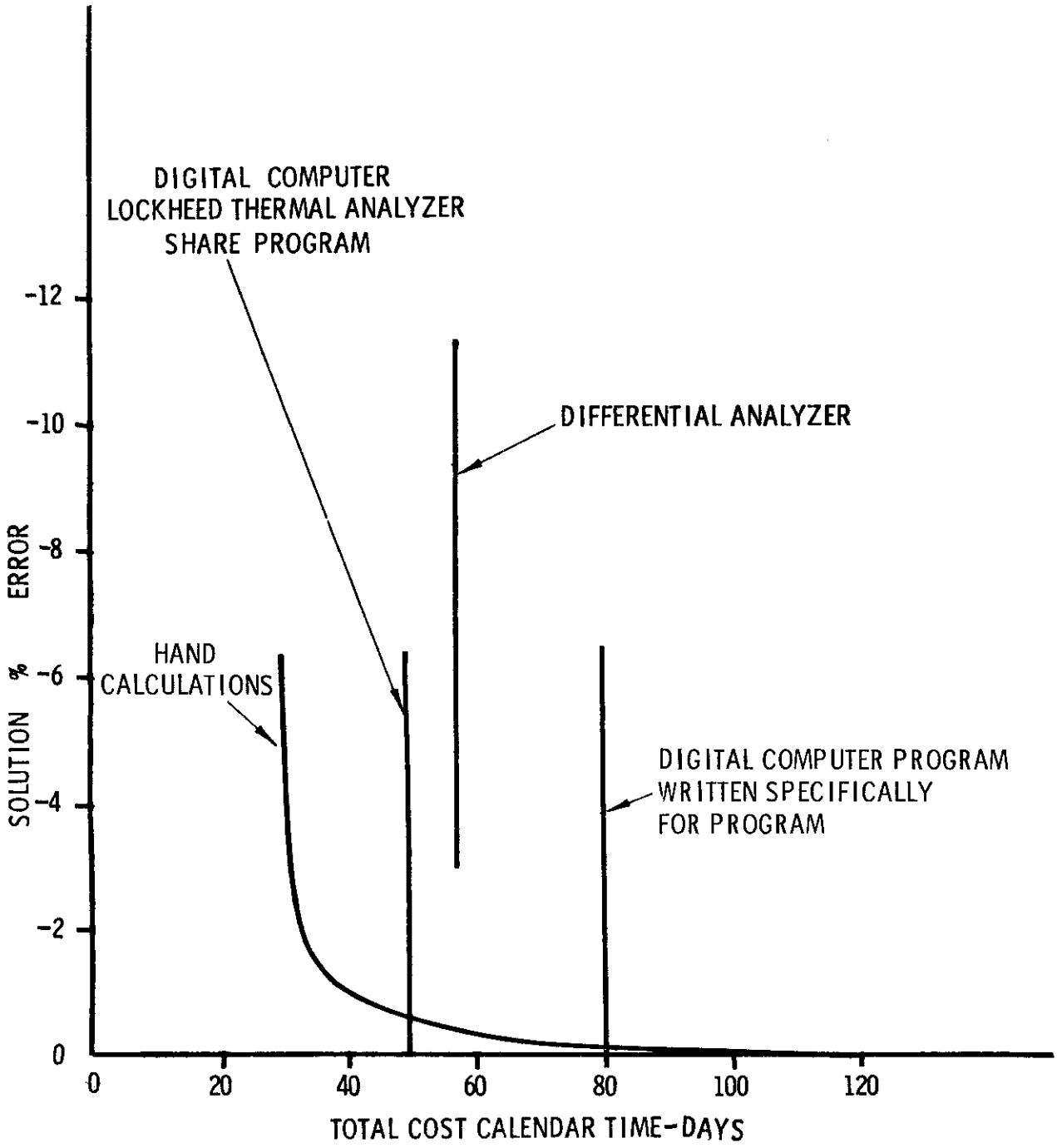

FIG. 26 SOLUTION % ERROR VS CALENDAR TIME-DRAG VEHICLE

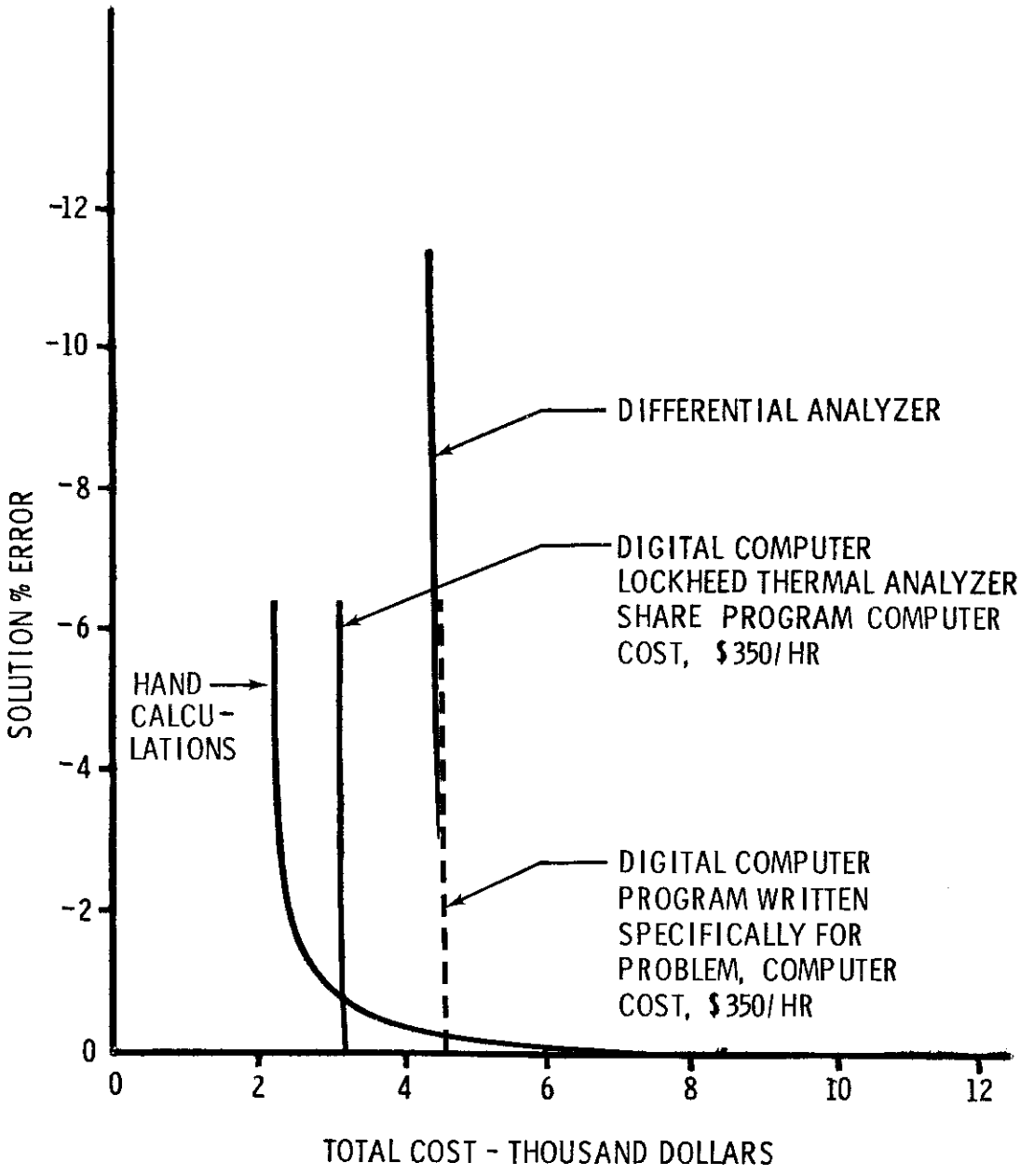

FIG. 27 - SOLUTION % ERROR VS DOLLAR COST-DRAG VEHICLE

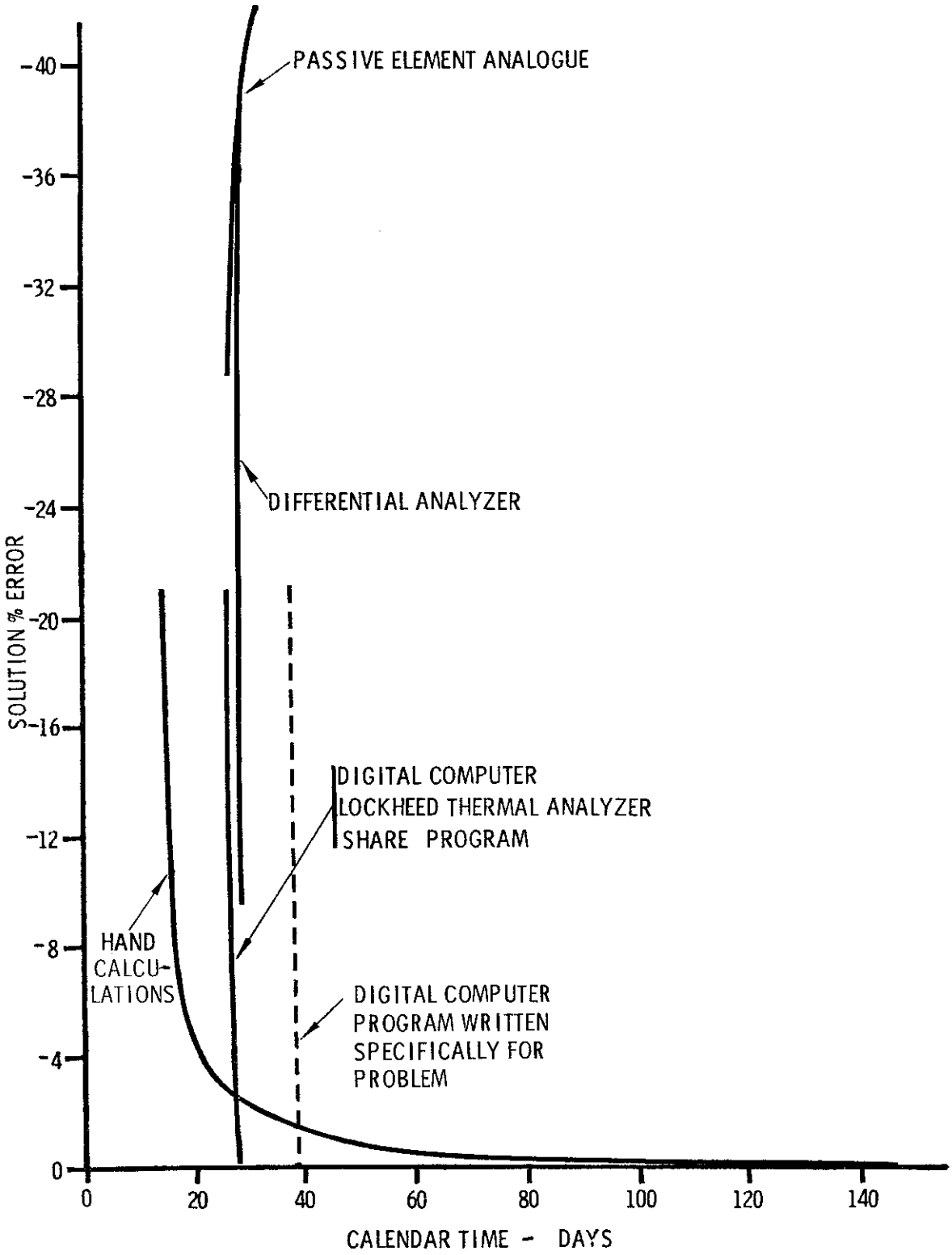

FIG. 28 SOLUTION % ERROR VS CALENDAR TIME FORWARD SIDE DRAG VEHICLE

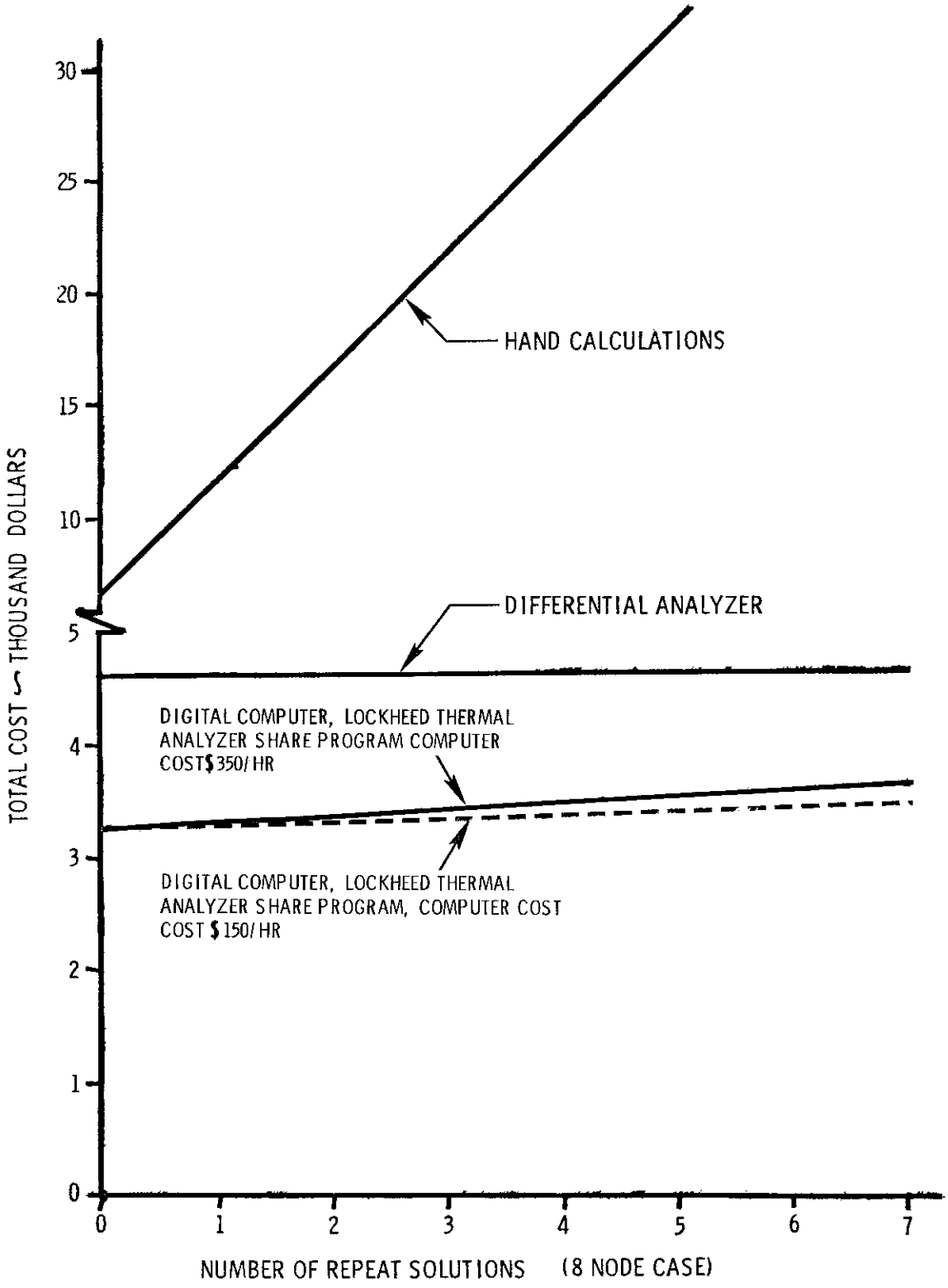

FIG. 29 – TOTAL DOLLAR COST VS NUMBER REPEAT SOLUTIONS-DRAG VEHICLE

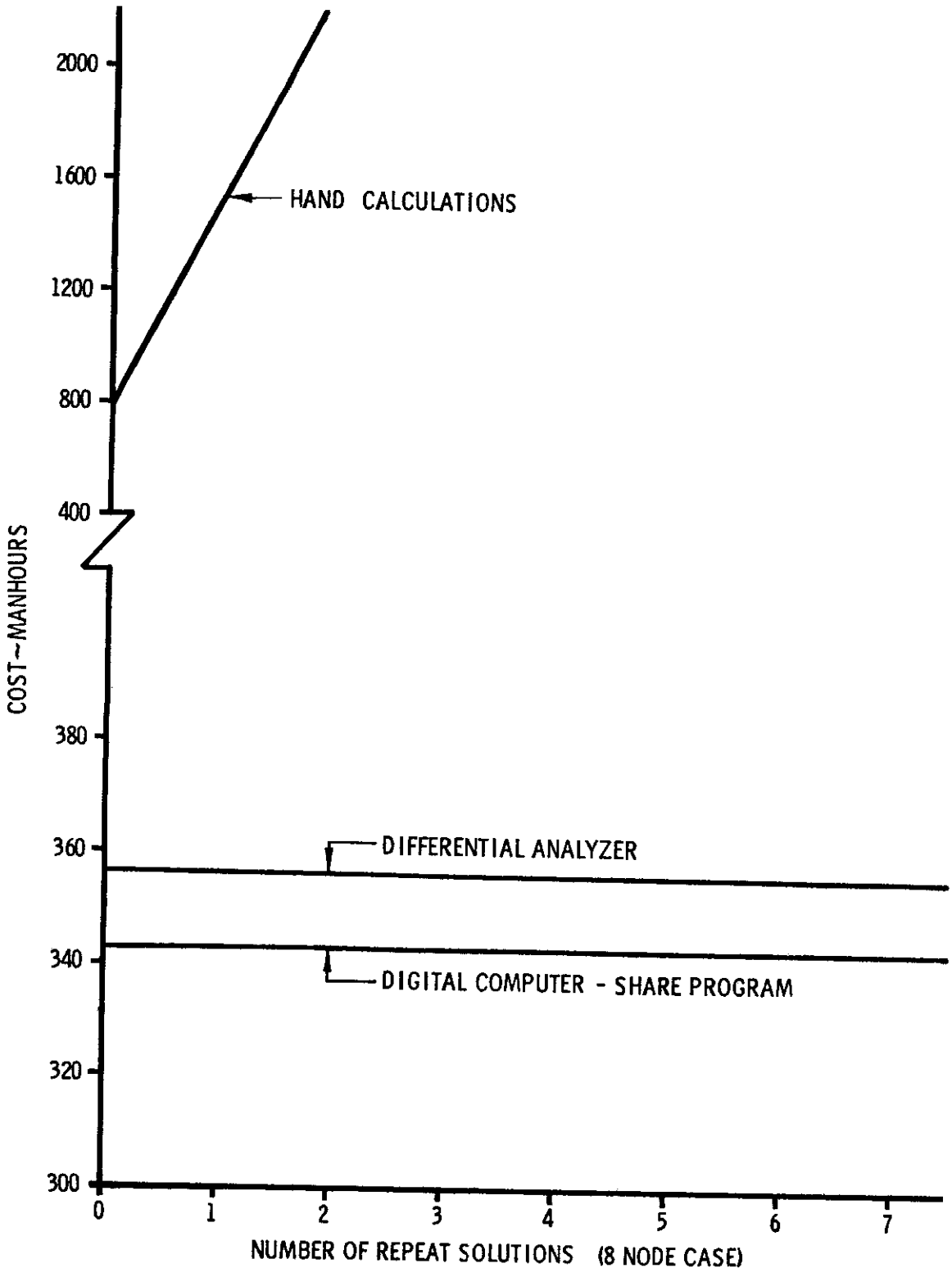

FIG. 30 MAN HOUR COST VS. NUMBER REPEAT SOLUTIONS ~ DRAG VEHICLE

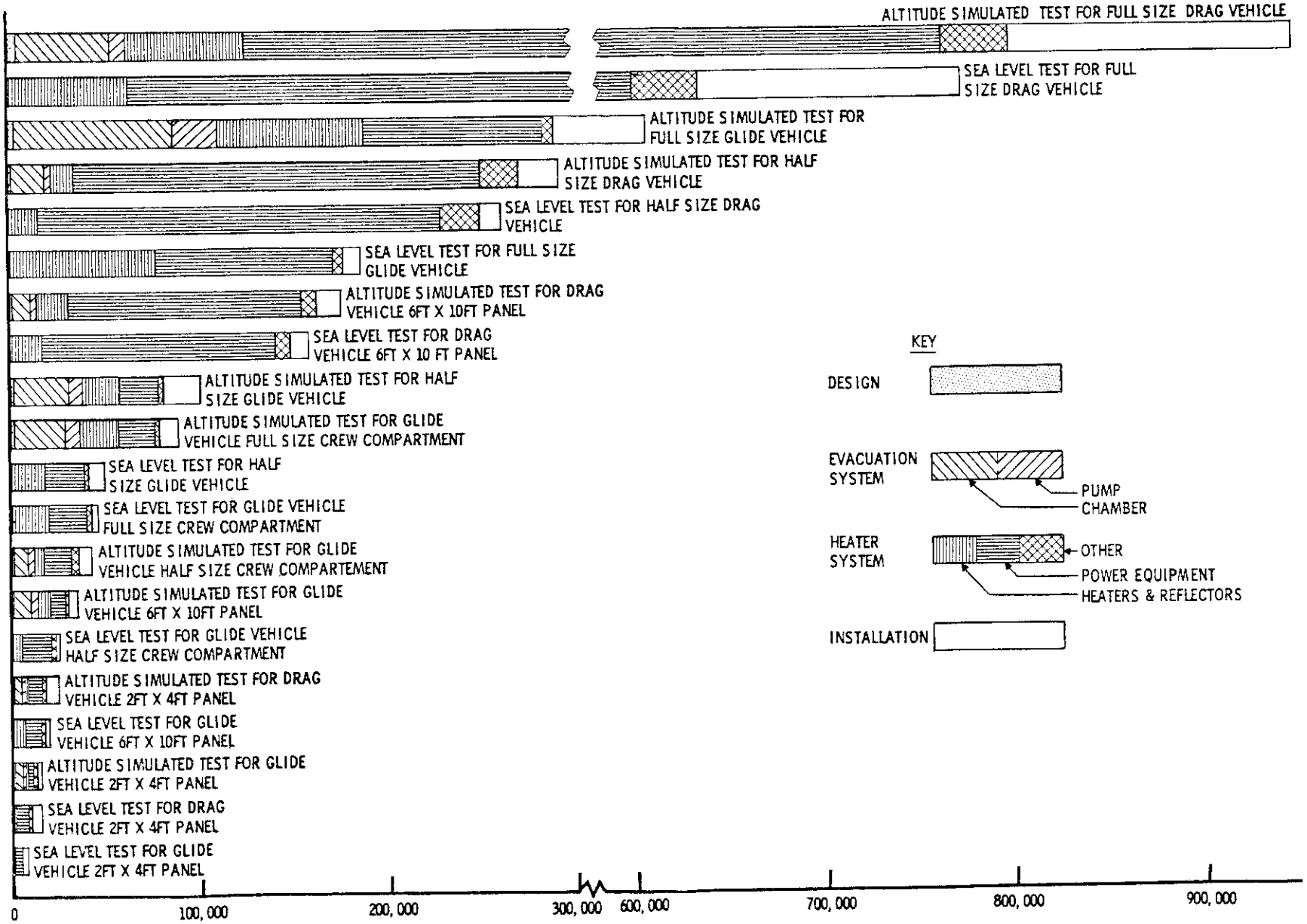

FIG. 31 RADIANT HEAT TEST FACILITIES COST

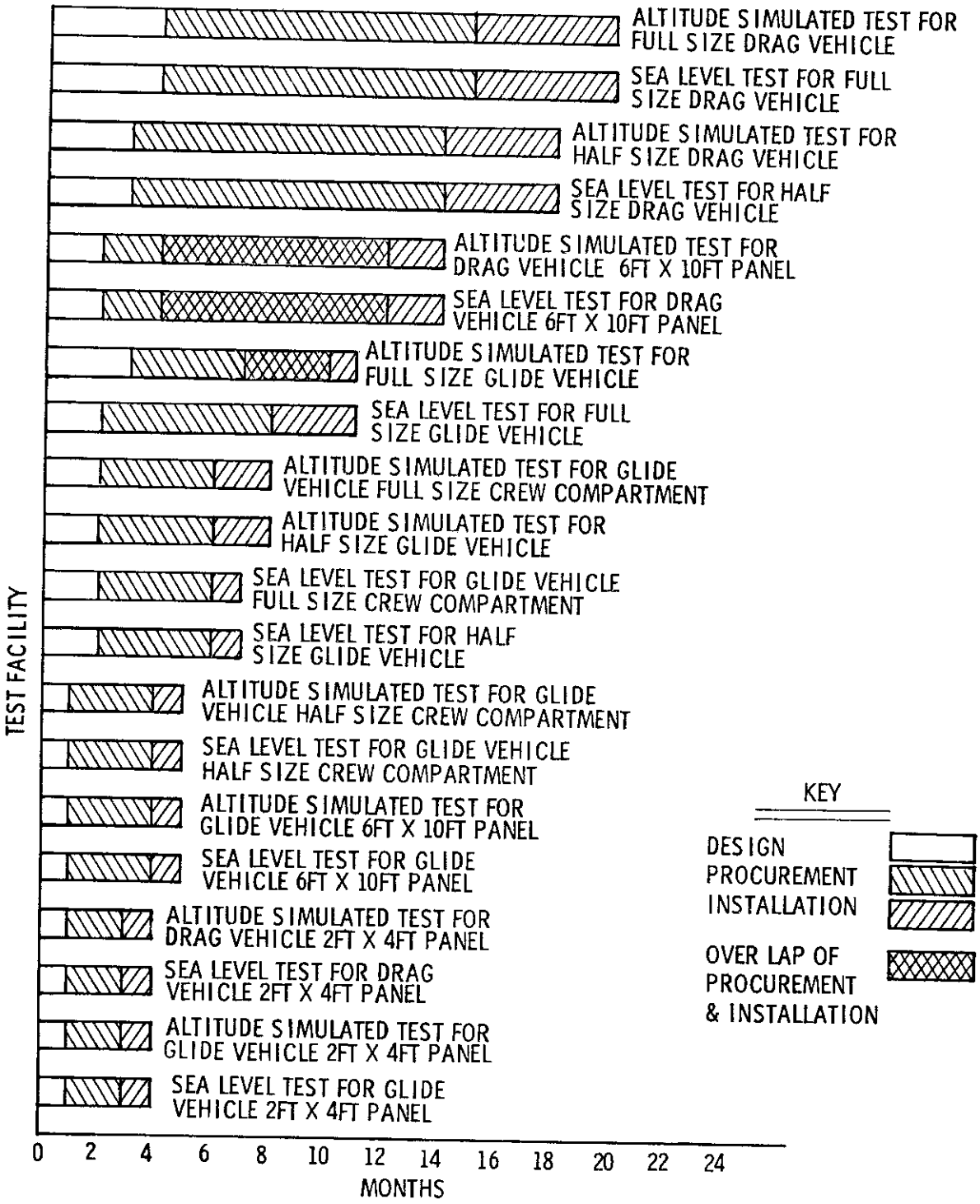

FIGURE 32 RADIANT HEAT TEST FACILITIES CALENDAR LEAD TIME

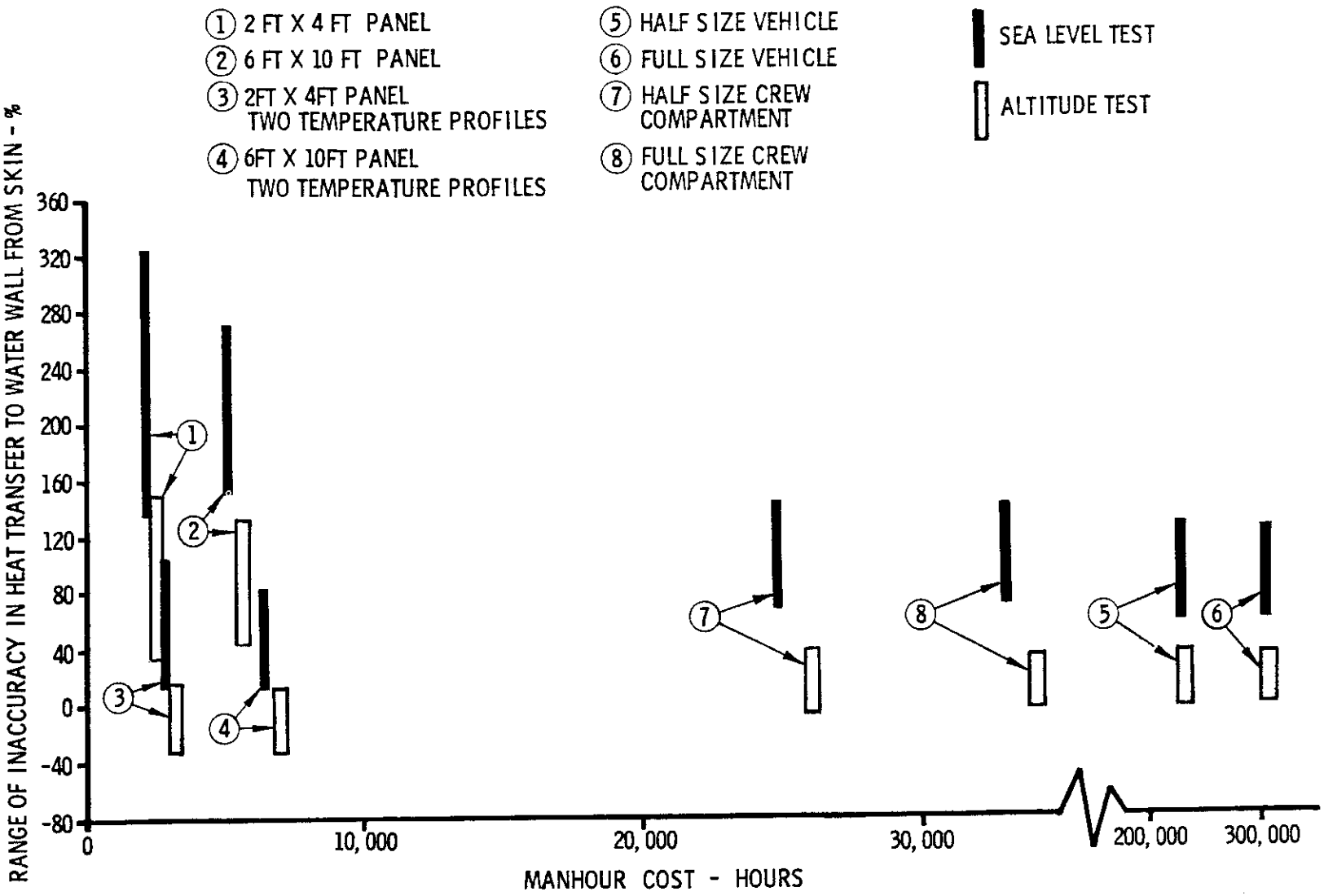

FIG. 33 EXPERIMENTAL MANHOURS VERSUS ACCURACY - GLIDE VEHICLE

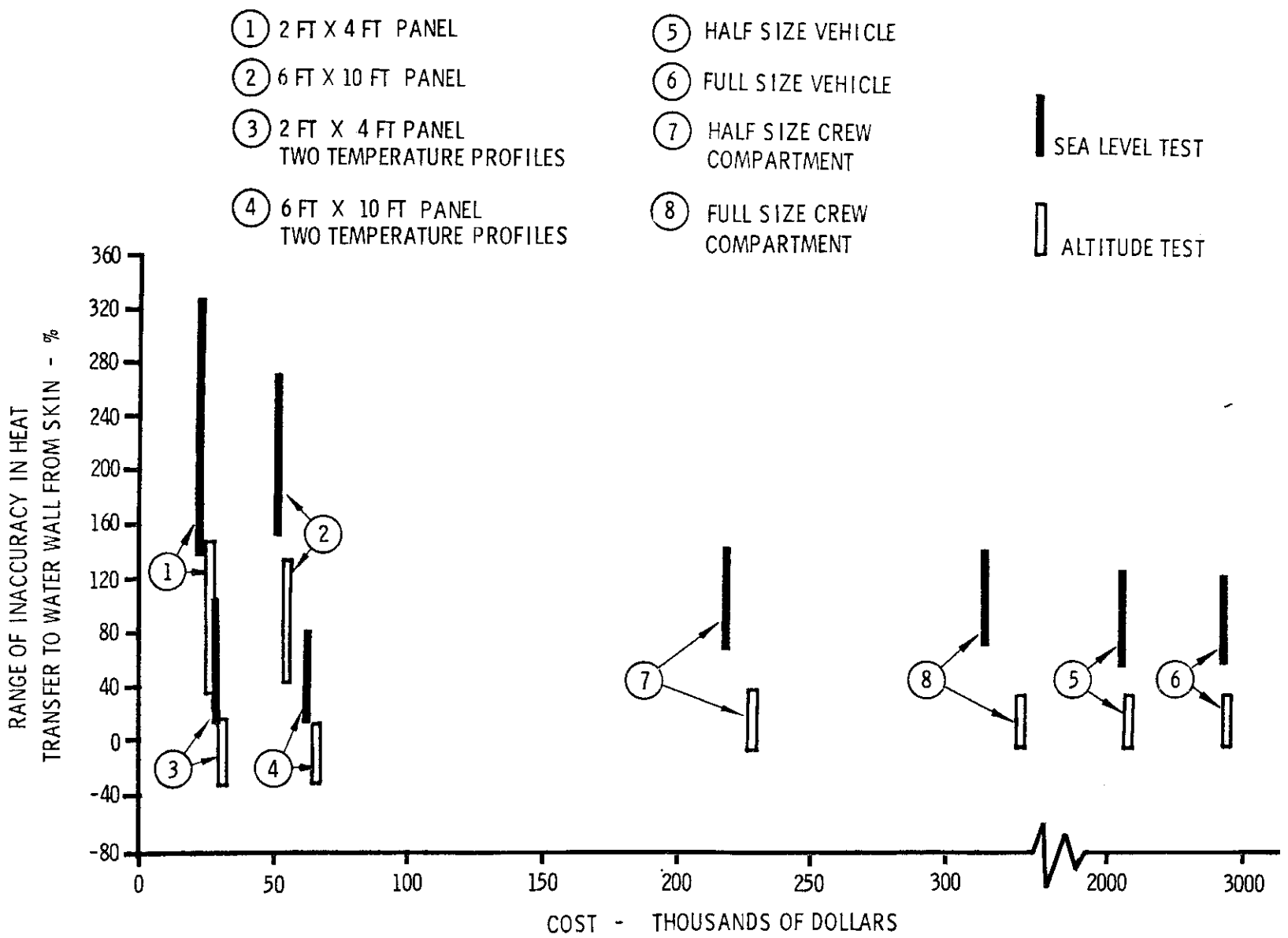

FIG. 34 EXPERIMENTAL DOLLAR COST VERSUS ACCURACY - GLIDE VEHICLE

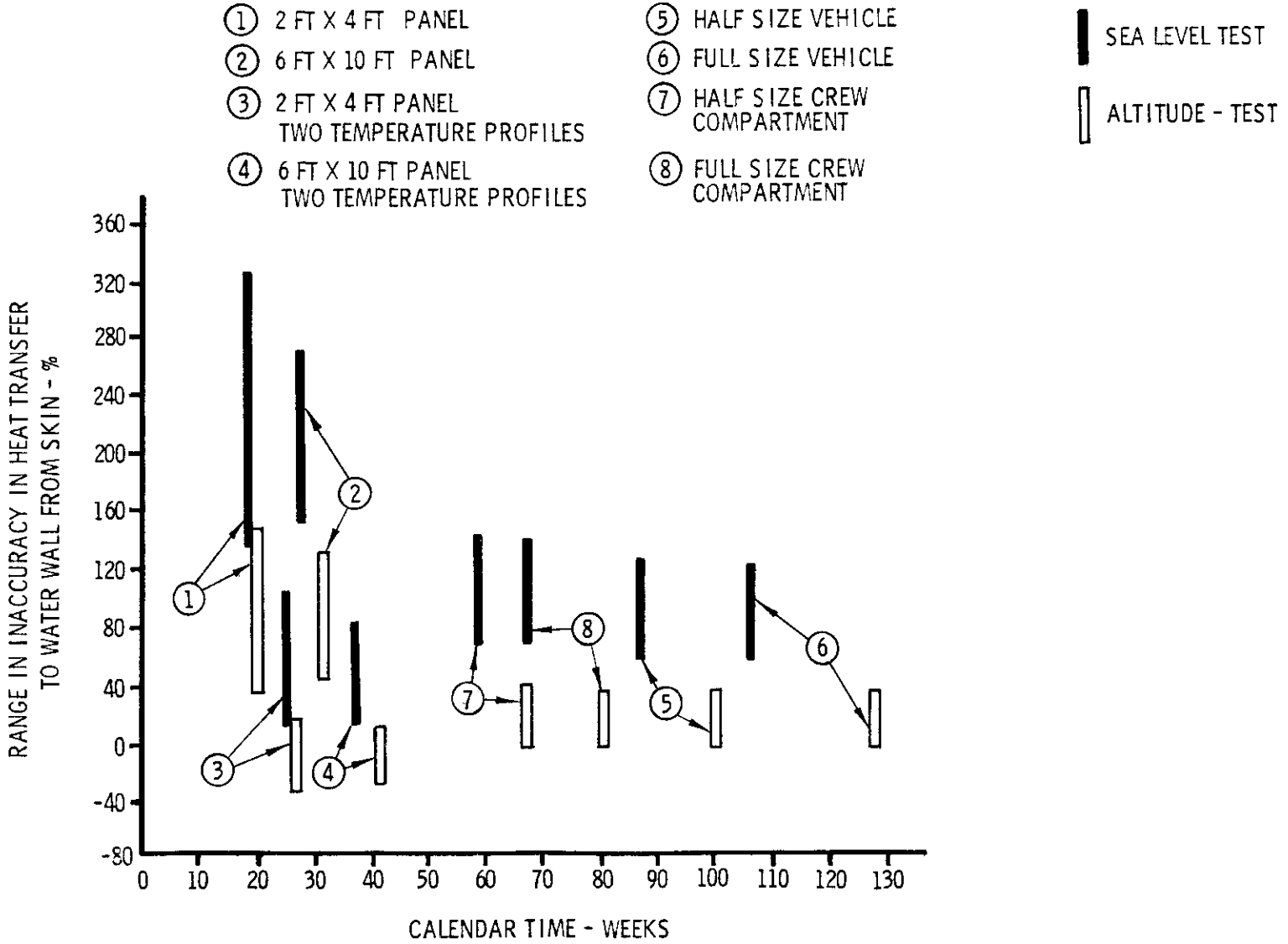

FIG. 35 EXPERIMENTAL CALENDAR TIME VERSUS ACCURACY - GLIDE VEHICLE

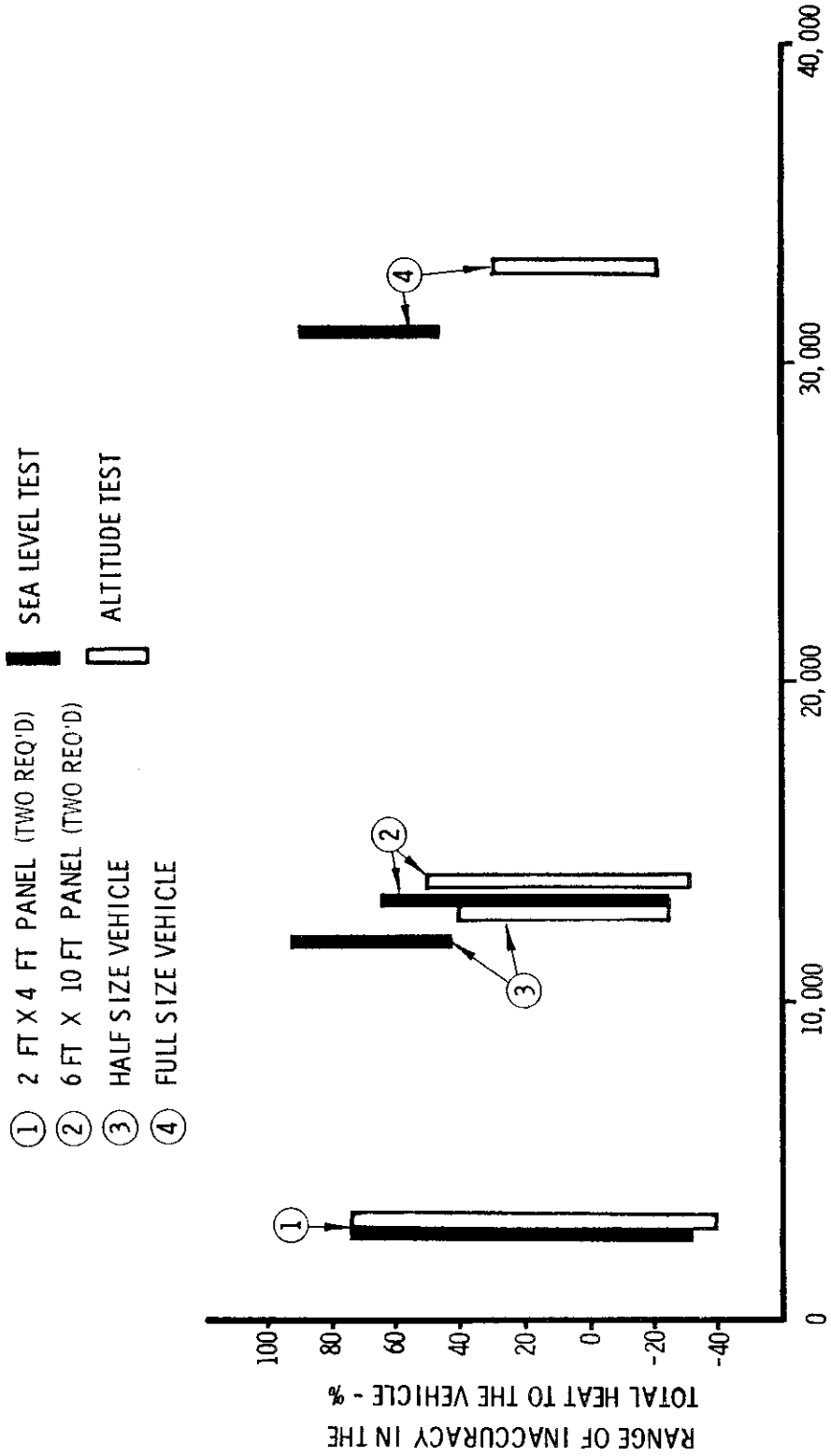

FIG. 36 EXPERIMENTAL MANHOURS VERSUS ACCURACY - DRAG VEHICLE

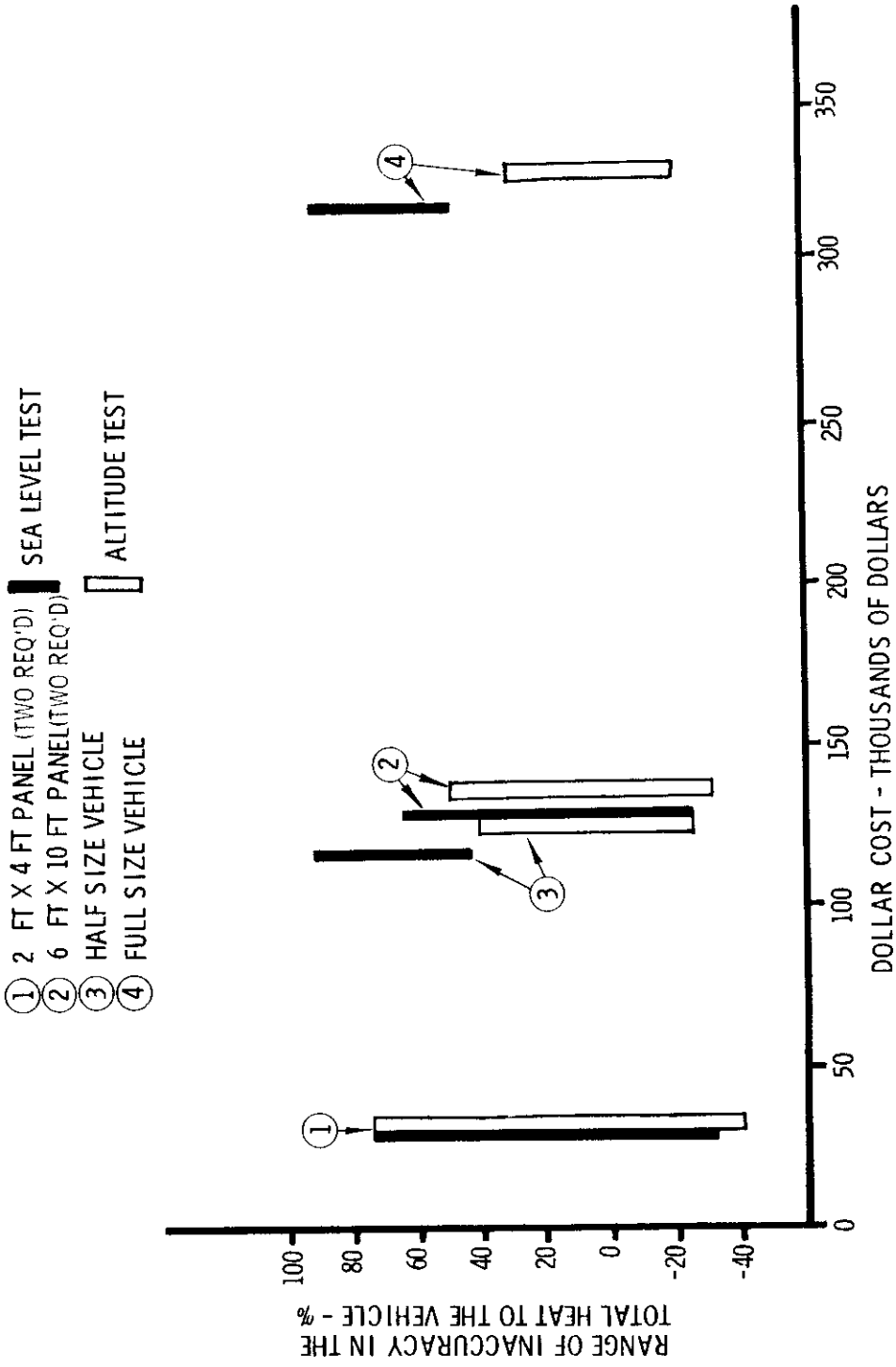

FIG. 37 EXPERIMENTAL DOLLAR COST VERSUS ACCURACY - DRAG VEHICLE

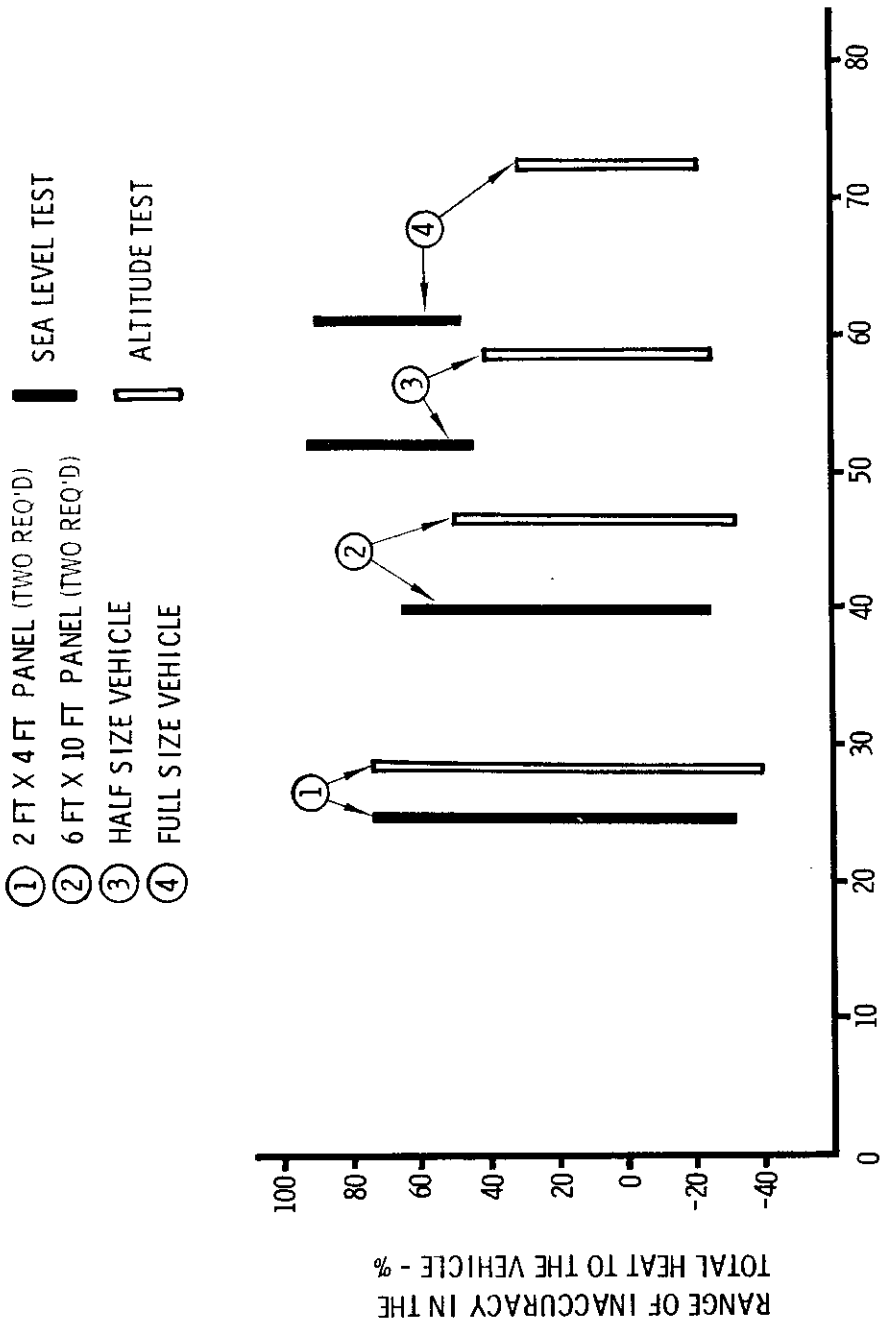

FIG. 38 EXPERIMENTAL CALENDAR TIME VERSUS ACCURACY - DRAG VEHICLE

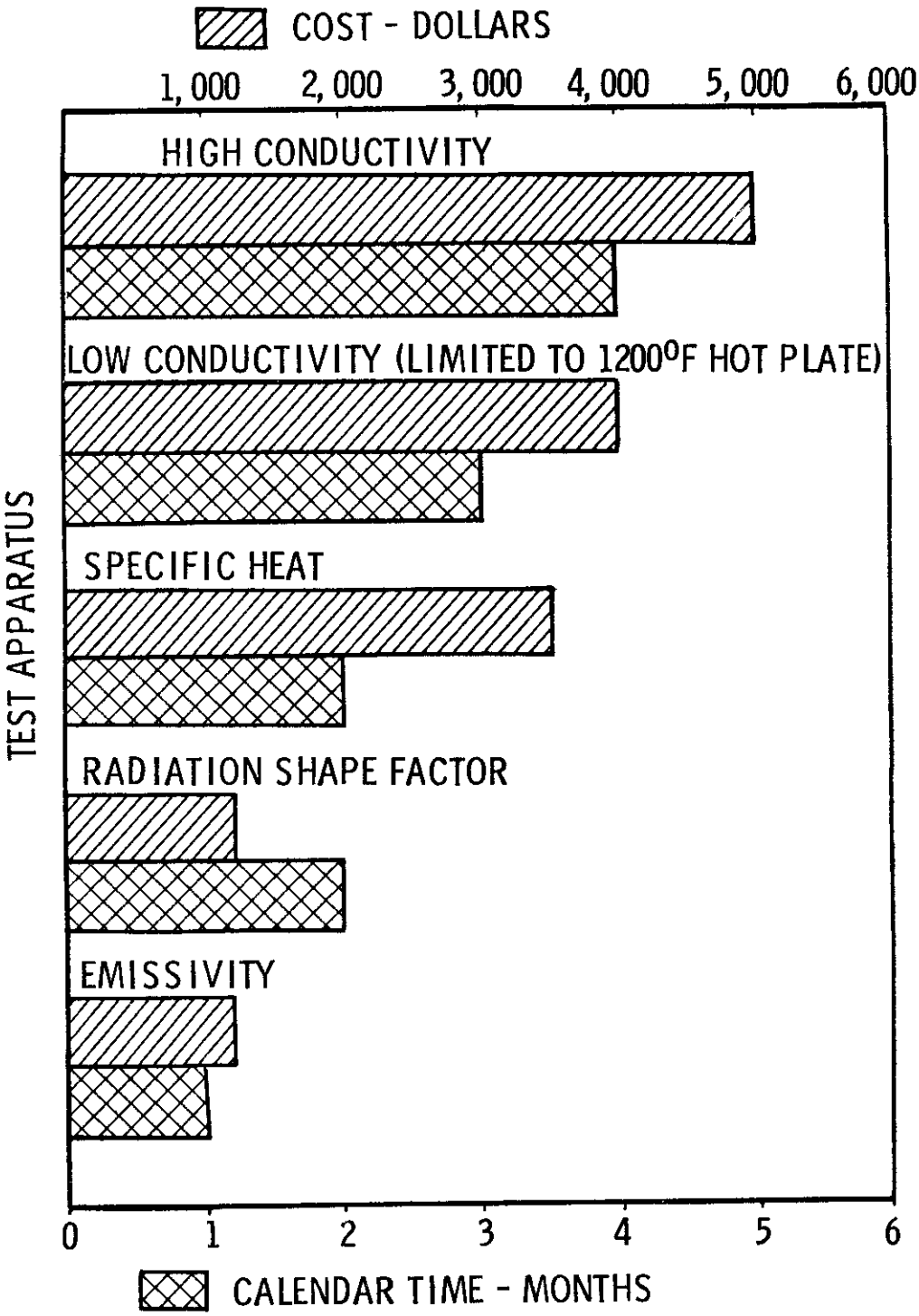

FIGURE 39 MATERIAL PROPERTY TEST APPARATUS COST & CALENDAR LEAD TIME

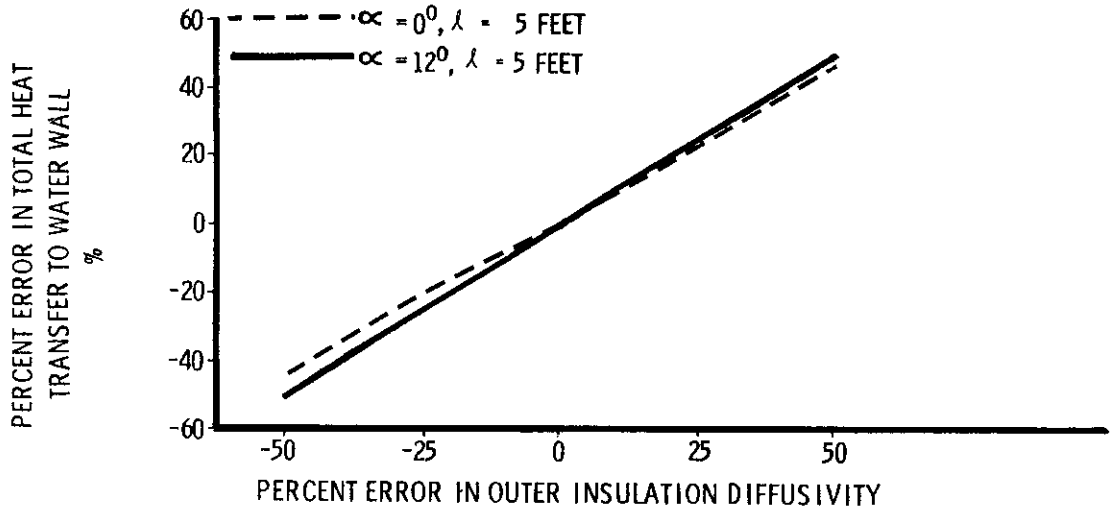

FIG. 40 EFFECT ON HEAT TRANSFER OF ERRORS IN THE OUTER INSULATION DIFFUSIVITY - GLIDE VEHICLE

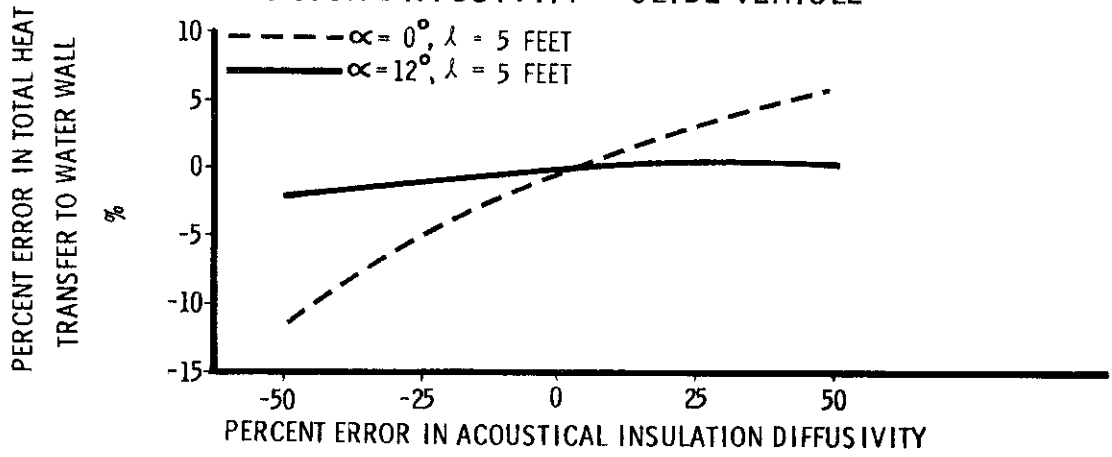

FIG. 41 EFFECT ON HEAT TRANSFER OF ERRORS IN THE ACOUSTICAL INSULATION DIFFUSIVITY - GLIDE VEHICLE

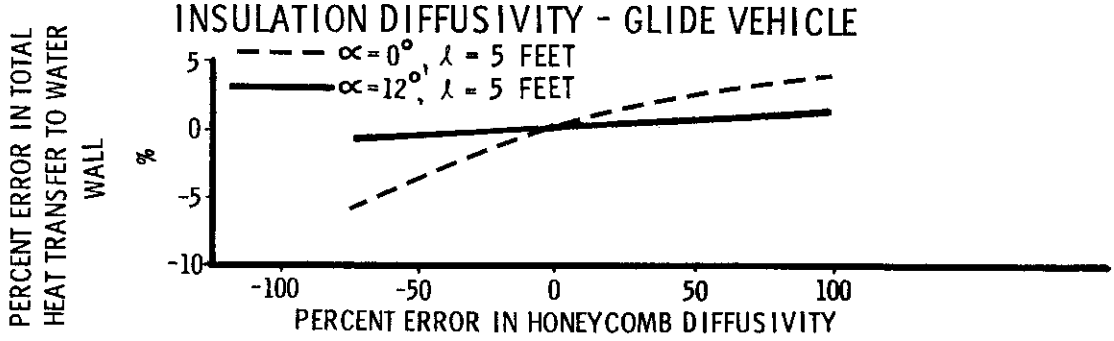

FIG. 42 EFFECT ON HEAT TRANSFER OF ERRORS IN THE HONEYCOMB DIFFUSIVITY - GLIDE VEHICLE

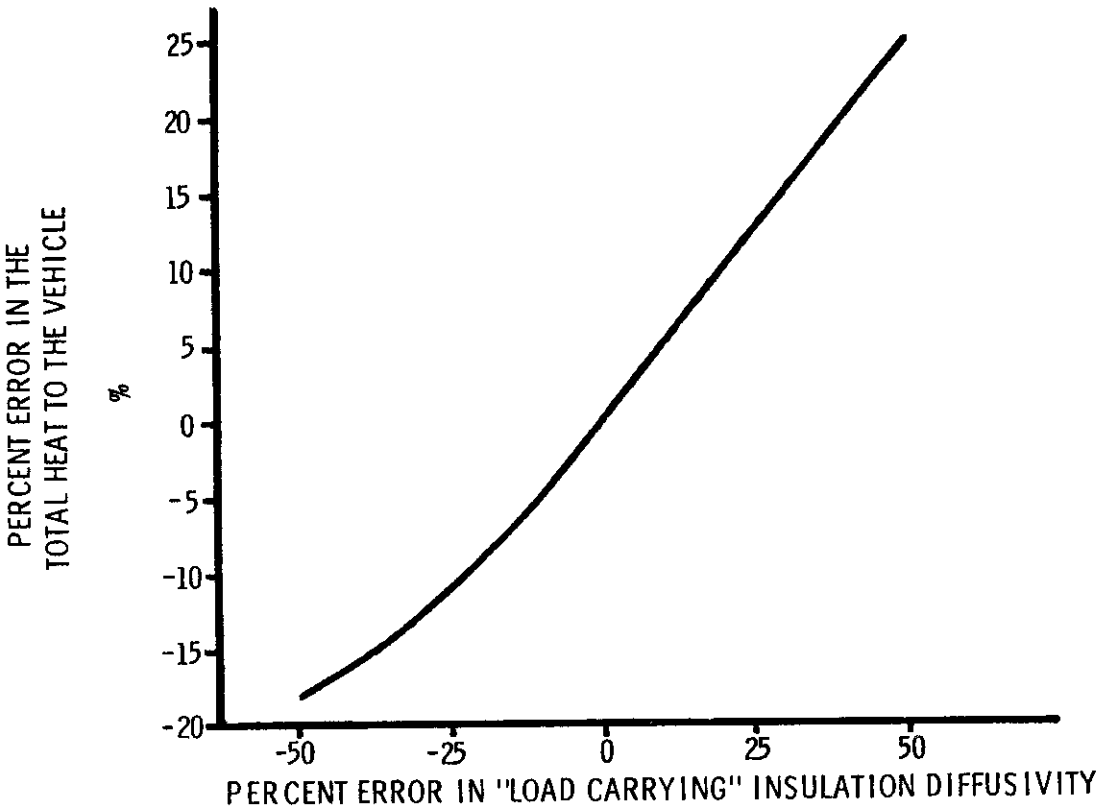

FIG 43 EFFECT ON HEAT TRANSFER OF ERRORS IN THE "LOAD CARRYING" INSULATION DIFFUSIVITY - DRAG VEHICLE

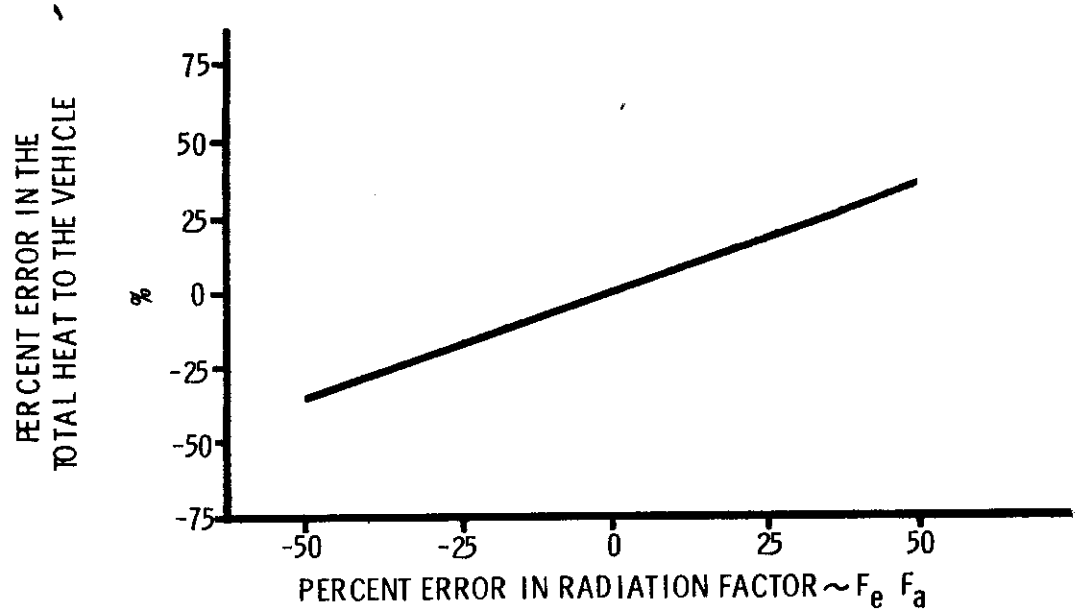

FIG 44 EFFECT ON HEAT TRANSFER OF ERRORS IN THE RADIATION FACTOR - DRAG VEHICLE.

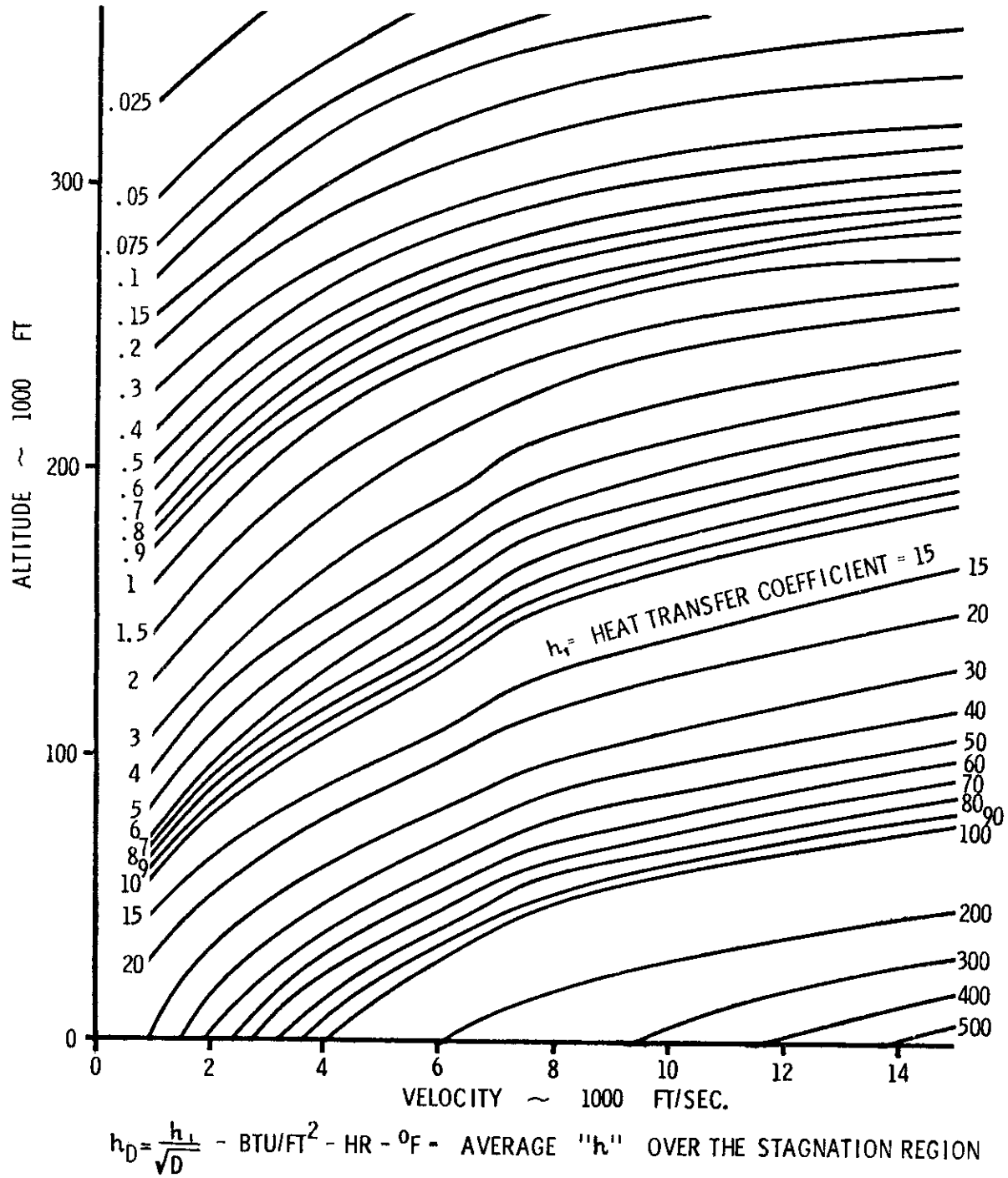

FIG. 45 SPHERICAL NOSE HEAT TRANSFER COEFFICIENT FOR ONE FOOT DIA. NOSE VELOCITY UP TO 14,000 FT/SEC

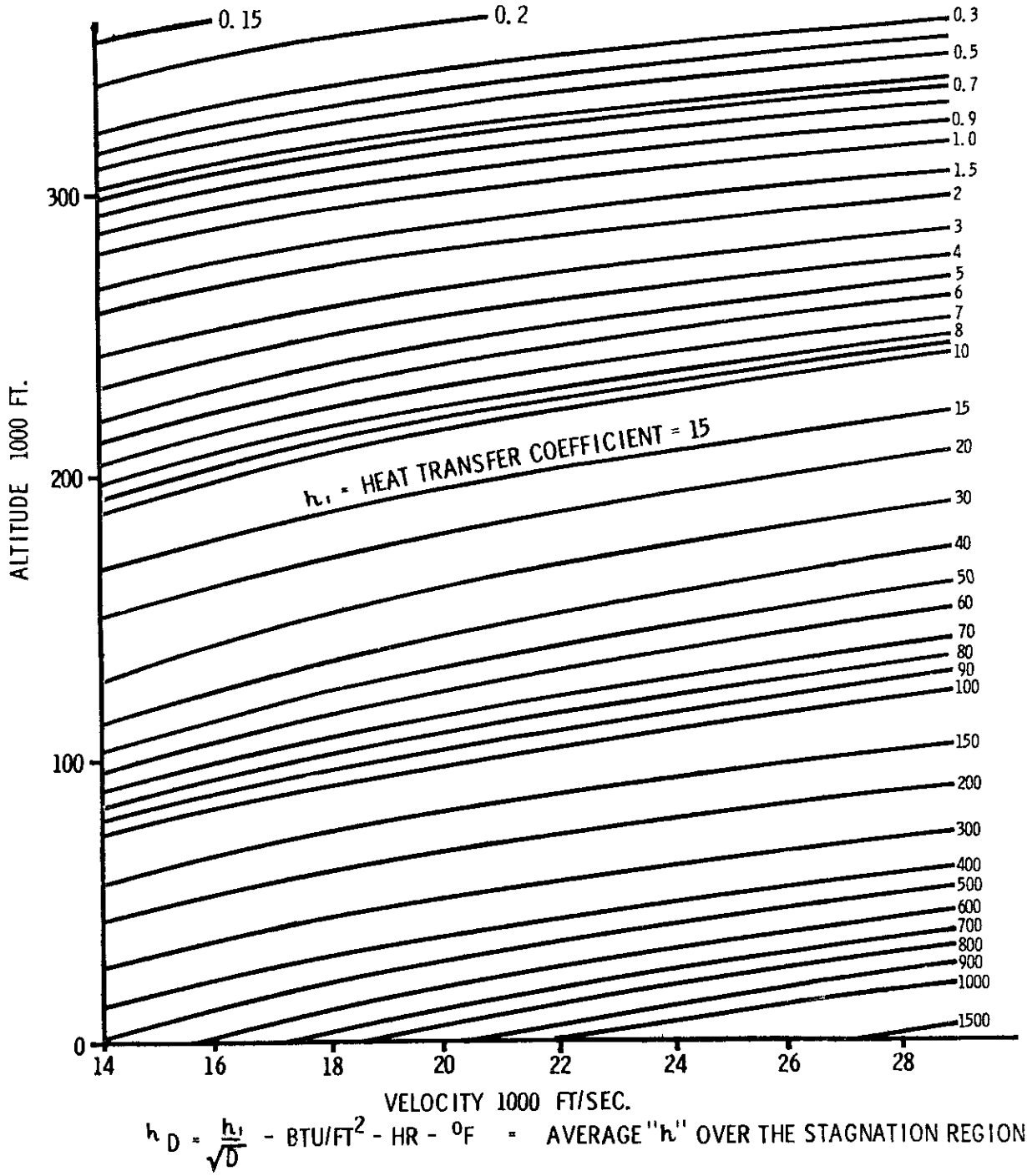

FIG. 46 SPHERICAL NOSE HEAT TRANSFER COEFFICIENT FOR ONE FOOT DIA. NOSE VELOCITY UP TO 28,000 FT/SEC

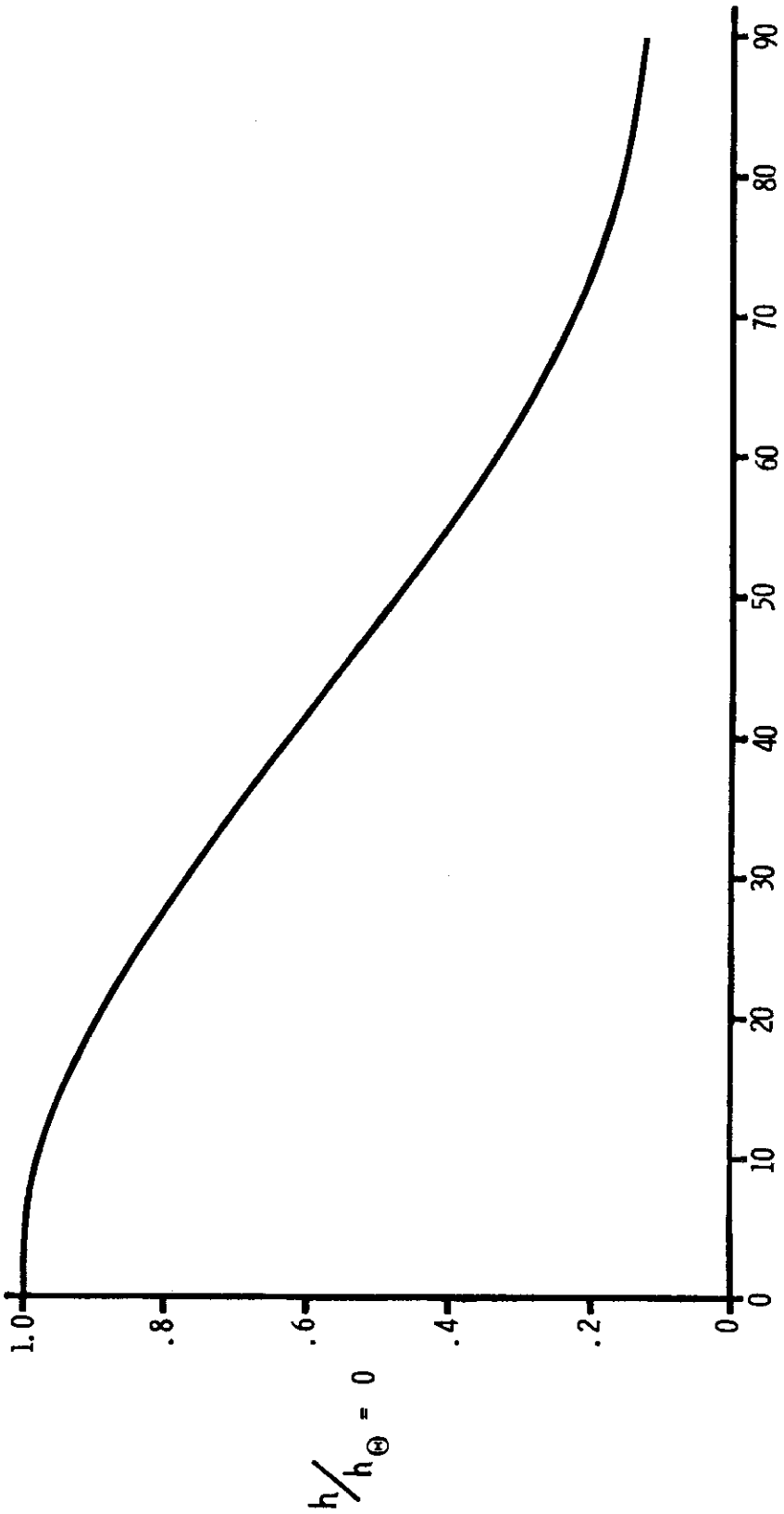

FIG. 47 STAGNATION REGION FACTOR-LAMINAR FLOW

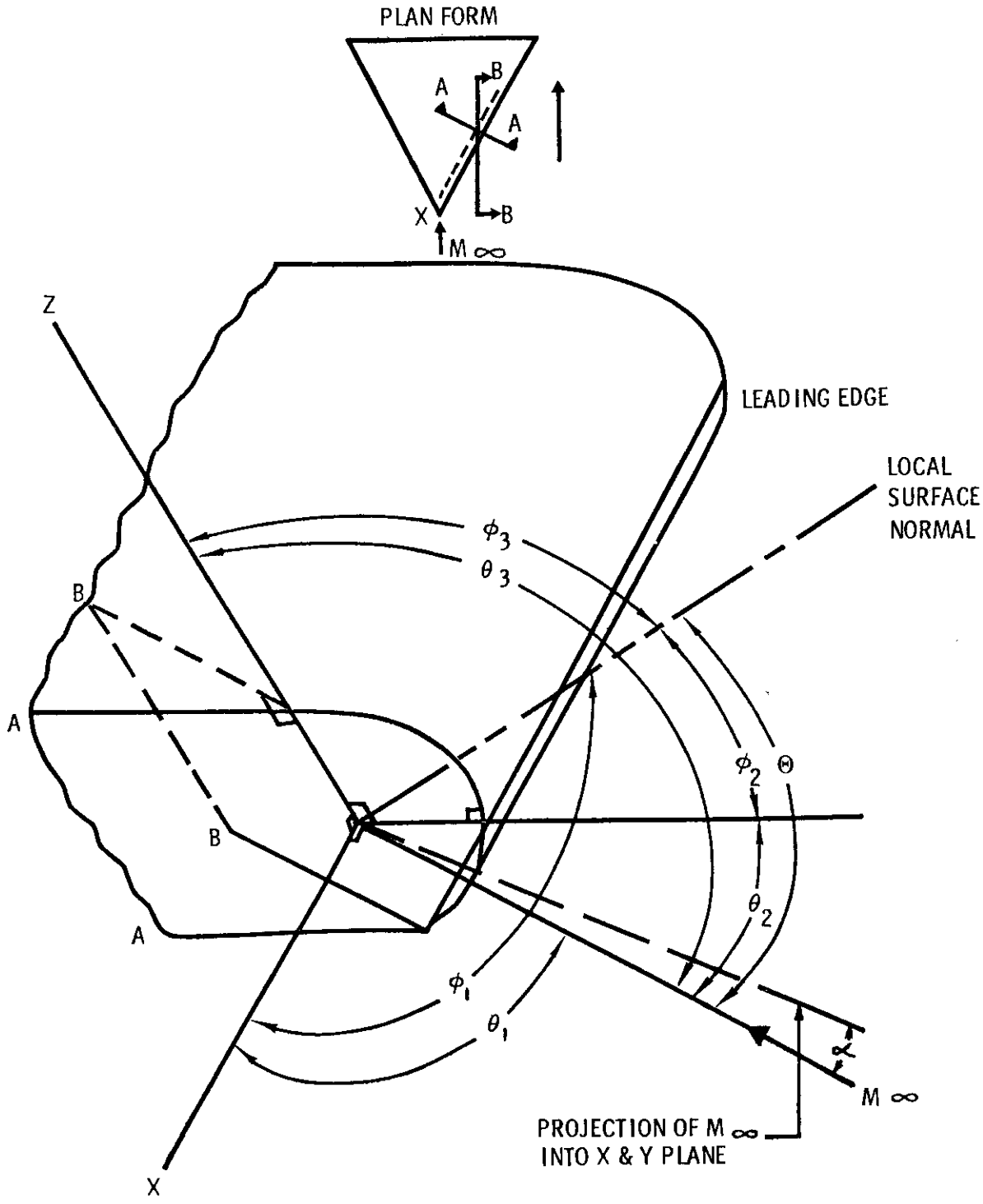

FIG. 48 GEOMETRIC DEFINITION OF ANGLES USED TO FIND ANGLE BETWEEN FLOW AND SURFACE NORMAL

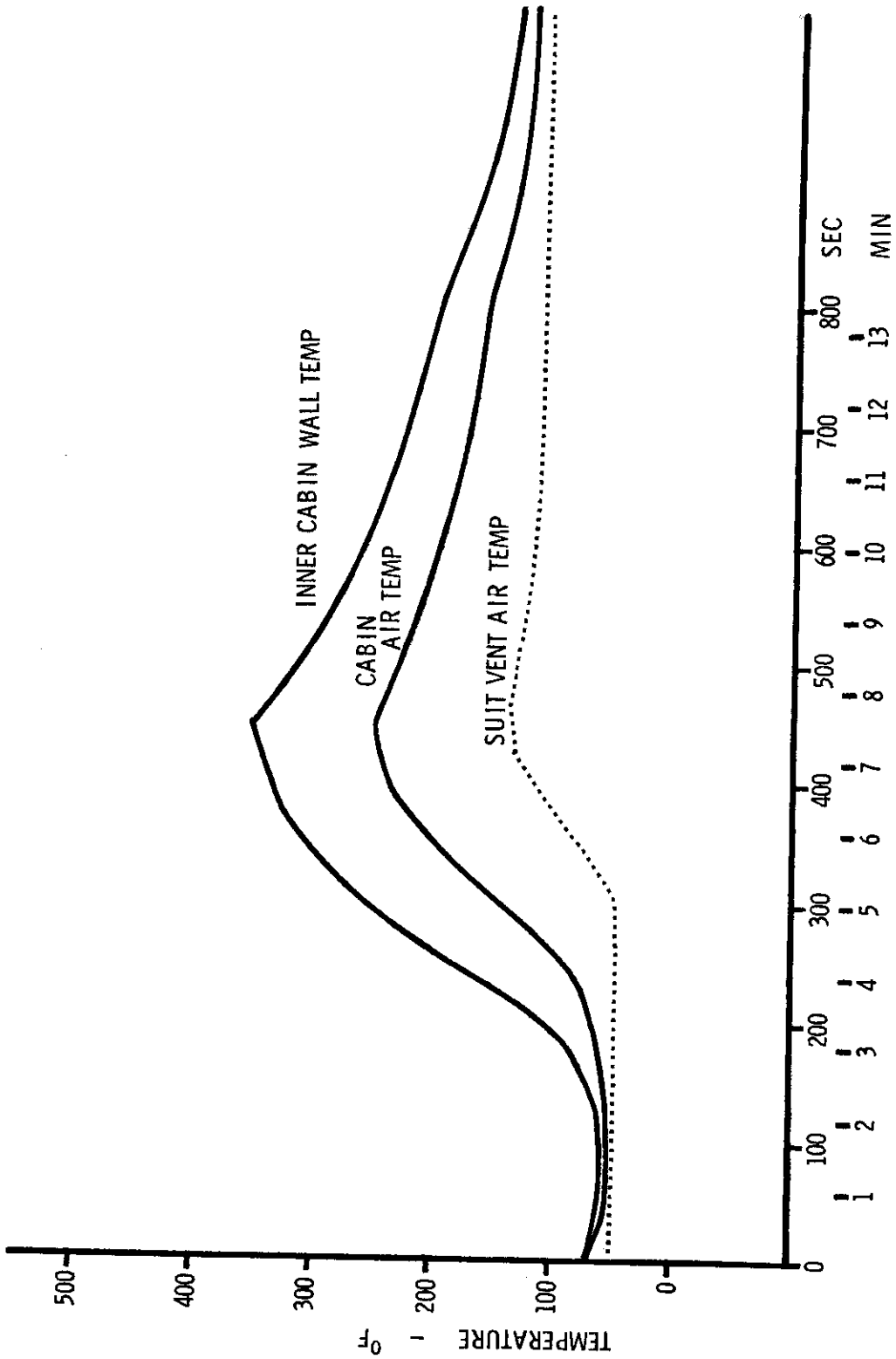

FIG. 49 TYPICAL RE-ENTRY VEHICLE WALL TEMPERATURE

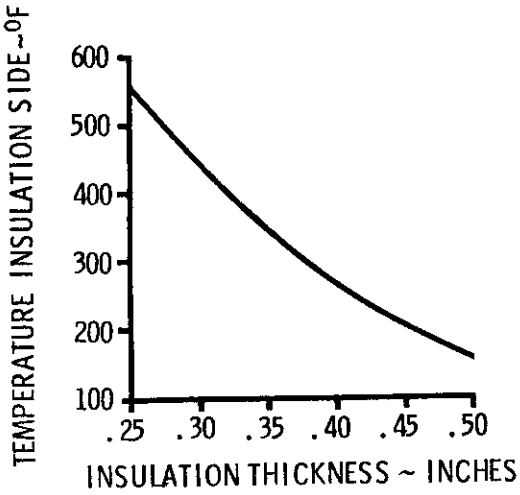

FIG. 50 MAXIMUM CABIN WALL TEMPERATURE VS INSULATION THICKNESS FORWARD SIDE - DRAG VEHICLE

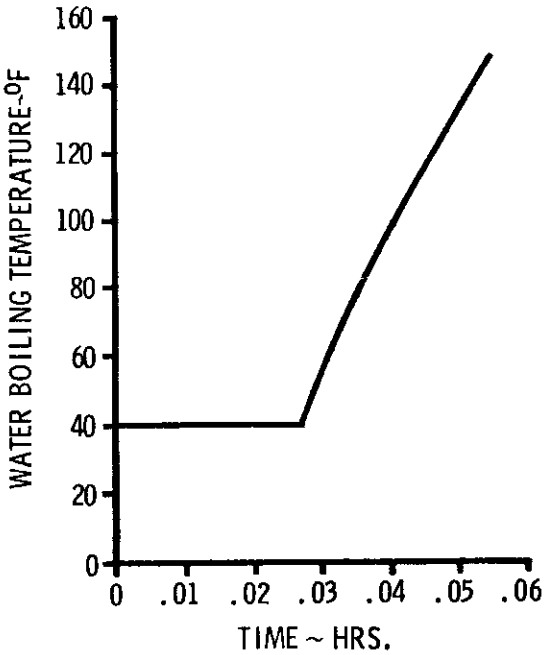

FIG. 51 WATER BOILING TEMPERATURE - DRAG VEHICLE

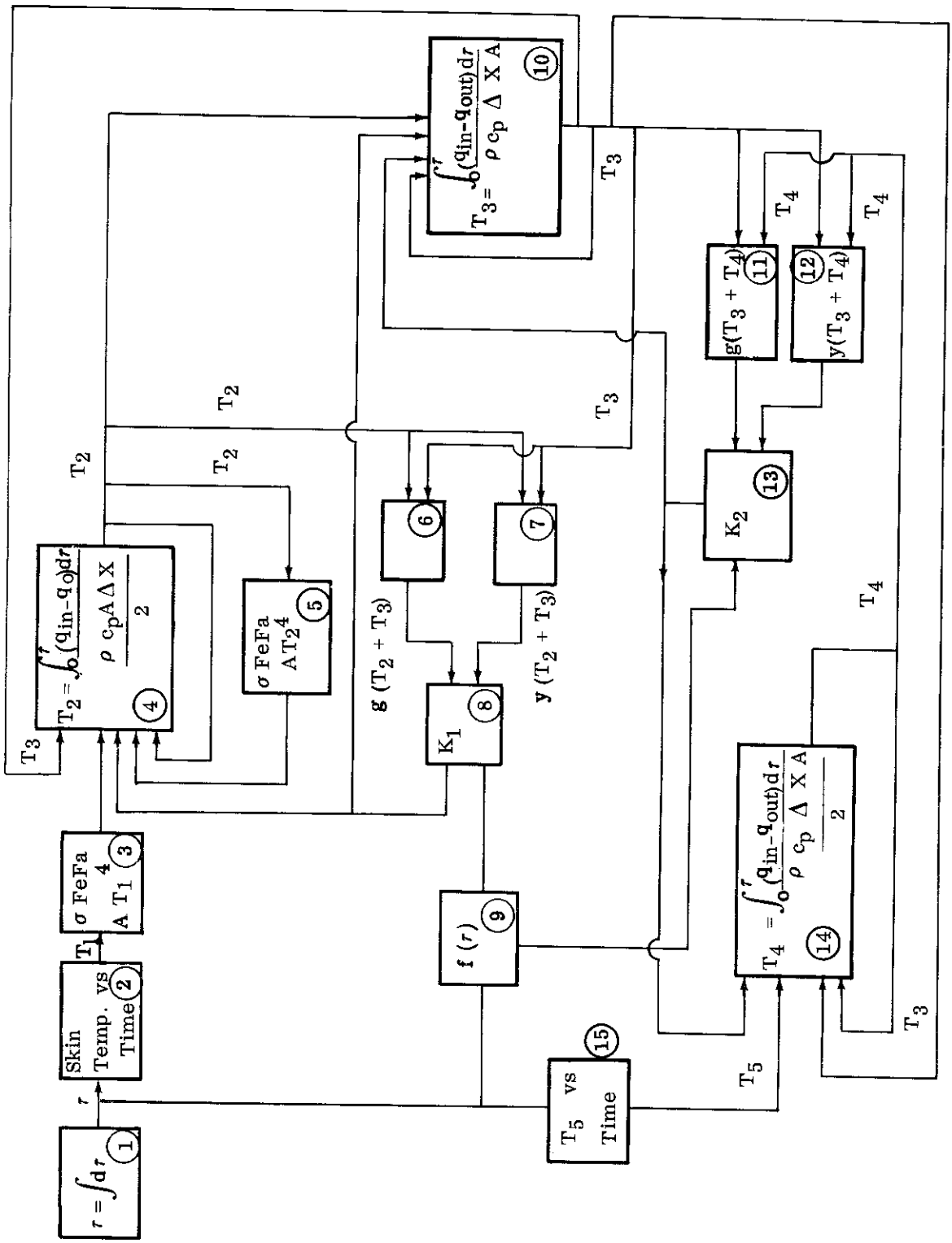

FIG. 52 BLOCK DIAGRAM OF DIFFERENTIAL ANALYZER SETUP

1 $\Sigma \Delta r$	2 T_1 as function of r input data	3 σ A FeFa T_1	4 σ A FeFa T_2^4	5 $T_1 - T_2$ ② - ⑱	6 hr ③ - ④ / ⑤	7 R_1 $\frac{1}{⑥}$ A
8 $\frac{C_1}{R_1}$ $\frac{\rho c_p A \Delta X}{2}$ ⑦	9 $\frac{T_2 + T_3}{2}$ $\frac{⑱ + ㉙}{2}$	10 K_1 from a plot of K as a function of altitude and mean temperature	11 $\frac{1}{R_2}$ $\frac{K_1 A}{\Delta X} = ⑩ \frac{A}{\Delta X}$	12 $\frac{C_1}{R_2}$ $\frac{\rho A c_p \Delta X ⑪}{(2)}$	13 $\left[\frac{C_1}{R_1} + \frac{C_1}{R_2}\right] \Delta r$ $\left[⑫ + ⑧\right] \Delta r$	14 $1 \left[\frac{C_1}{R_1} + \frac{C_1}{R_2}\right] \Delta r$ $1 -$ ⑬
15 $T_2 \times$ ⑭ ⑯ x ⑭	16 $\frac{C_1 \Delta r T_1}{R_1}$ ⑧ x ② Δr	17 $\frac{C_1 \Delta r T_3}{R_2}$ ⑫ x ㉙ Δr	18 T_2' ⑮ + ⑯ + ⑰	19 $\frac{T_3 + T_4}{2}$ $\frac{㉙ + ㊳}{2}$	20 K_2 from a plot of K as a function of altitude and mean temperature	21 $\frac{1}{R_3}$ $\frac{K_2 A}{\Delta X} = \frac{⑳ A}{\Delta X}$
22 $\frac{C_2}{R_3}$ $(\rho A \Delta X c_p)$ ㉑	23 $\frac{C_2}{R_2}$ $(\rho A \Delta X c_p)$ ⑪	24 $\left[\frac{C_2}{R_2} + \frac{C_2}{R_3}\right] \Delta r$ $\left[㉒ + ㉓\right] \Delta r$	25 1 - ㉔	26 $T_3 \left[1 - \left(\frac{C_2}{R_2} + \frac{C_3}{R_3}\right) \Delta r\right]$ ㉙ x ㉕	27 $\frac{C_2}{R_2} \Delta r T_2$ ㉓ x ⑯ Δr	28 $\frac{C_2}{R_3} \Delta r T_4$ ㉒ x ㊳ Δr
29 T_3' ㉖ + ㉗ + ㉘	30 $\frac{C_3}{R_3}$ $\left(\frac{\rho A c_p \Delta X}{2}\right)$ ㉑	31 $\frac{1}{R_4}$ h A	32 $\frac{C_3}{R_4}$ $\left(\frac{\rho A c_p \Delta X}{2}\right)$ ㉛	33 $\left[\frac{C_3}{R_3} + \frac{C_3}{R_4}\right] \Delta r$ $\left[㉚ + ㉜\right] \Delta r$	34 1 - ㉝	35 $T_4 \left[1 - \left(\frac{C_3}{R_3} + \frac{C_4}{R_4}\right) \Delta r\right]$ ㊳ x ㉝
36 $\frac{C_3 \Delta r T_3}{R_4}$ ㉜ x ㊴ Δr	37 $\frac{C_3 \Delta r T_5}{R_4}$ ㉜ x ㊴ Δr	38 T_4' ㉟ + ㊱ + ㊲	39 T_5 Cabin. Temperature input data			

FIGURE 53
HAND CALCULATION
DATA SHEET

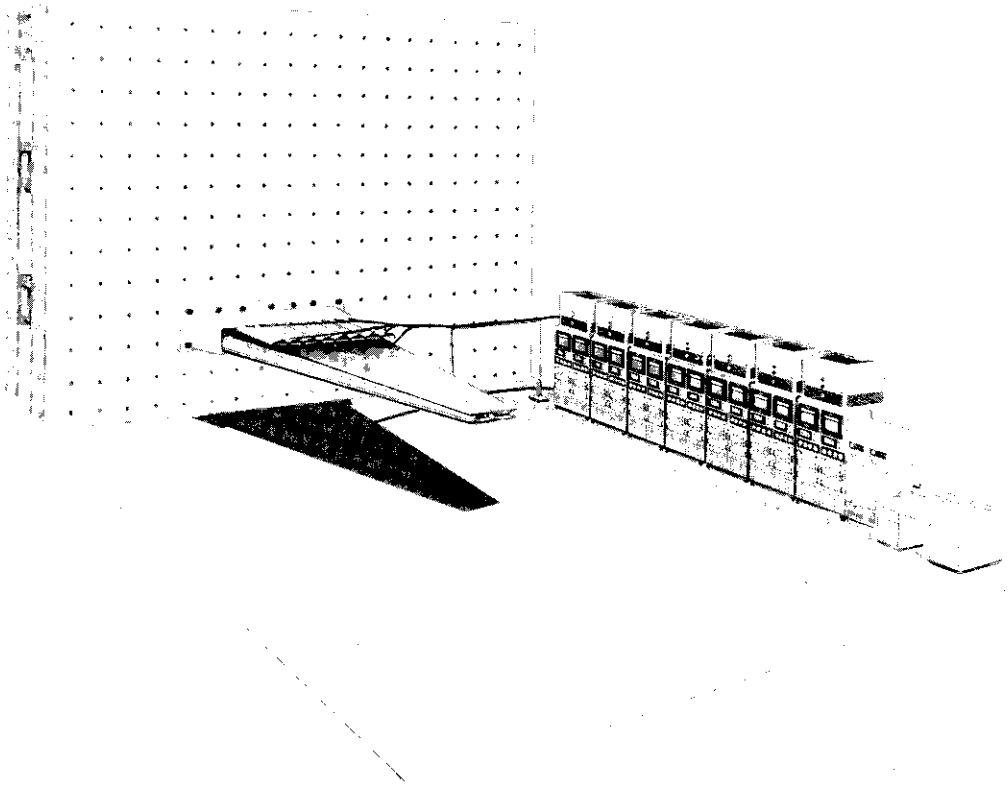

FIG. 54 RADIANT HEATING EQUIPMENT

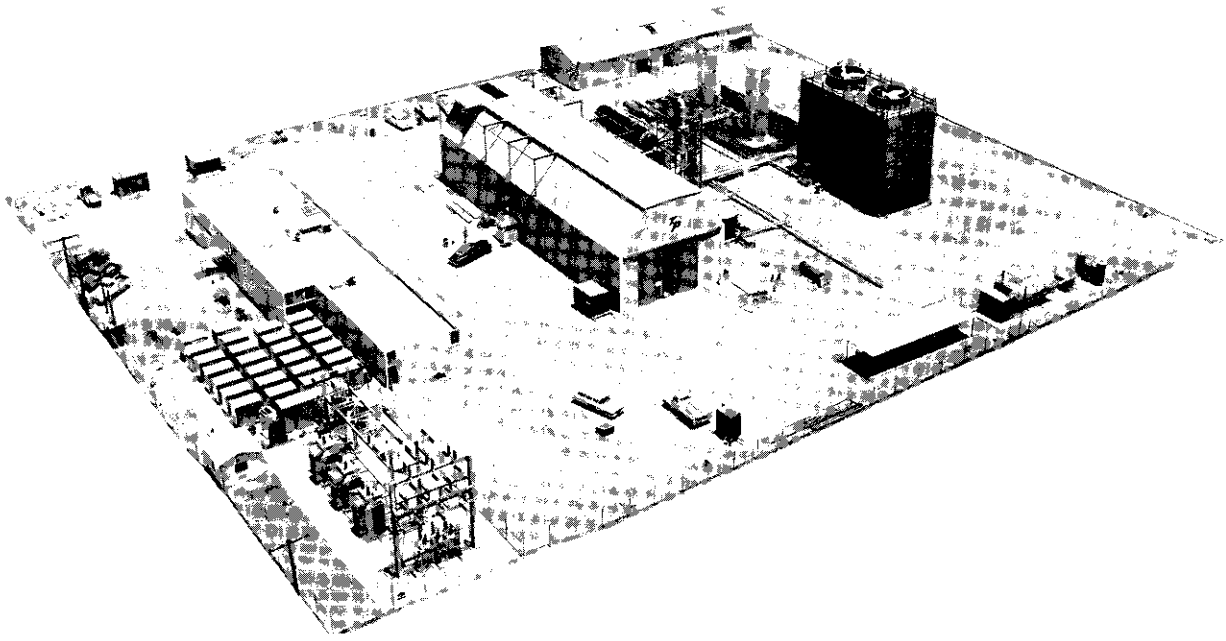

FIG. 55 AIR FORCE HEAT TEST FACILITY LOCATED AT INGLEWOOD, CALIFORNIA (PHOTO COURTESY OF THOMPSON RAMO WOOLDRIDGE INC.)

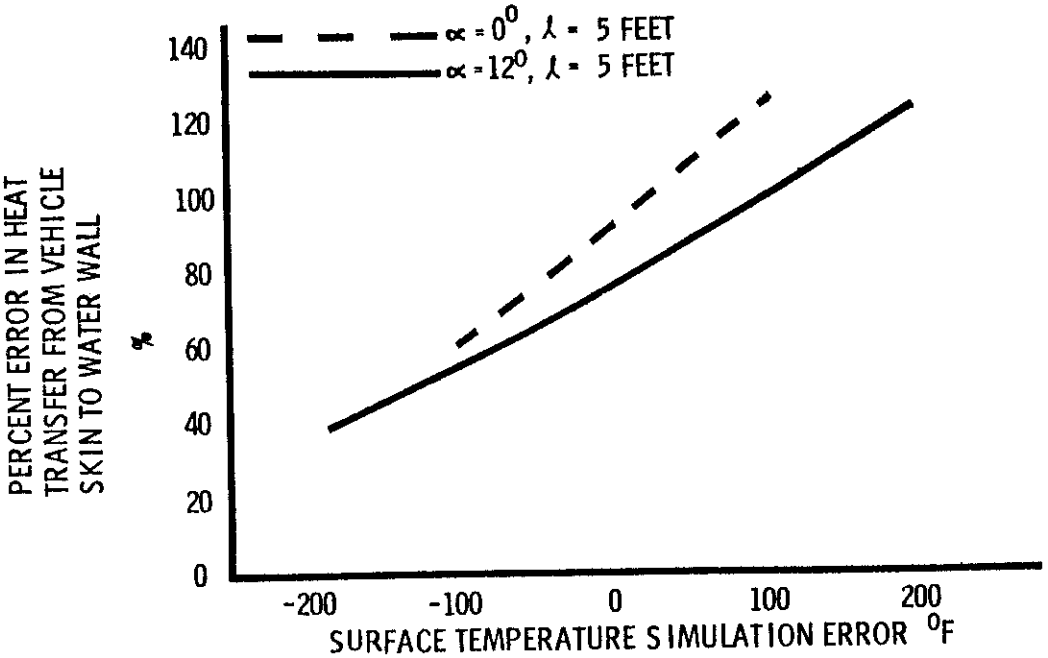

FIGURE 56 ERROR IN HEAT TRANSFER FROM VEHICLE SKIN TO WATER WALL RESULTING FROM ERRORS IN SURFACE TEMP. SIMULATION FOR SEA LEVEL TESTING - GLIDE VEHICLE.

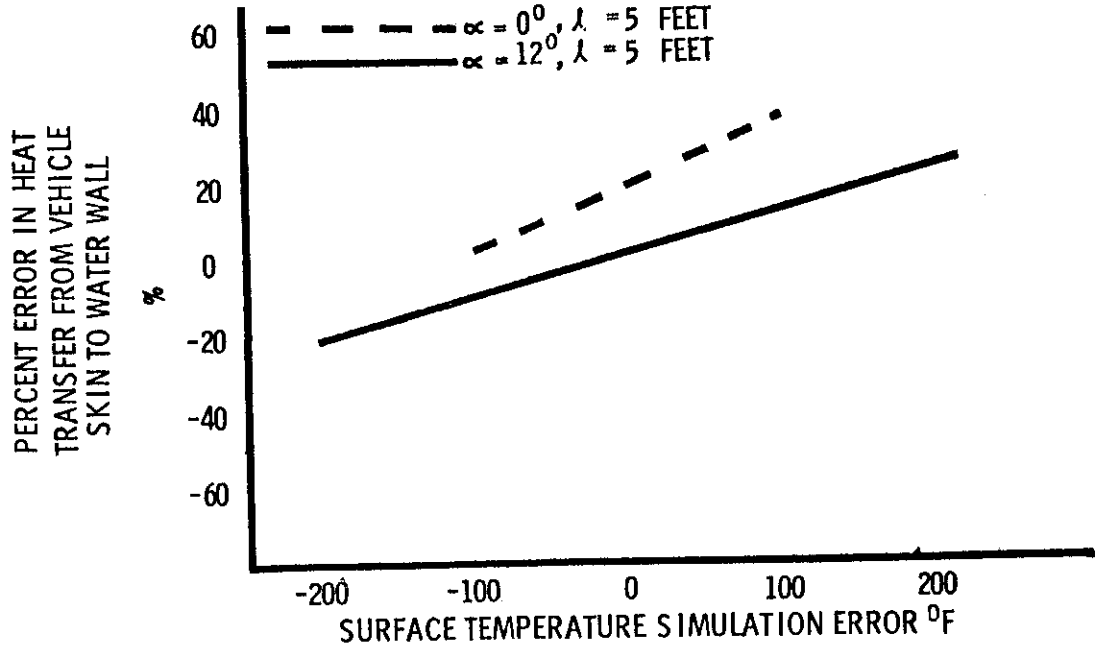

FIGURE 57 ERROR IN HEAT TRANSFER FROM VEHICLE SKIN TO WATER WALL RESULTING FROM ERRORS IN SURFACE TEMP. SIMULATION WITH ALTITUDE ERROR CURVE "A" OF FIGURE 59-GLIDE VEHICLE.

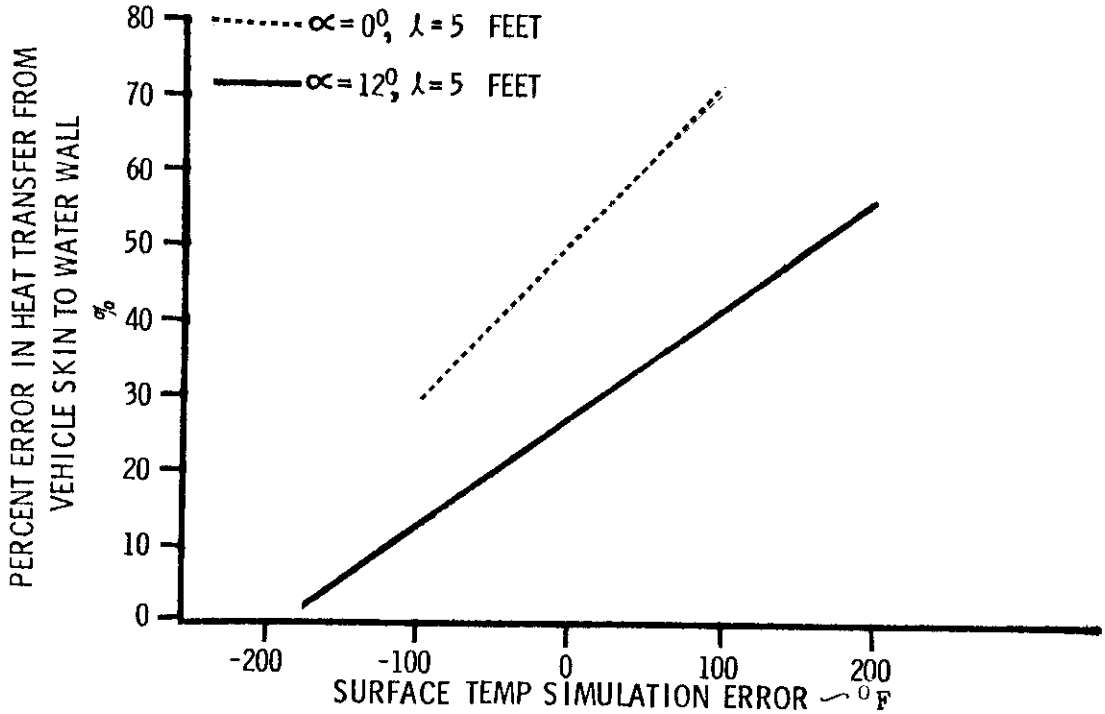

FIGURE 58 ERROR IN HEAT TRANSFER FROM VEHICLE SKIN TO WATER WALL RESULTING FROM ERRORS IN SURFACE TEMP SIMULATION WITH ALTITUDE ERROR CURVE "B" OF FIG. 59 - GLIDE VEHICLE

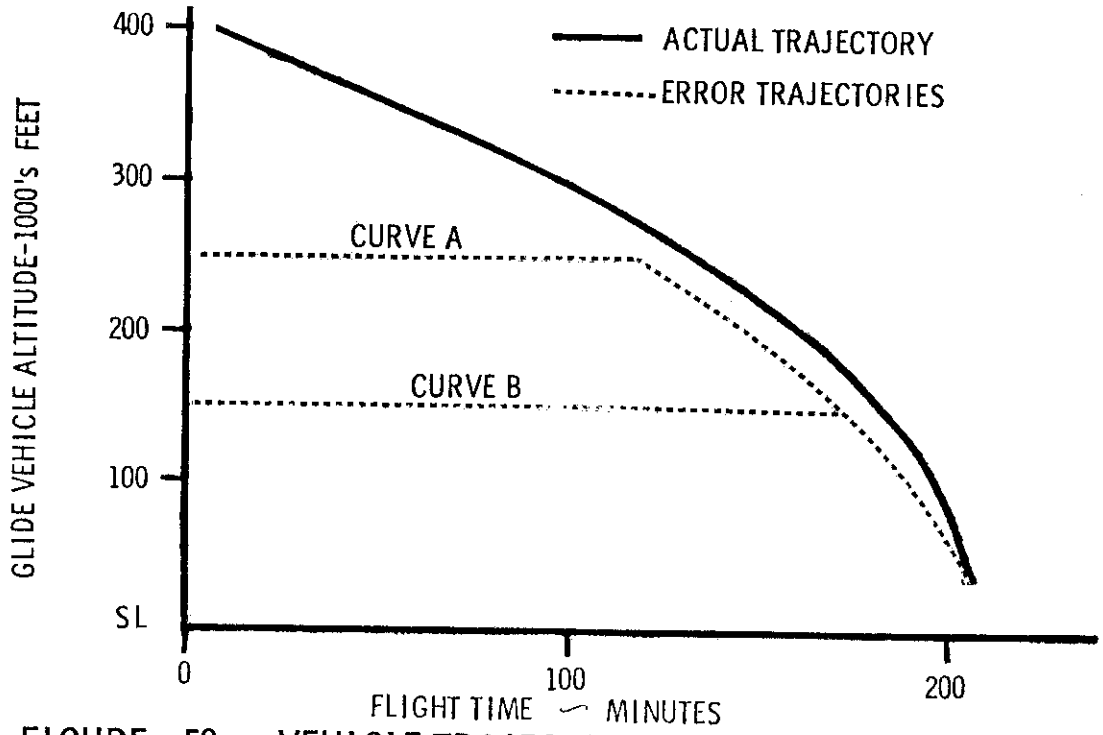

FIGURE 59 VEHICLE TRAJECTORY ERROR CURVES USED FOR FIGURES 57 AND 58 – GLIDE VEHICLE.

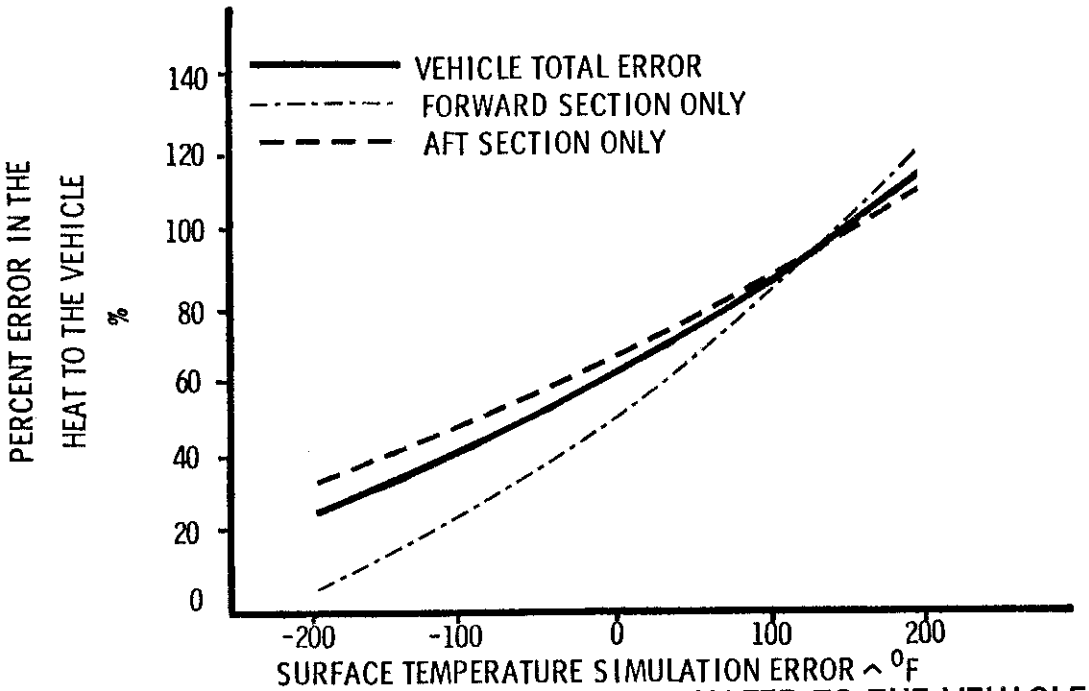

FIGURE 60 ERROR IN THE HEAT TRANSFER TO THE VEHICLE RESULTING FROM ERRORS IN SURFACE TEMPERATURE SIMULATION FOR SEA LEVEL TESTING - DRAG VEHICLE

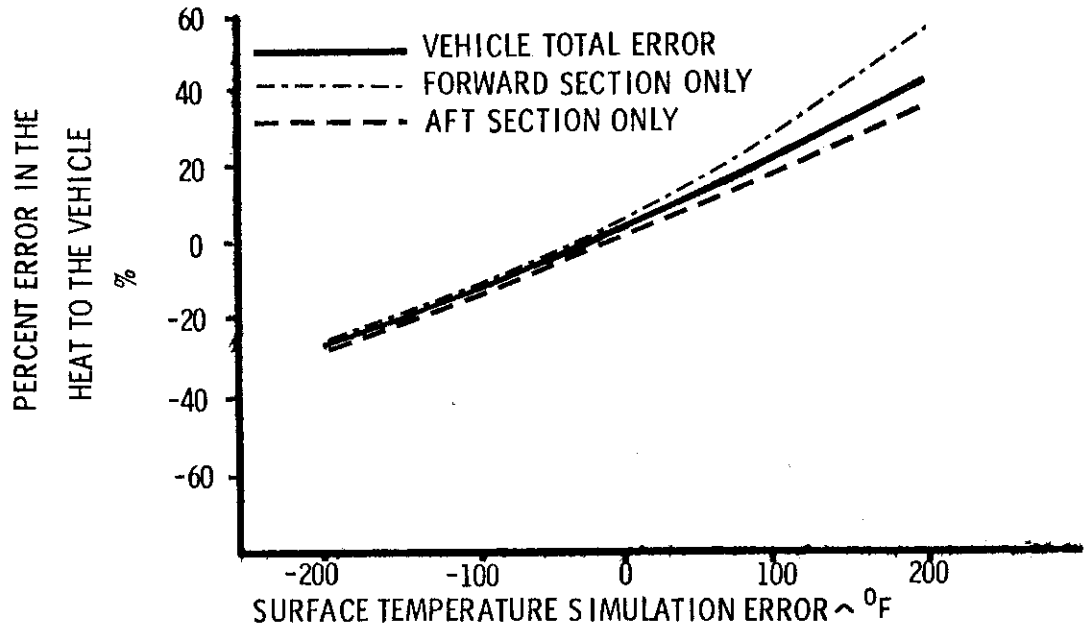

FIGURE 61 ERROR IN THE HEAT TRANSFER TO THE VEHICLE RESULTING FROM ERRORS IN SURFACE TEMPERATURE SIMULATION WITH ALTITUDE ERROR CURVE "A" OF FIGURE 63 -DRAG VEHICLE.

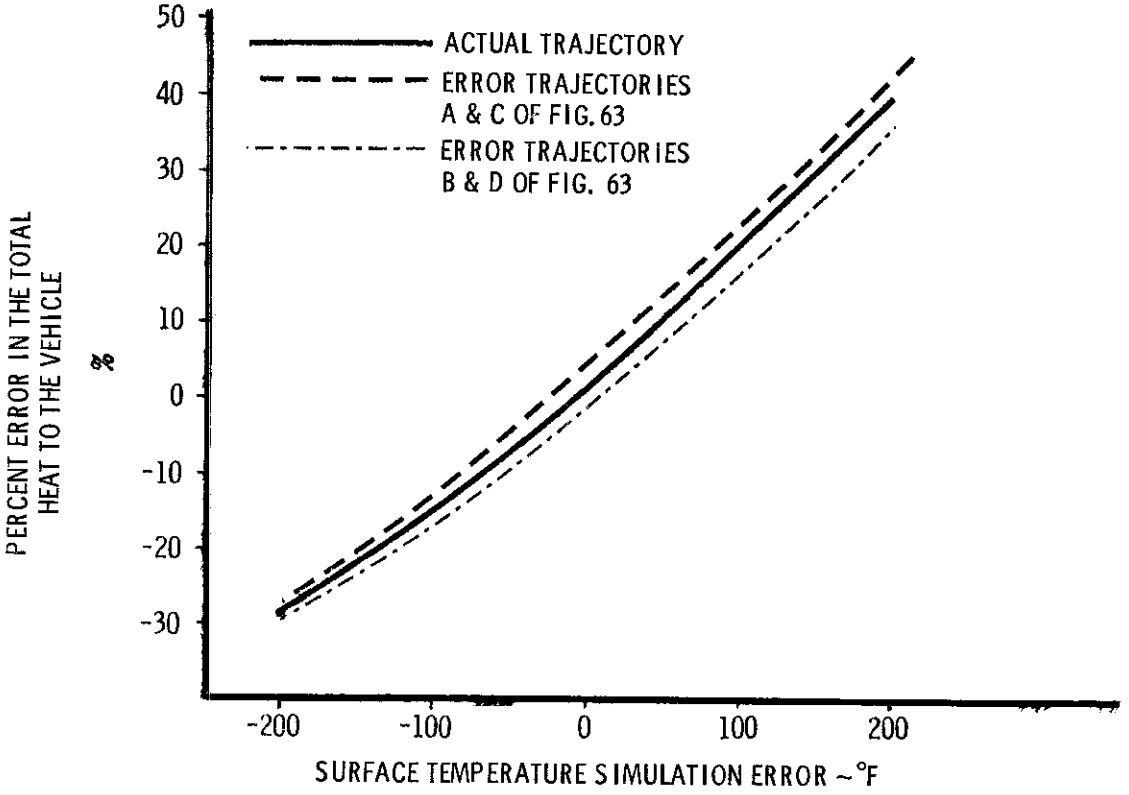

FIGURE 62 TOTAL ERROR IN THE HEAT TRANSFER TO THE VEHICLE RESULTING FROM ERRORS IN SURFACE TEMPERATURE SIMULATION FOR ALTITUDE SIMULATION ERRORS OF FIGURE 63-DRAG VEHICLE

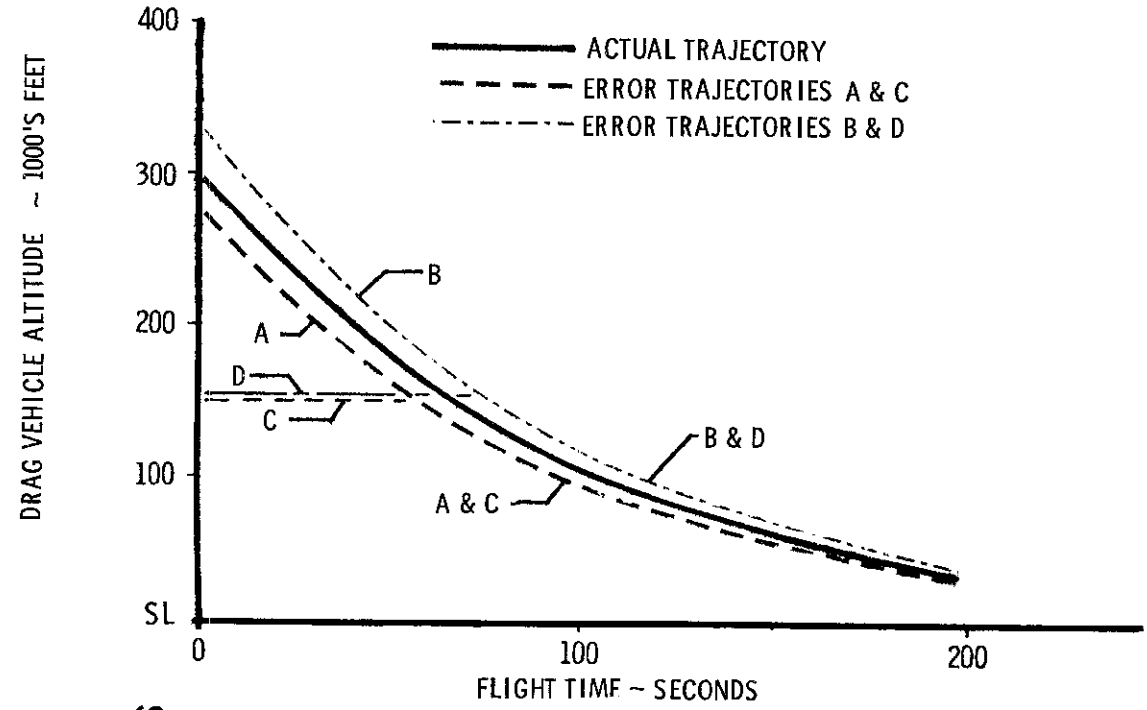

FIGURE 63 VEHICLE TRAJECTORY ERROR CURVES USED FOR FIGURES 61 & 62-DRAG VEHICLE